NIST NCSTAR 1-3C

Federal Building and Fire Safety Investigation of the World Trade Center Disaster

Damage and Failure Modes of Structural Steel Components

Stephen W. Banovic
Timothy Foecke

NIST National Institute of Standards and Technology • Technology Administration • U.S. Department of Commerce

NIST NCSTAR 1-3C

Federal Building and Fire Safety Investigation of the World Trade Center Disaster

Damage and Failure Modes of Structural Steel Components

Stephen W. Banovic
Timothy Foecke
Materials Science and Engineering Laboratory
National Institute of Standards and Technology

September 2005

<u>Disclaimer No. 1</u>

Certain commercial entities, equipment, products, or materials are identified in this document in order to describe a procedure or concept adequately or to trace the history of the procedures and practices used. Such identification is not intended to imply recommendation, endorsement, or implication that the entities, products, materials, or equipment are necessarily the best available for the purpose. Nor does such identification imply a finding of fault or negligence by the National Institute of Standards and Technology.

<u>Disclaimer No. 2</u>

The policy of NIST is to use the International System of Units (metric units) in all publications. In this document, however, units are presented in metric units or the inch-pound system, whichever is prevalent in the discipline.

<u>Disclaimer No. 3</u>

Pursuant to section 7 of the National Construction Safety Team Act, the NIST Director has determined that certain evidence received by NIST in the course of this Investigation is "voluntarily provided safety-related information" that is "not directly related to the building failure being investigated" and that "disclosure of that information would inhibit the voluntary provision of that type of information" (15 USC 7306c).

In addition, a substantial portion of the evidence collected by NIST in the course of the Investigation has been provided to NIST under nondisclosure agreements.

<u>Disclaimer No. 4</u>

NIST takes no position as to whether the design or construction of a WTC building was compliant with any code since, due to the destruction of the WTC buildings, NIST could not verify the actual (or as-built) construction, the properties and condition of the materials used, or changes to the original construction made over the life of the buildings. In addition, NIST could not verify the interpretations of codes used by applicable authorities in determining compliance when implementing building codes. Where an Investigation report states whether a system was designed or installed as required by a code *provision*, NIST has documentary or anecdotal evidence indicating whether the requirement was met, or NIST has independently conducted tests or analyses indicating whether the requirement was met.

<u>Use in Legal Proceedings</u>

No part of any report resulting from a NIST investigation into a structural failure or from an investigation under the National Construction Safety Team Act may be used in any suit or action for damages arising out of any matter mentioned in such report (15 USC 281a; as amended by P.L. 107-231).

National Institute of Standards and Technology National Construction Safety Team Act Report 1-3C
Natl. Inst. Stand. Technol. Natl. Constr. Sfty. Tm. Act Rpt. 1-3C, 532 pages (September 2005)
CODEN: NSPUE2

U.S. GOVERNMENT PRINTING OFFICE
WASHINGTON: 2005

_____

For sale by the Superintendent of Documents, U.S. Government Printing Office
Internet: bookstore.gpo.gov — Phone: (202) 512-1800 — Fax: (202) 512-2250
Mail: Stop SSOP, Washington, DC 20402-0001

ABSTRACT

This report describes damage characteristics, failure modes, and fire-related degradation of the recovered structural components from the World Trade Center (WTC) 1 and WTC 2. Assessment of the structural components was divided into pre- and post-collapse analysis. Pre-collapse analysis concentrated on impact damage sustained by the exterior panel sections, with assessment based solely upon photographic and video images. These images were also used to locate areas on the recovered and identified (i.e., known as-built location) panels with pre-collapse fire exposure. The second portion of the analysis focused on direct visual examination of the recovered steel elements. Of particular importance were the samples located near the airplane impacts (north face of WTC 1 and south face of WTC 2) and those where fire was known to exist prior to collapse of the buildings. Metallographic analysis of components with specific or unique damage patterns was also conducted. The findings of this report were used for validation of the modeling efforts in the baseline structural performance and aircraft impact damage analysis, the reconstruction of the thermal environment, and the structural fire response and collapse analysis. WTC 7 steel was not evaluated in this study of the tower damage and failure modes.

Keywords: Damage characteristics, failure analysis, failure modes, fire-related damage, steel, World Trade Center.

This page intentionally left blank.

TABLE OF CONTENTS

Chapter 8
References 285

Appendix A
Examples of Perimeter Panel Floor Truss Connectors 287

Appendix B
Recovered Perimeter Panel Floor Truss Connectors from Identified Panels ... 295

Appendix C
Recovered Core Floor Truss Connectors 417

Appendix D
Forensic Thermometry Technique Development 433

Appendix E
Paint Mapping Study of WTC Structural Elements 447

Appendix F
**Visual Observations of the Steel Recovered from the World Trade Center Site
Reported by Wiss, Janney, Elstner Associates, Inc. 455**

Appendix G
Summary and NIST Review of Appendix F 473

LIST OF FIGURES

LIST OF TABLES

LIST OF ACRONYMS AND ABBREVIATIONS

Acronyms

AISC	American Institute of Steel Construction
AISI	American Iron and Steel Institute
ASCE	American Society of Civil Engineers
ASTM	ASTM International
AWS	American Welding Society
BPAT	Building Performance Assessment Team
BPS	Building Performance Study
DTA	differential thermal analyzer
EDM	Electrical Discharge Machining
EDS	Energy Dispersive Spectroscopy
FCAW	Flux Cored Arc Welding
FDNY	New York City Fire Department
FEMA	Federal Emergency Management Agency
HAZ	heat affected zone
HLSA	High-strength, low alloy
JIS	Japan Industrial Standard
LERA	Leslie E. Robertson Associates
NIST	National Institute of Standards and Technology
NYPD	New York Police Department
PANYNJ	Port Authority of New York and New Jersey
PC&F	Pacific Car and Foundry
PONYA	Port of New York Authority
SEAoNY	Structural Engineers Association of New York
SFRM	sprayed fire-resistive material
SHCR	Skilling, Helle, Christiansen, & Robertson
SMAW	Shielded Metal Arc Welding
USC	United States Code
WF	wide flange (a type of structural steel shape now usually called a W-shape)

WJE	Wiss, Janney, Elstner Associates, Inc.
WTC	World Trade Center
WTC 1	World Trade Center 1 (North Tower)
WTC 2	World Trade Center 2 (South Tower)
WTC 7	World Trade Center 7

Abbreviations

°C	degrees Celsius
°F	degrees Fahrenheit
µm	micrometer
2D	two dimensional
3D	three dimensional
cm	centimeter
ft	foot
ft^2	square feet
Fe	iron
F_y	yield strength (AISC usage)
g	acceleration (gravity)
g	gram
gal	gallon
h	hour
in.	inch
kg	kilogram
kip	a force equal to 1,000 pounds
kJ	kilojoule
kN	kilonewton
kPa	kilopascal
klb	1,000 pounds
ksi	1,000 pounds per square inch
kW	kilowatt
kW/m^2	kilowatts per square meter
L	liter

NIST NCSTAR 1-3C, WTC Investigation

lb	pound
m	meter
m^2	square meter
mm	millimeter
Mn	magnesium
m/s	meters per second
min	minute
MJ	megajoule
MPa	megapascal
mph	miles per hour
ms	millisecond
Msi	millions of pounds per square inch
MW	megawatt
N	newton
Pa	pascal
pcf	pounds per cubic foot
plf	pounds per linear foot
psf	pounds per square foot
psi	pounds-force per square inch
s	second
yd	yard

This page intentionally left blank.

METRIC CONVERSION TABLE

To convert from	to	Multiply by
AREA AND SECOND MOMENT OF AREA		
square foot (ft^2)	square meter (m^2)	9.290 304 E-02
square inch (in.^{2})	square meter (m^2)	6.4516 E-04
square inch (in.^{2})	square centimeter (cm^2)	6.4516 E+00
square yard (yd^2)	square meter (m^2)	8.361 274 E-01
ENERGY (includes WORK)		
kilowatt hour (kW · h)	joule (J)	3.6 E+06
quad (1015 BtuIT)	joule (J)	1.055 056 E+18
therm (U.S.)	joule (J)	1.054 804 E+08
ton of TNT (energy equivalent)	joule (J)	4.184 E+09
watt hour (W · h)	joule (J)	3.6 E+03
watt second (W · s)	joule (J)	1.0 E+00
FORCE		
dyne (dyn)	newton (N)	1.0 E-05
kilogram-force (kgf)	newton (N)	9.806 65 E+00
kilopond (kilogram-force) (kp)	newton (N)	9.806 65 E+00
kip (1 kip=1000 lbf)	newton (N)	4.448 222 E+03
kip (1 kip=1000 lbf)	kilonewton (kN)	4.448 222 E+00
pound-force (lbf)	newton (N)	4.448 222 E+00
FORCE DIVIDED BY LENGTH		
pound-force per foot (lbf/ft)	newton per meter (N/m)	1.459 390 E+01
pound-force per inch (lbf/in)	newton per meter (N/m)	1.751 268 E+02
HEAT FLOW RATE		
calorieth per minute (calth/min)	watt (W)	6.973 333 E-02
calorieth per second (calth/s)	watt (W)	4.184 E+00
kilocalorieth per minute (kcalth/min)	watt (W)	6.973 333 E+01
kilocalorieth per second (kcalth/s)	watt (W)	4.184 E+03

To convert from	to	Multiply by
LENGTH		
foot (ft)	meter (m)	3.048 E-01
inch (in.)	meter (m)	2.54 E-02
inch (in.)	centimeter (cm)	2.54 E+00
micron (m)	meter (m)	1.0 E-06
yard (yd)	meter (m)	9.144 E-01
MASS and MOMENT OF INERTIA		
kilogram-force second squared per meter (kgf · s^2/m)	kilogram (kg)	9.806 65 E+00
pound foot squared (lb · ft^2)	kilogram meter squared (kg · m^2)	4.214 011 E-02
pound inch squared (lb · in^2)	kilogram meter squared (kg · m^2)	2.926 397 E-04
ton, metric (t)	kilogram (kg)	1.0 E+03
ton, short (2000 lb)	kilogram (kg)	9.071 847 E+02
MASS DIVIDED BY AREA		
pound per square foot (lb/ft^2)	kilogram per square meter (kg/m^2)	4.882 428 E+00
pound per square inch (not pound force) (lb/in^2)	kilogram per square meter (kg/m^2)	7.030 696 E+02
MASS DIVIDED BY LENGTH		
pound per foot (lb/ft)	kilogram per meter (kg/m)	1.488 164 E+00
pound per inch (lb/in.)	kilogram per meter (kg/m)	1.785 797 E+01
pound per yard (lb/yd)	kilogram per meter (kg/m)	4.960 546 E-01
PRESSURE or STRESS (FORCE DIVIDED BY AREA)		
kilogram-force per square centimeter (kgf/cm^2)	pascal (Pa)	9.806 65 E+04
kilogram-force per square meter (kgf/m^2)	pascal (Pa)	9.806 65 E+00
kilogram-force per square millimeter (kgf/mm^2)	pascal (Pa)	9.806 65 E+06
kip per square inch (ksi) (kip/in.^{2})	pascal (P)	6.894 757 E+06
kip per square inch (ksi) (kip/in.^{2})	kilopascal (kPa)	6.894 757 E+03
pound-force per square foot (lbf/ft^2)	pascal (Pa)	4.788 026 E+01
pound-force per square inch (psi) (lbf/in.^{2})	pascal (Pa)	6.894 757 E+03
pound-force per square inch (psi) (lbf/in.^{2})	kilopascal (kPa)	6.894 757 E+00
psi (pound-force per square inch) (lbf/in.^{2})	pascal (Pa)	6.894 757 E+03
psi (pound-force per square inch) (lbf/in.^{2})	kilopascal (kPa)	6.894 757 E+00

To convert from	to	Multiply by
TEMPERATURE		
degree Celsius (°C)	kelvin (K)	$T/K = t/°C + 273.15$
degree centigrade	degree Celsius (°C)	$t/°C \approx t$ /deg. cent.
degree Fahrenheit (°F)	degree Celsius (°C)	$t/°C = (t/°F\ 2\ 32)/1.8$
degree Fahrenheit (°F)	kelvin (K)	$T/K = (t/°F + 459.67)/1.8$
kelvin (K)	degree Celsius (°C)	$t/°C = T/K - 273.15$
TEMPERATURE INTERVAL		
degree Celsius (°C)	kelvin (K)	1.0
degree centigrade	gree Celsius (°C)	1.0 E+00
degree Fahrenheit (°F)	degree Celsius (°C)	555 556
degree Fahrenheit (°F)	lvin (K)	.555 556 E-01
degree Rankine (°R)	lvin (K)	.555 556 E-01
VELOCITY (includes SPEED)		
foot per second (ft/s)	ter per second (m/s)	3.048 E-01
inch per second (in/s)	ter per second (m/s)	2.54 E-02
kilometer per hour (km/h)	ter per second (m/s)	2.777 778 E-01
mile per hour (mi/h)	lometer per hour (km/h)	1.609 344
mile per minute (mi/min)	ter per second (m/s)	.682 24 E+01
VOLUME (includes CAPACITY)		
cubic foot (ft^3)	bic meter (m^3)	.831 685 E-02
cubic inch (in^3)	cubic meter (m^3)	1.638 706 E-05
cubic yard (yd^3)	cubic meter (m^3)	7.645 549 E-01
gallon (U.S.) (gal)	cubic meter (m^3)	3.785 412 E-03
gallon (U.S.) (gal)	liter (L)	3.785 412
liter (L)	cubic meter (m^3)	1000
ounce (U.S. fluid) (fl oz)	cubic meter (m^3)	2.957 353 E-05
ounce (U.S. fluid) (fl oz)	milliliter (mL)	2.957 353 E+01

This page intentionally left blank.

PREFACE

Genesis of This Investigation

Immediately following the terrorist attack on the World Trade Center (WTC) on September 11, 2001, the Federal Emergency Management Agency (FEMA) and the American Society of Civil Engineers began planning a building performance study of the disaster. The week of October 7, as soon as the rescue and search efforts ceased, the Building Performance Study Team went to the site and began its assessment. This was to be a brief effort, as the study team consisted of experts who largely volunteered their time away from their other professional commitments. The Building Performance Study Team issued its report in May 2002, fulfilling its goal "to determine probable failure mechanisms and to identify areas of future investigation that could lead to practical measures for improving the damage resistance of buildings against such unforeseen events."

On August 21, 2002, with funding from the U.S. Congress through FEMA, the National Institute of Standards and Technology (NIST) announced its building and fire safety investigation of the WTC disaster. On October 1, 2002, the National Construction Safety Team Act (Public Law 107-231), was signed into law. The NIST WTC Investigation was conducted under the authority of the National Construction Safety Team Act.

The goals of the investigation of the WTC disaster were:

- To investigate the building construction, the materials used, and the technical conditions that contributed to the outcome of the WTC disaster.

- To serve as the basis for:

    - Improvements in the way buildings are designed, constructed, maintained, and used;

    - Improved tools and guidance for industry and safety officials;

    - Recommended revisions to current codes, standards, and practices; and

    - Improved public safety.

The specific objectives were:

1. Determine why and how WTC 1 and WTC 2 collapsed following the initial impacts of the aircraft and why and how WTC 7 collapsed;

2. Determine why the injuries and fatalities were so high or low depending on location, including all technical aspects of fire protection, occupant behavior, evacuation, and emergency response;

3. Determine what procedures and practices were used in the design, construction, operation, and maintenance of WTC 1, 2, and 7; and

4. Identify, as specifically as possible, areas in current building and fire codes, standards, and practices that warrant revision.

NIST is a nonregulatory agency of the U.S. Department of Commerce's Technology Administration. The purpose of NIST investigations is to improve the safety and structural integrity of buildings in the United States, and the focus is on fact finding. NIST investigative teams are authorized to assess building performance and emergency response and evacuation procedures in the wake of any building failure that has resulted in substantial loss of life or that posed significant potential of substantial loss of life. NIST does not have the statutory authority to make findings of fault nor negligence by individuals or organizations. Further, no part of any report resulting from a NIST investigation into a building failure or from an investigation under the National Construction Safety Team Act may be used in any suit or action for damages arising out of any matter mentioned in such report (15 USC 281a, as amended by Public Law 107-231).

Organization of the Investigation

The National Construction Safety Team for this Investigation, appointed by the then NIST Director, Dr. Arden L. Bement, Jr., was led by Dr. S. Shyam Sunder. Dr. William L. Grosshandler served as Associate Lead Investigator, Mr. Stephen A. Cauffman served as Program Manager for Administration, and Mr. Harold E. Nelson served on the team as a private sector expert. The Investigation included eight interdependent projects whose leaders comprised the remainder of the team. A detailed description of each of these eight projects is available at http://wtc.nist.gov. The purpose of each project is summarized in Table P–1, and the key interdependencies among the projects are illustrated in Fig. P–1.

Table P–1. Federal building and fire safety investigation of the WTC disaster.

Technical Area and Project Leader	Project Purpose
Analysis of Building and Fire Codes and Practices; Project Leaders: Dr. H. S. Lew and Mr. Richard W. Bukowski	Document and analyze the code provisions, procedures, and practices used in the design, construction, operation, and maintenance of the structural, passive fire protection, and emergency access and evacuation systems of WTC 1, 2, and 7.
Baseline Structural Performance and Aircraft Impact Damage Analysis; Project Leader: Dr. Fahim H. Sadek	Analyze the baseline performance of WTC 1 and WTC 2 under design, service, and abnormal loads, and aircraft impact damage on the structural, fire protection, and egress systems.
Mechanical and Metallurgical Analysis of Structural Steel; Project Leader: Dr. Frank W. Gayle	Determine and analyze the mechanical and metallurgical properties and quality of steel, weldments, and connections from steel recovered from WTC 1, 2, and 7.
Investigation of Active Fire Protection Systems; Project Leader: Dr. David D. Evans; Dr. William Grosshandler	Investigate the performance of the active fire protection systems in WTC 1, 2, and 7 and their role in fire control, emergency response, and fate of occupants and responders.
Reconstruction of Thermal and Tenability Environment; Project Leader: Dr. Richard G. Gann	Reconstruct the time-evolving temperature, thermal environment, and smoke movement in WTC 1, 2, and 7 for use in evaluating the structural performance of the buildings and behavior and fate of occupants and responders.
Structural Fire Response and Collapse Analysis; Project Leaders: Dr. John L. Gross and Dr. Therese P. McAllister	Analyze the response of the WTC towers to fires with and without aircraft damage, the response of WTC 7 in fires, the performance of composite steel-trussed floor systems, and determine the most probable structural collapse sequence for WTC 1, 2, and 7.
Occupant Behavior, Egress, and Emergency Communications; Project Leader: Mr. Jason D. Averill	Analyze the behavior and fate of occupants and responders, both those who survived and those who did not, and the performance of the evacuation system.
Emergency Response Technologies and Guidelines; Project Leader: Mr. J. Randall Lawson	Document the activities of the emergency responders from the time of the terrorist attacks on WTC 1 and WTC 2 until the collapse of WTC 7, including practices followed and technologies used.
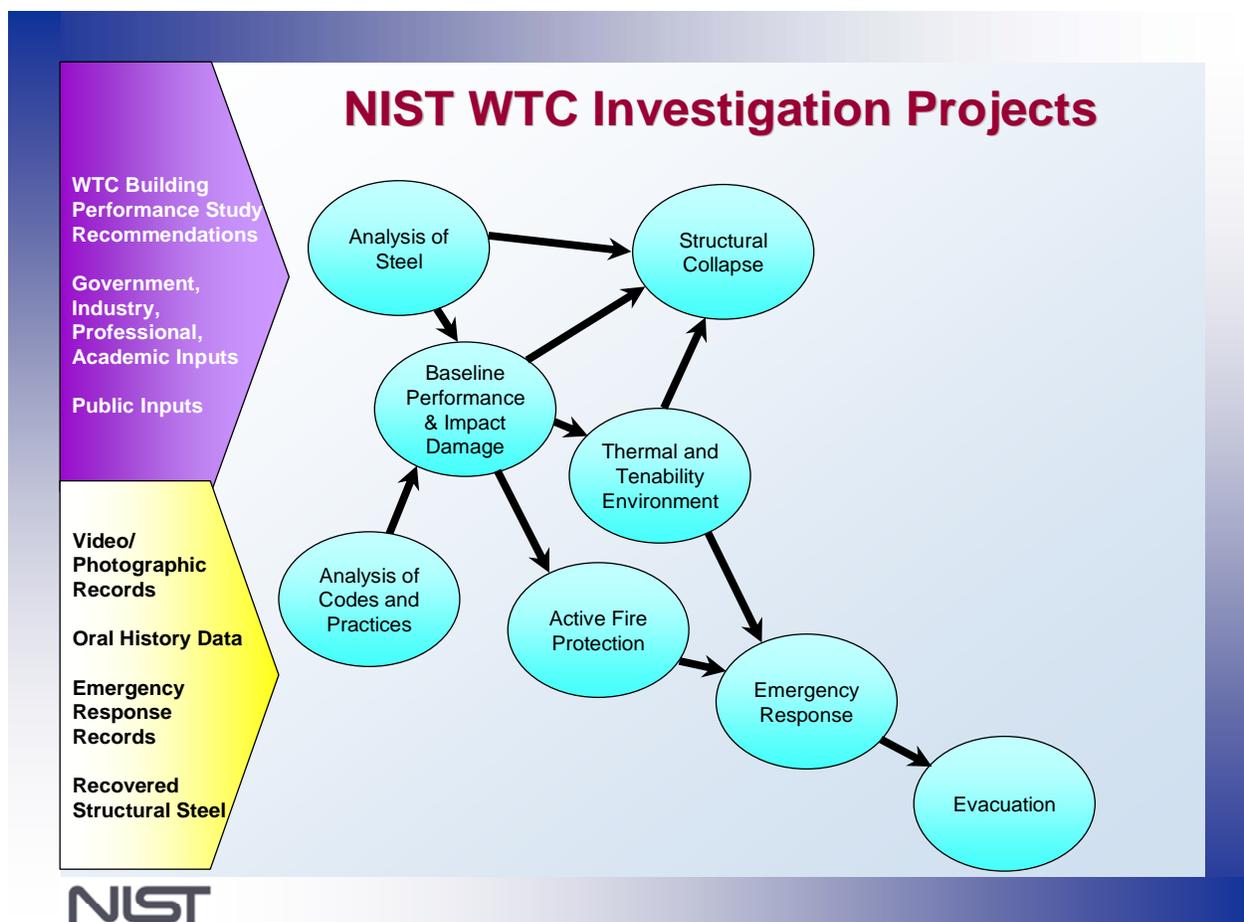
Figure P–1. The eight projects in the federal building and fire safety investigation of the WTC disaster.

National Construction Safety Team Advisory Committee

The NIST Director also established an advisory committee as mandated under the National Construction Safety Team Act. The initial members of the committee were appointed following a public solicitation. These were:

- Paul Fitzgerald, Executive Vice President (retired) FM Global, National Construction Safety Team Advisory Committee Chair

- John Barsom, President, Barsom Consulting, Ltd.

- John Bryan, Professor Emeritus, University of Maryland

- David Collins, President, The Preview Group, Inc.

- Glenn Corbett, Professor, John Jay College of Criminal Justice

- Philip DiNenno, President, Hughes Associates, Inc.

- Robert Hanson, Professor Emeritus, University of Michigan

- Charles Thornton, Co-Chairman and Managing Principal, The Thornton-Tomasetti Group, Inc.

- Kathleen Tierney, Director, Natural Hazards Research and Applications Information Center, University of Colorado at Boulder

- Forman Williams, Director, Center for Energy Research, University of California at San Diego

This National Construction Safety Team Advisory Committee provided technical advice during the Investigation and commentary on drafts of the Investigation reports prior to their public release. NIST has benefited from the work of many people in the preparation of these reports, including the National Construction Safety Team Advisory Committee. The content of the reports and recommendations, however, are solely the responsibility of NIST.

Public Outreach

During the course of this Investigation, NIST held public briefings and meetings (listed in Table P–2) to solicit input from the public, present preliminary findings, and obtain comments on the direction and progress of the Investigation from the public and the Advisory Committee.

NIST maintained a publicly accessible Web site during this Investigation at http://wtc.nist.gov. The site contained extensive information on the background and progress of the Investigation.

NIST's WTC Public-Private Response Plan

The collapse of the WTC buildings has led to broad reexamination of how tall buildings are designed, constructed, maintained, and used, especially with regard to major events such as fires, natural disasters, and terrorist attacks. Reflecting the enhanced interest in effecting necessary change, NIST, with support from Congress and the Administration, has put in place a program, the goal of which is to develop and implement the standards, technology, and practices needed for cost-effective improvements to the safety and security of buildings and building occupants, including evacuation, emergency response procedures, and threat mitigation.

The strategy to meet this goal is a three-part NIST-led public-private response program that includes:

- A federal building and fire safety investigation to study the most probable factors that contributed to post-aircraft impact collapse of the WTC towers and the 47-story WTC 7 building, and the associated evacuation and emergency response experience.

- A research and development (R&D) program to (a) facilitate the implementation of recommendations resulting from the WTC Investigation, and (b) provide the technical basis for cost-effective improvements to national building and fire codes, standards, and practices that enhance the safety of buildings, their occupants, and emergency responders.

Table P–2. Public meetings and briefings of the WTC Investigation.

Date	Location	Principal Agenda
June 24, 2002	New York City, NY	Public meeting: Public comments on the *Draft Plan* for the pending WTC Investigation.
August 21, 2002	Gaithersburg, MD	Media briefing announcing the formal start of the Investigation.
December 9, 2002	Washington, DC	Media briefing on release of the *Public Update* and NIST request for photographs and videos.
April 8, 2003	New York City, NY	Joint public forum with Columbia University on first-person interviews.
April 29–30, 2003	Gaithersburg, MD	NCST Advisory Committee meeting on plan for and progress on WTC Investigation with a public comment session.
May 7, 2003	New York City, NY	Media briefing on release of *May 2003 Progress Report.*
August 26–27, 2003	Gaithersburg, MD	NCST Advisory Committee meeting on status of the WTC investigation with a public comment session.
September 17, 2003	New York City, NY	Media and public briefing on initiation of first-person data collection projects.
December 2–3, 2003	Gaithersburg, MD	NCST Advisory Committee meeting on status and initial results and release of the *Public Update* with a public comment session.
February 12, 2004	New York City, NY	Public meeting on progress and preliminary findings with public comments on issues to be considered in formulating final recommendations.
June 18, 2004	New York City, NY	Media/public briefing on release of *June 2004 Progress Report.*
June 22–23, 2004	Gaithersburg, MD	NCST Advisory Committee meeting on the status of and preliminary findings from the WTC Investigation with a public comment session.
August 24, 2004	Northbrook, IL	Public viewing of standard fire resistance test of WTC floor system at Underwriters Laboratories, Inc.
October 19–20, 2004	Gaithersburg, MD	NCST Advisory Committee meeting on status and near complete set of preliminary findings with a public comment session.
November 22, 2004	Gaithersburg, MD	NCST Advisory Committee discussion on draft annual report to Congress, a public comment session, and a closed session to discuss pre-draft recommendations for WTC Investigation.
April 5, 2005	New York City, NY	Media and public briefing on release of the probable collapse sequence for the WTC towers and draft reports for the projects on codes and practices, evacuation, and emergency response.
June 23, 2005	New York City, NY	Media and public briefing on release of all draft reports for the WTC towers and draft recommendations for public comment.
September 12–13, 2005	Gaithersburg, MD	NCST Advisory Committee meeting on disposition of public comments and update to draft reports for the WTC towers.
September 13–15, 2005	Gaithersburg, MD	WTC Technical Conference for stakeholders and technical community for dissemination of findings and recommendations and opportunity for public to make technical comments.

- A dissemination and technical assistance program (DTAP) to (a) engage leaders of the construction and building community in ensuring timely adoption and widespread use of proposed changes to practices, standards, and codes resulting from the WTC Investigation and the R&D program, and (b) provide practical guidance and tools to better prepare facility owners, contractors, architects, engineers, emergency responders, and regulatory authorities to respond to future disasters.

The desired outcomes are to make buildings, occupants, and first responders safer in future disaster events.

National Construction Safety Team Reports on the WTC Investigation

A final report on the collapse of the WTC towers is being issued as NIST NCSTAR 1. A companion report on the collapse of WTC 7 is being issued as NIST NCSTAR 1A. The present report is one of a set that provides more detailed documentation of the Investigation findings and the means by which these technical results were achieved. As such, it is part of the archival record of this Investigation. The titles of the full set of Investigation publications are:

NIST (National Institute of Standards and Technology). 2005. *Federal Building and Fire Safety Investigation of the World Trade Center Disaster: Final Report on the Collapse of the World Trade Center Towers.* NIST NCSTAR 1. Gaithersburg, MD, September.

NIST (National Institute of Standards and Technology). 2008. *Federal Building and Fire Safety Investigation of the World Trade Center Disaster: Final Report on the Collapse of World Trade Center 7.* NIST NCSTAR 1A. Gaithersburg, MD, November.

Lew, H. S., R. W. Bukowski, and N. J. Carino. 2005. *Federal Building and Fire Safety Investigation of the World Trade Center Disaster: Design, Construction, and Maintenance of Structural and Life Safety Systems.* NIST NCSTAR 1-1. National Institute of Standards and Technology. Gaithersburg, MD, September.

> Fanella, D. A., A. T. Derecho, and S. K. Ghosh. 2005. *Federal Building and Fire Safety Investigation of the World Trade Center Disaster: Design and Construction of Structural Systems.* NIST NCSTAR 1-1A. National Institute of Standards and Technology. Gaithersburg, MD, September.

> Ghosh, S. K., and X. Liang. 2005. *Federal Building and Fire Safety Investigation of the World Trade Center Disaster: Comparison of Building Code Structural Requirements.* NIST NCSTAR 1-1B. National Institute of Standards and Technology. Gaithersburg, MD, September.

> Fanella, D. A., A. T. Derecho, and S. K. Ghosh. 2005. *Federal Building and Fire Safety Investigation of the World Trade Center Disaster: Maintenance and Modifications to Structural Systems.* NIST NCSTAR 1-1C. National Institute of Standards and Technology. Gaithersburg, MD, September.

> Grill, R. A., and D. A. Johnson. 2005. *Federal Building and Fire Safety Investigation of the World Trade Center Disaster: Fire Protection and Life Safety Provisions Applied to the Design and Construction of World Trade Center 1, 2, and 7 and Post-Construction Provisions Applied after Occupancy.* NIST NCSTAR 1-1D. National Institute of Standards and Technology. Gaithersburg, MD, September.

> Razza, J. C., and R. A. Grill. 2005. *Federal Building and Fire Safety Investigation of the World Trade Center Disaster: Comparison of Codes, Standards, and Practices in Use at the Time of the Design and Construction of World Trade Center 1, 2, and 7.* NIST NCSTAR 1-1E. National Institute of Standards and Technology. Gaithersburg, MD, September.

> Grill, R. A., D. A. Johnson, and D. A. Fanella. 2005. *Federal Building and Fire Safety Investigation of the World Trade Center Disaster: Comparison of the 1968 and Current (2003) New*

York City Building Code Provisions. NIST NCSTAR 1-1F. National Institute of Standards and Technology. Gaithersburg, MD, September.

Grill, R. A., and D. A. Johnson. 2005. *Federal Building and Fire Safety Investigation of the World Trade Center Disaster: Amendments to the Fire Protection and Life Safety Provisions of the New York City Building Code by Local Laws Adopted While World Trade Center 1, 2, and 7 Were in Use.* NIST NCSTAR 1-1G. National Institute of Standards and Technology. Gaithersburg, MD, September.

Grill, R. A., and D. A. Johnson. 2005. *Federal Building and Fire Safety Investigation of the World Trade Center Disaster: Post-Construction Modifications to Fire Protection and Life Safety Systems of World Trade Center 1 and 2.* NIST NCSTAR 1-1H. National Institute of Standards and Technology. Gaithersburg, MD, September.

Grill, R. A., D. A. Johnson, and D. A. Fanella. 2005. *Federal Building and Fire Safety Investigation of the World Trade Center Disaster: Post-Construction Modifications to Fire Protection, Life Safety, and Structural Systems of World Trade Center 7.* NIST NCSTAR 1-1I. National Institute of Standards and Technology. Gaithersburg, MD, September.

Grill, R. A., and D. A. Johnson. 2005. *Federal Building and Fire Safety Investigation of the World Trade Center Disaster: Design, Installation, and Operation of Fuel System for Emergency Power in World Trade Center 7.* NIST NCSTAR 1-1J. National Institute of Standards and Technology. Gaithersburg, MD, September.

Sadek, F. 2005. *Federal Building and Fire Safety Investigation of the World Trade Center Disaster: Baseline Structural Performance and Aircraft Impact Damage Analysis of the World Trade Center Towers.* NIST NCSTAR 1-2. National Institute of Standards and Technology. Gaithersburg, MD, September.

Faschan, W. J., and R. B. Garlock. 2005. *Federal Building and Fire Safety Investigation of the World Trade Center Disaster: Reference Structural Models and Baseline Performance Analysis of the World Trade Center Towers.* NIST NCSTAR 1-2A. National Institute of Standards and Technology. Gaithersburg, MD, September.

Kirkpatrick, S. W., R. T. Bocchieri, F. Sadek, R. A. MacNeill, S. Holmes, B. D. Peterson, R. W. Cilke, C. Navarro. 2005. *Federal Building and Fire Safety Investigation of the World Trade Center Disaster: Analysis of Aircraft Impacts into the World Trade Center Towers,* NIST NCSTAR 1-2B. National Institute of Standards and Technology. Gaithersburg, MD, September.

Gayle, F. W., R. J. Fields, W. E. Luecke, S. W. Banovic, T. Foecke, C. N. McCowan, T. A. Siewert, and J. D. McColskey. 2005. *Federal Building and Fire Safety Investigation of the World Trade Center Disaster: Mechanical and Metallurgical Analysis of Structural Steel.* NIST NCSTAR 1-3. National Institute of Standards and Technology. Gaithersburg, MD, September.

Luecke, W. E., T. A. Siewert, and F. W. Gayle. 2005. *Federal Building and Fire Safety Investigation of the World Trade Center Disaster: Contemporaneous Structural Steel Specifications.* NIST Special Publication 1-3A. National Institute of Standards and Technology. Gaithersburg, MD, September.

Banovic, S. W. 2005. *Federal Building and Fire Safety Investigation of the World Trade Center Disaster: Steel Inventory and Identification.* NIST NCSTAR 1-3B. National Institute of Standards and Technology. Gaithersburg, MD, September.

Banovic, S. W., and T. Foecke. 2005. *Federal Building and Fire Safety Investigation of the World Trade Center Disaster: Damage and Failure Modes of Structural Steel Components.* NIST NCSTAR 1-3C. National Institute of Standards and Technology. Gaithersburg, MD, September.

Luecke, W. E., J. D. McColskey, C. N. McCowan, S. W. Banovic, R. J. Fields, T. Foecke, T. A. Siewert, and F. W. Gayle. 2005. *Federal Building and Fire Safety Investigation of the World Trade Center Disaster: Mechanical Properties of Structural Steels.* NIST NCSTAR 1-3D. National Institute of Standards and Technology. Gaithersburg, MD, September.

Banovic, S. W., C. N. McCowan, and W. E. Luecke. 2005. *Federal Building and Fire Safety Investigation of the World Trade Center Disaster: Physical Properties of Structural Steels.* NIST NCSTAR 1-3E. National Institute of Standards and Technology. Gaithersburg, MD, September.

Evans, D. D., R. D. Peacock, E. D. Kuligowski, W. S. Dols, and W. L. Grosshandler. 2005. *Federal Building and Fire Safety Investigation of the World Trade Center Disaster: Active Fire Protection Systems.* NIST NCSTAR 1-4. National Institute of Standards and Technology. Gaithersburg, MD, September.

Kuligowski, E. D., D. D. Evans, and R. D. Peacock. 2005. *Federal Building and Fire Safety Investigation of the World Trade Center Disaster: Post-Construction Fires Prior to September 11, 2001.* NIST NCSTAR 1-4A. National Institute of Standards and Technology. Gaithersburg, MD, September.

Hopkins, M., J. Schoenrock, and E. Budnick. 2005. *Federal Building and Fire Safety Investigation of the World Trade Center Disaster: Fire Suppression Systems.* NIST NCSTAR 1-4B. National Institute of Standards and Technology. Gaithersburg, MD, September.

Keough, R. J., and R. A. Grill. 2005. *Federal Building and Fire Safety Investigation of the World Trade Center Disaster: Fire Alarm Systems.* NIST NCSTAR 1-4C. National Institute of Standards and Technology. Gaithersburg, MD, September.

Ferreira, M. J., and S. M. Strege. 2005. *Federal Building and Fire Safety Investigation of the World Trade Center Disaster: Smoke Management Systems.* NIST NCSTAR 1-4D. National Institute of Standards and Technology. Gaithersburg, MD, September.

Gann, R. G., A. Hamins, K. B. McGrattan, G. W. Mulholland, H. E. Nelson, T. J. Ohlemiller, W. M. Pitts, and K. R. Prasad. 2005. *Federal Building and Fire Safety Investigation of the World Trade Center Disaster: Reconstruction of the Fires in the World Trade Center Towers.* NIST NCSTAR 1-5. National Institute of Standards and Technology. Gaithersburg, MD, September.

Pitts, W. M., K. M. Butler, and V. Junker. 2005. *Federal Building and Fire Safety Investigation of the World Trade Center Disaster: Visual Evidence, Damage Estimates, and Timeline Analysis.* NIST NCSTAR 1-5A. National Institute of Standards and Technology. Gaithersburg, MD, September.

Hamins, A., A. Maranghides, K. B. McGrattan, E. Johnsson, T. J. Ohlemiller, M. Donnelly, J. Yang, G. Mulholland, K. R. Prasad, S. Kukuck, R. Anleitner and T. McAllister. 2005. *Federal Building and Fire Safety Investigation of the World Trade Center Disaster: Experiments and Modeling of Structural Steel Elements Exposed to Fire.* NIST NCSTAR 1-5B. National Institute of Standards and Technology. Gaithersburg, MD, September.

Ohlemiller, T. J., G. W. Mulholland, A. Maranghides, J. J. Filliben, and R. G. Gann. 2005. *Federal Building and Fire Safety Investigation of the World Trade Center Disaster: Fire Tests of Single Office Workstations.* NIST NCSTAR 1-5C. National Institute of Standards and Technology. Gaithersburg, MD, September.

Gann, R. G., M. A. Riley, J. M. Repp, A. S. Whittaker, A. M. Reinhorn, and P. A. Hough. 2005. *Federal Building and Fire Safety Investigation of the World Trade Center Disaster: Reaction of Ceiling Tile Systems to Shocks.* NIST NCSTAR 1-5D. National Institute of Standards and Technology. Gaithersburg, MD, September.

Hamins, A., A. Maranghides, K. B. McGrattan, T. J. Ohlemiller, and R. Anleitner. 2005. *Federal Building and Fire Safety Investigation of the World Trade Center Disaster: Experiments and Modeling of Multiple Workstations Burning in a Compartment.* NIST NCSTAR 1-5E. National Institute of Standards and Technology. Gaithersburg, MD, September.

McGrattan, K. B., C. Bouldin, and G. Forney. 2005. *Federal Building and Fire Safety Investigation of the World Trade Center Disaster: Computer Simulation of the Fires in the World Trade Center Towers.* NIST NCSTAR 1-5F. National Institute of Standards and Technology. Gaithersburg, MD, September.

Prasad, K. R., and H. R. Baum. 2005. *Federal Building and Fire Safety Investigation of the World Trade Center Disaster: Fire Structure Interface and Thermal Response of the World Trade Center Towers.* NIST NCSTAR 1-5G. National Institute of Standards and Technology. Gaithersburg, MD, September.

Gross, J. L., and T. McAllister. 2005. *Federal Building and Fire Safety Investigation of the World Trade Center Disaster: Structural Fire Response and Probable Collapse Sequence of the World Trade Center Towers.* NIST NCSTAR 1-6. National Institute of Standards and Technology. Gaithersburg, MD, September.

Carino, N. J., M. A. Starnes, J. L. Gross, J. C. Yang, S. Kukuck, K. R. Prasad, and R. W. Bukowski. 2005. *Federal Building and Fire Safety Investigation of the World Trade Center Disaster: Passive Fire Protection.* NIST NCSTAR 1-6A. National Institute of Standards and Technology. Gaithersburg, MD, September.

Gross, J., F. Hervey, M. Izydorek, J. Mammoser, and J. Treadway. 2005. *Federal Building and Fire Safety Investigation of the World Trade Center Disaster: Fire Resistance Tests of Floor Truss Systems.* NIST NCSTAR 1-6B. National Institute of Standards and Technology. Gaithersburg, MD, September.

Zarghamee, M. S., S. Bolourchi, D. W. Eggers, Ö. O. Erbay, F. W. Kan, Y. Kitane, A. A. Liepins, M. Mudlock, W. I. Naguib, R. P. Ojdrovic, A. T. Sarawit, P. R Barrett, J. L. Gross, and

T. P. McAllister. 2005. *Federal Building and Fire Safety Investigation of the World Trade Center Disaster: Component, Connection, and Subsystem Structural Analysis.* NIST NCSTAR 1-6C. National Institute of Standards and Technology. Gaithersburg, MD, September.

Zarghamee, M. S., Y. Kitane, Ö. O. Erbay, T. P. McAllister, and J. L. Gross. 2005. *Federal Building and Fire Safety Investigation of the World Trade Center Disaster: Global Structural Analysis of the Response of the World Trade Center Towers to Impact Damage and Fire.* NIST NCSTAR 1-6D. National Institute of Standards and Technology. Gaithersburg, MD, September.

Averill, J. D., D. S. Mileti, R. D. Peacock, E. D. Kuligowski, N. Groner, G. Proulx, P. A. Reneke, and H. E. Nelson. 2005. *Federal Building and Fire Safety Investigation of the World Trade Center Disaster: Occupant Behavior, Egress, and Emergency Communication.* NIST NCSTAR 1-7. National Institute of Standards and Technology. Gaithersburg, MD, September.

Fahy, R., and G. Proulx. 2005. *Federal Building and Fire Safety Investigation of the World Trade Center Disaster: Analysis of Published Accounts of the World Trade Center Evacuation.* NIST NCSTAR 1-7A. National Institute of Standards and Technology. Gaithersburg, MD, September.

Zmud, J. 2005. *Federal Building and Fire Safety Investigation of the World Trade Center Disaster: Technical Documentation for Survey Administration.* NIST NCSTAR 1-7B. National Institute of Standards and Technology. Gaithersburg, MD, September.

Lawson, J. R., and R. L. Vettori. 2005. *Federal Building and Fire Safety Investigation of the World Trade Center Disaster: The Emergency Response Operations.* NIST NCSTAR 1-8. National Institute of Standards and Technology. Gaithersburg, MD, September.

McAllister, T., R. G. Gann, J. D. Averill, J. L. Gross, W. L. Grosshandler, J. R. Lawson, K. B. McGrattan, H. E. Nelson, W. M. Pitts, K. R. Prasad, F. H. Sadek. 2008. *Federal Building and Fire Safety Investigation of the World Trade Center Disaster: Structural Fire Response and Probable Collapse Sequence of World Trade Center Building 7.* NIST NCSTAR 1-9. National Institute of Standards and Technology. Gaithersburg, MD, November.

MacNeill, R., S. Kirkpatrick, B. Peterson, and R. Bocchieri. 2008. *Federal Building and Fire Safety Investigation of the World Trade Center Disaster: Global Structural Analysis of the Response of World Trade Center Building 7 to Fires and Debris Impact Damage.* NIST NCSTAR 1-9A. National Institute of Standards and Technology. Gaithersburg, MD, November.

ACKNOWLEDGMENTS

This page intentionally left blank.

EXECUTIVE SUMMARY

E.1   INTRODUCTION

This report describes damage characteristics, failure modes, and fire-related degradation of the recovered structural components from the World Trade Center (WTC) towers. Knowledge of damage sustained by the steel elements plays an important role in the investigation by:

1. Helping ascertain the response of the structural steel of the towers to the impact of the aircrafts, and

2. Providing guidance and validation for models in the investigation involving impact damage, dynamics of the fires in the towers, and the thermal response and collapse of the towers.

Analysis of the structural elements was divided into two sections. Pre-collapse analysis concentrated on impact damage sustained by the exterior panel sections, with assessment based solely upon photographic and video images. These images were also used to locate areas on the recovered and identified (i.e., known as-built location) panels with pre-collapse fire exposure. The second analysis focused on direct visual examination of the recovered steel elements. Of particular importance were the samples located near the airplane impacts (north face of WTC 1 and south face of WTC 2) and those where fire was known to exist prior to collapse of the buildings. Metallographic analysis of components with specific or unique damage patterns was conducted. Sprayed fire-resistive material and building response to fire were analyzed

In support of this task, Wiss, Janney, Elstner Associates, Inc. (WJE) was retained to perform two tasks: (1) provide independent identification of recovered steel of particular interest to the furtherance of other tasks under this project; and (2) through unaided visual examination, identify and describe the various failure mechanisms and damage types observed on the recovered structural steel members. WJE team members surveyed and documented possible local failure mechanisms from a structural engineering perspective on exterior panels, core columns, floor trusses, and structural connections (spandrel splice plates, floor truss seat connectors). The complete report can be found in Appendix F with a summary of the main observations and NIST review of the contractor report in Appendix G.

WTC 7 steel was not evaluated in this study of the tower damage and failure modes.

E.2   STRUCTURAL DAMAGE AS A RESULT OF AIRPLANE IMPACT – PERIMETER PANELS

Analysis of enhanced photographs taken of the impact hole in WTC 1 allowed for the identification of about 95 percent of the modes of failure for the exterior wall columns damaged in the collision. Gross

deformation behavior observed from the photographs, coupled with analysis of the recovered steel, included:

- Whole exterior panels pushed inside the envelope of the building as a result of column connection bolt failures in the area of fuselage impact;

- Individual perimeter columns torn in a tensile mode surrounding the area of fuselage impact;

- Individual perimeter columns sliced through with little disturbance of surrounding material in areas where engines, heavier sections of the wings, and wing sections containing fuel impacted; and

- Minor damage to individual perimeter columns where lighter airplane components (e.g., wing tips) impacted and sieved through the panel openings.

Of the five panels recovered from the impact zone of WTC 1, four were directly hit by the airplane. Correlation between pre-collapse photographs and the recovered panels from the impact zone indicates that two of the four recovered impact-damaged panels (M-2 and M-30) were in a condition similar to that just prior to building collapse. Some damage can be attributed to the events during and after collapse, but the shape and appearance of the recovered pieces generally match the damage photographs. There was a lack of detailed pre-collapse visual evidence of the impact damage sustained by panels M-27 and S-9, and it was not possible to make such a comparison. The lower portion of panel N-7 did incur some damage; however, it could not be positively correlated with pre-collapse images.

The number and particularly the resolution of the photos taken of the damage to WTC 2 were much less than those available for the analysis of WTC 1, allowing identification of only 70 percent of the exterior column failure modes. Gross deformation behavior was similar to that observed for WTC 1. In addition, failures of exterior columns due to impact by aircraft components and debris that had passed through the building and exited on the opposite side were characterized.

Of particular interest was the fracture behavior of the plates composing the recovered columns that were directly impacted by the airplane. Fractures of the outer webs of panels M-30 and S-9 exhibited ductile behavior, including necking and thinning away from the fracture, indicating that the steel behaved ductilely under very high strain rates.

Conversely, fractures occurring parallel and directly next to welded joints exhibited few or no ductile characteristics. The geometry of the joint with respect to the direction of impact, stress concentrations due to the geometry, diminished properties of the heat-affected zone in the base metal, and the orientation of the crack propagation with respect to the rolling direction of the plate are expected to have contributed to the lack of ductility. There was no evidence to indicate that the type of joining method, materials, or welding procedures were improper. The welds appeared to perform as intended.

In general, severing of the perimeter columns hit by the heavier sections of the aircraft occurred at the internal stiffener plates or diaphragm plates (associated with the spandrel connection to column). There was a tendency for the columns hit by the plane to fracture along heat-affected zones adjacent to welds. This behavior was not observed for columns outside the impact zone.

E.3   STRUCTURAL DAMAGE AS A RESULT OF AIRPLANE IMPACT - CORE COLUMNS

Failure of the limited number (three) of recovered core columns in the impact zone was a result of both splice connection failures and fracture of the columns themselves. One recovered core column (WTC 2, column line 801, floors 77 through 80) may have sustained damage as a direct result of the airplane impact in terms of a flange bent in a direction consistent with the travel of the airplane. However, the welded splice connection to the column above survived intact.

E.4   DAMAGE TO SPRAYED FIRE-RESISTIVE MATERIAL AS A RESULT OF AIRPLANE IMPACT

Damage to sprayed fire-resistive material on the perimeter columns was examined in pre-collapse photographs. As expected, sprayed fire-resistive material was removed from pieces struck by the incoming aircraft or debris exiting the far side of the buildings. In addition, the impact caused sprayed fire-resistive material and aluminum facade panels to spall off many perimeter columns, which were not directly struck nor severed, but apparently suffered strong accelerations and forces otherwise transmitted through the structure.

A band of white features was apparent on the sprayed fire-resistive material wherever two aluminum panels met on the exterior columns of the buildings, becoming visible when the panels were dislodged. This appears to be a coating applied to protect the SFRM from moisture infiltration at the aluminum panel joints. This coating appears to have prevented the loss of SFRM in a number of locations where the SFRM was knocked off both above and below this location.

E.5   FIRE EXPOSURE AND TEMPERATURES REACHED BY THE STEEL

The pre-collapse photographic analysis showed that 16 recovered exterior panels were exposed to fire prior to collapse of WTC 1. None of the nine recovered panels from within the fire floors of WTC 2 were observed to have been directly exposed.

A method was developed using microscopic observations of paint cracking to determine whether steel members had experienced temperatures in excess of 250 °C. More than 170 areas were examined on 21 exterior panels. Note that these 21 panels represent only about 3 percent of the panels from fire-involved floors, and that results on these panels cannot be considered indicative of exposure of other panels. Only three locations had a positive result indicating that the steel and paint may have reached temperatures in excess of 250 °C (note that exposure could have occurred pre- or post-collapse). These areas were:

- WTC 1, east face, floor 98, column 210, inner web;

- WTC 1, east face, floor 92, column 236, spandrel; and

- WTC 1, north face, floor 98, column 143, floor truss connector.

Annealing studies on recovered steels (from NIST NCSTAR 1-3E[1]) established the set of time and temperature conditions necessary to alter the steel microstructure. The microstructures of steels known to have been exposed to fire, based on the pre-collapse photographic evidence, were characterized. These microstructures show no evidence of exposure to temperatures above 600 °C for any significant time.

Perimeter columns exposed to pre-collapse fire (determined from pre-collapse photographs) had a greater tendency for local buckling of the inner web; a similar correlation did not exist for fracture in the base metal near welds.

In the two buildings, there were 329 core columns (each three stories tall) traversing floors involved in fires. NIST has portions of four of these columns, and on average about half of each column was recovered. While these pieces allow some comparison of metal and paint condition with the predications of the fire model, the recovered steel represents less than one percent of all the core columns intersecting floors with fire. Thus, the forensic analysis indicating moderate temperature excursions in the recovered core columns does not, and cannot, give a picture of temperatures seen by the vast majority of the core columns.

E.6   TIME-DEPENDENT DEFORMATION OF PERIMETER WALLS DUE TO FIRE AND LOAD REDISTRIBUTION

Images of WTC 1 showed gross deformations of an exterior wall prior to final collapse. Images of the south face of the tower taken approximately 5 min prior to collapse showed inward bowing of the exterior columns, reaching an observable maximum of 55 in. near column 316 on the 96th floor. The inward deflection appears to extend over the entire south face of the building at this time and is visible vertically between the 94th and 100th floors. Photographs taken approximately 30 min prior to this time do not show any inward bowing of the south face of WTC 1.

Images of WTC 2 revealed some details of how the building deformed during the time between aircraft impact and collapse and revealed how the portion of the building above the impact zone moved relative to the bottom of the building during initial stages of collapse. Approximately 18 min after the impact of the aircraft, the east face of WTC 2 exhibited inward bowing of up to 10 in. in the region of the 79th to 83rd floors. This inward bowing increased to 20 in. at a time 5 min before collapse of the tower.

Hanging floor slabs at the 82nd and 83rd floors were visible in window openings on the east and north faces, respectively, and the positions of these slabs changed over time, suggesting a slow collapse mechanism of certain parts of the flooring in this area of the tower.

At the moment of collapse of WTC 2, the top portion of the building moved to the west as it tilted to the southeast. During this tilting, a complex kink developed at the southeast corner of the top portion in the region of the 106th floor. In addition, the top portion twisted slightly clockwise (as viewed from the top) as the collapse progressed.

---

[1] This reference is to one of the companion documents from this Investigation. A list of these documents appears in the Preface to this report.

E.7 STRUCTURAL DAMAGE AND FAILURES AS A RESULT OF COLLAPSE

The failure mode of spandrel connections on perimeter panels differed above and below the impact zone. Spandrel connections on exterior panels at or above the impact zone were more likely to experience bolt hole tear out as a failure mode. For those exterior panels below the impact zone, there was a higher propensity for portions of the spandrels to be torn from the panels. There did not appear to be any difference in failure mode for the spandrel connections whether the exterior panels were exposed to fire or not.

With the exception of the mechanical floors, the major failure mechanism concerning perimeter panel column splices was fracture of the bolts. At mechanical floors, where column splices were welded in addition to being bolted, the majority of the splices did not fail, rather the web and flange plates composing the columns fractured near the splice.

The damage to truss seats on perimeter panels differed above and below the impact zone. The majority of perimeter panel floor truss connectors (perimeter seats) below the impact floors were either missing or bent downward. Above this level, the failure modes were more randomly distributed. This trend was observed for both towers.

Failure of the perimeter panel floor truss seats typically occurred in the heat-affected zones near welds, and the fracture location was associated with the weld geometry (i.e., in the component with the lowest cross-sectional area). These areas with the lowest cross-sectional area were typically the standoff plates. However, there was no evidence to indicate that the type of joining method, materials, or welding procedures were improper.

Of the 31 core floor truss connectors (core truss seats) recovered, 90 percent were still intact though extensive damage may have occurred. Only two were observed to have been completely torn from the channel. (This distribution may have resulted from the selection process at the salvage yards).

In the floor trusses, failure of a large majority of the electric resistance welds at the web-to-chord connections was observed. Failure of the connection between the floor truss and the perimeter panel floor truss connectors was typically a result of gusset plate (attached to top truss chord) weld and bolt failure.

E.8 STRUCTURAL STEEL IN IMPACT ZONE

Though representative examples of all strength/gauge combinations of steel plate used to fabricate the exterior panels from the impact regions of the towers have not been recovered, numerous gauges for all 12 specified grades of steel used for the perimeter panels have been recovered. Of the 28 different strength/gauge combinations for plates composing the perimeter columns in the impact region of both towers, NIST has recovered representative samples for 14. Of the 14 unrecovered strength/gauge combinations, 10 combinations had gauges very close to those in the NIST inventory (within 0.0625 in.), while three were 0.125 in. away, and one combination had a difference of 0.1875 in. Similarly, seven of the thirteen strength/gauge combinations used for the spandrel plates in the impact region were recovered. All six of these missing strength/gauge combinations of spandrel plate were within 0.0625 in. of those in the NIST inventory.

This page intentionally left blank.

Chapter 1
INTRODUCTION

The purpose of the mechanical and metallurgical analysis of structural steel of the National Institute of Standards and Technology (NIST) World Trade Center (WTC) Investigation was to analyze structural steel available from WTC 1, 2, and 7 to determine the metallurgical and mechanical properties and quality of the metal, weldments, and connections, and to provide these data to other investigation projects. The properties determined under this project were used in two ways: (1) properties were correlated with the design requirements of the buildings to determine if the specified steel was in place in the towers, and (2) properties were supplied for other projects in the investigation as input for or validation of models of building performance.

1.1   SCOPE OF REPORT

This report describes damage characteristics, failure modes, and fire-related degradation of the recovered structural components from WTC 1 and WTC 2. Knowledge of damage to the steel elements plays an important role in the investigation in the following roles:

1.   Ascertaining the response of the structural steel of the towers to the impact of the planes;

2.   Providing information on perimeter column damage for correlations with impact damage modeled in the baseline structural performance and aircraft impact damage analysis;

3.   Providing information on thermal excursions experienced by the structural steel for use in the reconstruction of the thermal environment. It should be noted, however, that the model of the fire was not intended to match the actual fire on a column by column basis, and thus, the observations on thermal excursions of the steel are not expected to match the model in detail; and

4.   Providing input to the structural fire response and collapse analysis covering observations of missing sprayed fire-resistive material on the perimeter columns due to impact. This information is vital as sprayed fire-resistive material was the primary factor determining whether fire-exposed steel reached temperatures where there was significant strength loss. In addition, NIST used the detailed characterization of damage observations as a basis for modeling the damaged towers and the subsequent collapse of the buildings.

This report details the information available on structural elements prior to the collapse of the buildings and on the recovered steel components considered significant to the investigation. In particular, information from this analysis was used for validation of the modeling efforts in the baseline structural performance and aircraft impact damage analysis (NIST NCSTAR 1-2[1]), the reconstruction of the thermal

---

[1]   This reference is to one of the companion documents from this Investigation. A list of these documents appears in the Preface to this report.

environment (NIST NCSTAR 1-5), and the structural fire response and collapse analysis
(NIST NCSTAR 1-6).

To accomplish this task, two sets of observations were made. Post-impact, pre-collapse analysis
concentrated on impact damage sustained by the exterior panel sections, including the spandrel and
endplate connections between individual panels. The panels were the only structural components
observable during this time frame, with assessment based solely upon photographic and video images.
Further, the pre-collapse images were used to locate areas on the panels with pre-collapse fire exposure.
The second analysis focused on observations of the recovered steel elements. The exterior panels and
connections, as well the connectors or seat assemblies used to attach the floor trusses to the exterior
column panels, the inner core columns, and the seat assemblies attached to the channels of the core
columns were again evaluated. Of particular importance were the samples located near the airplane
impacts (north face of WTC 1 and south face of WTC 2) and those where fire was known to exist before
the collapse of the buildings, as the findings were important input in modeling the possible collapse
mechanism(s) of the towers.

For this report, only those samples with known as-built locations were documented to the fullest extent.
For samples without identifications, the information regarding damage and failure mechanisms were
collected for statistical purposes only.

Throughout this report, it should be recognized that while the physical damage and failure mechanisms
observed were reported in their present condition, in most cases it was difficult or impossible to conclude
which extreme loading event may have led to the damage. In other words, the damage may have been a
result of the aircraft impact, the subsequent fires, the ensuing collapse of the buildings, or the subsequent
handling related to the recovery efforts. It should also be recognized that in many cases it was difficult or
impossible to conclude when fire exposure occurred, that is, whether the fire exposure transpired prior to
collapse or during the time period that the piece was in the debris pile at the WTC site (for some samples,
possibly up to 4 months).

WTC 7 steel was not evaluated in this study of damage to the tower.

1.2   DIVISION OF STRUCTURAL ELEMENTS BY BUILDING AND LOCATION

The recovered structural elements were divided into categories depending upon their as-built location
within the towers and the post-impact, pre-collapse environmental conditions they may have experienced
in order to determine the extreme loading conditions that resulted in the damage and the time frame in
which fire exposure occurred. The samples were separated into the following categories:
(1) unambiguously identified samples with possible impact damage, (2) unambiguously identified
samples with exposure to pre-collapse fires (as determined by NIST), (3) unambiguously identified
samples not part of the previous two groups, and (4) those samples for which identification of the as-built
location was not possible. Section 2.0 defines the parameters used to assign the samples to the
appropriate category.

1.3 RECOVERED STRUCTURAL ELEMENTS FROM WTC 1 AND WTC 2

As a result of the recovery efforts of the Structural Engineers Association of New York (SEAoNY), Federal Emergency Management Agency (FEMA)/American Society of Civil Engineers (ASCE), and the investigation team, NIST possesses 236 structural steel elements from the WTC buildings. The report entitled "Inventory and Identification of Steels Recovered from WTC Buildings" (NIST NCSTAR 1-3B) contains a catalog of the recovered components and describes the process of collecting and cataloging the physical evidence (structural steel components and connections) and other available data, such as the as-built location of the steel pieces within the buildings and the specified steel properties. The primary location of most of these samples was the NIST Gaithersburg, MD, campus; some samples were located at an additional site, John F. Kennedy International Airport.

1.3.1 Review of the WTC Tower Design

In order to help understand damage observed on the recovered components, a brief review of the general building design for the towers is given. (Another report, NIST NCSTAR 1-1, discusses the design in detail.) Both WTC 1 and WTC 2 had similar framed-tube construction consisting of outer perimeter columns, a rectangular service core, and a floor truss system tying these two components together, Fig. 1–1. With a square footprint of approximately 207 ft on a side and chamfered corners, each floor contained roughly 31,000 ft^2 of unobstructed office space. There were 110 floors, starting at the plaza level, with a six-story subterranean structure beneath a large portion of the main WTC plaza and WTC 1, 2, 3, and 6.

The perimeter wall was designed to carry 40 percent of the gravitational loads, as well as all wind loads imposed on the building. From the 9th floor to 107th floor, the majority of the perimeter walls were composed of closely spaced, built-up box columns with approximate dimensions of 14 in. square sections by 36 ft long. Fifty-nine of these columns, each distinctly numbered (Fig. 1–2), were spaced at 3 ft 4 in. on center along each face of the building. Adjacent perimeter columns were interconnected at each floor level by deep spandrels, typically 52 in. in depth. In general, three full columns were connected to form exterior column "panels," Fig. 1–3, which were prefabricated and shipped to the construction site. These panel assemblies were raised into position and attached by bolting the end plates of the columns and splice plates of the spandrels. Each panel was typically three stories tall and spanned four floors in the building, as shown in Fig. 1–4. Therefore, each panel contained the upper half of one floor, two full floors, and the lower portion of a fourth. Figure 1–4 also shows that the panels were staggered so that only one third of the units were spliced at a given floor level. Panels spanning mechanical floors and sky lobbies, as well as at the corners of the building, were similar in nature, but had varying dimensions. Additionally, the panels were not staggered at these floors.

The core of the towers was designed to carry 60 percent of the gravitational load as well as provide room for building services (i.e., elevator shafts, stairwells, utility hardware). Core columns consisted of two types; box beam columns were typically used in the lower floors with a transition to rolled wide-flange sections at the upper floors. Some examples are shown in Fig. 1–5; a wide range of dimensions can be found for both types of core columns.

The floor outside of the core area was composed of deep, composite floor trusses (Fig. 1–6a) that spanned between the core and outer wall. Spaced at 6 ft 8 in., the trusses were attached to the exterior walls by

truss seats located at the interior intersection of the columns and spandrels, Fig. 1–3. Gusset plates with diagonal bracing straps were used to provide horizontal shear transfer between the floor slab and exterior wall, as well as out-of-plane bracing for the perimeter columns not directly supporting the floor trusses. To reduce wind-induced building motion, viscoelastic damper units tied the lower chords of the truss to the outer wall by a gusset plate below each truss seat, Detail A of Fig. 1–6b. Seats, welded to channels running along the perimeter of the building core, were also used to connect the trusses to the inner core columns, as in Detail B of Fig. 1–6b.

1.3.2 Summary of Recovered Structural Steel Elements

Structural steel components recovered from the WTC towers included partial and complete exterior column panels, core columns, floor truss members, channels used to attach the floor trusses to the core columns, and other smaller structural components (e.g., bolts, diagonal bracing straps, aluminum façade, etc.) (NIST NCSTAR 1-3B). These pieces were collected from four recovery yards where debris, including the steel, was taken during the clean-up effort. Once identified for recovery in the yard, the samples were marked as "SAVE" and given an alphanumeric code designating the recovery yard and an accession number. The samples were tested for asbestos and abated, if necessary, and then shipped to NIST. Upon arrival at NIST, the samples were catalogued, documented, and when possible, identified as to their precise, as-built location within the buildings. The vast majority of the recovered structural components obtained by NIST were from WTC 1 and WTC 2. It was estimated that roughly 0.25 percent to 0.5 percent of the 200,000 tons of steel used in the construction of the two towers was recovered. The following lists the recovered structural steel elements:

- Portions of 90 exterior panels were recovered with the as-built location of 42 distinct sections unambiguously identified within WTC 1 and WTC 2 (Table 1–1):

    - 26 panels from WTC 1: 22 from near the impact floors, 4 hit directly by the airplane and an additional panel that may have experienced impact damage;

    - 16 panels from WTC 2: 4 from near the impact floors.

- Portions of 55 wide flange sections and built-up box sections were recovered with 12 core columns positively identified from WTC 1 and WTC 2 (Table 1–2):

    - two columns from the fire floors of WTC 1;

    - two columns from the impact zone of WTC 2.

- 23 pieces of floor truss material from WTC 1 and WTC 2 were recovered; however, the as-built location of the trusses within the buildings could not be identified. The sizes of the recovered portions were significantly smaller than their as-fabricated dimensions due to a combination of their lightweight design and the excessive loads experienced during the collapse.

- 25 pieces of channel material that connected the floor trusses to the core columns in WTC 1 and WTC 2 were recovered; however, the as-built location of the channels within the buildings could not be identified.

- Seven coupons from WTC 5 were removed in the field and sent to NIST.

- No pieces could be unambiguously identified as being from WTC 7.

Figures 1–7 and 1–8 display the exterior wall impact damage along with nearby structural elements recovered from WTC 1 and WTC 2, respectively. The floors where pre-collapse fires were observed are also shown in these images.

In the design drawings for WTC 1 and WTC 2, 14 different grades (or strengths) of steel for the exterior panels, four different grades for the core columns, and two grades for the floor trusses were specified. From the recovered and identified columns, whether perimeter or core, a one to one correlation was observed between the minimum yield strength specified by the design drawings and the observed stampings and/or stencilings on the samples, with the exception of the 85 ksi and 90 ksi material that was substituted with 100 ksi plate, leading to only 12 grades of steel in the perimeter columns in the as-built structures (NIST NCSTAR 1-3A). To date, the recovered structural elements have yielded representative samples for the following:

- All 12 grades of exterior panel material,

- Two grades of the core column material (representing 99 percent, by total number, of the columns),

- Both grades for the floor truss material.

From these samples observations were made on the damage characteristics, failure modes, and possible fire-related damage of the structural elements.
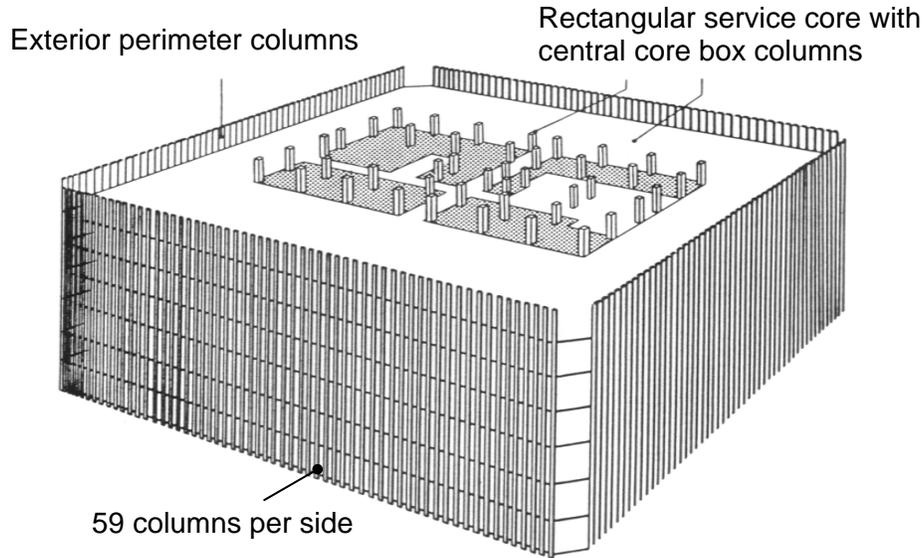
Figure 1–1. Tubular construction for WTC 1 and WTC 2 consisting of a rectangular service core and exterior perimeter columns.
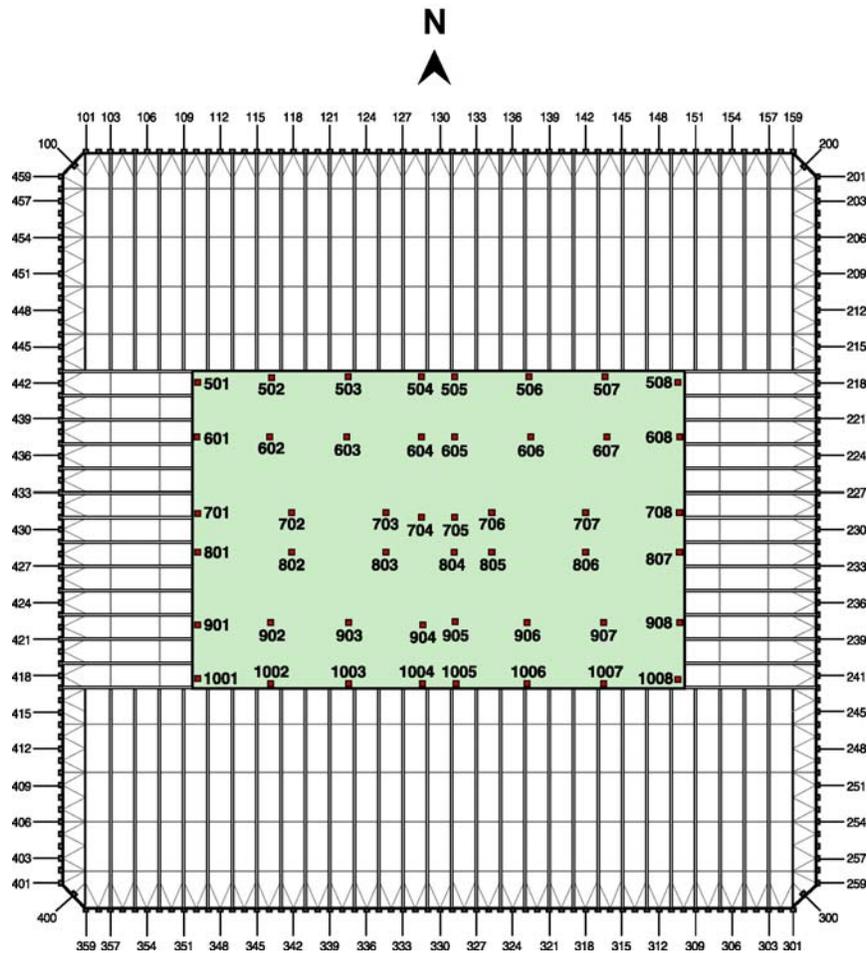
Figure 1–2. Floor plan for WTC 1. Perimeter and core column are numbered.
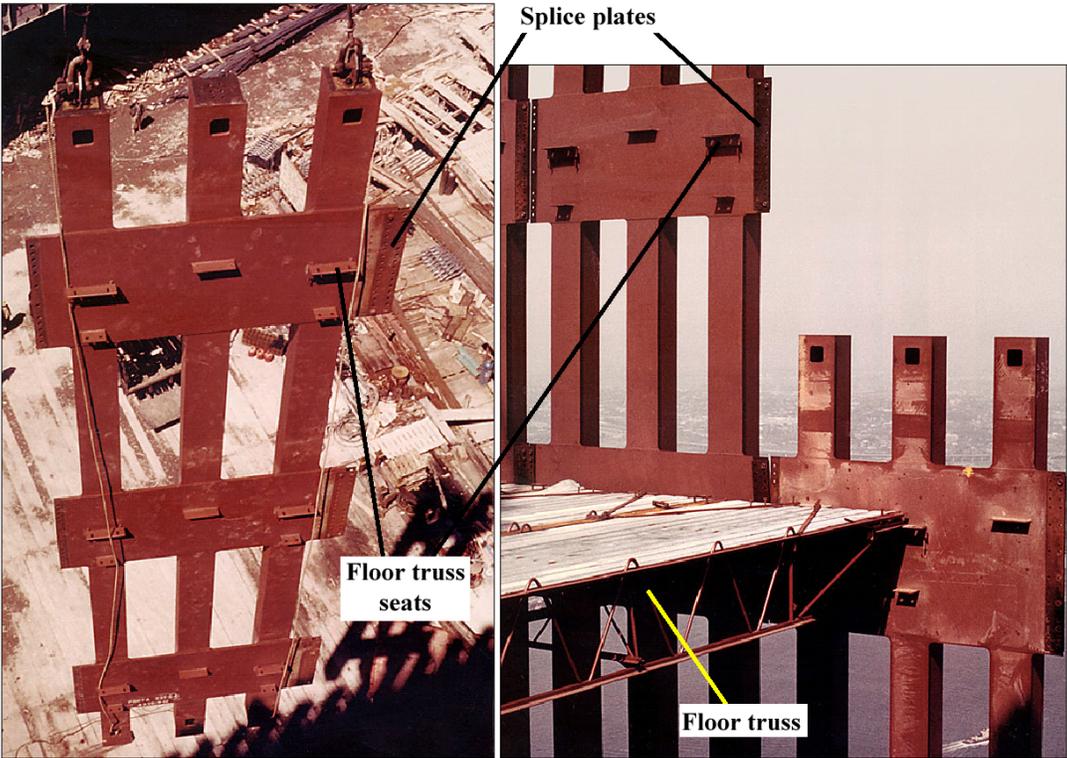
Source: unknown.

Figure 1–3. Construction photographs showing the exterior column panel consisting of three full columns connected by three spandrels (left image). Floor trusses and seats used to connect the floor trusses to the exterior wall can also be seen (right image).
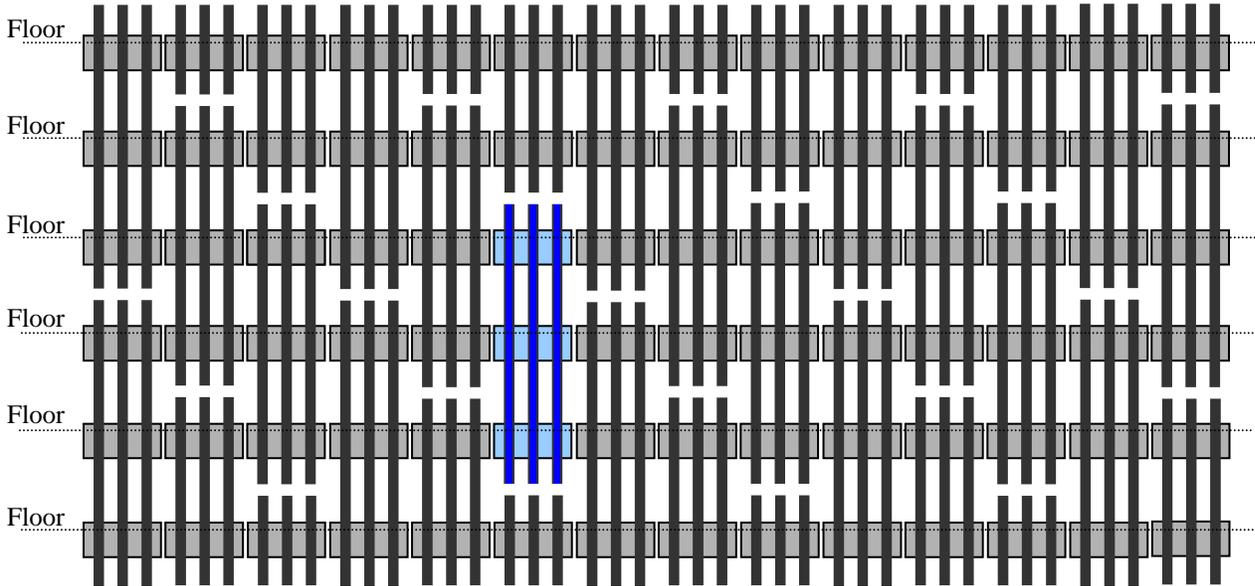
Figure 1–4. Partial elevation of exterior bearing-wall frame showing exterior wall module construction. Highlighted panel is three stories tall (36 ft) and spans 4 floors. Distance between panels has been exaggerated.
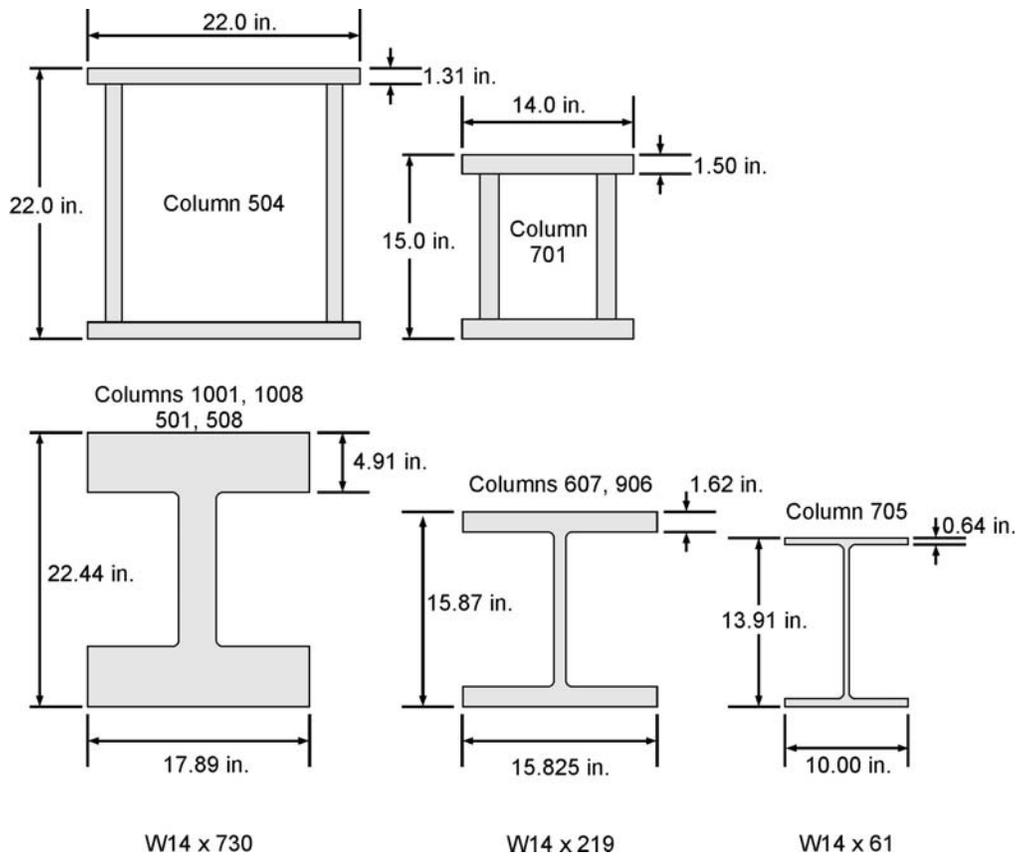
Figure 1–5. Typical welded box members and rolled wide flange shapes used for core columns between the 83rd and 86th floors (to scale).

Source: unknown.

Figure 1–6. a) Construction photograph of a composite floor truss.
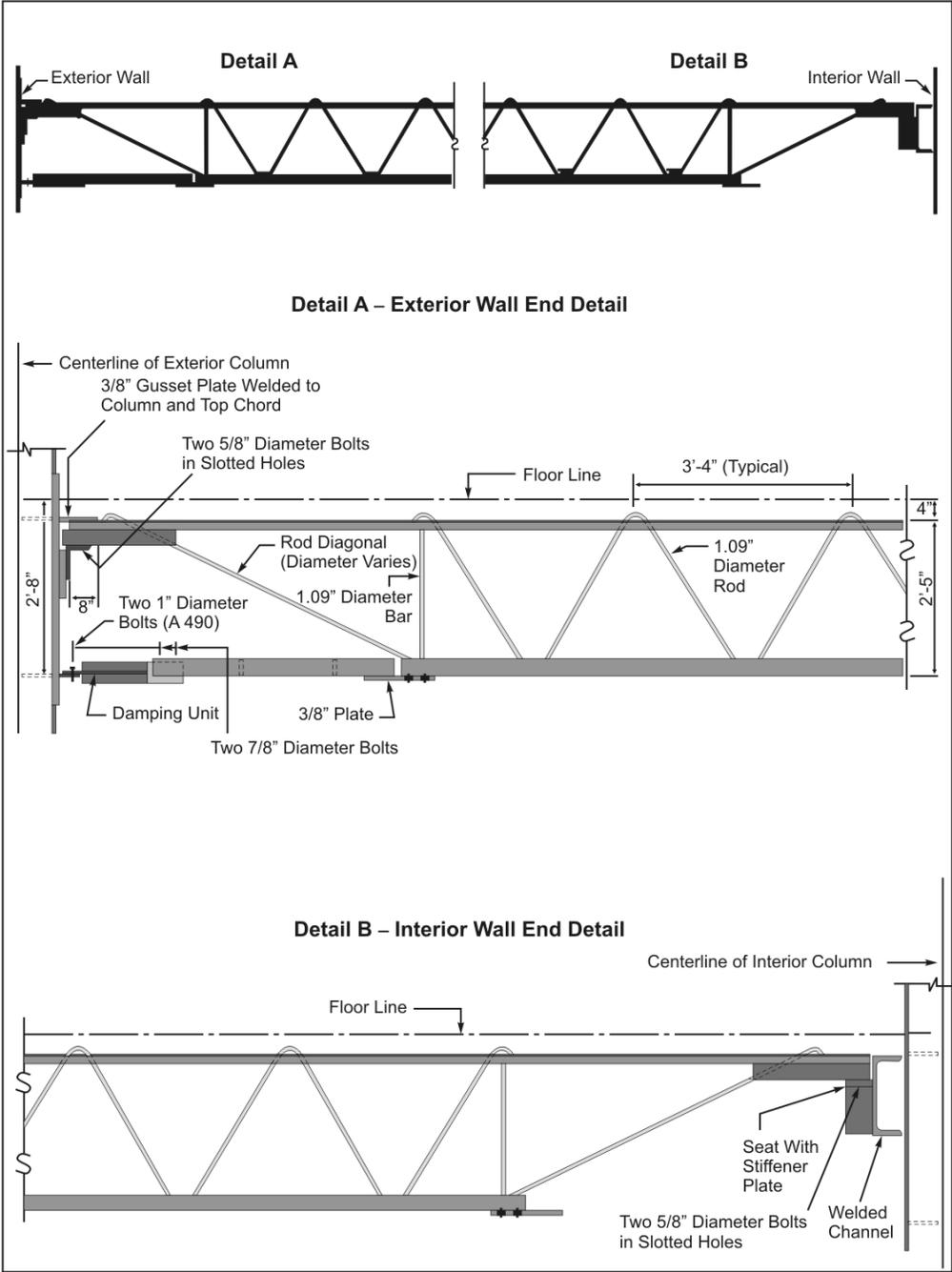
Figure 1–6. b) Schematic showing the attachment of the floor truss to the exterior wall and interior core columns.
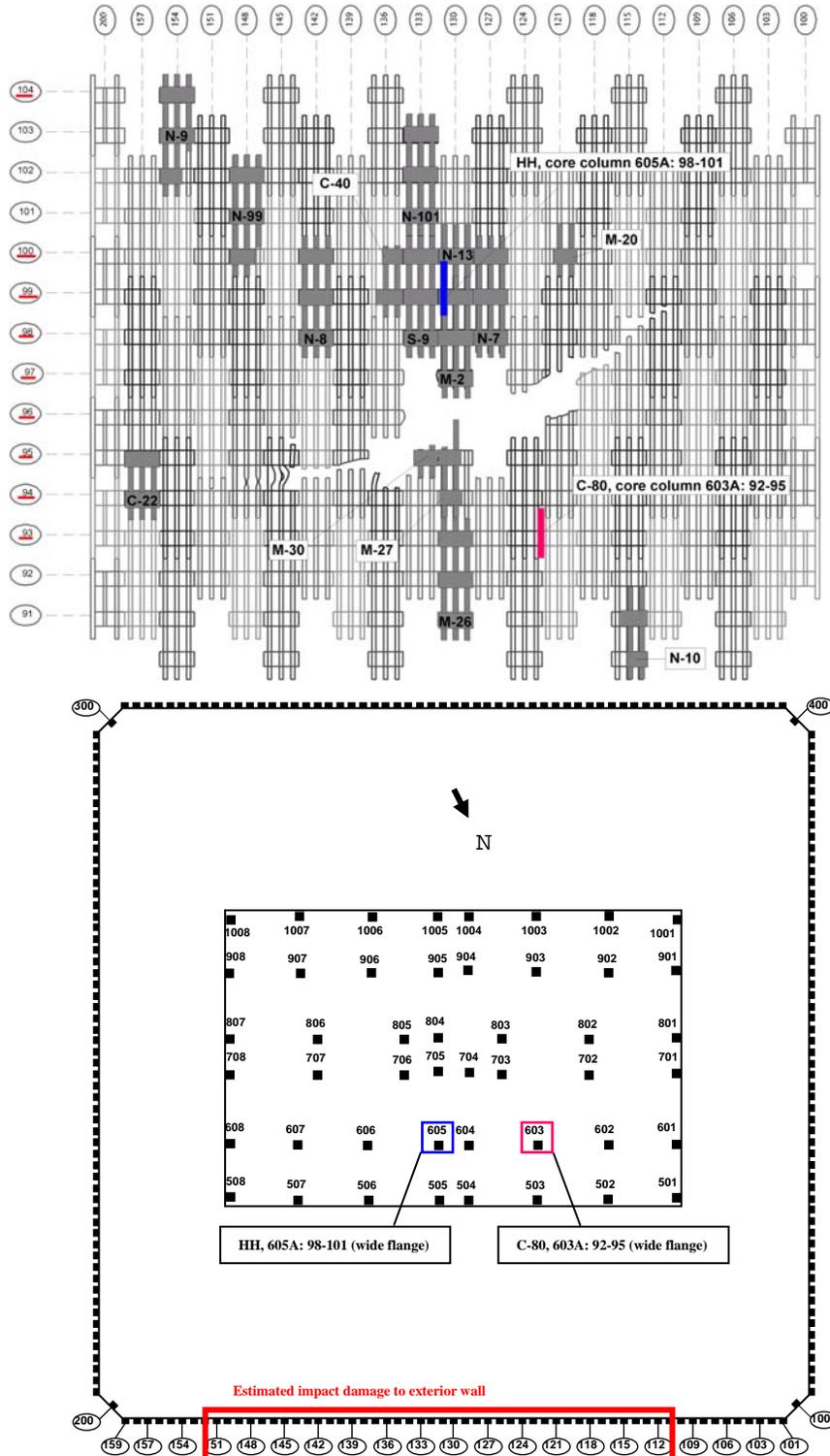
Figure 1–7. Impact damage location and recovered structural elements from WTC 1. Visual evidence of pre-collapse fires was observed on floors highlighted in red.
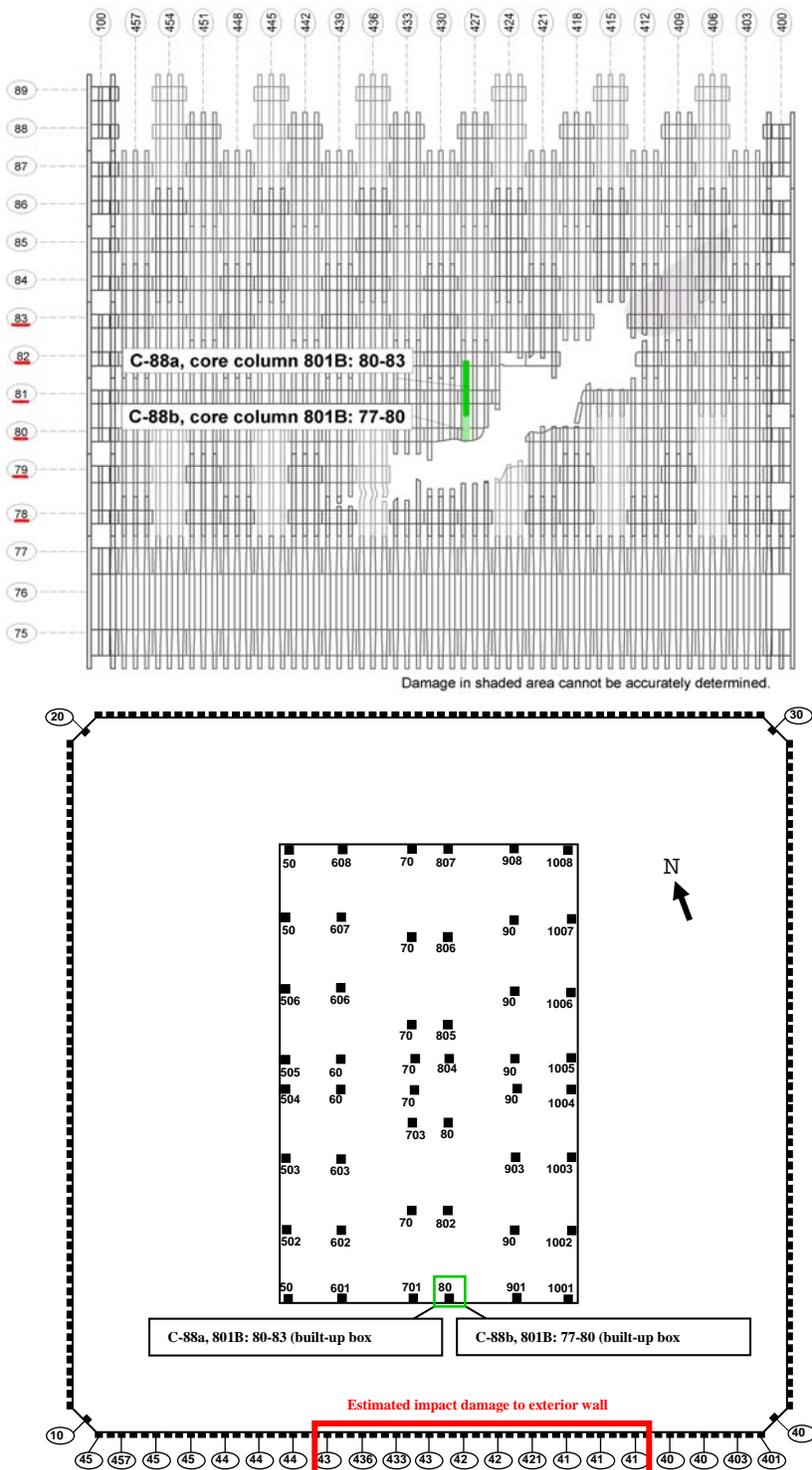
Figure 1–8. Impact damage location and recovered structural elements from WTC 2. Visual evidence of pre-collapse fires was observed on floors highlighted in red.

Table 1–1. Exterior panel sections with identified, as-built locations.

NIST label	Description	Bldg	Column	Floors
ASCE-2	1 full column	WTC 2	329	40 - 43
B-1024	Full panel	WTC 2	154	21 - 24
B-1043	Full panel	WTC 2	406	40 - 43
B-1044	Full panel	WTC 2	409	40 - 43
C-10	Full panel	WTC 1	451	85 - 88
C-13	Rectangular column with spandrel	WTC 2	200	90 - 92
C-13a	Partial of single column	WTC 2	159	90 - 92
C-14	1 column, lower $1/3^{rd}$	WTC 2	300	85 - 87
C-18	3 columns, bottom $2/3^{rds}$	WTC 2	230	93 - 96
C-22	3 columns, lower ½	WTC 1	157	93 - 96
C-24	3 columns, upper $1/3^{rd}$	WTC 2	203	74 - 77
C-25	1 column, lower ½	WTC 1	206	89 - 92
C-40	2 columns, lower $2/3^{rds}$	WTC 1	136	98 - 101
C-46	Nearly full panel	WTC 2	157	68 - 71
C-48	Nearly 2 full columns	WTC 2	442	91 - 94
C-55	1 column, lower $1/3^{rd}$	WTC 1	209	94 - 97
C-89	2 full columns	WTC 2	215	12 – 15
C-92	1 column, lower $1/3^{rd}$	WTC 2	130	93 - 96
C-93	1 column, lower $1/3^{rd}$	WTC 1	339	99 - 102
CC	2 full columns	WTC 1	124	70 - 73
K-1	3 columns, lower $1/3^{rd}$	WTC 1	209	97 - 100
K-2	1 column, lower $2/3^{rds}$	WTC 1	236	92 - 95
M-2	Full panel	WTC 1	130	96 - 99
M-10a	3 columns, middle section $1/3^{rd}$	WTC 2	209	82 - 85
M-10b	3 columns, lower ½	WTC 2	206	83 - 86
M-20	2 columns, lower $1/3^{rd}$	WTC 1	121	99 - 102
M-26	Full panel	WTC 1	130	90 - 93
M-27	2 columns, lower $3/4^{ths}$	WTC 1	130	93 - 96
M-28	3 columns, lower $1/4^{th}$	WTC 2	345	98 - 101
M-30	2 columns, lower $1/3^{rd}$	WTC 1	133	94 - 97
N-1	2 full columns	WTC 1	218	82 - 85
N-7	Full panel	WTC 1	127	97 - 100
N-8	Full panel	WTC 1	142	97 - 100
N-9	Nearly full panel	WTC 1	154	101 - 104
N-10	2 columns, lower $2/3^{rds}$	WTC 1	115	89 - 92
N-12	2 full columns	WTC 1	206	92 - 95
N-13	3 columns, lower $1/3^{rd}$	WTC 1	130	99 - 102
N-99	Nearly full panel	WTC 1	148	99 - 102
N-101	Full panel	WTC 1	133	100 - 103
S-1	2 columns, lower $1/3^{rd}$	WTC 1	433	79 - 82
S-9	Full panel	WTC 1	133	97 - 100
S-10	2 columns, lower 1/2	WTC 1	224	92 - 95
S-14	Full panel	WTC 2	218	91 - 94

Source: NIST NCSTAR 1-3B.

Table 1–2. Core columns with identified, as-built locations.

NIST Name	Type	Description	Bldg	Column	Floors	F_y (ksi)
B-1011	RB	Rectangular box column	WTC 1	508	51 – 54	36
B-6152-1	RB	Rectangular box column	WTC 1	803	15 – 18	36
B-6152-2	RB	Rectangular box column	WTC 1	504	33 - 36	36
C-88a	RB	Rectangular box column	WTC 2	801	80 – 83	42
C-88b	RB	Rectangular box column	WTC 2	801	77 - 80	42
C-90	RB	Rectangular box column	WTC 2	701	12 – 15	36
C-30 or S-12	W	Wide flange section	WTC 2	1008	104 – 106	36
C-65 or S-8	W	Wide flange section	WTC 1	904	86 – 89	36
C-71	W	Wide flange section	WTC 1	904	77 - 80	36
C-80	W	Wide flange section	WTC 1	603	92 – 95	36
C-155	W	Wide flange section	WTC 1	904	83 – 86	36
HH or S-2	W	Wide flange section	WTC 1	605	98 – 101	42

Source: NIST NCSTAR 1-3B.

This page intentionally left blank.

Chapter 2
PRE-COLLAPSE DAMAGE AND FIRE EXPOSURE OF STRUCTURAL ELEMENTS

This chapter of the report covers observable impact damage, failure modes, and possible exposure to fire of the pre-fabricated, exterior column panels of the World Trade Center (WTC) towers prior to their collapse. This analysis was based upon photographic images, video images, engineering drawings, and other relevant resources. From this information, the recovered panels (Table 1–1) were assigned to the four categories listed above in Sec. 1.2.

It was not possible to view the internal damage caused by the impact and subsequent travel of the higher density airframe components (e.g., landing gear, engines) through the buildings. However, structural damage due to aircraft impact computed in the aircraft impact damage analysis (NIST NCSTAR 1-2B) was discussed. General information on the types/shapes and strengths of the core columns located in and around the impact zones can be found in (NIST NCSTAR 1-3A).

2.1 DESCRIPTION OF IMPACT DAMAGED PANELS

2.1.1 WTC 1

As determined by National Institute of Standards and Technology (NIST), the estimated amount of missing/damaged sections of full panels/individual perimeter columns for WTC 1 is shown in Fig. 2–1. The impact damage occurred in the center of the north face between the 94th and 99th floors, bounded by column lines 111 and 152. (Superficial damage to the aluminum facade for the 93rd floor in the area of the left wing tip was observed visually, but it was believed that structural damage did not occur.) Two exterior panels appear to be pushed inside the envelope of the building, while 25 additional panels experienced varying degrees of damage. A listing of these panels, with the dimensions of the columns and spandrels and grades of steel for WTC 1 can be found in Table 2–1. The impacted exterior columns had required minimum yield strengths between 50 ksi and 65 ksi with gauges from 0.25 in. to 0.5625 in. Of the 81 damaged columns, there were 16 strength/gauge combinations. The breakdown of this data can be found in Table 2–2 for WTC 1, with Fig. 2–2b pictorially displaying the required minimum yield strength for the individual columns overlaid on the damage diagram. The spandrels were also an integral strengthening component of the exterior walls. As shown in Table 2–1, all spandrels located in the impact region had a gauge of 0.375 in. with minimum yield strengths of 36 ksi, 42 ksi, or 45 ksi. Figure 2–3 shows the location of these spandrels, with the breakdown of this data found in Table 2–3.

2.1.2 WTC 2

The impact damage to WTC 2 occurred off-center on the south face toward the eastern side of the building between the 77th and 85th floors, Fig. 2–4. While the damage appears to be bordered by column lines 411 and 440, columns closer to the south-east corner of the building may also have been affected. However, smoke continually obscured this region and few images were obtained where portions of the damaged area to the south face of WTC 2 could be observed. It appears that up to 18 panels may have

experienced varying degrees of impact damage. A listing of these panels, with the dimensions of the columns and spandrels and grades of steel for WTC 2 can be found in Table 2–4. The exterior columns located in this region had specified minimum yield strengths between 50 ksi and 100 ksi with varying gauges between 0.25 in. and 0.625 in. Of the 54 columns experiencing damage, there were 18 strength/gauge combinations. The breakdown of this data can be found in Table 2–2 for WTC 2, with Fig. 2–5b pictorially displaying the specified minimum yield strength for the individual columns overlaid on the damage diagram. Table 2–4 also lists the spandrel strengths associated with these panels. Unlike WTC 1, the strengths and gauges were more varied in WTC 2 with 11 different combinations. The minimum yield strength values ranged between 36 ksi and 65 ksi with gauges of either 0.375 in. or 0.4375 in. Table 2–3 shows these combinations, and Fig. 2–6 shows the location of the strengths with respect to the impact of the airplane.

2.1.3   Correlation of Pre-Collapse Images with Recovered Exterior Panel Sections

The panel identifications in Tables 2–1 and 2–4 were cross-referenced with 42 recovered exterior panels with known as-built locations (Table 1–1). Of the 42 panels, there were five recovered from WTC 1 that had been either directly impacted by the airplane or had possible damage as a result of the impact, Table 2–5 and Fig. 1–7. No corresponding panels were recovered for the impact region of WTC 2. From these five samples from WTC 1, damage features to and failure modes of the panels and individual components of the panels were visually observed and documented for possible insights into the behavior of the material/component(s) upon impact of the airplane. See Chapter 3.

Ninety-seven individual columns were specifically identified as to their strength/gauge combination from the 42 recovered panel sections with known as-built locations. There were an additional nine columns from unidentified panel sections where the column type and minimum strength values could be deciphered from the stampings located on the base of the columns (NIST NCSTAR 1-3B), yielding a total of 106 recovered columns of known strength and gauge. From these recovered columns, there were 36 different strength/gauge combinations (Table 2–2). Out of the 28 different strength/gauge combinations for columns in the impact region of both towers, NIST has recovered representative samples for 14.

Though representative examples of all the strength/gauge combinations have not been recovered from the impact regions of the towers, numerous gauges for all 12 specified grades of steel used for the perimeter panels have been recovered (NIST NCSTAR 1-3B). Most of the missing strength/gauge combinations for the impact regions were due to small variations in the thickness of the flange section of the column. Of the 14 un-recovered strength/gauge combinations, 10 combinations had differences of 0.0625 in. to their nearest recovered strength/gauge combination, while three were 0.125 in. away, and one combination had a difference of 0.1875 in.

Similar to the column material, the recovered spandrel material consisted of various strengths and gauges (Table 2–3). There were 87 distinct portions of spandrel plate recovered with 20 different strength/gauge combinations. Considering both towers, 7 of the 13 strength/gauge combinations in the impact region were recovered. As seen with the column material, all six of the missing strength/gauge combinations were only 0.0625 in. from their nearest recovered strength/gauge combination, thus, sufficient samples were available for the investigation.

2.2 PHOTOGRAPHIC ANALYSIS OF PRE-COLLAPSE DAMAGE TO EXTERIOR WALL PANELS

As part of the investigation, the investigative team put out requests to news organizations and the public for any photographs or video footage taken of the impact damage to either tower prior to collapse (NIST NCSTAR 1-5A). These images were analyzed to produce preliminary damage assessments and maps of the progression of fires and window damage between the times of airplane impact and collapse for each tower (NIST NCSTAR 1-5A). The present analysis goes into more detail into the pre-collapse damage, focusing on structural issues and damage to sprayed fire-resistive material (SFRM).

A large number of images of the impact area in the north face of WTC 1 were obtained. However, the number of images of the damage to the south face of WTC 2 was limited and spatially incomplete. This was largely due to the fact that the damaged face was on the south side, and close-up photographs were not taken, as the area south of the WTC complex was evacuated, and most images taken from farther away proved to be of insufficient resolution to allow extraction of failure mode information.

Extensive image processing in the form of filtering, contrast enhancement, and montaging was used on the available images to provide as many details as possible. In all cases where image processing was used, this was indicated in either the figures or described in the figure captions. The processing techniques were limited to enhancement, and not re-touching or changing the content of the image. Arrows and other notations were added as needed to enhance clarity for reporting purposes.

2.2.1 Structural Damage to WTC 1

Eleven photos had sufficiently high resolution to be of use in this part of the investigation. Figure 2–7 shows one important photograph in its original state. The damage to the building caused by the outermost tip of the starboard wing was not shown in this image, so a small portion of another photograph was color adjusted, rotated, and pasted onto the image of Fig. 2–7 to complete the damage zone. The image was then adjusted for contrast, and the levels were expanded so as to bring out important features hidden in the darker regions (Fig. 2–8). This was done in a piecewise manner within 27 individual regions. In this manner, it was possible to bring out the maximum number of details over the entire image.

Superimposed onto this figure is an outline of a Boeing 767 aircraft as it would appear sitting on the runway (Boeing 2004), scaled to correct dimensions with regard to the image of the building (Fig. 2–9). However, as the plane was traveling at a high rate of speed and was experiencing a turn at the time of impact, the shape of the hole does not correspond to the outline of the plane at rest. In the next image (Fig. 2–10), the outline of the plane was distorted to approximately match the outline of the hole in the building. Note that this outline was not based on any calculations, but merely an approximate fit to the image. It was seen that all of the major features of the hole in the building were accounted for by some part of the aircraft, from holes formed by the engines to the damage from the wingtips and the top of the tail.

In Fig. 2–11, colored rectangles have been added to identify observable failure modes in the exterior columns, whether at the ends or at some location along their length. The specific failure modes identified are described in the figure caption. Blue rectangles indicate where the bolted connections between two vertically adjacent exterior wall panels have failed. In many instances, this was indicated by a trio of

truncated columns at the same vertical location that corresponded with a known column connection. In other instances, notably seven columns from the leftmost damaged column, bolted connection failures were visible as a small horizontal dark line on the column. The fact that the junction indeed had broken was verified by examining other photographs taken at oblique angles from the ground, showing that one or the other of the column ends making up the joint was pushed in or out of the plane of the exterior building face. Rectangles shaded red indicate where there was a high likelihood of failure of the steel of the columns via tearing or cracking, not located at a bolted column connection. At many locations it could be seen in the various photographs that the longitudinal welds used to form the box columns from four plates of steel have failed, and these are indicated in green. Finally, there were several broken exterior column connection failures that could not be definitely identified, and these are colored in yellow.

Several general observations were made about the spatial distribution of failure modes around the impact hole of WTC 1. The regions to the left and right, where the wings impacted, showed a higher concentration of columns that failed by cutting or splitting of the steel of the columns, rather than at connections. The far ends of the wings did not sever the columns, however; the wing apparently sieved through the columns. Where the fuselage went through, there were higher concentrations of failures at the bolted column connections between the exterior panel sections. For visualization purposes, Fig. 2–12 shows the location of these bolted joints in the exterior wall. Failures farther removed from the impact holes tended to be in the bolted vertical connections, as panels cut loose at one end bent into the interior of the building, loading the other end in tension and breaking the bolts. In most instances, the column failures that could not be identified were obscured by what remains of the decorative aluminum façade on the exterior of the building. Figure 2–13 shows the as-built locations and remaining portions of the recovered and identified panels in NIST's possession as they existed in the impact region. Comparison of these photographs to the current state of the recovered panels allowed for the identification of impact damage and the location of fracture surfaces and other failures caused by the plane collision, as discussed in Sec. 3.0.

Five exterior wall panels were recovered and identified as having been directly impacted by the aircraft. As seen in Fig. 2–13, these are the panels labeled M-30, S-9, M-27, M-2, and N-7. The available photographs were examined, and portions of the best views of each of these panels have been extracted and shown in Figs. 2–14 through 2–18. These were described in detail below.

- **M-30:** (location A133: 94-97) This panel was observed to have been displaced and pushed inside the envelope of the building while still being attached by the 95th floor spandrel to M-27; thus, its orientation was diagonal as shown in Fig. 2–14. The bolted column splice connections at the 94th floor level of columns 132 and 133 have broken at the bolts.

- **S-9:** (location A133: 97-100) Panel S-9 was above the impact hole and to the left of panel M-2 (Fig. 2–15). This panel was hit by the vertical tail assembly. Damage to the aluminum exterior panels of the building was evident, though this region was obscured by smoke in all photographs available. The panel appears relatively straight after impact; however, substantial local damage to column 134 may be present below the damaged aluminum façade.

- **M-27:** (location A130: 93-96) This panel, hit by the nose of the aircraft, was directly below panel M-2, and the upper part was observed bent over at roughly a 90 degree angle into the building after the collapse (Fig. 2–6). Column 130 appears to be sliced off at the 95th floor, while column 131 was bent over and lying on the 95th floor. It appears that the spandrel connection at the 95th floor level of column 131 was still attached, while the connection associated with column 129 was broken.

- **M-2:** (location A133: 96-99) Panel M-2 was originally immediately above panel M-27, (Fig. 2–17). The lower end was hit directly by the fuselage of the aircraft. The bottom of each of the box columns of the panel showed failure of the vertical column connection bolts, as well as extensive splitting of the longitudinal welds of the box from the end plate to the first spandrel. The bottom end of the panel was pushed several feet into the building. The right end of the lower spandrel remained, and its length implied failure of the middle of the connection with the adjoining panel. The left end of this spandrel was not visible. In all photographs, smoke obscured the bolted vertical connection at the top of the panel.

- **N-7:** (location A127: 97-100) This panel (Fig. 2–18) was above the impact hole, to the right of and above panel M-2. The vertical column connections in the 97th floor level of columns 126, 127, and 128 broke at the bolts. The panel appeared otherwise relatively undamaged after the plane impact.

2.2.2 Damage to Sprayed Fire-Resistive Material in WTC 1

According to construction documents (Feld 1971), the SFRM (i.e. sprayed fire-resistive material) applied to the exterior of the outer columns within the impact regions of both towers was the same material and application process used for insulating both the core columns and the floor trusses. One of the parameters in the impact and fire analysis was the condition of the SFRM, so the available photographs were examined for evidence of its condition after impact.

Areas of particular interest were around the impact holes in each tower, as well as regions where the exterior walls were impacted from the inside by debris, causing the exterior facade to be damaged. The photos were enhanced digitally as necessary to reveal the condition of the SFRM. The image processing techniques involve changing the range of displayed levels, changing the effective gamma, the application of filters such as unsharp mask and edge sharpening, and subtracting filtered images from the original to highlight specific features. For an explanation of these image processing techniques, the reader is referred to Russ (1995).

Figure 2–19 shows a diagram indicating how the SFRM was to be applied to the exterior columns, with a relatively evenly thick coating to all exterior portions of the column. In practice, as evidenced by the photographs to follow, it appears the SFRM was sprayed on so as to fill the depression formed by the outer web of the column and the protrusions of the two column flanges, so that the outer face of the column appeared flat (Fig. 2–20). Figure 2–21 shows details of the architectural aluminum panel attachment to the window frames, suggesting how the blowout of windows and frames could possibly pull off the aluminum panels as well.

There was extensive photographic evidence of SFRM damage around the impact hole on the north face of WTC 1. This was not surprising, considering the energy of the impact. However, some of the damage was a considerable distance from the impact site. Since damage to the SFRM can only be detected at locations where the exterior aluminum panels have been dislodged, this analysis is not to be considered a comprehensive map of the damage to the SFRM on the north face of WTC 1.

Figure 2–22 shows the east side of the impact hole in the north face of WTC 1. Arrows indicate where the SFRM was damaged, and in several locations the underlying paint showed through. Examining these images further, it was possible to view the trusses on the underside of the floors that collapsed into the impact hole (Fig. 2–23). In the two instances indicated on the figure, the details of the structure and the paint color of the lower chord of the trusses were quite visible, indicating that most if not all of the SFRM had been dislodged.

2.2.3   Photographic Evidence of Pre-Collapse Distortion of Exterior Wall: South Face of WTC 1

In several photographs it was possible to see an inward bowing of the exterior walls of each tower at different times. The following methodology and assumptions were used to measure the positions of the exterior columns and their deviation from straight and vertical. The aluminum façade panels were 11 in. in depth in the installed position, measured from the window frame outward. They were also 19 in. wide across the exposed face. The aluminum panels were joined at seams that lay at right angles to the long axis of the external columns, and which were generally located at the top edge of a window opening of a particular floor. Each aluminum panel extended one full floor, measuring 12 ft in length.

The governing assumption of this analysis was that the bending of the columns inward preserved the direction and length of the seam across the 11 in. wide face of the façade pieces. The wall bowed inward parallel to the line of this seam. A line was drawn along the undeformed column sections that were visible far above and below the bent columns to establish the original profile of the column. Since the lens of the camera that took the pictures suffered from a considerable barrel distortion (lines at the outer region of the image are not parallel to the centerline, but rather curved slightly), this was corrected in the data to avoid introducing artificial distortion of the columns. A line parallel to the columns was established on each side of the image, with each line being the same distance from the edge of the photo. This established two lines equidistant from the center of the lens. These outer columns were determined to be straight in other images. The distortion of the columns adjacent to these lines from straight was established at each floor level at the line of the top of the windows. A linear interpolation function for the barrel distortion was calculated for the image at each floor level. It was assumed to vary from a rightward distortion of the image on the right hand side through perfect alignment in the center to a leftward distortion on the left hand side.

For each column, a vertical line was drawn to establish the original alignment of the column, wherever possible. This was done by tracing from unbowed sections far above and below the section that was bowed inward. Most commonly, if a line could not be drawn, it was because the columns above the inward bowing were not visible due to smoke. At each measurement site, when possible, the length of the 11 in. long seam, as well as its deviation angle from horizontal, was measured on the photo as a calibration. If the seam was not visible precisely at the measurement location, the length and angle were measured at as close a location as possible. It was found that this length did not vary by more than

1 percent over a vertical distance of three floors or sideways up to four columns in either direction, so establishing this length not exactly at the location did not introduce much error. A measurement was then made at the same angle as the seam from the upper left corner of the window (or window opening) to the previously drawn true line. The correction for barrel distortion was calculated and subtracted from this value. This established the amount of inward bending of the column. A ratio of this length to the seam length was calculated and multiplied by 11 in. to estimate inward bowing in in. This measurement was made at every location where the aluminum façade panels were intact, straight, and still attached to the building.

This measurement was performed on an image taken from a NYPD helicopter at approximately 10:23 a.m., several minutes before the collapse of WTC 1. The image is shown in nearly its entirety in Fig. 2–24, and the analysis is shown in Fig. 2–25. Due to the limited resolution of the digital camera that took the image, as well as artifacts introduced into the image by the JPEG compression routine, the resolution of these measurements are estimated to be +/- 6 in. This resolution limitation and the presence of such a large region obscured by smoke required that the aforementioned measurement procedure be modified slightly. Instead of establishing the vertical true lines using undeformed sections above and below the region of interest, the large area visible below this area was utilized by establishing the true line along 20 floors below the damaged region. This was extended along the same line through the smoke filled region. In addition, as the seam of the aluminum façade panels was not visible, the distance the columns were deformed into the building perpendicular to the south face was established by measuring angles and distances on the west face at the southwest corner of the building (see Fig. 2–25, lower left). This established the angle (167 degrees from right horizontal) and base magnitude (120 ft per 88 pixels) of the inward bowing vector. The foreshortening of the south face due to perspective was calculated and applied to the distances measured on the south face, and increased the measurements by a maximum of approximately 15 percent over the physical distance measured on the image. Note that later analysis of the inward bowing of the east face of WTC 2 did not require this correction, due to a more normal orientation of the photographer's view of the building.

The region over which the exterior columns of WTC 1 appear to bow inward spans nearly the entire face, and extends vertically over at least 4 floors, if we assume continuity between the inwardly bowed sections on the east and west sides of the south face. The maximum inward bowing at this time (10:23 a.m.) is 55 +/- 6 in. near column 316 on the 97th floor. Note that this is the maximum that is visible, but a large portion of the south face is obscured by smoke. Figure 2–26 shows an image taken at 9:25 a.m., or 58 min after aircraft impact. This image shows that the columns shown to be inwardly bowed in Fig. 2–25 are straight at this time, indicating that the inward bowing developed quite some time after impact, and was not due to initial impact damage.

2.2.4 Structural Damage to WTC 2

As mentioned previously, the availability of images showing details of the impact hole in WTC 2 was much more limited than the number of images available for WTC 1, and many of the images were taken from a much greater distance than those of WTC 1. Also, many photographers tended to frame their fields of view to encompass a shot showing both towers being on fire and damaged, so that the portion of the image showing the WTC 2 impact hole, even if very high resolution, was very small. Most of the useful images for the analysis came from videotape shot by staff from the New York City Fire Department (FDNY) very near the site, but these frame grabs suffer from limited resolution.

Figure. 2–27 shows a clear view of the damaged south face. The image was adjusted for contrast, and the levels were changed to bring out the most features and to correct for the general blue cast (Fig. 2–28). Small local regions were adjusted in a manner similar to Fig. 2–8, but the resolution of the image was too low for any new features to be revealed using this method. Fitting of an outline of a 767 to this image was found to be extremely difficult, as the angle of impact of the aircraft with the wall and the angle from which the image was taken with respect to the building face were not well known, and distorting the outline of the plane to match the damage did not produce acceptable results.

In the next image (Fig. 2–29), colored rectangles were added to identify any observable failure modes in the exterior columns, whether at the ends or at some location along their length. The specific failure modes identified are described in the figure caption. Blue rectangles indicate where the bolted connections between two vertically adjacent exterior wall panels have failed. In many instances, this was indicated by a trio of truncated columns at the same vertical location that corresponded with a known column connection. Rectangles shaded red indicate where there was a high likelihood of failure of the steel of the columns via tearing or cracking, not located at a vertical column connection. The number of longitudinal weld splits, designated by green rectangles, that could be seen was very limited due to image resolution. There were several broken exterior column connection failures that could not be definitely identified, and these are colored in yellow. In addition, the region encompassing the starboard wing tip damage area, outlined roughly in yellow, was unobservable in all available photographs and video footage, due to the large and persistent volume of smoke being emitted from those floors.

Several general observations were made about the spatial distribution of failure modes around the impact hole of WTC 2, though the patterns of damage were less well-defined than those in WTC 1. The region to the far left, where the wing impacted, shows a higher concentration of columns that may have failed by cutting or splitting of the steel of the columns, but the images do not provide a clear determination for most columns. It was evident that the damage was very localized at the point of impact and that the columns were not pushed into the interior of the building as seen for WTC 1. Where the fuselage went through, there was a somewhat higher concentration of failures at the bolted vertical connections between the exterior panel sections,but contrary to the observations on WTC 1 where the columns were bent inward into the building envelope, there were also a number of columns that were cut by the impact of the main body of the aircraft observed for WTC 2. This may be due to the fact that the fuselage did not enter the building at the roughly right angle that was the case for WTC 1, but at a more side-sliding acute angle for WTC 2. Thus, at any given point around what would be considered the fuselage entry point, components of the main body, wing, and perhaps even engine may have impacted a given exterior wall panel during the event. For visualization purposes, Fig. 2–30 shows the location of these bolted joints in the exterior wall.

No identified panels in NIST's possession correspond to any panels around the impact hole in WTC 2, so detailed post-collapse analysis of the failures was not possible.

Parts of the aircraft that impacted the south face of WTC 2 exited the building on the north face and landed some distance from the building. In particular, it was believed that an engine exited the NE corner of the building from the 81st floor, and a landing gear strut component cut through the wall on the north face near the northeast corner of the same floor. Images were examined to determine what damage was caused by these pieces in order to feed this information back to both the impact damage model and the stability models.

Several images taken from different angles and with different smoke and lighting configurations were examined to characterize the damage. Fig. 2–31 is a view of the northeast corner of WTC 2 centered on approximately the 82nd floor. The 81st floor, where the engine exited, was piled full of burning debris. The corners of the buildings were designed such that every other floor had a column in this space, an example of which can be seen above the hole, indicated by the arrow. The plans of the building show that the 81st floor was one without a column, consistent with the image, so that the exiting engine did not remove one as it exited the hole. Also, examination of this and two other images showed that the columns that border the hole to the left and right appear undamaged, so that the engine appears to have not damaged the building structurally as it exited.

On the right side of the image in Fig. 2–31 is the north face of WTC 2. It was believed that a large component of a landing gear exited the building on this face near the northeast corner in the region of the 80th floor. On Fig. 2–32, the arrows indicate where the columns have been cut (regions of missing column denoted by blue arrows) or where a bolted connection has broken and bent the column ends outward slightly (green arrows). The bolted connections were broken at the 81st floor in columns 257 and 258. The entire column was cut through at columns number 254 and 255, also at the 81st floor. Once these exterior columns had been severed, they were no longer load bearing.

In addition to the missing piece of column, column 254 exhibited an intact outer web (red arrows). This piece had fractured free of the rest of the column over a distance of slightly more than two floors. Since the flange tips can be seen on either side of the outer web, the fractures occurred within the flange plate.

2.2.5 Damage to Sprayed Fire-Resistive Material in WTC 2

North Face Near Northeast Corner

The north face of WTC 2 contained the exit holes for some of the debris from the collision of the aircraft. This debris consisted of aircraft components, building contents, and possibly structural parts of the building damaged during the event. This debris impacted the interior of the north wall, blowing out windows, damaging exterior columns, and removing aluminum exterior panels and SFRM from the columns.

A region of the north face of WTC 2 spanning columns 230 through 259 and the 79th through 82nd floors had the exterior aluminum panels and SFRM damaged or removed due to debris impact from within the building. In particular, a rectangular region consisting of columns 239 through 249 on floors 79 through 81 were found to be completely free of aluminum panels, and the best observations of SFRM damage were in this region as well. Figure 2–33 shows the region of interest. Red arrows indicate where the SFRM was dislodged from the outer web between the protruding tips of the flanges. This determination was made using this image and other higher resolution images (see forthcoming figures). The appearance of white linear features on the edge of the columns, at this angle of solar illumination, shows the absence of at least some, if not most, SFRM from the center region of the outer web of the column. In contrast, column 246 (green arrow) shows bright contrast across the entire face, and this and other photos confirm that the SFRM was nearly intact along this column for the entire exposed three floors, despite the fact that the aluminum facade had been dislodged.

Additional images taken of the region at higher resolution (Fig. 2–34) showed more subtle details about the SFRM damage. The arrows indicate where the SFRM has been dislodged completely from the

flanges, as evidenced by the exposed red Tnemec paint on the columns. It was not possible to make an unambiguous determination as to whether the insulation on the exteriors of the spandrels was damaged in any of the photographs. This photo also reveals details about the loss of the SFRM. The blue arrow in Fig. 2–34 points to an example of a band of white features that occurred wherever two aluminum panels met on the exterior of the building, the white feature becoming visible when the panels were dislodged. This may be a coating applied to protect the SFRM from moisture infiltration at the aluminum panel joints. This coating appears to have prevented the loss of SFRM in a great many locations where the SFRM was knocked off both above and below this location.

East Face of WTC 2

The interior of the east face of the tower was not impacted as directly as the north face, but experienced damage to both aluminum exterior panels and SFRM. However, the damage was more scattered across a larger fraction of the face on the 79th through 82nd floors (Fig. 2–35). Clearly, there were areas where the SFRM had been damaged or removed to the level of the paint (red arrows). Loss of SFRM was not found south of column 316 on this face of WTC 2, but since dislodged SFRM can only be seen if the aluminum panels were also dislodged, and the panels south of column 316 were intact, this does not mean that the insulation necessarily was intact.

2.2.6 Photographic Evidence of Pre-Collapse Distortion of Exterior Walls: East Face of WTC 2

Several high-resolution photographs taken of the east face of WTC 2 in the region of the 80th floor show an inward bowing of the exterior columns. The timestamps of these photos ranged from 9:21:29 a.m. until just before collapse. Three photographs were of sufficiently high resolution to enable measurement of the inward bowing over the surface of the face of the building. The estimated error in each measurement, given all the sources of error detailed previously in the discussion of the methodology (Sec. 2.2.3), was approximately 1 in. to 2 in. for these measurements. One image was taken at 9:21:29 a.m., or 18.5 min after impact (Fig. 2–36), and the other two images were taken by the same photographer at nearly the same location 10 s apart beginning at 9:52:54 a.m., or roughly 6 min before collapse of WTC 2 (Fig. 2–37 shows one of these images). These images were analyzed extensively to spatially map the inward bowing of the exterior columns across the face of the building to provide insight into when this bowing formed and how it changed with time. (Additional figures with much lower resolution were examined to determine the amount of deflection as close to the moment of collapse as possible. However, due to the low resolution and obscuration, these did not produce any usable results.)

The resulting data are plotted in Figs. 2–38 and 2–39. (The results from the two images that went into Fig. 2–39 were combined since they were taken from the same location with the same camera only 10 s apart, and it was assumed that the inward bowing of the columns did not change appreciably in that time). It was clear that only 18.5 min after the impact of the plane, there was significant inward bowing of the east face of the building. After an additional 31.5 min, the deflections nearly doubled in most locations.

2.2.7 Photographic Evidence of Damage to the Flooring System of WTC 2

An image showing what appears to be a hanging floor slab in the windows on the east face of WTC 2 is shown in Fig. 2–40. This image, which was of relatively low resolution and suffers from considerable

sun glare, shows a displaced floor slab on the east face of WTC 2 through the windows bounded by columns 315 and 343 on the 82nd floor.

A number of photographs of the north face of WTC 2 in the region of the 80th floor appeared to show floor slabs that had fallen from their original positions. The thickness and color of the feature indicated by arrows in the images were consistent with that of the concrete slab of the floor assembly (NIST NCSTAR 1-6C). The floor slab in Fig. 2–41 appeared in the windows bounded by columns 241 and 248 on the 80th floor, and in Fig. 2–42 bounded by columns 245 and 248 on the 80th floor. The timestamps for these two images were (pending) and (pending) respectively, so the floor slabs appear to have moved over time.

The details and implications of the presence and locations of these floor slabs are discussed in greater detail in McAllister et al. (2005).

2.2.8   Photographic Evidence of Details of Collapse of WTC 2

Some details of the early stages of collapse of WTC 2 were found in the photographic record and provided for validation of the models of collapse. The image in Fig. 2–43 was taken about one second after the tower began to collapse and shows the east face of the building. A noticeable kink was visible along the edge of the building in the region of the 106th floor at the SE corner (arrow).

A more detailed analysis of the geometry has been made of this distortion, shown in Fig. 2–44. The kink was in fact a double-kink, and the directions of the axes of bending are shown in the figure. It is likely that this distortion formed by the sideways shift of loads transmitted via the hat truss and rigid, beam-framed floors of floors 107 to 110, and a more detailed structural analysis can be found in McAllister et al. (2005). Examination of the right side of the image, after considerable image processing, shows that the edge of the building has bent, but shows no sharp discontinuity. Thus, the sharp kink had not propagated across the face of the building (Fig. 2–45). An image taken approximately 2 s before collapse (Fig. 2–46) shows no bending, so the kink must have developed at either the moment of collapse initiation or during the earliest moments of the collapse process.

2.3   PHOTOGRAPHIC ANALYSIS OF PRE-COLLAPSE EXPOSURE OF EXTERIOR PANELS TO FIRE

In the fire modeling project (NIST NCSTAR 1-5A), photographic images, video images, and other relevant information were utilized to develop detailed time lines for the spread and growth of fires at the peripheries of WTC 1 and WTC 2. From this information, it was determined if fire was present on a floor or near a specific exterior panel at a given time. In the analysis, the windows were numbered for a given floor, and the determination was made from the resources as to which category each individual window fell into for the given time frame. The categories were labeled as:

> 0: No fire was visible
> 1: Spot fire or small isolated fire
> 2: Fire visible inside
> 3: External flaming
> 9: Unable to be determined (typically as a result of smoke obscuring the window).

Cross-referencing this information with the recovered exterior panels, direct visual observations were made on samples to determine the extent of fire damage or if fire affected the structural integrity of the component.

Figure 2–47 displays a generic illustration of the combined data used in this portion of the analysis. On the right-hand side is a schematic of the recovered exterior panel along with the identification of its as-built location. The panel was drawn as if viewed from outside of the building, with the floors and column lines labeled. Portions of 16 different windows (labeled *a* through *p* on the schematic) were associated with each panel. These window locations correspond with areas located on the time-fire exposure sequence to the left of the panel schematic. Segments of the panel may be "grayed-out" indicating that this portion of the panel was not recovered. (The amount of recovered panel for each identified sample was documented in NIST NCSTAR 1-3B.) On the left-hand side of the illustration, the time line analysis for exposure to fire can be observed for that given panel, along with the color-coded, numerical key. The location of each window for a given time was consistent with the recovered panel diagram (windows labeled *a* through *p* for the 8:47 a.m. time frame). Similar to the "graying-out" of the panel schematic, the corresponding windows may be "grayed-out" in the time sequence; however, the numeric key was still visible. Only those panels in which fire was observed in at least one window (category 1, 2, or 3) were presented, regardless of whether that portion of the panel was recovered or not. All other panels not displayed were considered to have observations of category 0 (an absence of fire observations) or category 9 (the results were undeterminable). Observations for fire exposure were made from photographic and video images at roughly 2 min to 4 min intervals from the time of initial impact to collapse of the building. Thus, nearly 50 time frame observations were made for WTC 1 and 30 for WTC 2. For conciseness, only those time frames directly before, during, and directly after a visual confirmation of fire exposure in a window were shown (arrows between time frames indicate omitted observations due to lack of fire exposure during these times). The recovered panels found to have been exposed to fire were visually inspected and are discussed in Chapter 6.

2.3.1 WTC 1

Floors analyzed for exposure to fire in WTC 1 were from the 89th floor through the 110th floor. Figure 1–7 indicates the location of the fire floors with respect to the impact damage. These included all the floors above the impact zone and five stories below this zone. From the 26 recovered panels identified from WTC 1, 22 panels fall within this range, including the five from the impact region, Table 2–5. In general, fire was observed on floors 92 through 100, as well as the 104th floor. Correlating this data with the as-built location of the recovered samples, 16 panels were observed to have been exposed to fire sometime during the 1 h and 43 min that WTC 1 stood after the impact. Table 2–5 lists the specific floors where fire was observed, and Fig. 2–48 displays the time-fire exposure maps for these panels. Of these 16, 13 have recovered portions of the panel where fire exposure occurred. For the other three panels, the area where fire was observed prior to the collapse was not recovered.

2.3.2 WTC 2

WTC 2, from the 77th floor through the 110th floor, was analyzed for visual observations of fire. Figure 1–8 indicates the location of the fire floors with respect to the impact damage. Nine of the 16 panels recovered from WTC 2 resided within this region, Table 2–5. In general, fire was observed

from floors 78 through 83. No visual evidence of fire was observed (all windows were either category 0 or 9) near any of the recovered panels prior to the collapse of WTC 2.

2.4 CORE MATERIAL

Four core columns were identified as having as-built locations in the vicinity of the impacts. As seen in Fig. 1–7, two columns were from WTC 1, C-80 (603A: 92-95) and HH (605A: 98-101), and from Fig. 1–8, two were from WTC 2, C-88a (801B: 80-83) and C-88b (801B: 77-80). As stated above, the internal damage caused by the impact and subsequent travel of the higher density airframe components through the buildings could not be visually established prior to the collapse. Therefore, determination of which event caused the observed damage also was not firmly resolved from the available evidence. The following section presents computer model results of impact damage of these four core columns.

2.4.1 Computer Simulated Impact Damage of Core Columns

Computer simulation of impact damage determined that the recovered portion of the two core columns from WTC 1 (C-80 and HH) were not in the path of the aircraft debris (NIST NCSTAR 1-2B). This result was consistent with the physical location of the core columns with respect to the impact damage of the exterior panels (Fig. 1–7) as one column was above the external damage of the north face of WTC 1 and the other was below this region. Thus, damage observed on the core columns was assumed to be associated with events occurring during and after the collapse.

For the two core columns from WTC 2, the base case for aircraft impact damage indicated that the core columns were not damaged as a result of the impact. However, another analysis with parameters set to provide a more severe damage estimate indicated that the lower column sustained damage. From Fig. 1–8, the as-built location of the recovered core columns, particularly, the lower portion of C-88b (801B: 77-80), with respect to the external damage of the south face may support the latter evaluation. Therefore, impact damage may be present on this recovered core column.

2.5 SUMMARY

In correlating the post-impact, pre-collapse photographic and video images with the recovered structural elements, the following conclusions were made:

- Five exterior panels were recovered from the impact region of WTC 1; none were recovered from WTC 2. These panels were used to visually assess the amount of damage imposed on the structural elements as a direct result of the impact and evaluate the performance and/or behavior of the structural materials due to impact of the plane.

- Though representative examples of all strength/gauge combinations of steel plate used to fabricate the exterior panels from the impact regions of the towers have not been recovered, numerous gauges for all 12 grades of steel used for the perimeter panels have been recovered. Out of the 28 different strength/gauge combinations for perimeter columns in the impact region of both towers, NIST has recovered representative samples for 14. Of the 14 un-recovered strength/gauge combinations, 10 combinations were within 0.0625 in. of recovered pieces, while three were within 0.125 in., and one combination had a difference of 0.1875 in. Similarly, 7 of

the 13 strength/gauge combinations in the impact region were recovered. All six of the missing strength/gauge combinations were within 0.0625 in. of recovered strength/gauge combinations.

- Considering both towers, 7 of the 13 strength/gauge combinations in the impact regions were recovered. As seen with the column material, all six of these missing strength/gauge combinations were only 0.0625 in. from recovered strength/gauge combinations; thus, sufficient samples were available for the investigation. Computer image analysis of photographs taken of the impact hole in WTC 1 allowed for the identification of 95 percent of the modes of failure for the exterior wall columns damaged in the collision. The condition of five recovered and identified panels located around the hole before the building collapsed were largely determined.

- The number and particularly the resolution of the photos taken of the damage to WTC 2 were much less than those available for the analysis of WTC 1, allowing for identification of only 70 percent of the exterior column failure modes. Correlation to specific failure mechanisms on the panels was not possible, as none of the recovered identifiable exterior panels in NIST's possession were from the impact region of WTC 2.

- Sixteen exterior panels exposed to fire before the collapse were recovered from WTC 1; none were recovered from WTC 2. These panels were used to assess possible temperature excursions experienced by the material due to fire exposure, as well as to determine the extent of fire damage, or if fire affected the structural integrity of the structural steel component.

- Four core columns were recovered from the WTC towers; two were from each building. While pre-collapse damage could not be ascertained from photographic evidence, computer simulations indicated that impact damage may be found on the columns.

- Damage to sprayed fire-resistive material on the perimeter columns was examined in pre-collapse photographs. As expected, sprayed fire-resistive material was removed from pieces struck by the incoming aircraft or pieces exiting the far side of the building. In addition, the impact caused sprayed fire-resistive material and aluminum façade to spall off many perimeter columns which were not directly struck, but apparently suffered strong accelerations and forces otherwise transmitted through the building structure.

- Images of WTC 2 revealed some details of how the building deformed during the time between aircraft impact and collapse, and revealed how the portion of the building above the impact zone moved relative to the bottom of the building during initial stages of collapse. Approximately 18 min after the impact of the aircraft, the east face of WTC 2 exhibited inward bowing of up to 10 in. in the region of the 79th to 83rd floors. This inward bowing increased to 20 in. at a time 5 min before collapse of the tower.

- Hanging floor slabs at the 82nd and 83rd floors of WTC 2 were visible in window openings on the east and north faces, respectively, and the positions of these slabs changed over time, suggesting a slow progressive collapse mechanism of certain parts of the flooring in this area of the tower.

- At the moment of collapse of WTC 2, the top portion of the building was found to have moved to the west as it tilted to the southeast. During this tilting, a complex kink developed at the

southeast corner of the top portion in the region of the 106th floor. In addition, the top portion twisted slightly clockwise (as viewed from the top) as the collapse progressed.

From this analysis, the following 42 recovered exterior panel sections were grouped into one of four categories:

1. Unambiguously identified exterior panels with probable impact damaged

    WTC 1:   N-7, M-27, M-2, M-30, S-9

    WTC 2:   No panels recovered

2. Unambiguously identified exterior panels with exposure to pre-collapse fires

    WTC 1:   N-10, M-26, C-40, N-8, C-22, N-12, C-55, K-1, S-10, K-2, C-93
                (The panels N-7, M-27, M-2, M-30, S-9 are also considered part of this group but
                were handled separately in the first category)

    WTC 2:   No panels recovered

3. Unambiguously identified exterior panels not part of the first two groups

    WTC 1:   M-20, N-13, N-101, N-99, N-9, C-25, CC, N-1, S-1, C-10

    WTC 2:   ASCE-2, C-92, C-13/C-13a, M-10b, M-10a, S-14, C-18, C-14, M-28, C-48,
                B-1024, C-46, C-24, C-89, B-1043, B-1044

4. All other panels not identified.

Additionally, four core columns were identified as having importance to the investigation due to their as-built location with respect to the impact and fire floors:

- WTC 1:   C-80 and HH

- WTC 2:   C-88a and C-88b

The results of this work provided input for validation of the models from Projects 2, 5, and 6.
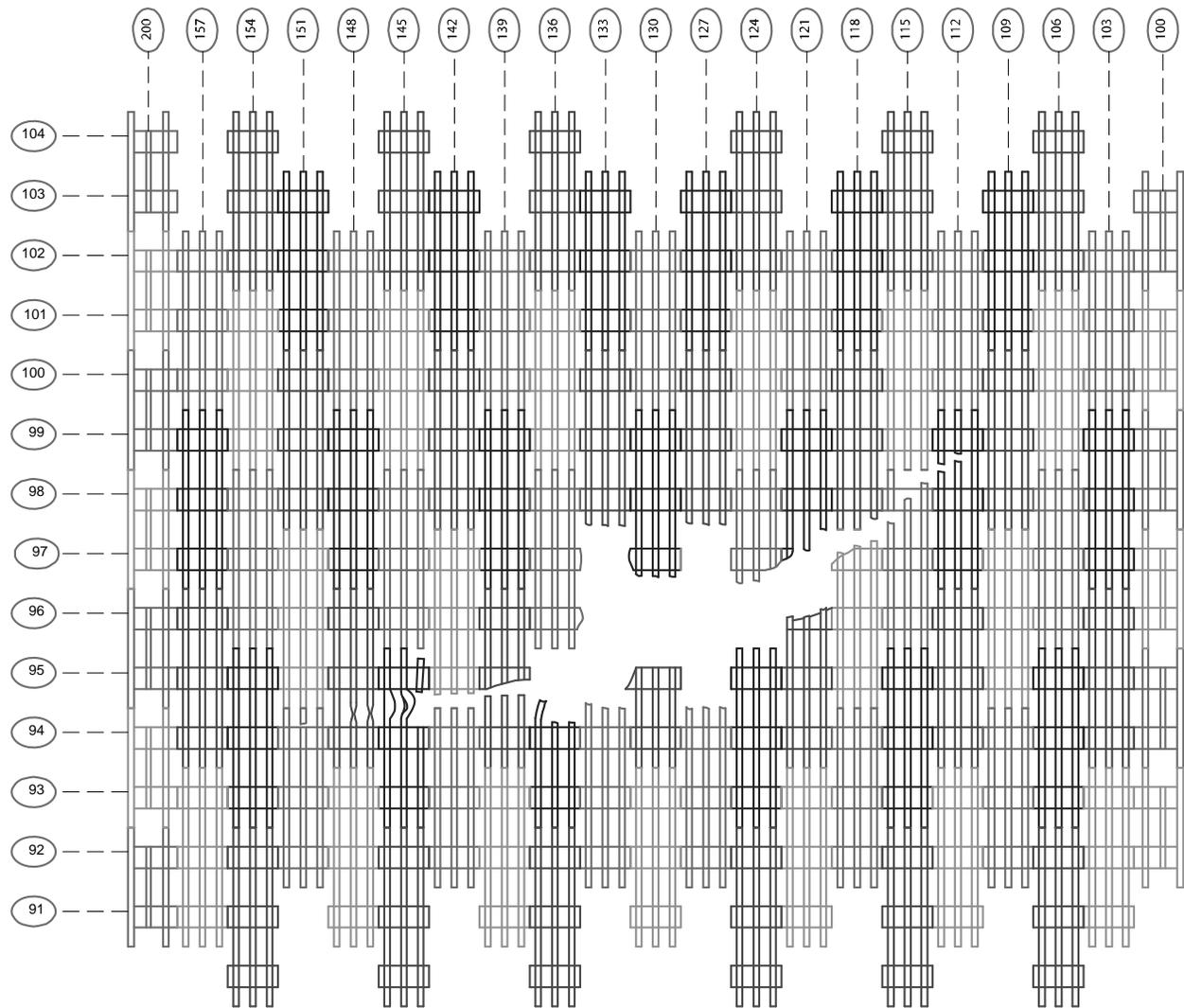
Figure 2–1. Estimated amount of damage to the north face of WTC 1, as determined by NIST.
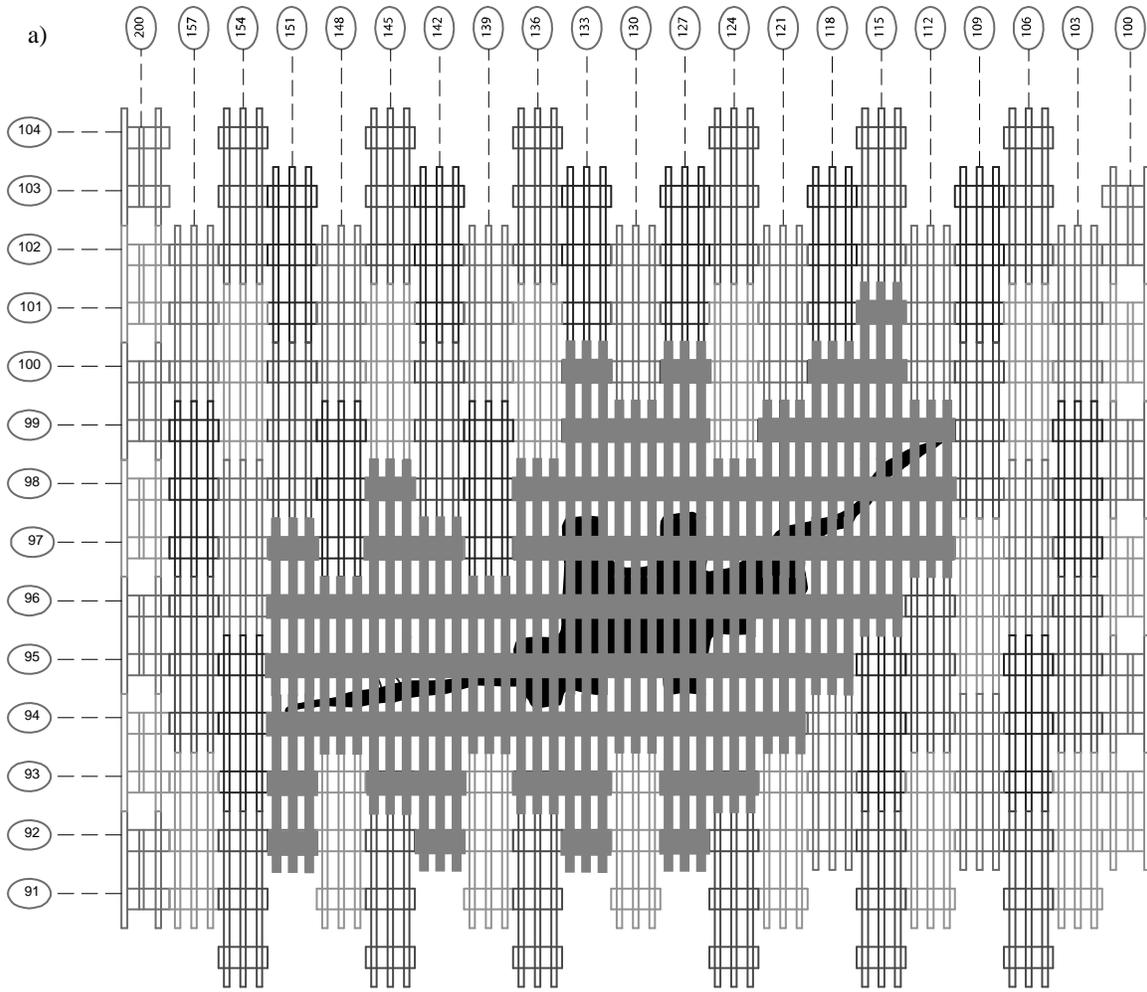
Figure 2–2a. Pictorial display showing the panels damaged on the north face of WTC 1 around the airplane impact region.

b)
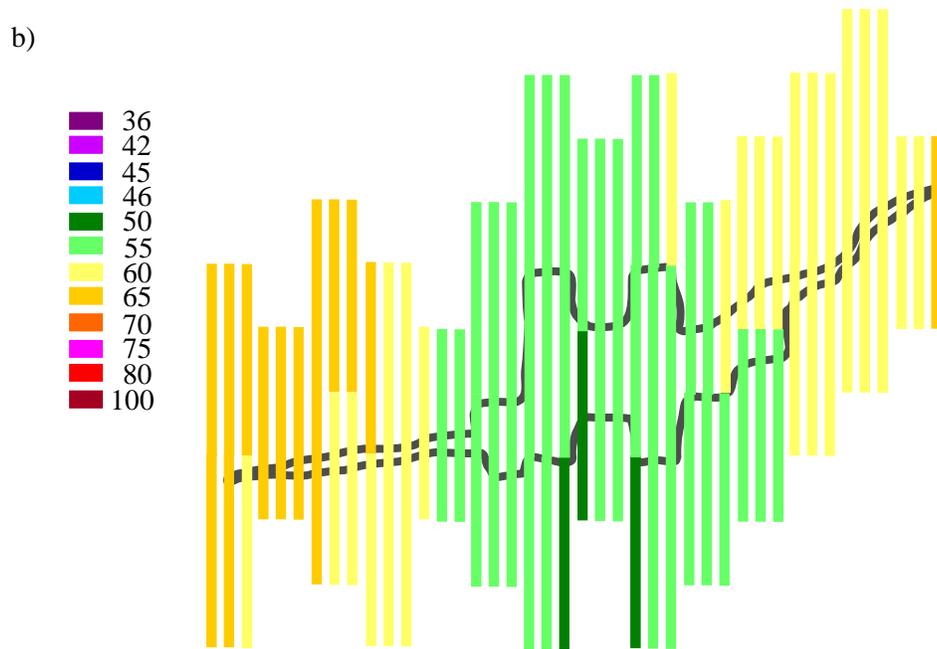
Figure 2–2b. The specified minimum yield strength of the exterior columns for WTC 1 shown in (a).
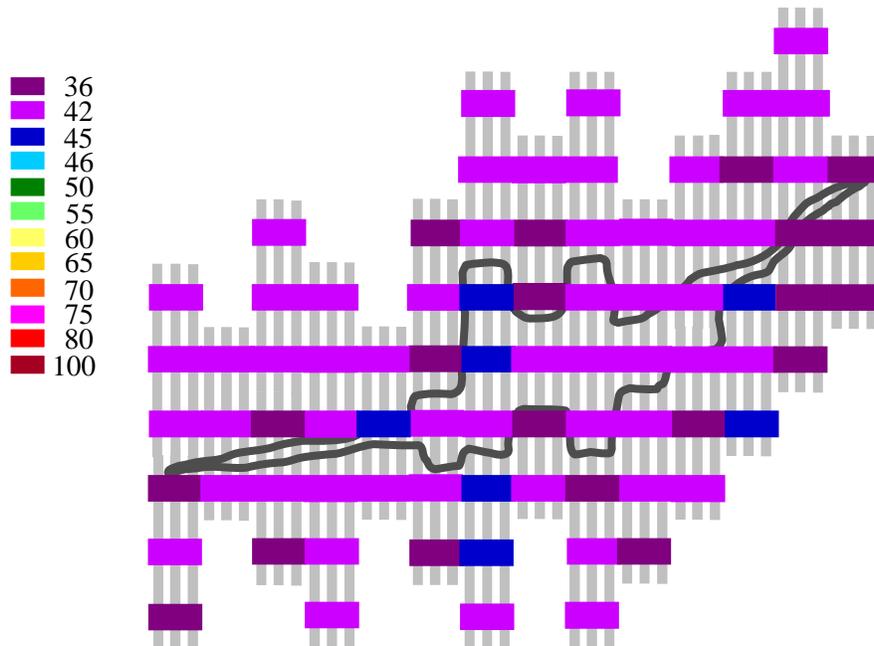
Figure 2–3. Pictorial display showing the required minimum yield strength of the spandrels on the north face of WTC 1 around the airplane impact region.

Damage in shaded area cannot be accurately determined.
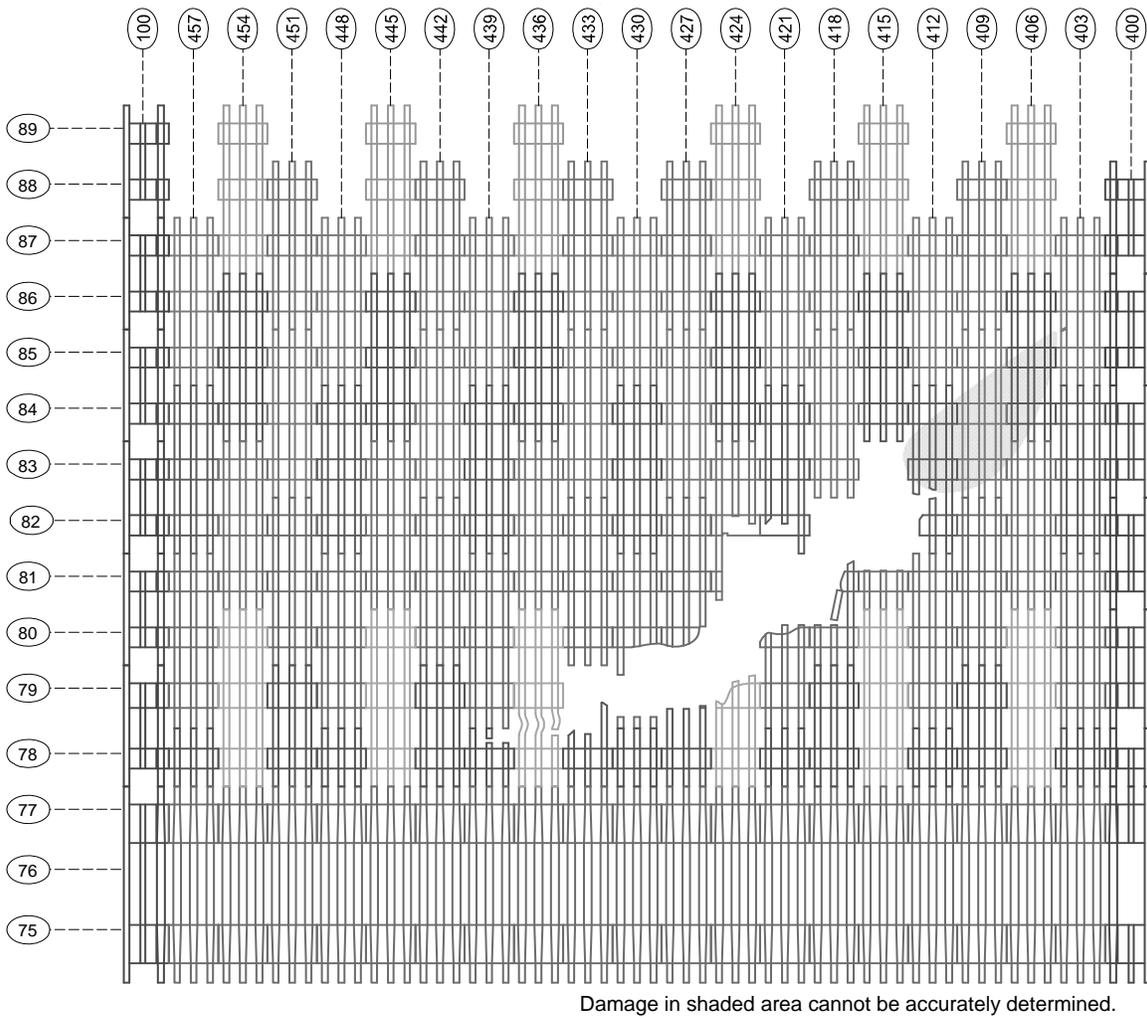
Figure 2–4. Estimated amount of damage to the south face of WTC 2, as determined by NIST.

Damage in shaded area cannot be accurately determined.
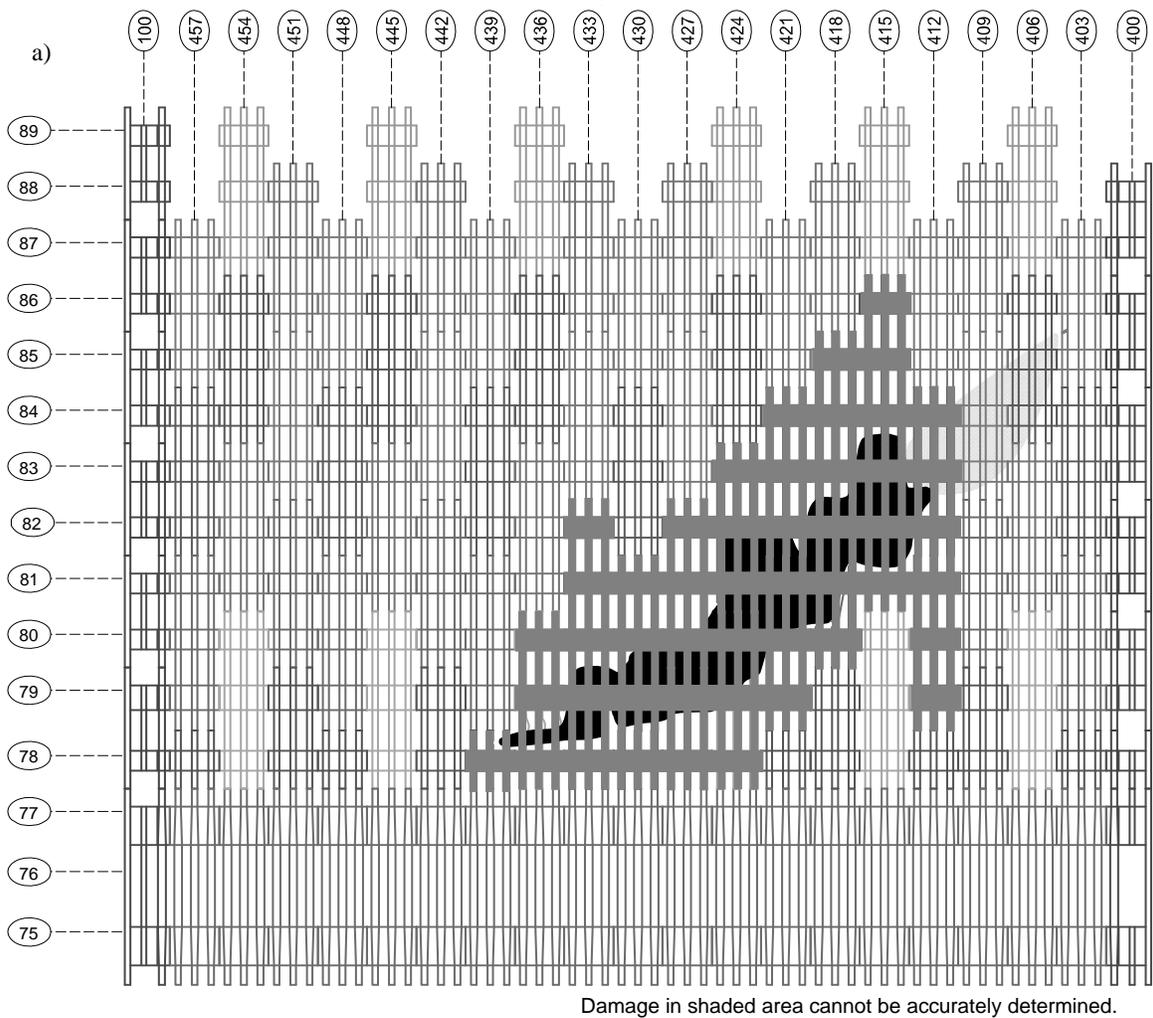
Figure 2–5a. Pictorial display showing the panels possibly damaged on the south face of WTC 2 around the airplane impact region.

b)
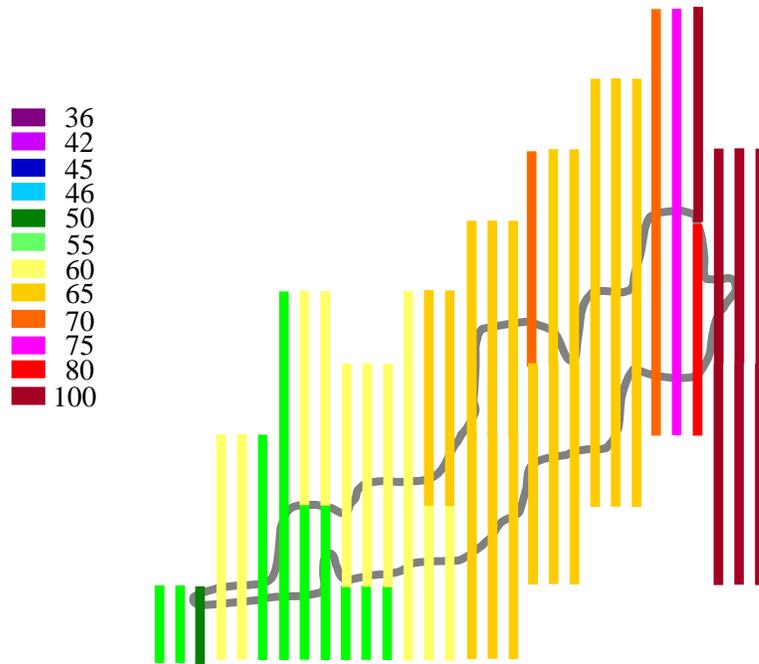
Figure 2–5b. The specified minimum yield strength of the exterior columns for WTC 2 shown in (a).
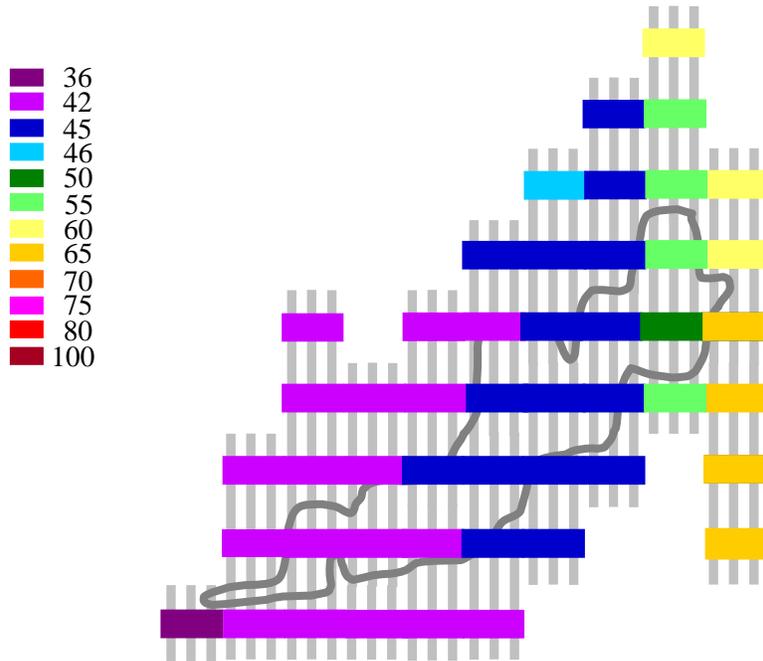
Figure 2–6. Pictorial display showing the required minimum yield strength of the spandrels on the south face of WTC 2 around the airplane impact region.

Figure 2–7. Unenhanced image Corbis_NRM161282 showing the impact hole in the north face of WTC 1.
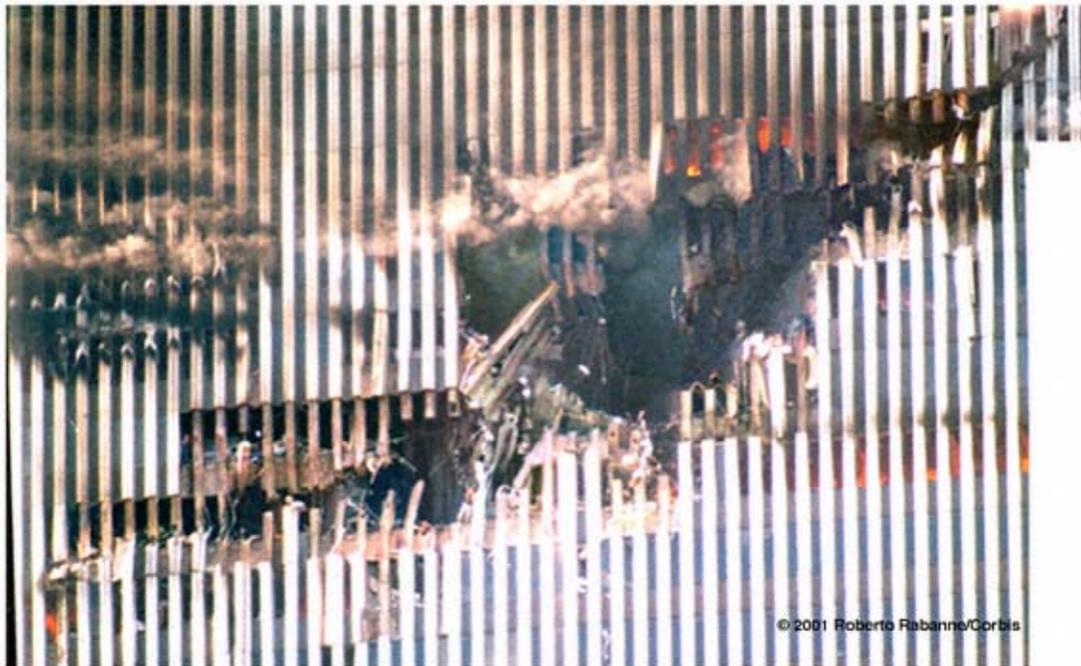
Figure 2–8. Image from Fig. 2–7 with addition of a small piece of image "7_1.jpg" (original photograph copyright Roberto Rabanne 2001), then computer image enhanced for maximum visibility of damage to exterior wall panels.

Figure 2–9. Image from Fig. 2–8 with overlay of the outline of a Boeing 767 as it appears at rest.
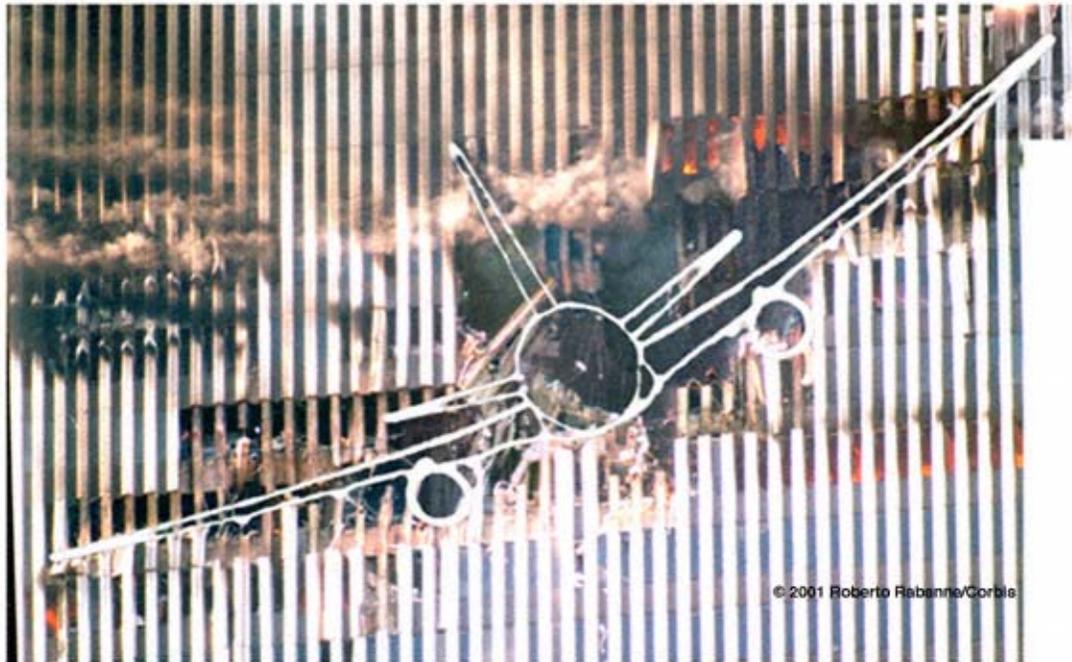
Figure 2–10. Image from Fig. 2–8 with overlay of the outline of a Boeing 767 that has been manually distorted in the computer to get a best approximate fit with damage to WTC 1.
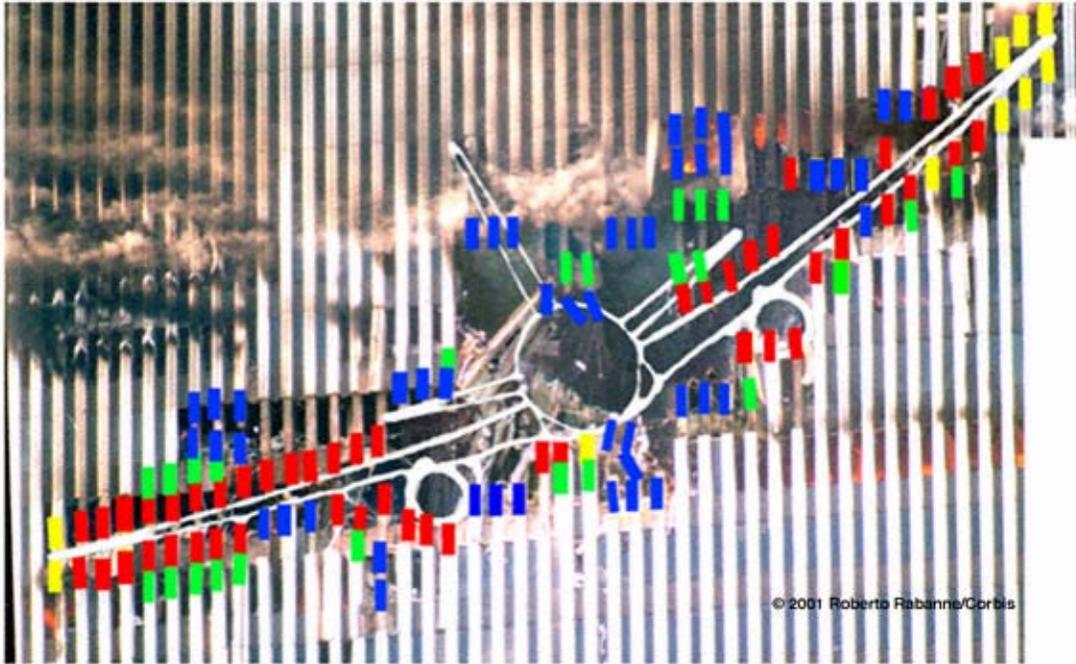
Figure 2–11. Image from Fig. 2–10 with indications of location and type of localized damage. Red designates cut metal components; blue, broken vertical column connection bolts; green, locations of failure of longitudinal welds in the box columns; and yellow shows regions that could not be identified from any photographic evidence.
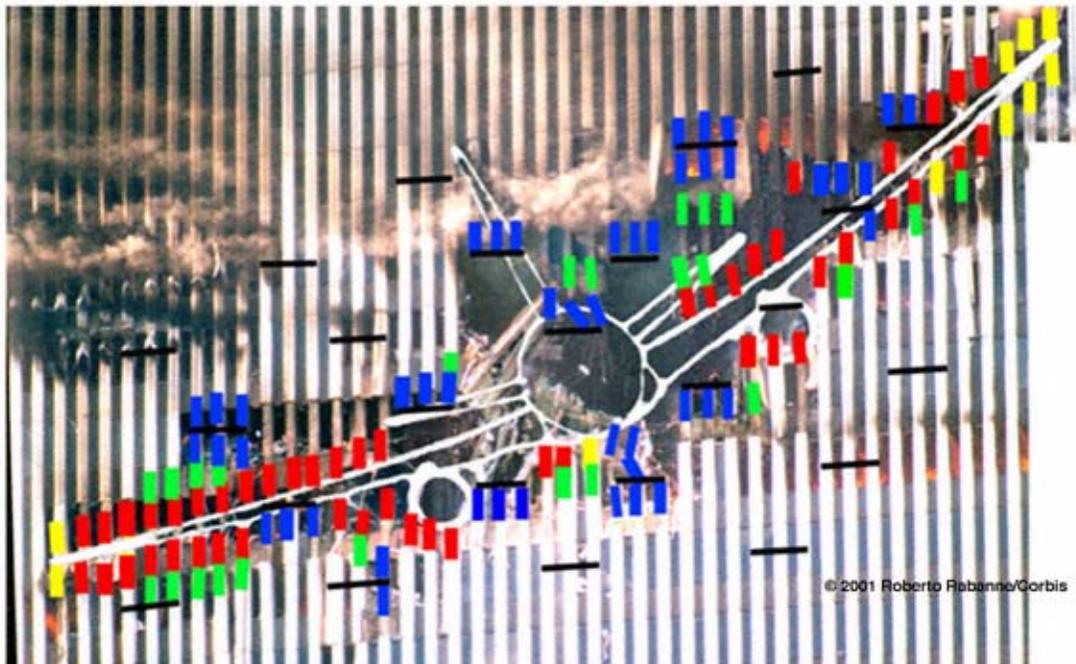
Figure 2–12. Image from Fig. 2–11 with black lines showing the location of bolted vertical column connections between panels.
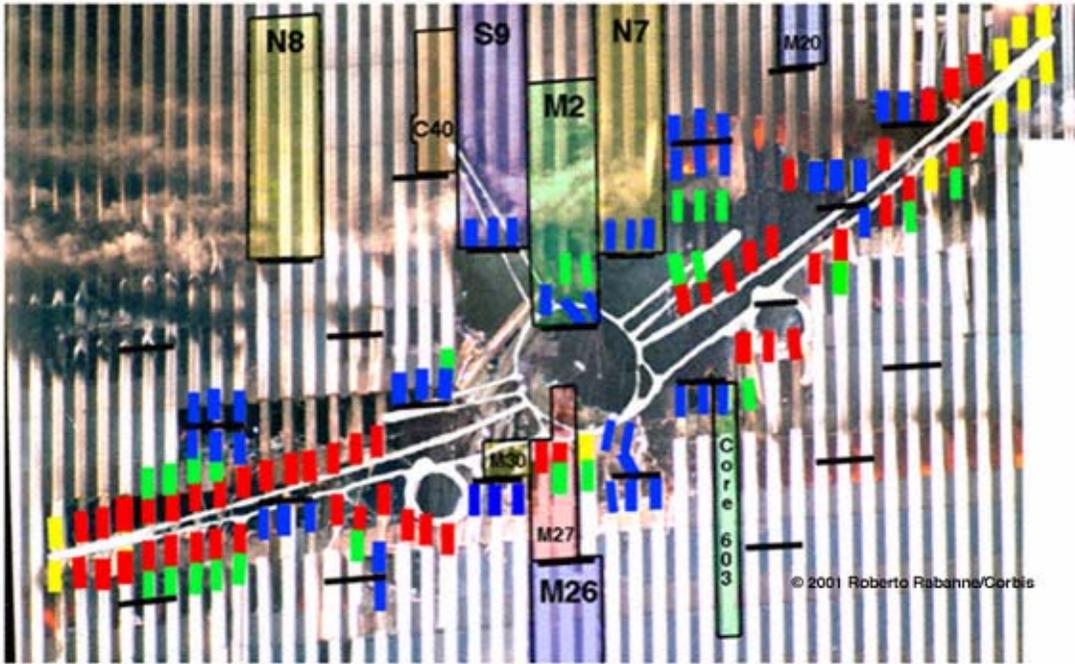
Figure 2–13. Image from Fig. 2–12 with shaded regions showing the locations of identified panels in NIST's possession from around the impact hole in WTC 1.
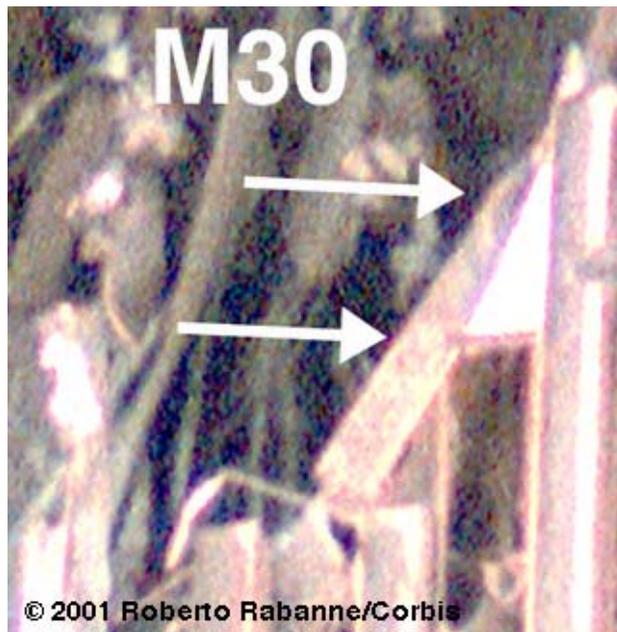
Figure 2–14. Close-up of pre-collapse condition of panel M-30 (A133: 94-97).

Figure 2–15. Close-up of pre-collapse condition of panel S-9 (A133: 97-100).

Figure 2–16. Close-up of pre-collapse condition of panel M-27 (A130: 93-96).

Figure 2–17. Close-up of pre-collapse condition of panel M-2 (A130: 96-99).

Figure 2–18. Close-up of pre-collapse condition of panel N-7 (A127: 97-100).
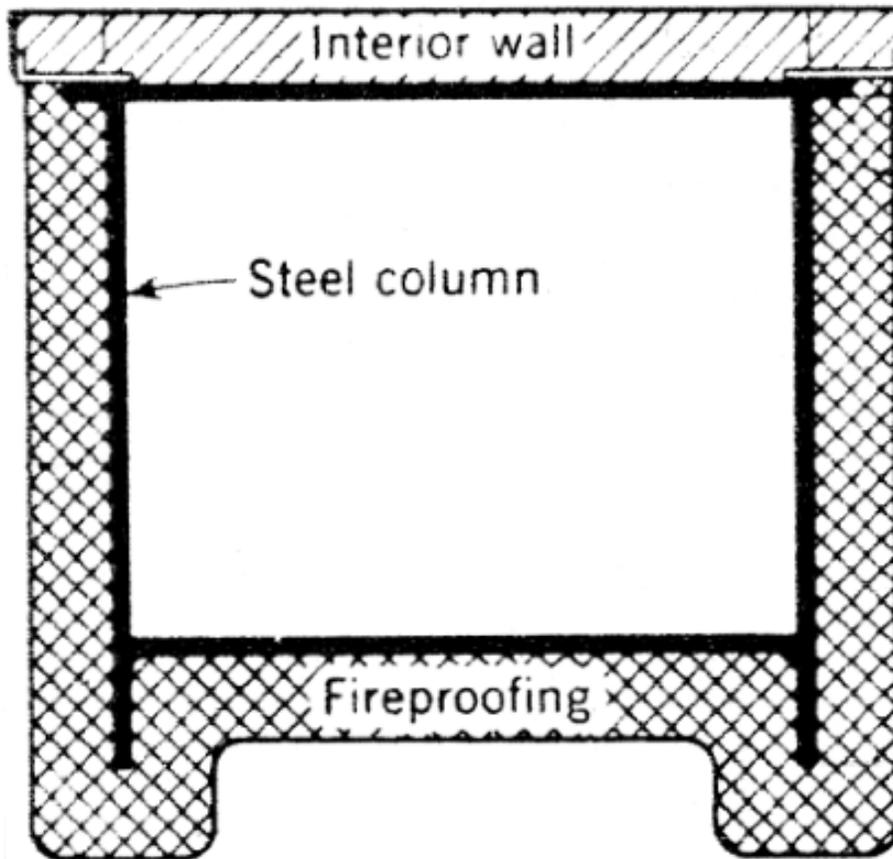
Source: Feld 1971.

Figure 2–19. Diagram showing how the sprayed fire-resistive material was to be applied to the exterior columns.
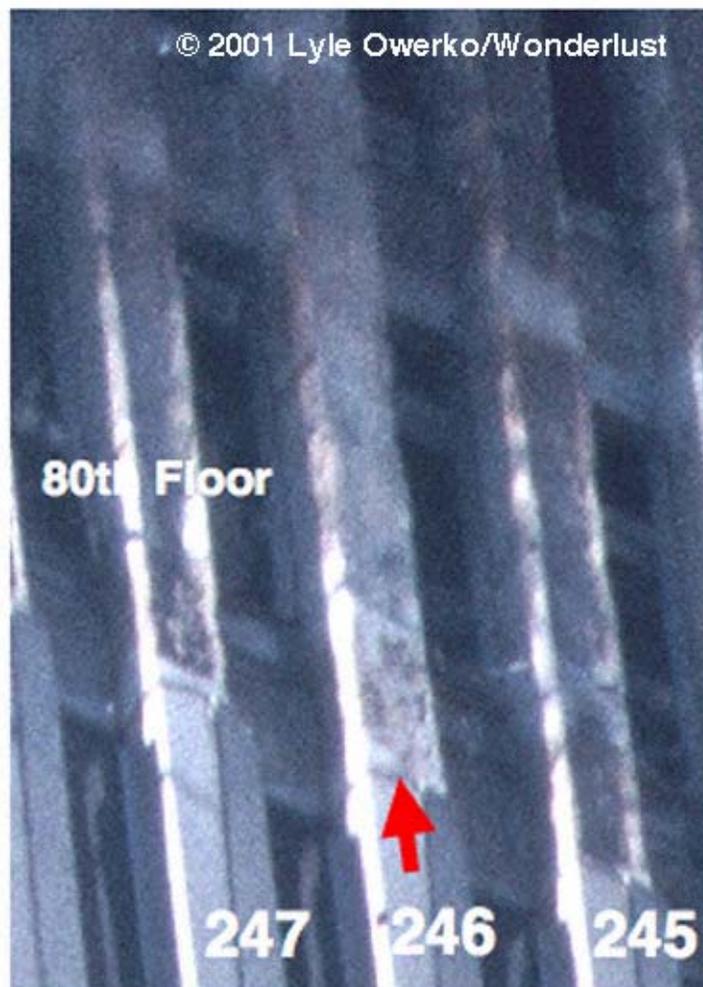
Source: Original photograph copyright Lyle Owerko 2001.

Figure 2–20. Image showing how the sprayed fire-resistive material was actually applied to the exterior columns. The depression formed by the outer web and the flange tips is completely filled in with sprayed fire-resistive material at the arrow. North face of WTC 2.
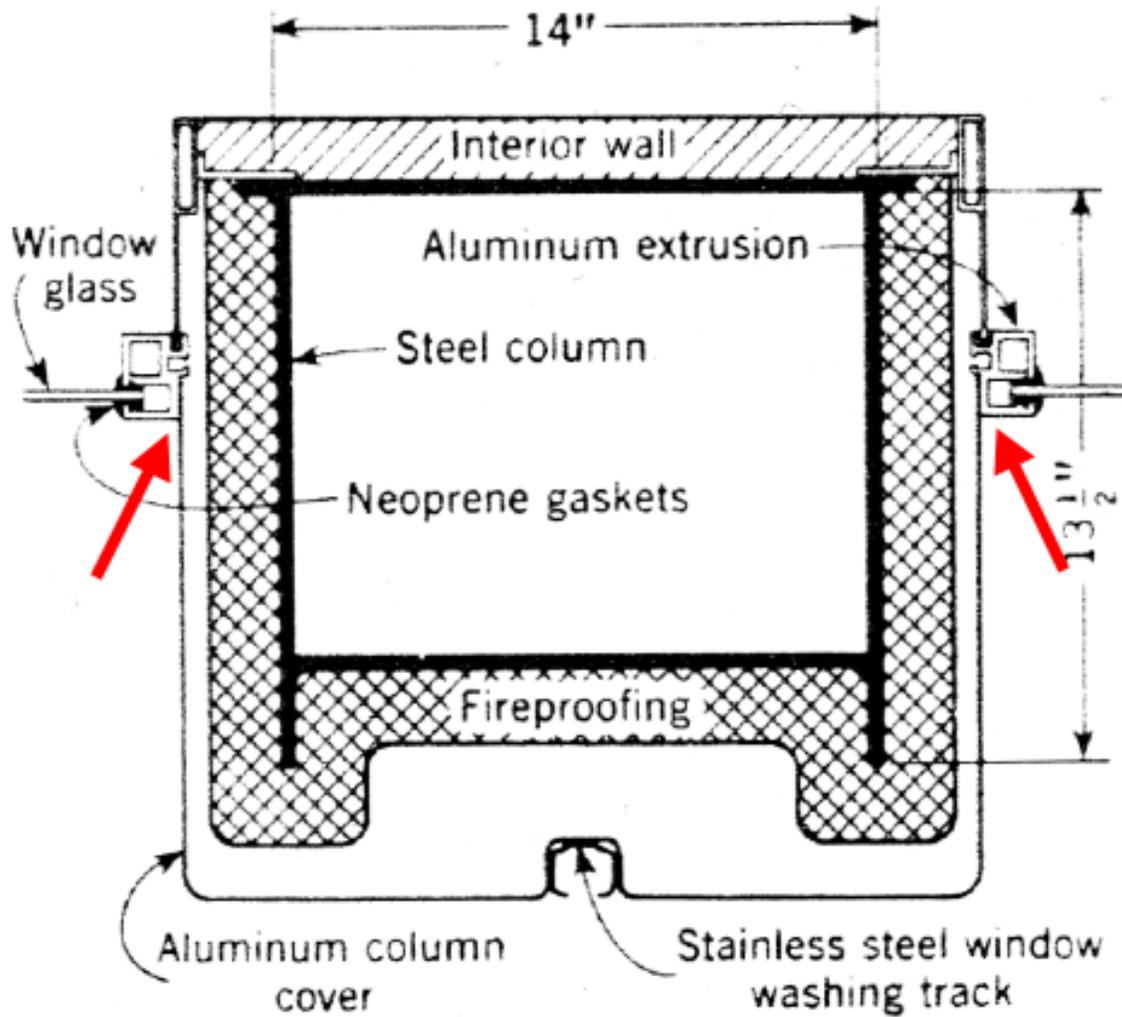
Source: Feld 1971.

**Figure 2–21. Diagram showing how the exterior
aluminum panels were attached to the window frames.**
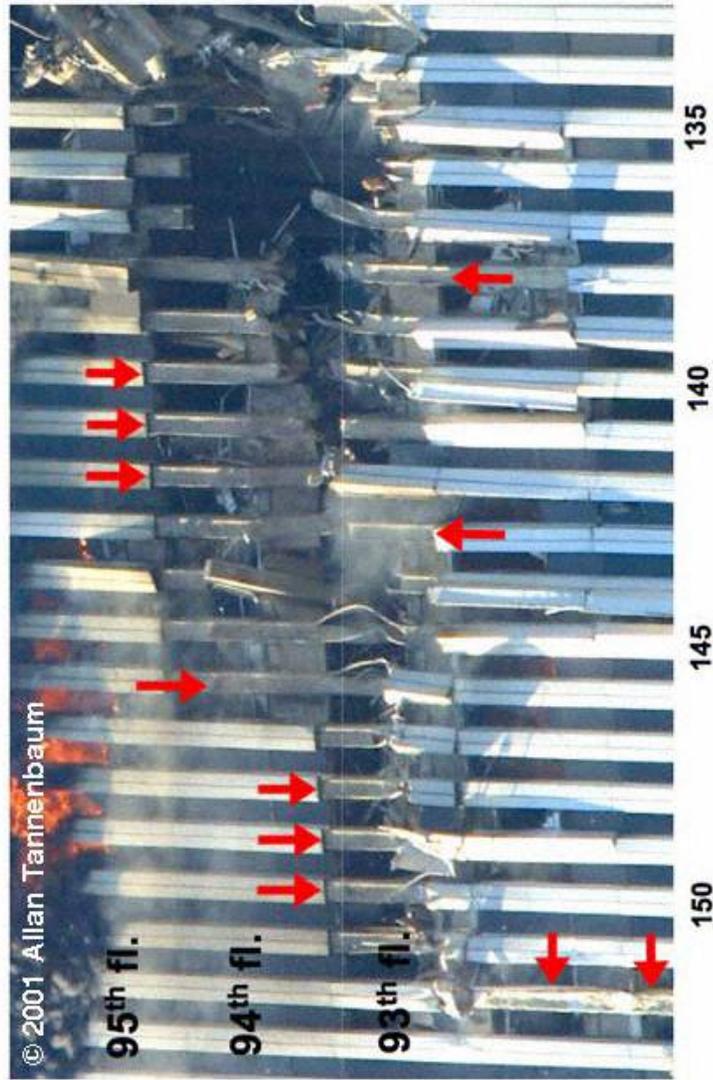
Figure 2–22. Port side of impact hole in north face of WTC 1 showing missing sprayed fire-resistive material. The red arrows indicate a few of the many instances of missing sprayed fire-resistive material around the impact hole. The region roughly approximated as the area where the aluminum panels were dislodge has been digitally enhanced for clarity.

Figure 2–23. Image showing missing sprayed fire-resistive material on floor trusses that fell into impact hole on north face of WTC 1. The arrows labeled "1" are three trusses where you can see the lower or upper chords, and can distinguish the line that separates the two angle iron components. The arrows labeled "2" lie at either end of a lower chord of a truss that fell farther inside the building, and is made up of 4 angle irons (a double truss). The red paint color being visible and the fact that the line between the angle iron can be seen indicated that the sprayed fire-resistive material was displaced.
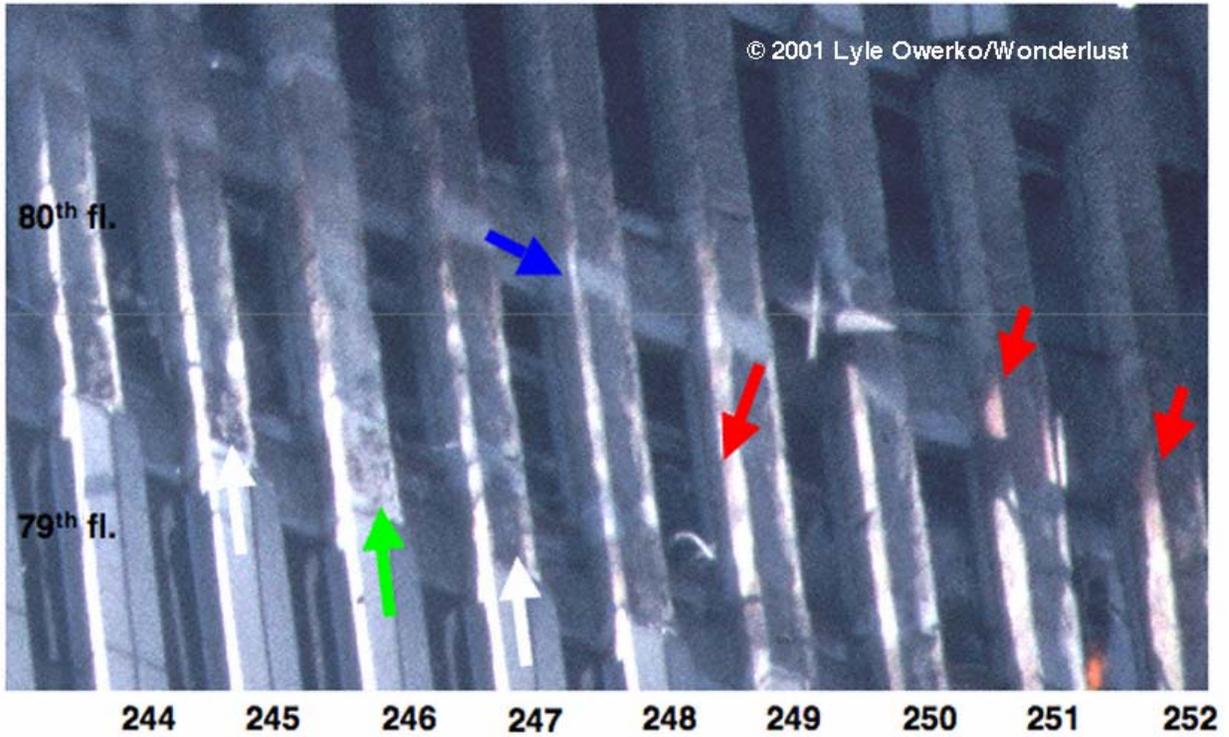
Figure 2–24. Image of inward bowing of south face (at right, with dark lines overdrawn) of WTC 1. This image was taken at 10:23 a.m. from a NYPD helicopter.
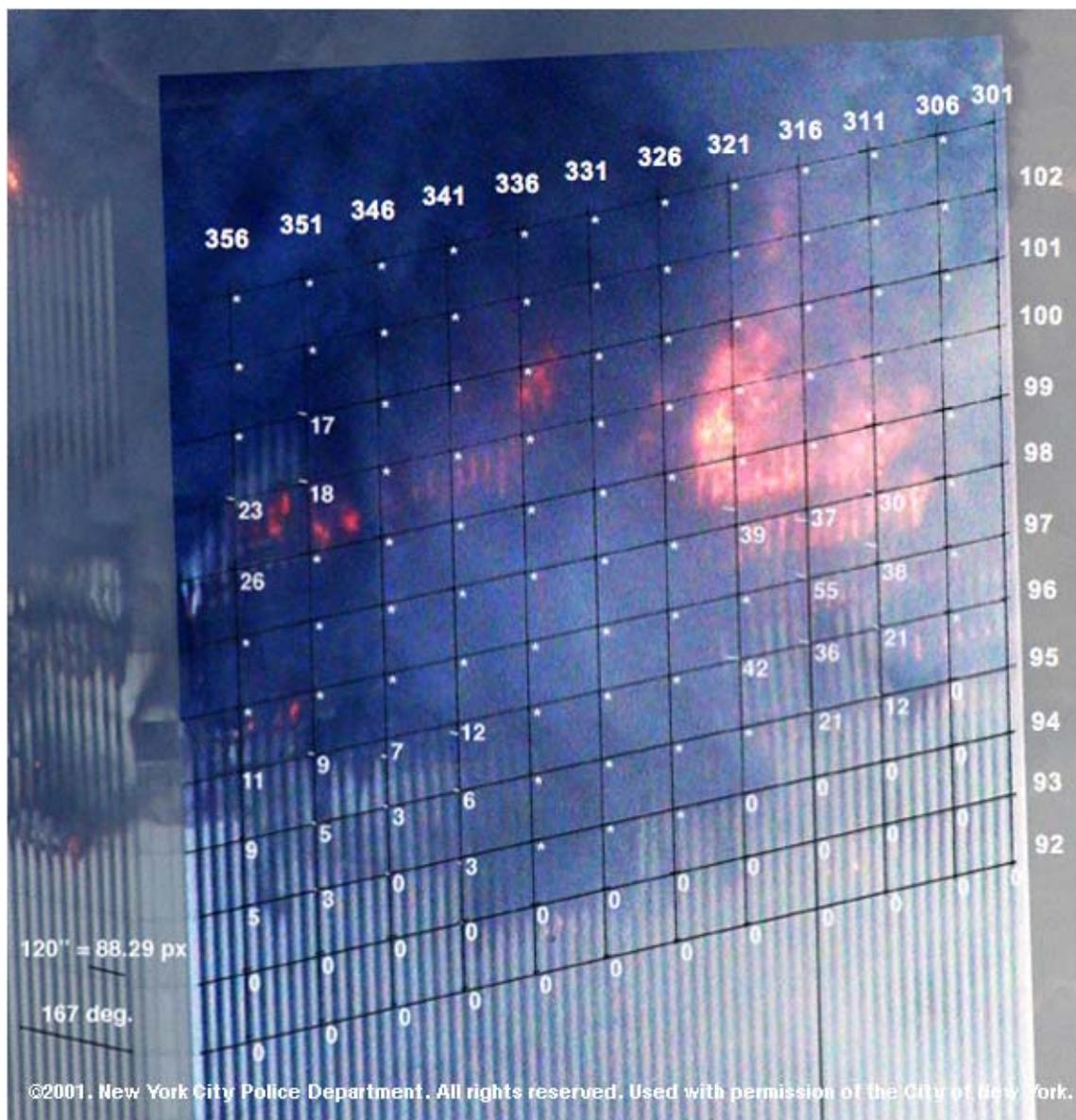
Figure 2–25. Image of pull in of south face of WTC 1 at 10:23 a.m. showing considerable displacements of the outer columns into the building. The faint white vertical features are the aluminum façade of the exterior. Maximum visible inward displacement of the columns is 55 +/- 6 in. Poor resolution of the image leads to large uncertainties in the measurements, and a large fraction of the south face of the building is obscured by smoke.

Figure 2–26. South face of WTC 1 58 min after (9:25 a.m.), showing no bowing in the outer columns.

Figure 2–27. Un-enhanced frame from "Sorensen 4 at 1-44-21.jpg" showing the impact hole in the south face of WTC 2.

Figure 2–28. Image from Fig. 2–27 computer image enhanced for maximum visibility of damage to exterior wall panels.

Figure 2–29. Image from Fig. 2–28 with indications of location and type of localized damage. Red designates cut metal components, blue indicates broken vertical column connection bolts, green indicates locations of failure of longitudinal welds in the box columns, and yellow shows regions that could not be identified from any photographic evidence.
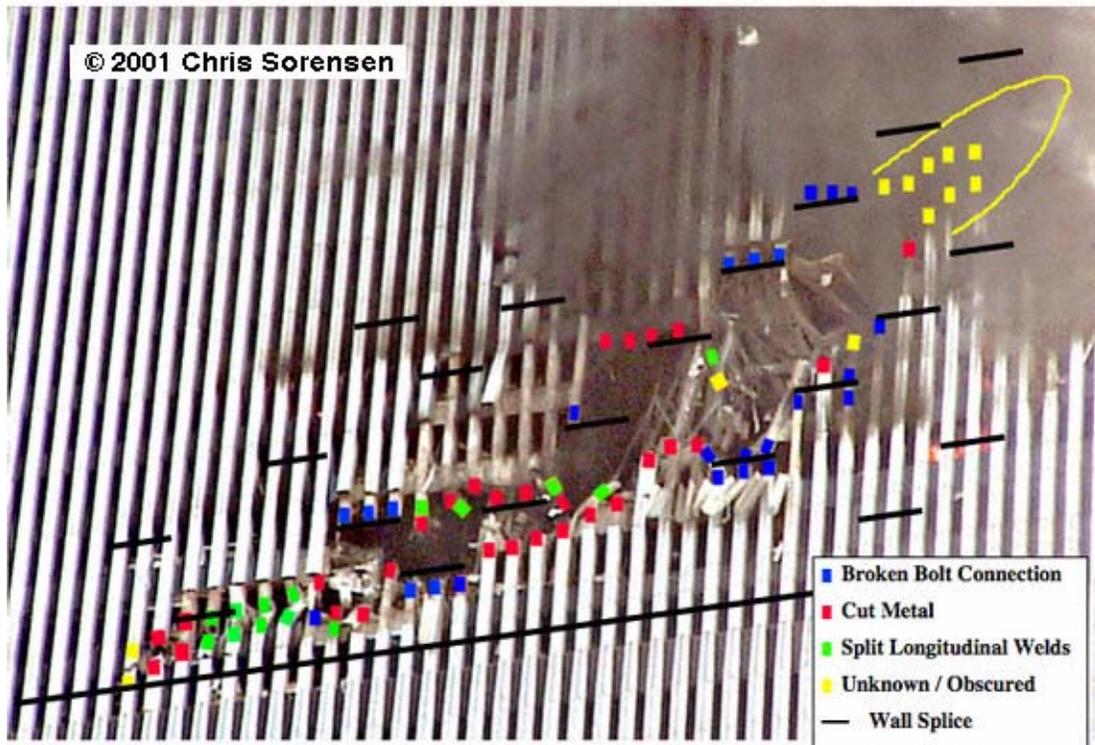
Figure 2–30. Image from Fig. 2–29 with black lines showing the location of bolted vertical column connections between panels.
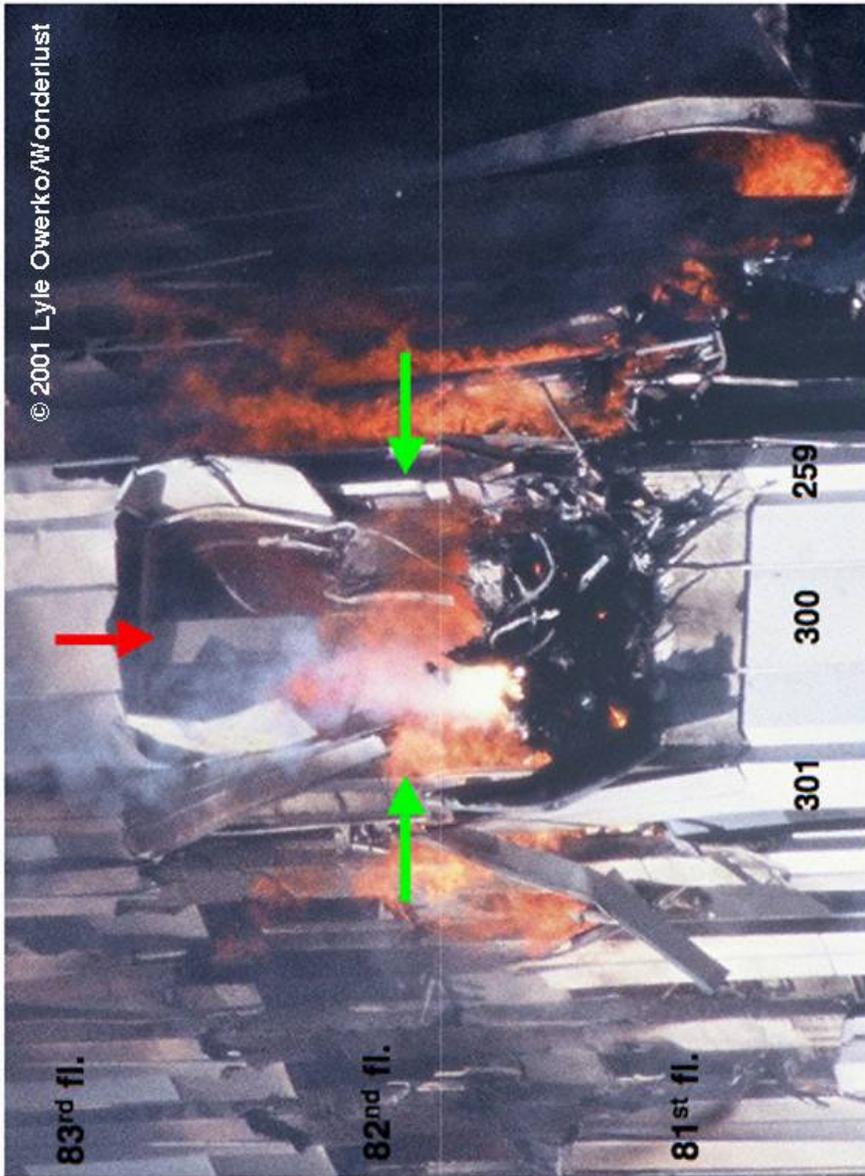
Figure 2–31. Image showing damage to NE corner of WTC 2 at 81st floor. The red arrow indicates an intact column 300 at the 82nd floor. Other photographs confirm that the spandrel connecting column 300 to columns 259 and 301 is also intact (location indicated by green arrows).
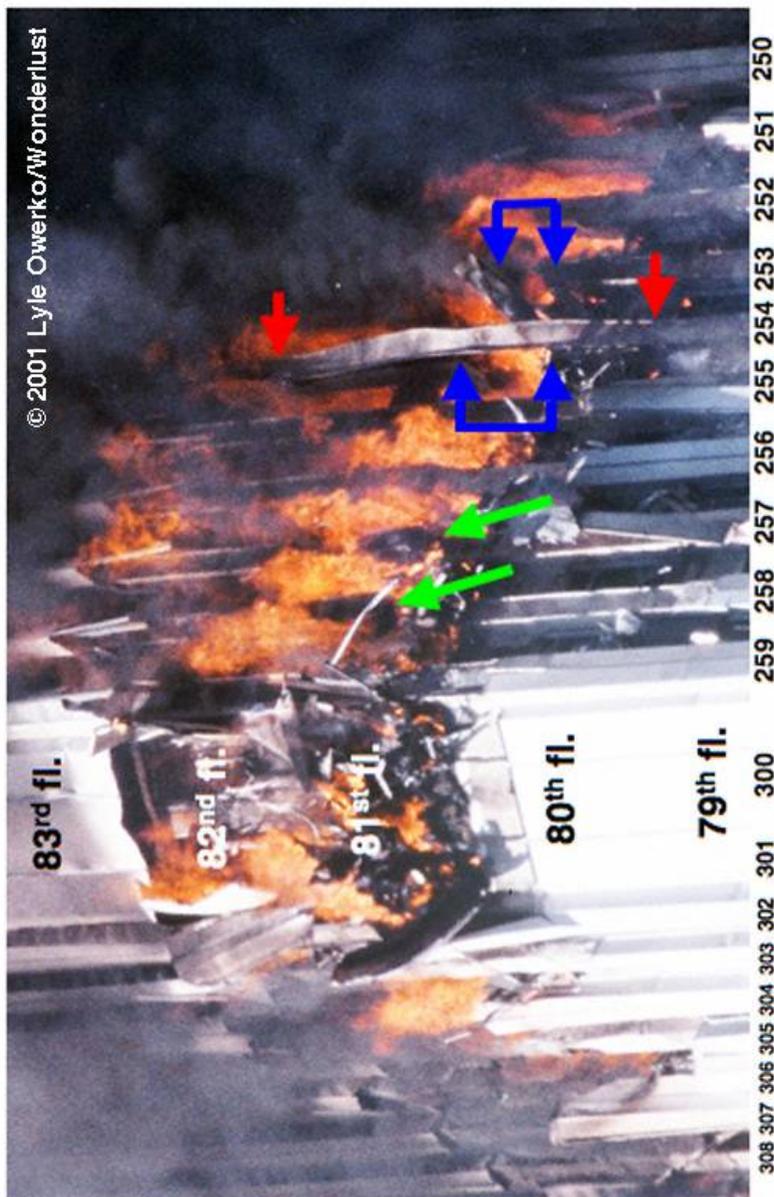
Figure 2–32. Image showing damage to columns on N face of WTC 2 near NE corner due to internal impact by debris. Broken vertical column bolted connections (green arrows) are visible, along with an intact outer web on column 254 (red arrows) and missing column sections (blue arrows).
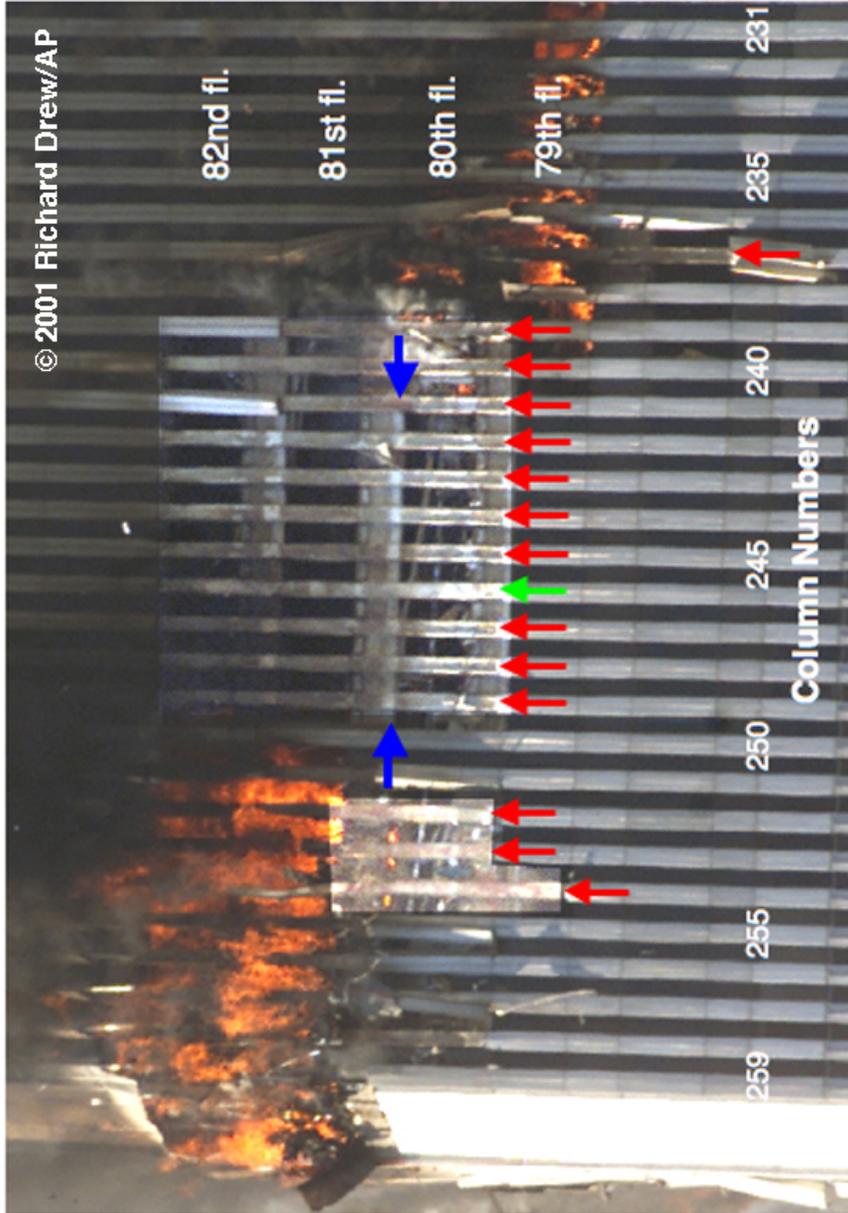
Figure 2–33. Image showing missing façade and sprayed fire-resistive material on N face of WTC 2. Two regions have had contrast and gamma adjusted to enhance visibility of the features. Red arrows indicate columns with missing or damaged sprayed fire-resistive material. Missing or damaged sprayed fire-resistive material determinations were made from this and several other photos taken at different times and angles. Blue arrows indicate white features where some sort of coating has preserved the sprayed fire-resistive material in place.
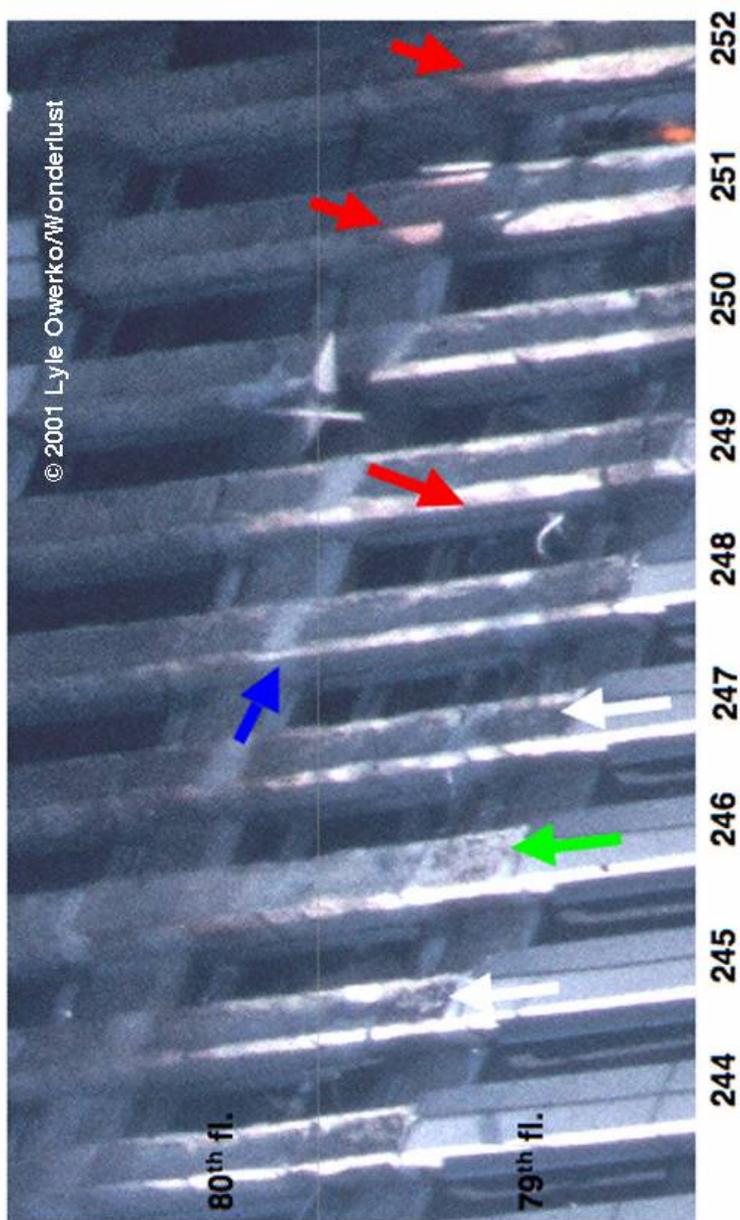
Figure 2–34. Image of missing sprayed fire-resistive material on flanges of exterior columns of N face of WTC 2. sprayed fire-resistive material has come off, revealing red Tnemec paint of the column (red arrows). This image also shows how the outer web regions have been partially or completely denuded of sprayed fire-resistive material. Damage is evidenced by shading by sunlight - compare green (undamaged sprayed fire-resistive material) and white (damaged sprayed fire-resistive material) arrows. Blue arrow indicates same type of white coated area of sprayed fire-resistive material as previous figure that adhered when material above and below was dislodged.
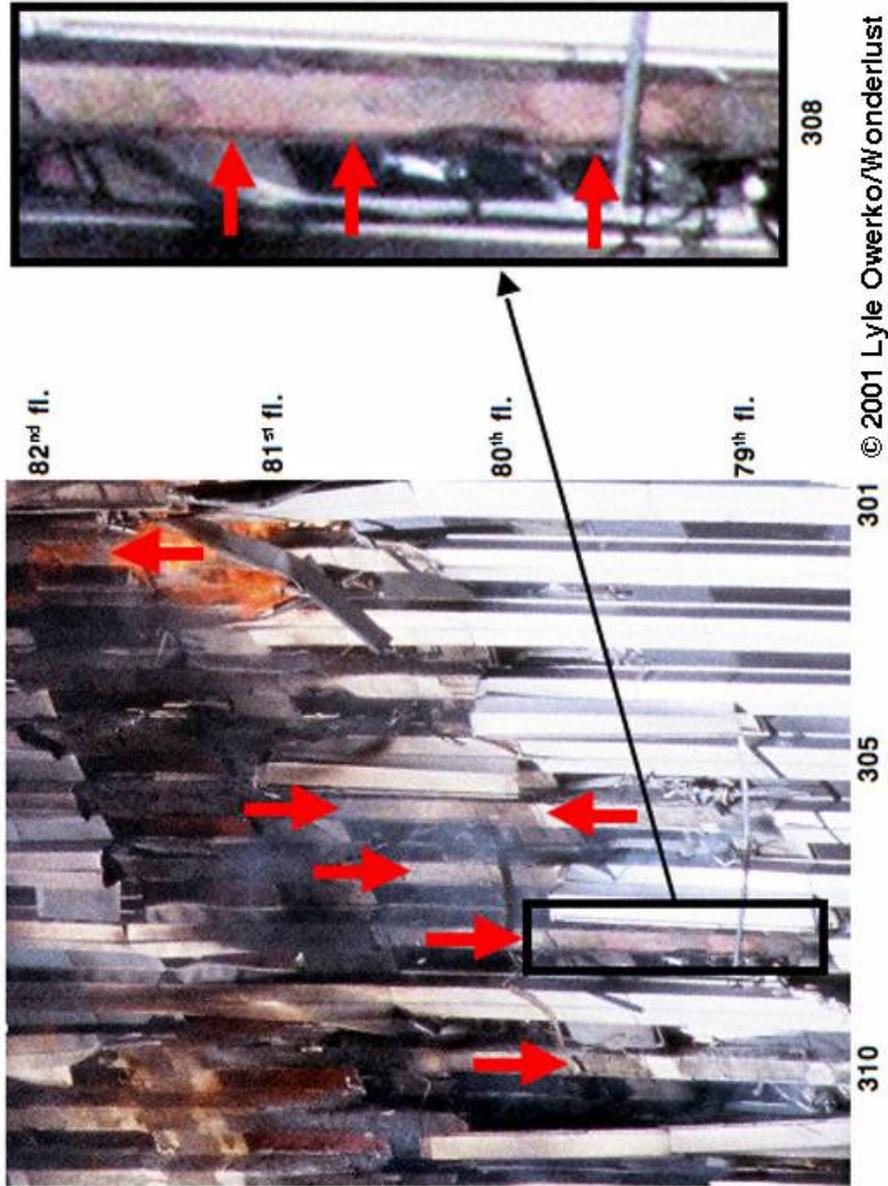
Figure 2–35. Image showing damage to sprayed fire-resistive material on east face of WTC 2 due to internal impact. Red arrows highlight areas where sprayed fire-resistive material has been damaged. The blowup to the right shows a column were the red Tnemec paint of the column is visible.

Figure 2–36. East face of WTC 2 at time 9:21:29, showing a small degree of inward deflection of the outer wall.
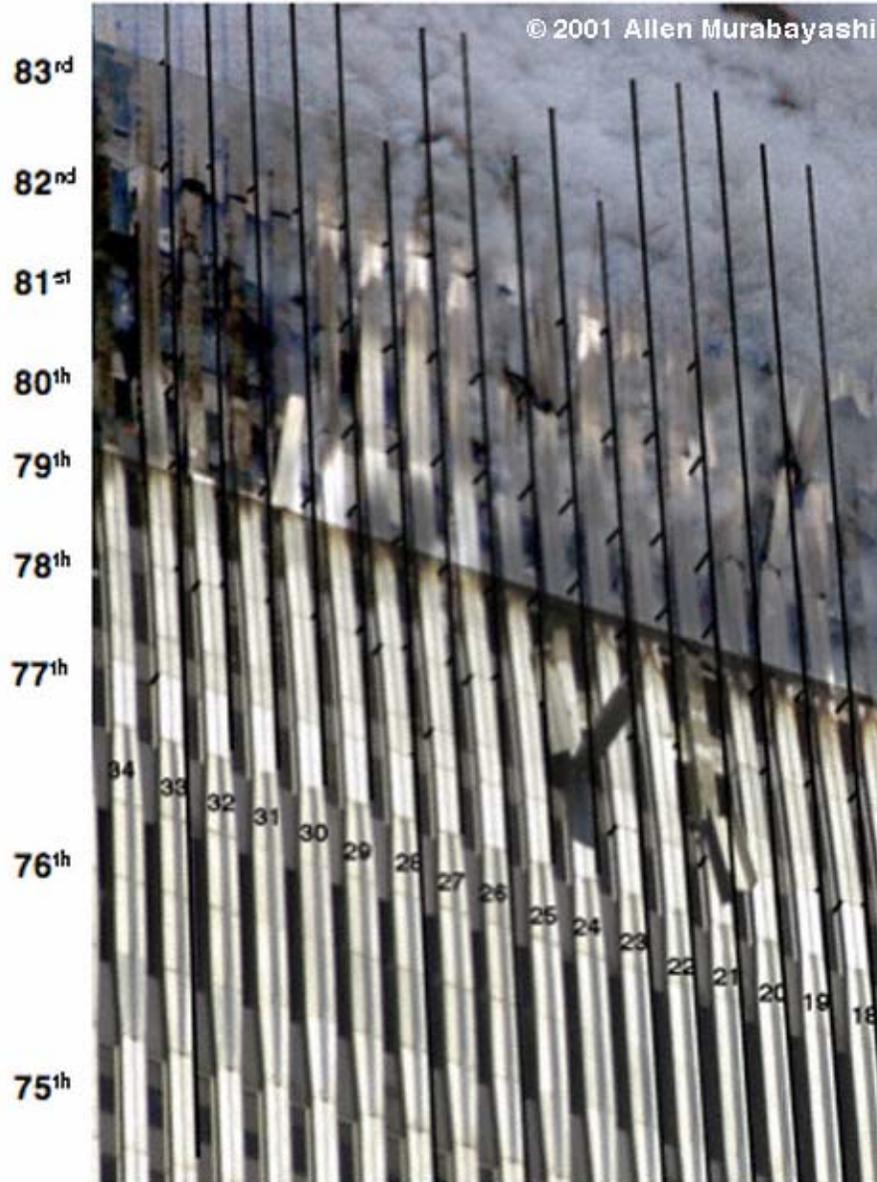
Figure 2–37. East face of WTC 2 at time 9:53:04 showing a larger amount of pull in. The vertical black lines were drawn to establish the original line of the exterior wall columns, and the shorter line segments were drawn at the same angle as the nearest observable joint in the exterior aluminum panels to establish the inward bowing distance. For actual column numbers, add a "3" to the front of the two-digit designations in the image.
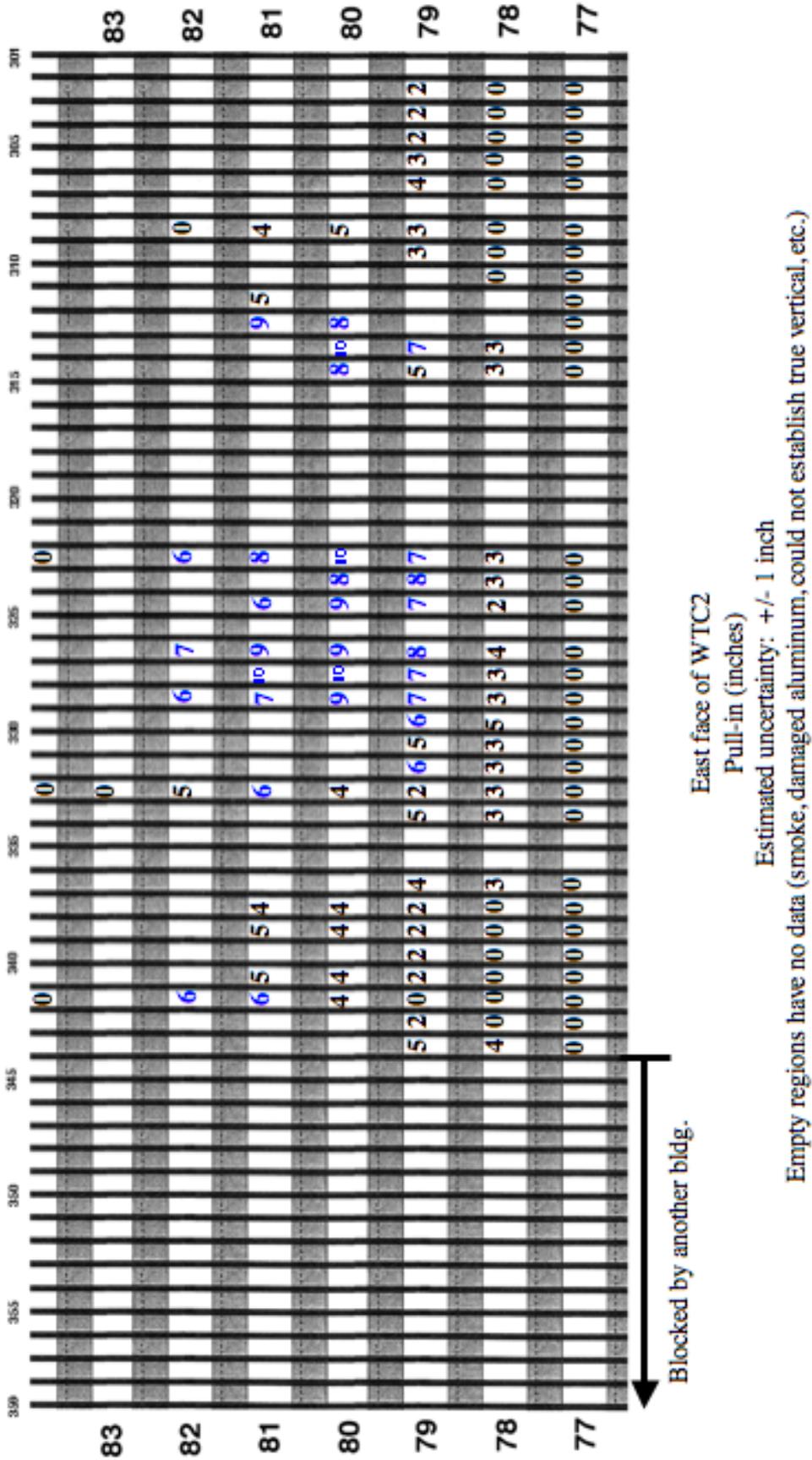
Figure 2–38. Map of inward displacements of the east outer face of WTC 2 inward at time 9:21:29 a.m. Each measurement refers to the upper left corner of the window within which the number resides. Measurements are in inches. The colors refer to groups of 5 inch displacements (0-5: black, 6-10: blue) for easier visualization.

Time: 9:52:54 AM to 9:53:04 AM

East face of WTC2

Pull-in (inches)

Estimated uncertainty: +/- 1 inch

Empty regions have no data (smoke, damaged aluminum, could not establish true vertical, etc.)

Blocked by another bldg.
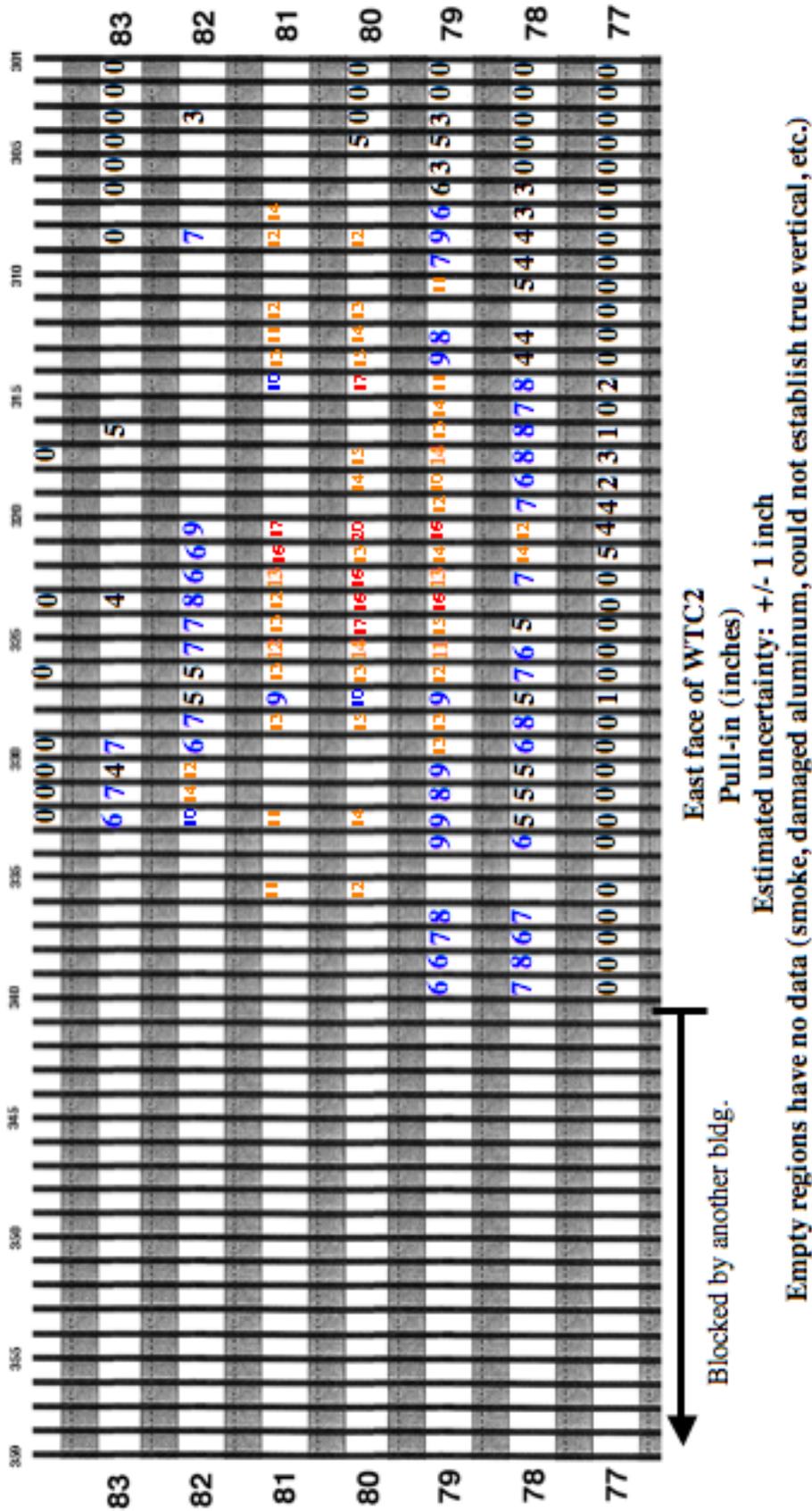
Figure 2–39. Map of pull in displacements of the east outer face of WTC 2 inward shortly before collapse. Each measurement refers to the upper left corner of the window within which the number resides. Measurements are in inches. The colors refer to groups of 5 inch displacements (0-5: black, 6-10: blue, 11-15: orange, 16-20: red) for easier visualization. This data was combined from two images taken by the same photographer at nearly the same location 10 s apart, and it is assumed that the inward deflection did not change appreciably during this time.
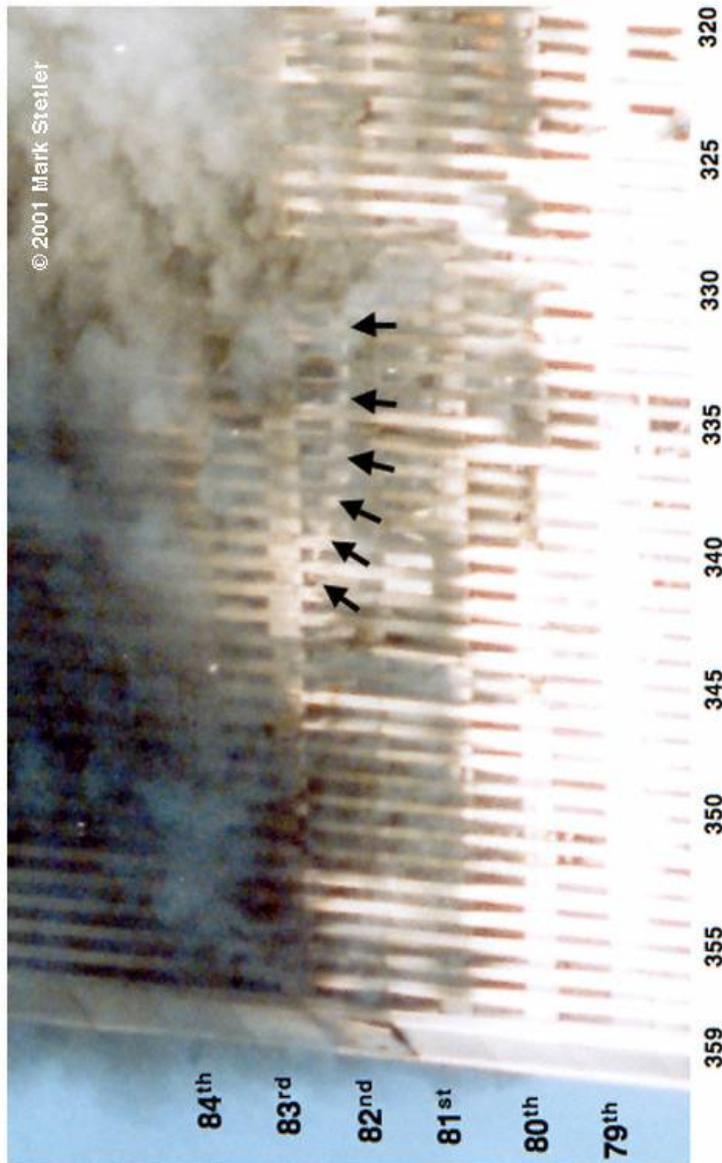
Figure 2–40. Image of dropped floor on east face of WTC 2. The slab of the 83rd floor has partially collapsed onto the 82nd floor.
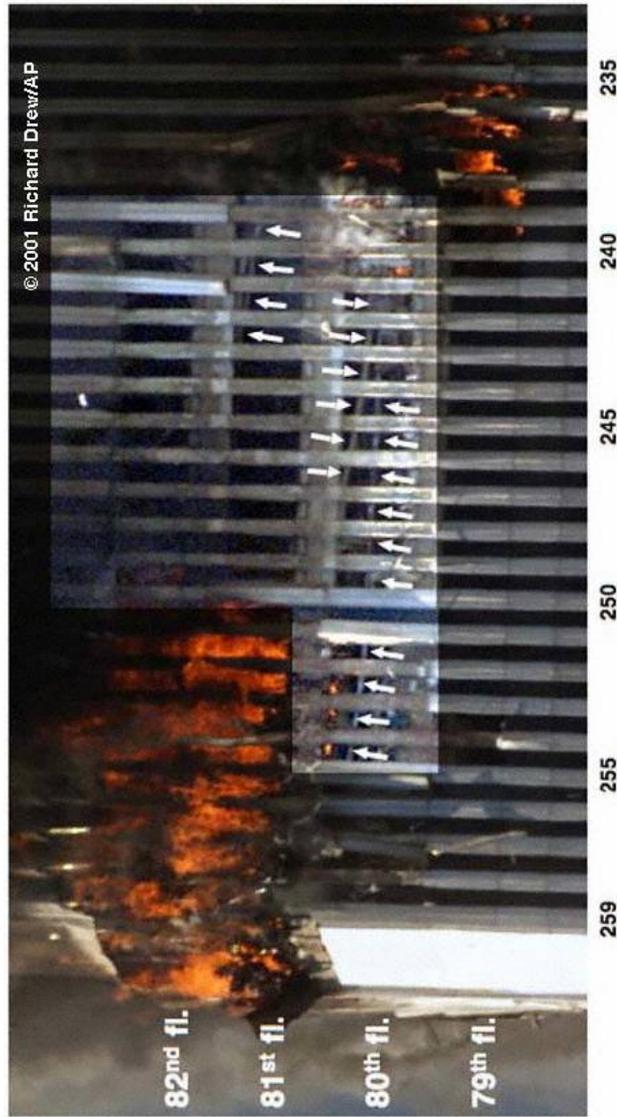
Figure 2–41. Image of dropped floors on north face of WTC 2.

Figure 2–42. Image of dropped floor on north face of WTC 2. The slab of the 81st floor has dropped into the office space of the 80th floor.

© 2001 Gulnara Samoilova /AP

Figure 2–43. Image showing initial seconds of collapse of WTC 2 viewed from the ENE, and kink in the SE edge of the building near the 106th floor (arrow).
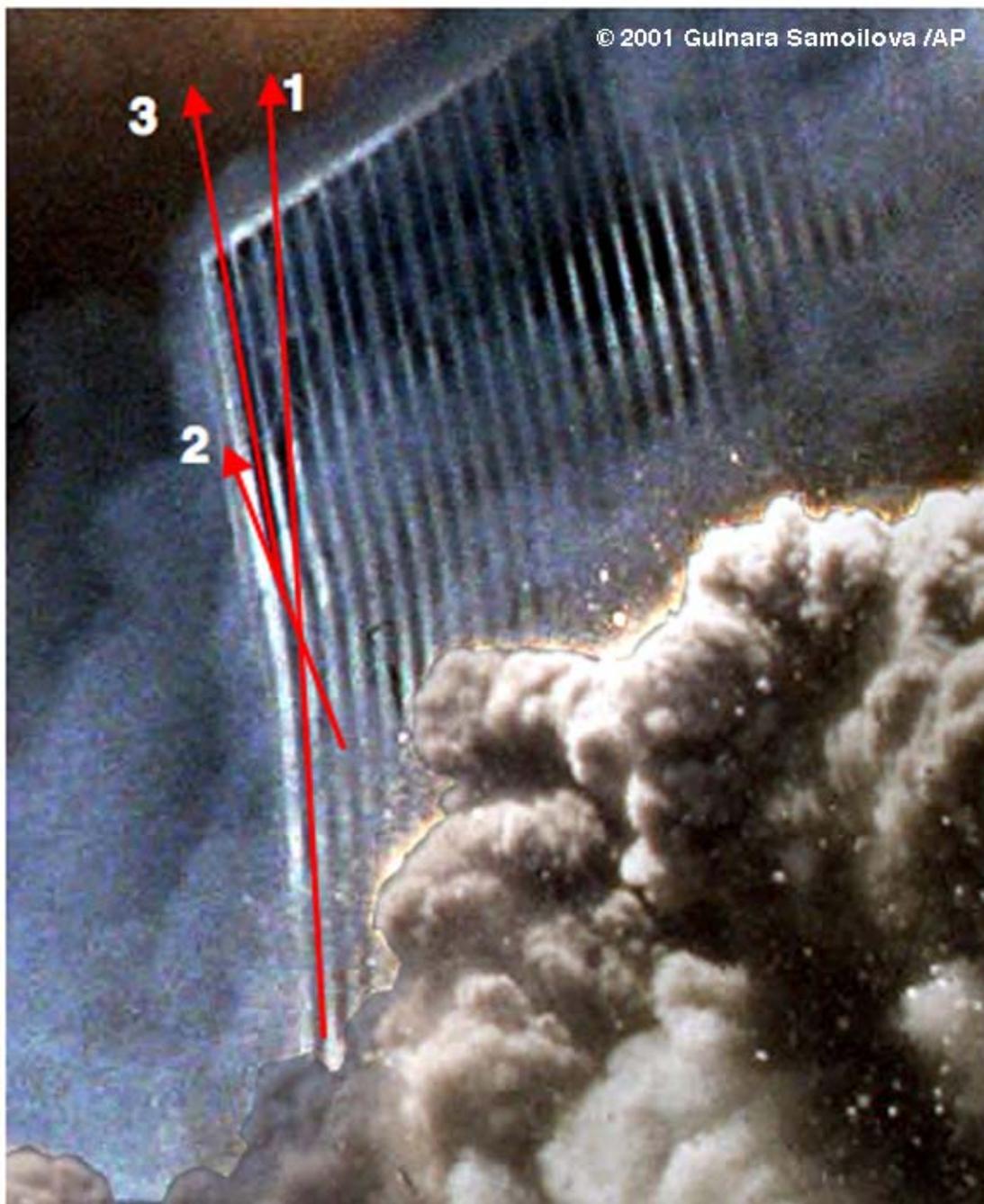
Figure 2–44. An enhanced close-up of the kink area in the previous figure (SE corner, WTC 2), with overlaid lines to highlight the details of the kink geometry. The edge of the building (1) bends an angle to another direction (2), then bends back somewhat toward the original direction (3).
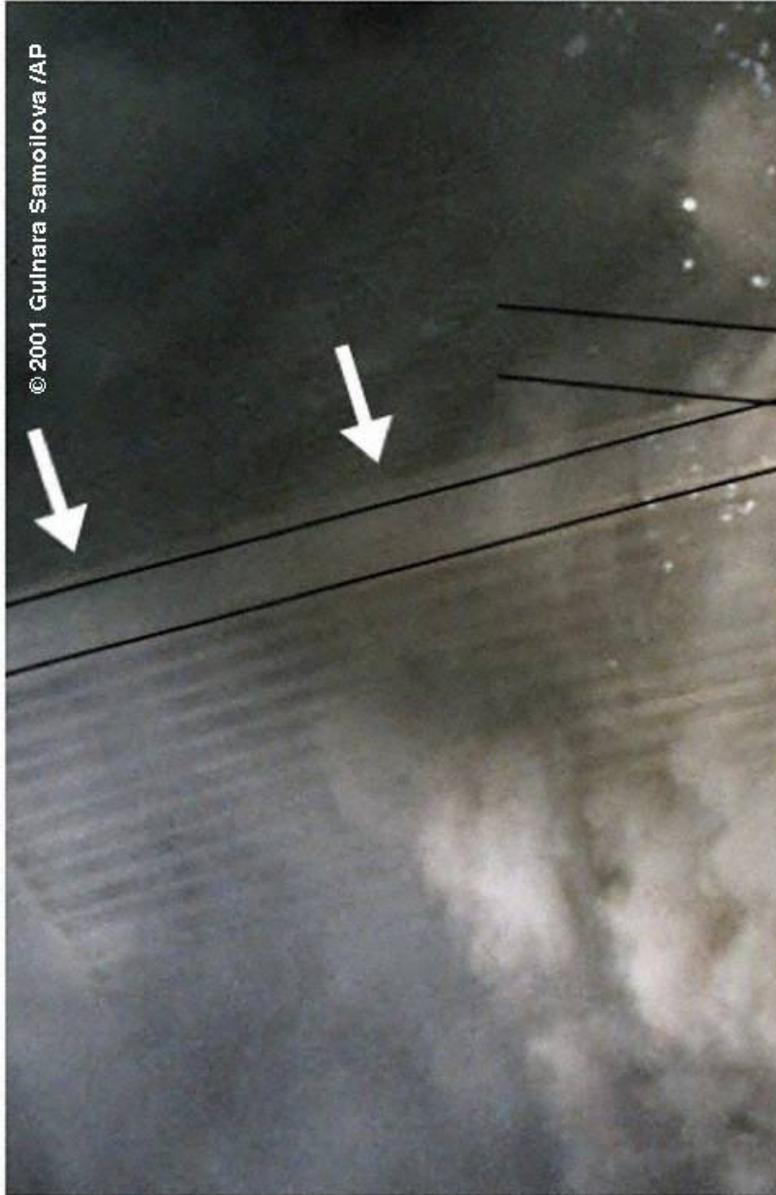
Figure 2–45. Close-up view of the northeast corner of WTC 2 during the first seconds of collapse. The white arrows indicate that the edge near column 259 bends gradually in the region that exhibits a kink at the SE corner.
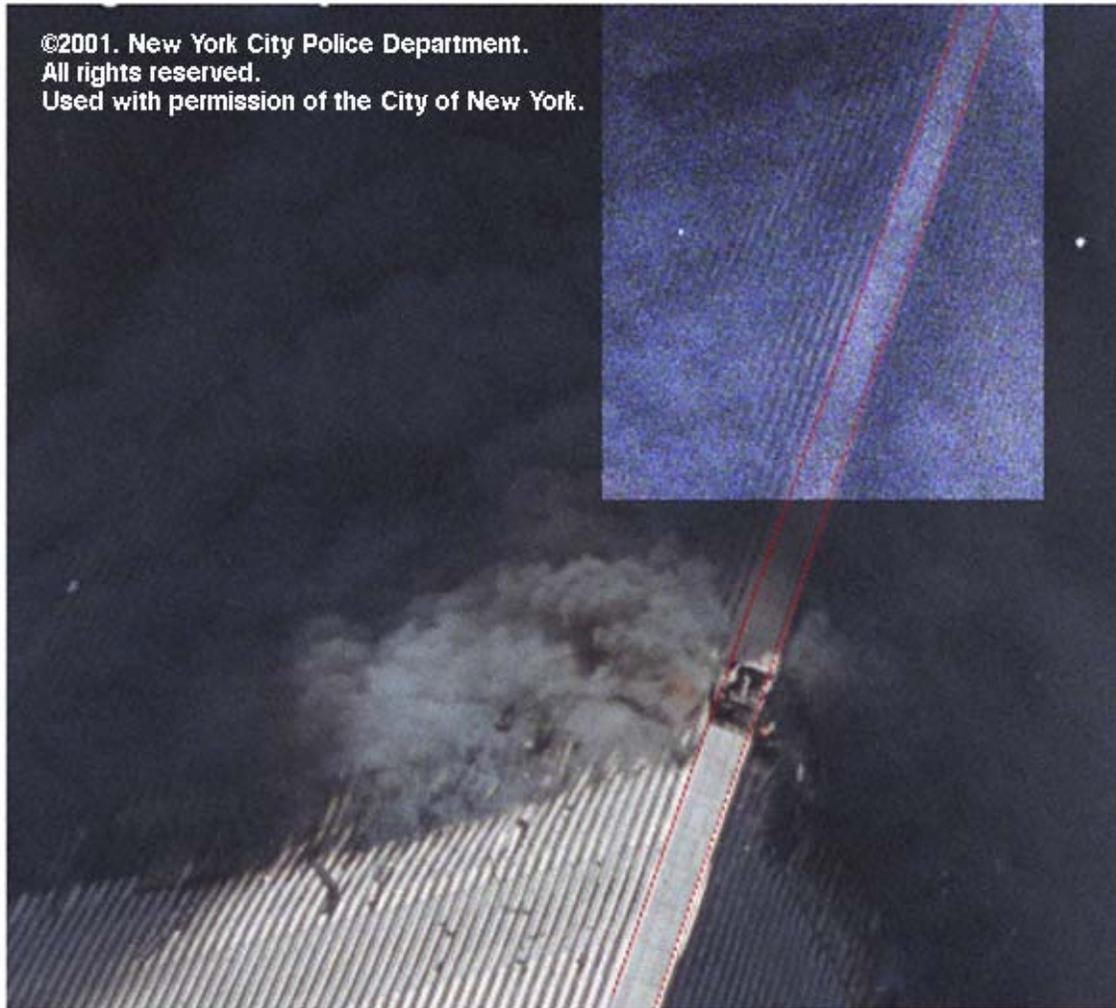
Figure 2–46. Image of the NE corner of WTC 2, several seconds before collapse. The corner shows no distortion of the type in the previous figure. This would imply that the distortion accompanied the collapse and did not precede it. The region in the upper right is enhanced for visibility.
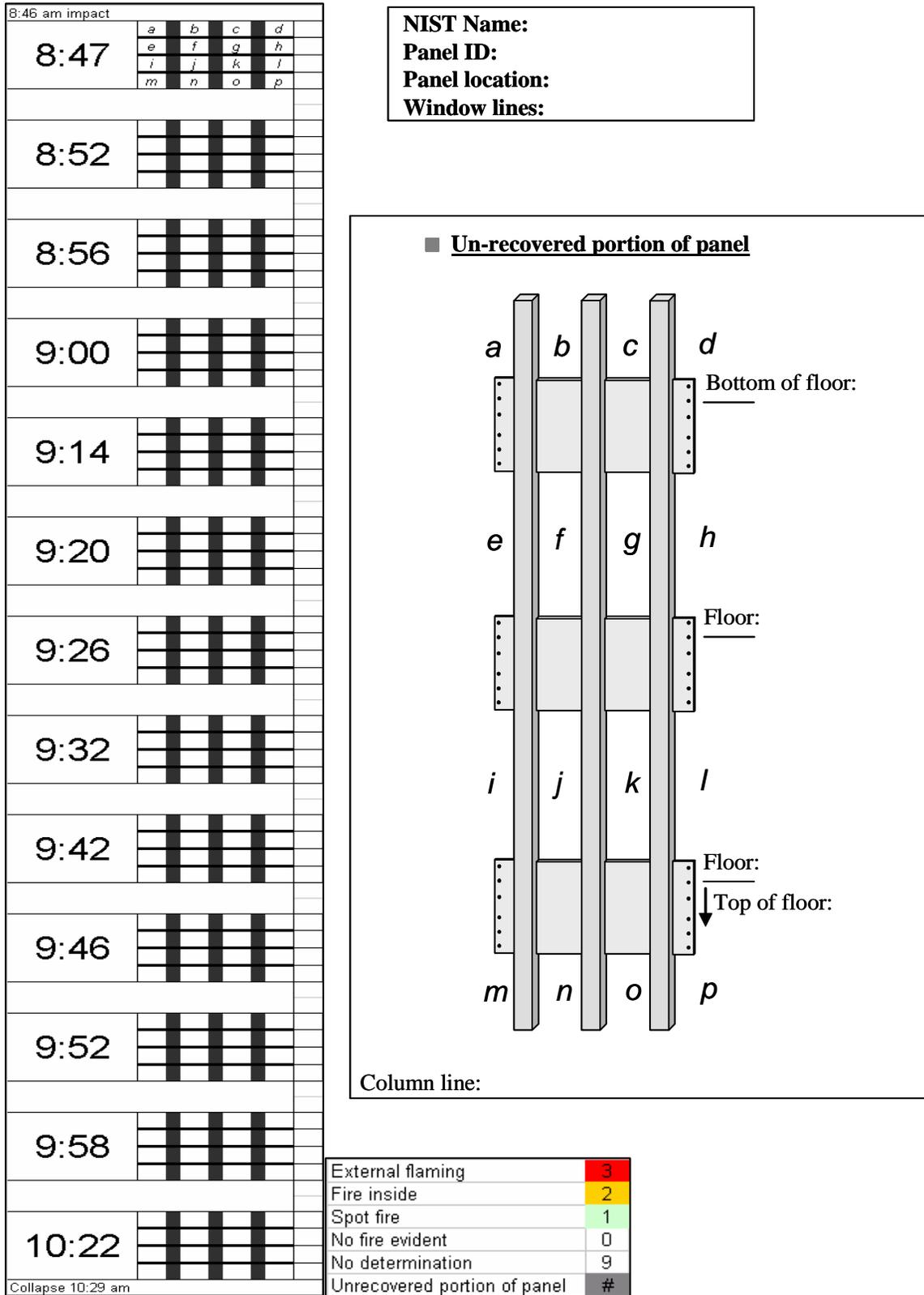
Figure 2–47. Generic illustration of the time sequence map used to analyze fire exposure of the recovered exterior panel sections prior to collapse of the WTC towers.
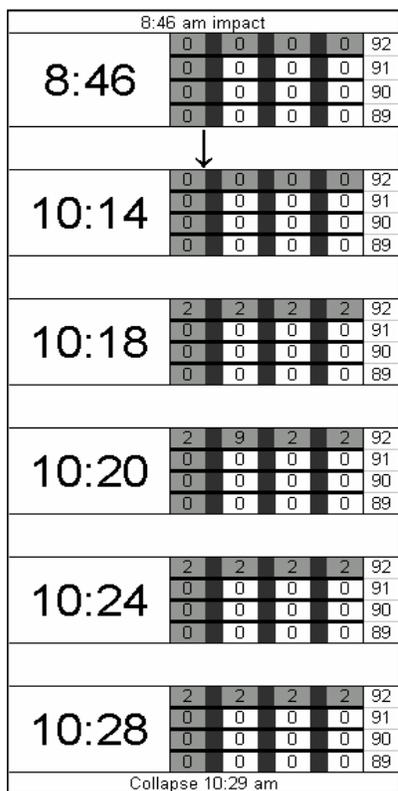
NIST Name:	N-10
Panel ID:	A115: 89-92
Panel location:	WTC 1, North face
Window lines:	13-16
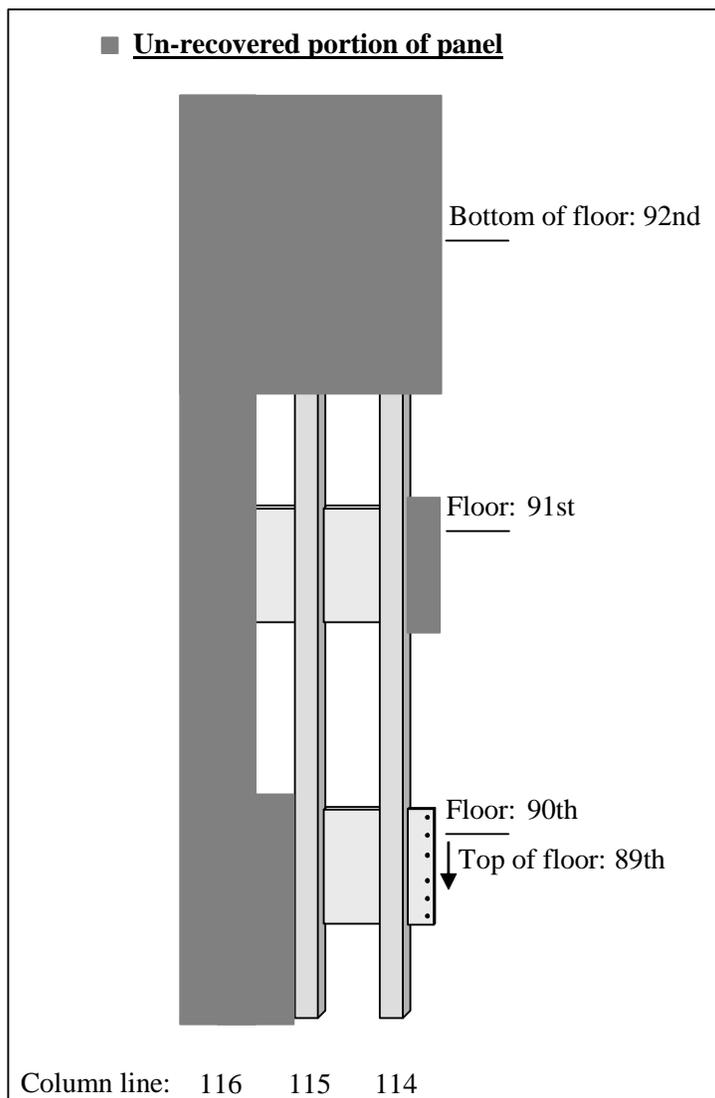
■ **Un-recovered portion of panel**

Bottom of floor: 92nd

Floor: 91st

Floor: 90th

Top of floor: 89th

Column line: 116   115   114

External flaming	3
Fire inside	2
Spot fire	1
No fire evident	0
No determination	9
Unrecovered portion of panel	#

Figure 2–48. Time sequence map for WTC 1 recovered panels. a) A115: 89-92 of the north face.

NIST Name:	N-7
Panel ID:	A127: 97-100
Panel location:	WTC 1, North face
Window lines:	25-28

■ **Un-recovered portion of panel**

Bottom of floor: 100th

Floor: 99th

Floor: 98th
Top of floor: 97th

Column line: 128   127   126

External flaming	3
Fire inside	2
Spot fire	1
No fire evident	0
No determination	9
Unrecovered portion of panel	#

Figure 2–48. Time sequence map for WTC 1 recovered panels. b) A127: 97-100 of the north face.

NIST Name:	M-26
Panel ID:	A130: 90-93
Panel location:	WTC 1, North face
Window lines:	28-31
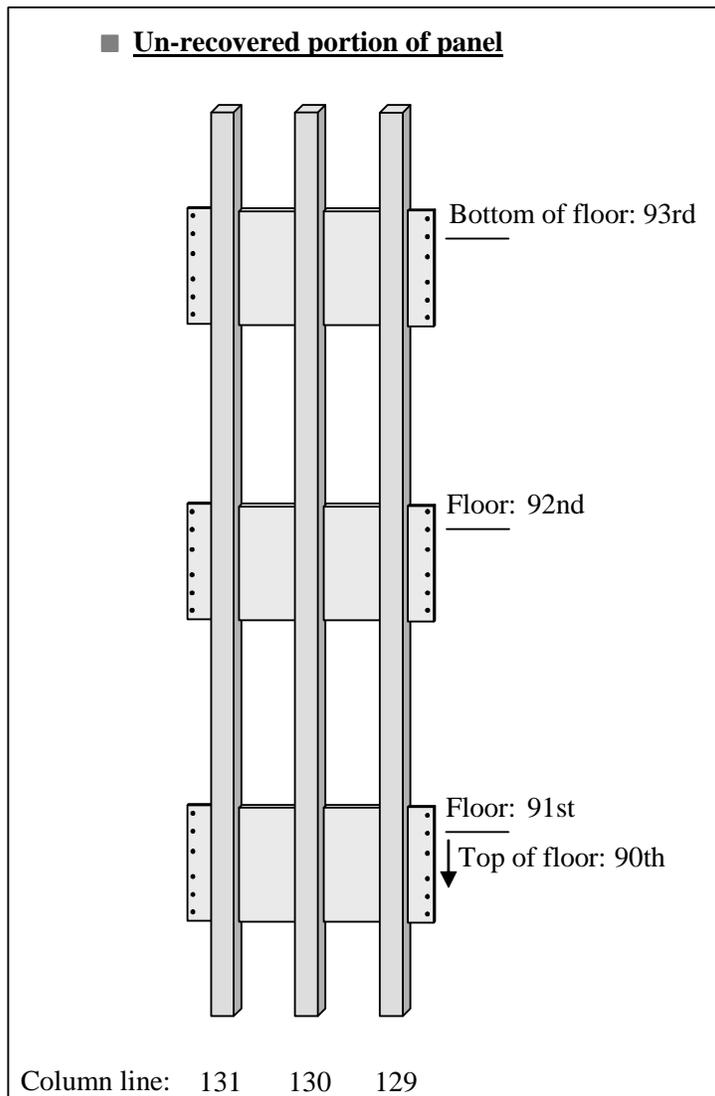
■ **Un-recovered portion of panel**

Bottom of floor: 93rd

Floor: 92nd

Floor: 91st

Top of floor: 90th

Column line: 131   130   129

External flaming	3
Fire inside	2
Spot fire	1
No fire evident	0
No determination	9
Unrecovered portion of panel	#

Figure 2–48. Time sequence map for WTC 1 recovered panels. c) A130: 90-93 of the north face.

NIST Name:	M-27
Panel ID:	A130: 93-96
Panel location:	WTC 1, North face
Window lines:	28-31
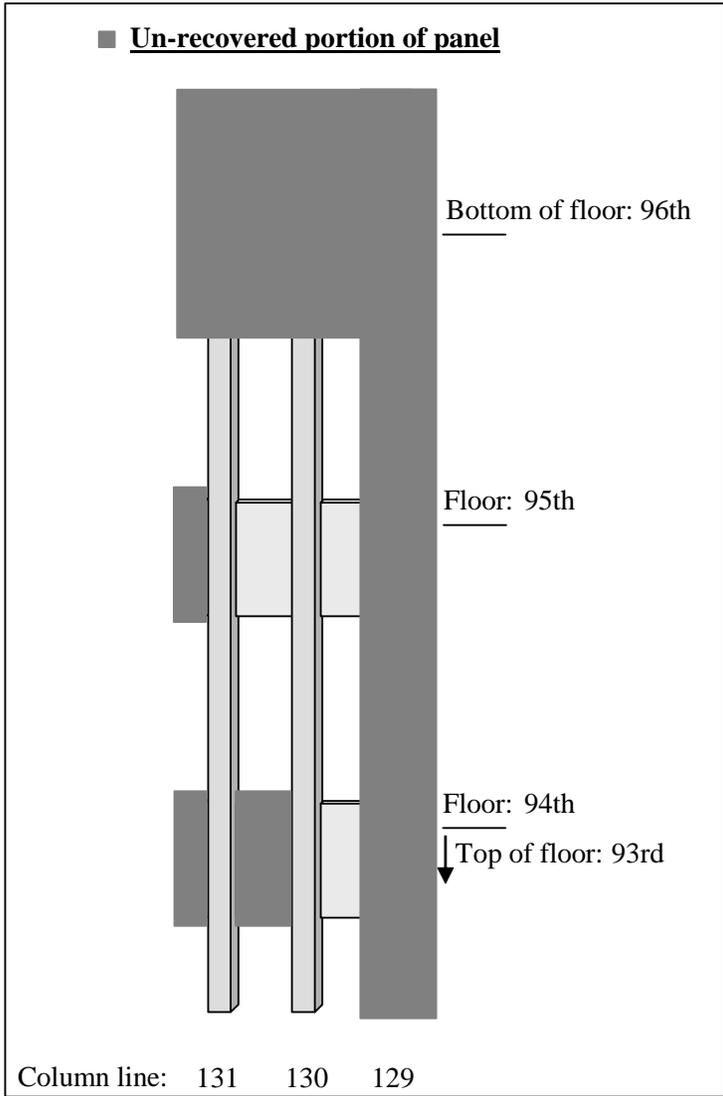
■ **Un-recovered portion of panel**

Bottom of floor: 96th

Floor: 95th

Floor: 94th

Top of floor: 93rd

Column line: 131   130   129

External flaming	3
Fire inside	2
Spot fire	1
No fire evident	0
No determination	9
Unrecovered portion of panel	#

Figure 2–48. Time sequence map for WTC 1 recovered panels. d) A130: 93-96 of the north face.

NIST Name:	M-2
Panel ID:	A130: 96-99
Panel location:	WTC 1, North face
Window lines:	28-31
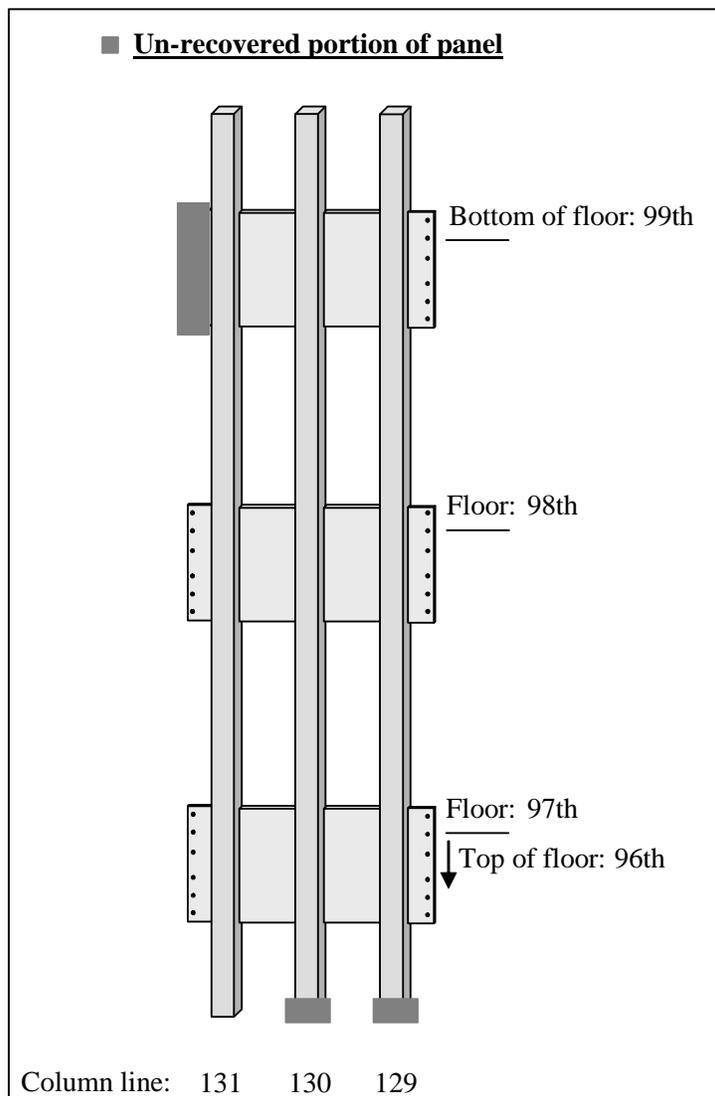
■ **Un-recovered portion of panel**

Bottom of floor: 99th

Floor: 98th

Floor: 97th

Top of floor: 96th

Column line: 131   130   129

External flaming	3
Fire inside	2
Spot fire	1
No fire evident	0
No determination	9
Unrecovered portion of panel	#

Figure 2–48. Time sequence map for WTC 1 recovered panels. e) A130: 96-99 of the north face.
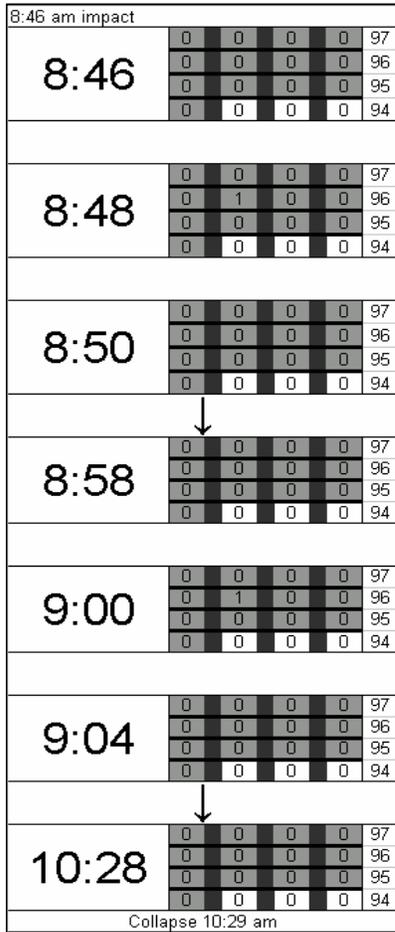
				NIST Name:	M-30
				Panel ID:	A133: 94-97
				Panel location:	WTC 1, North face
				Window lines:	31-34
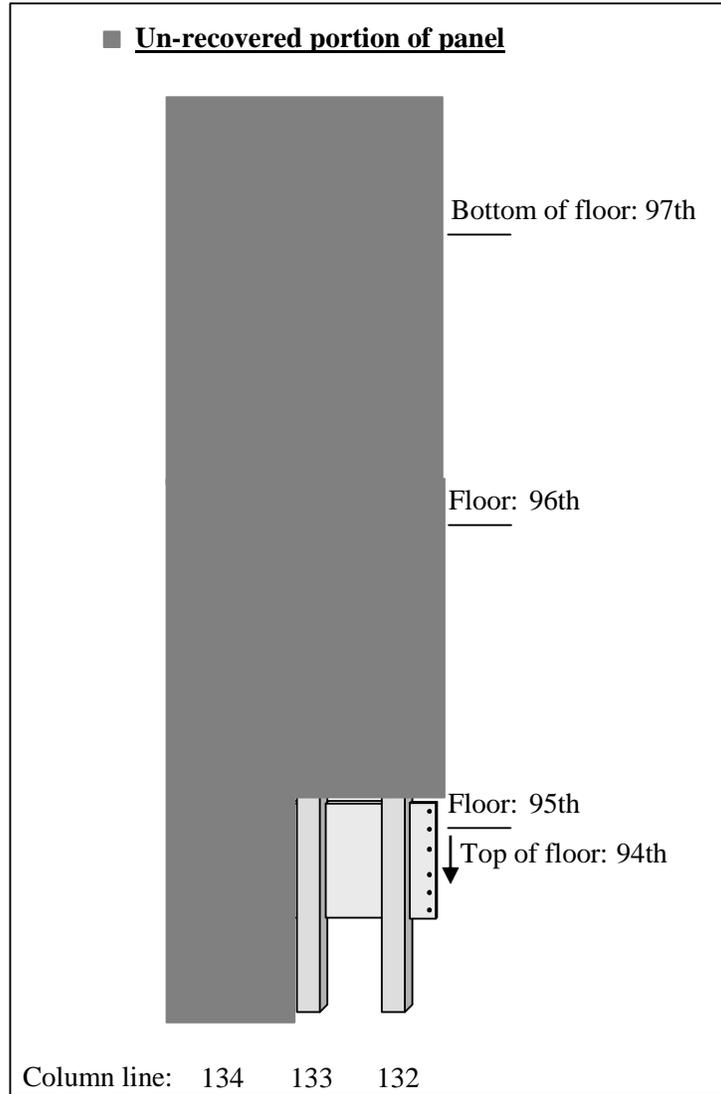
Figure 2–48. Time sequence map for WTC 1 recovered panels. f) A133: 94-97 of the north face.

External flaming	3
Fire inside	2
Spot fire	1
No fire evident	0
No determination	9
Unrecovered portion of panel	#

8:46 am impact

8:46

NIST Name: S-9
Panel ID: A133: 97-100
Panel location: WTC 1, North face
Window lines: 31-34
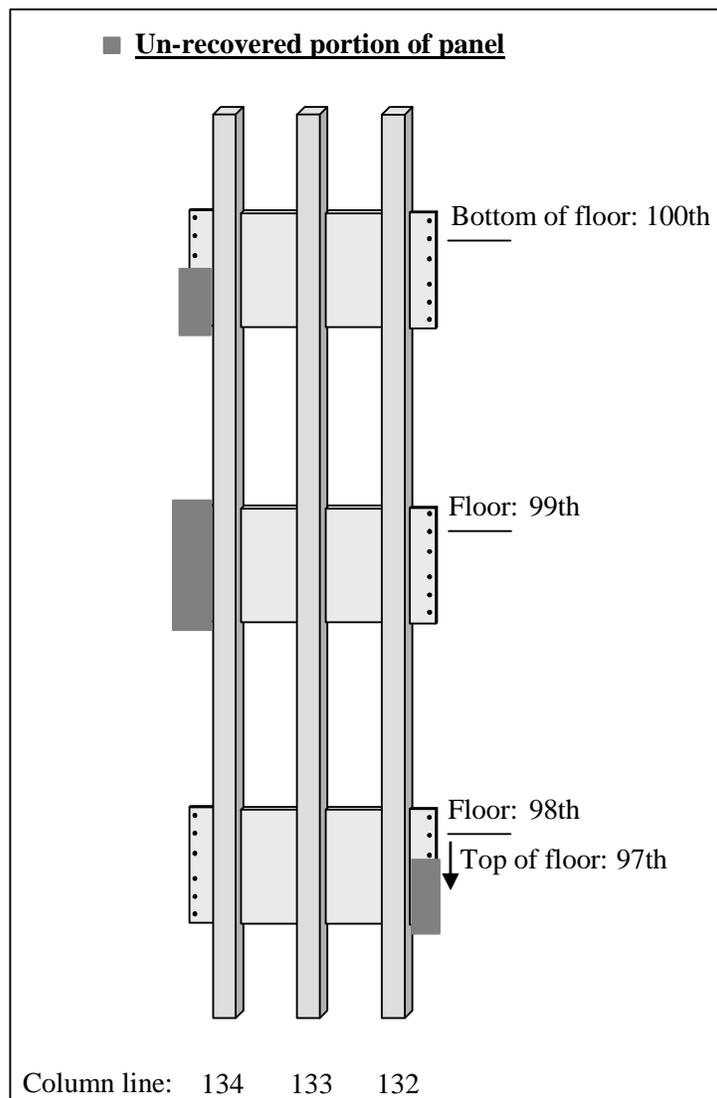
■ **Un-recovered portion of panel**

Bottom of floor: 100th

Floor: 99th

Floor: 98th

Top of floor: 97th

Column line: 134   133   132

Collapse 10:29 am

External flaming	3
Fire inside	2
Spot fire	1
No fire evident	0
No determination	9
Unrecovered portion of panel	#

Figure 2–48. Time sequence map for WTC 1 recovered panels. g) A133: 97-100 of the north face.
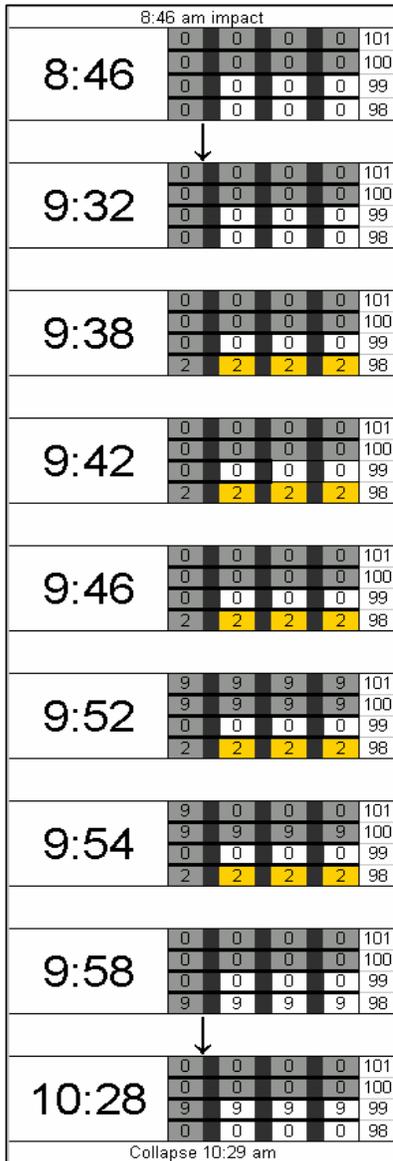
NIST Name:	C-40
Panel ID:	A136: 98-101
Panel location:	WTC 1, North face
Window lines:	34-37
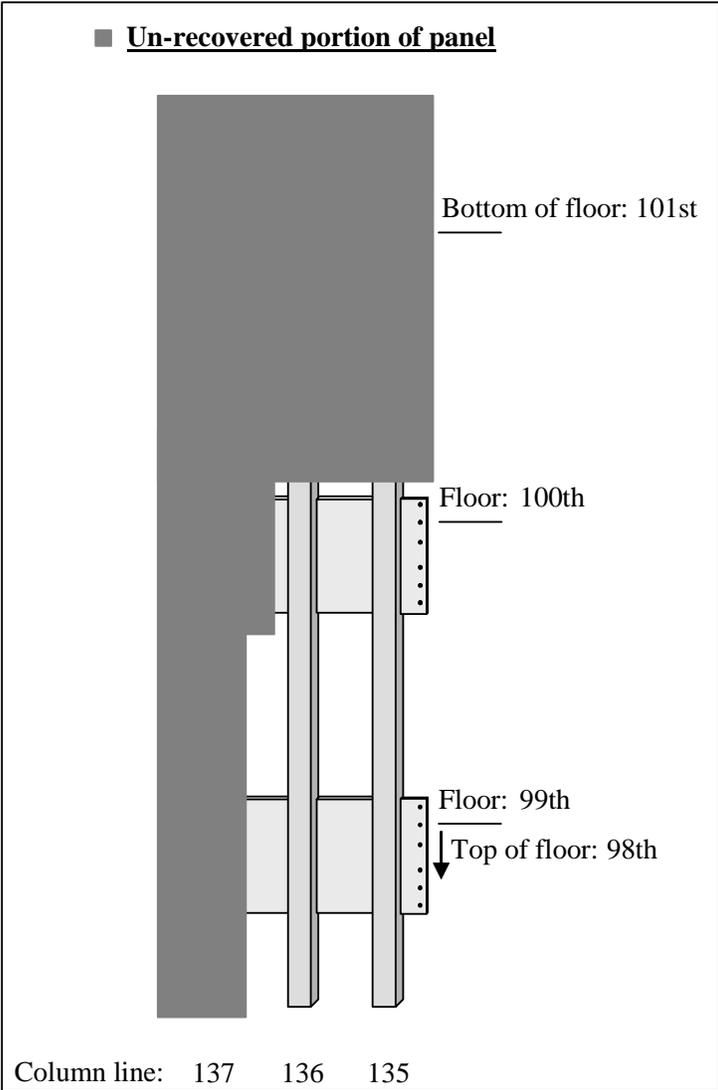
External flaming	3
Fire inside	2
Spot fire	1
No fire evident	0
No determination	9
Unrecovered portion of panel	#

Figure 2–48. Time sequence map for WTC 1 recovered panels. h) A136: 98-101 of the north face.

Figure 2–48. Time sequence map for WTC 1 recovered panels. i) A142: 97-100 of the north face.

9:42	0	0	0	0	100
	0	0	0	0	99
	2	2	2	2	98
	0	0	0	0	97

9:46	0	0	0	0	100
	0	0	0	0	99
	2	2	2	2	98
	0	0	0	0	97

9:52	9	9	9	9	100
	0	0	0	0	99
	2	2	2	2	98
	0	0	0	0	97

9:54	9	9	9	9	100
	0	0	0	0	99
	2	2	2	2	98
	0	0	0	0	97

9:58	0	0	0	0	100
	0	0	0	0	99
	0	0	0	0	98
	0	0	0	0	97

10:28	0	0	0	0	100
	9	9	9	9	99
	0	0	0	0	98
	0	0	0	0	97

Collapse 10:29 am
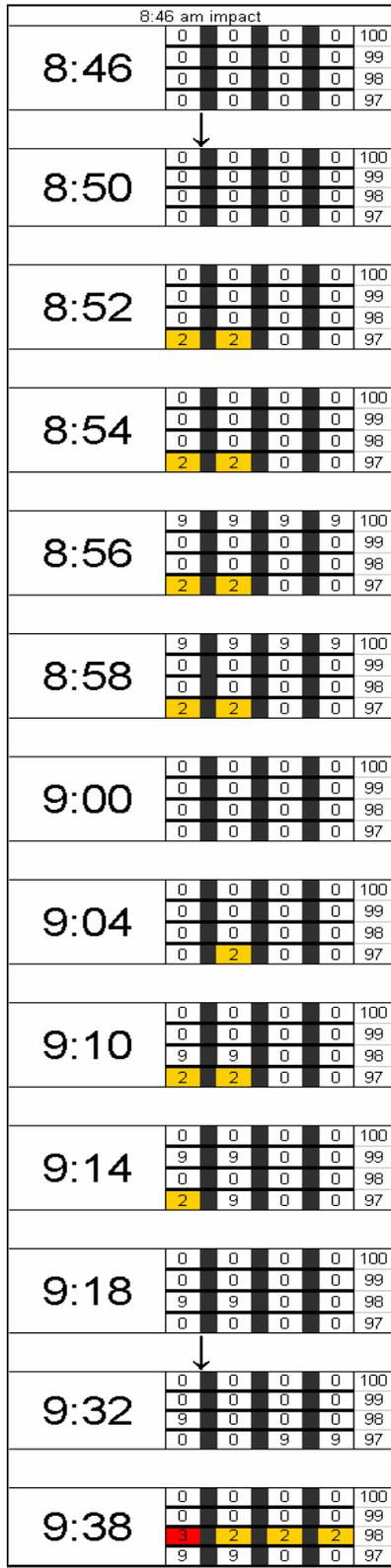
NIST Name:	N-8
Panel ID:	A142: 97-100
Panel location:	WTC 1, North face
Window lines:	40-43
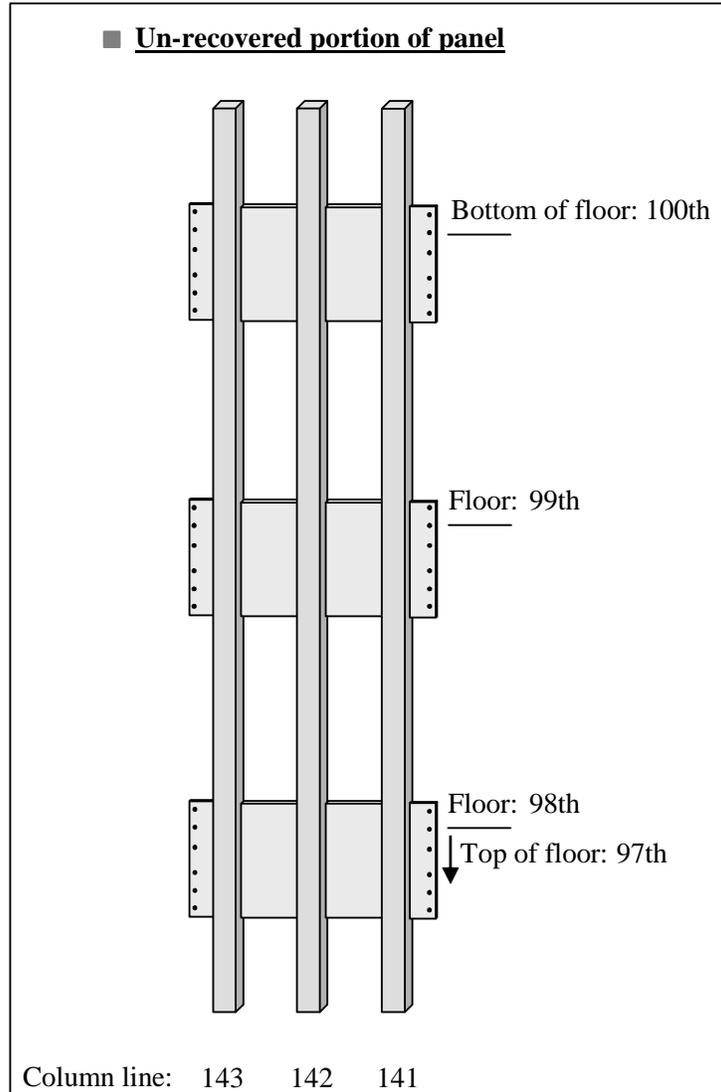
■ **Un-recovered portion of panel**

Bottom of floor: 100th

Floor: 99th

Floor: 98th
Top of floor: 97th

Column line: 143   142   141

External flaming	3
Fire inside	2
Spot fire	1
No fire evident	0
No determination	9
Unrecovered portion of panel	#

Figure 2–48. Time sequence map for WTC 1 recovered panels. i) A142: 97-100 of the north face.

NIST Name:	C-22
Panel ID:	A157: 93-96
Panel location:	WTC 1, North face
Window lines:	55-58

Un-recovered portion of panel

Bottom of floor: 96th

Floor: 95th

Floor: 94th

Top of floor: 93rd

Column line: 158 157 156

External flaming	3
Fire inside	2
Spot fire	1
No fire evident	0
No determination	9
Unrecovered portion of panel	#
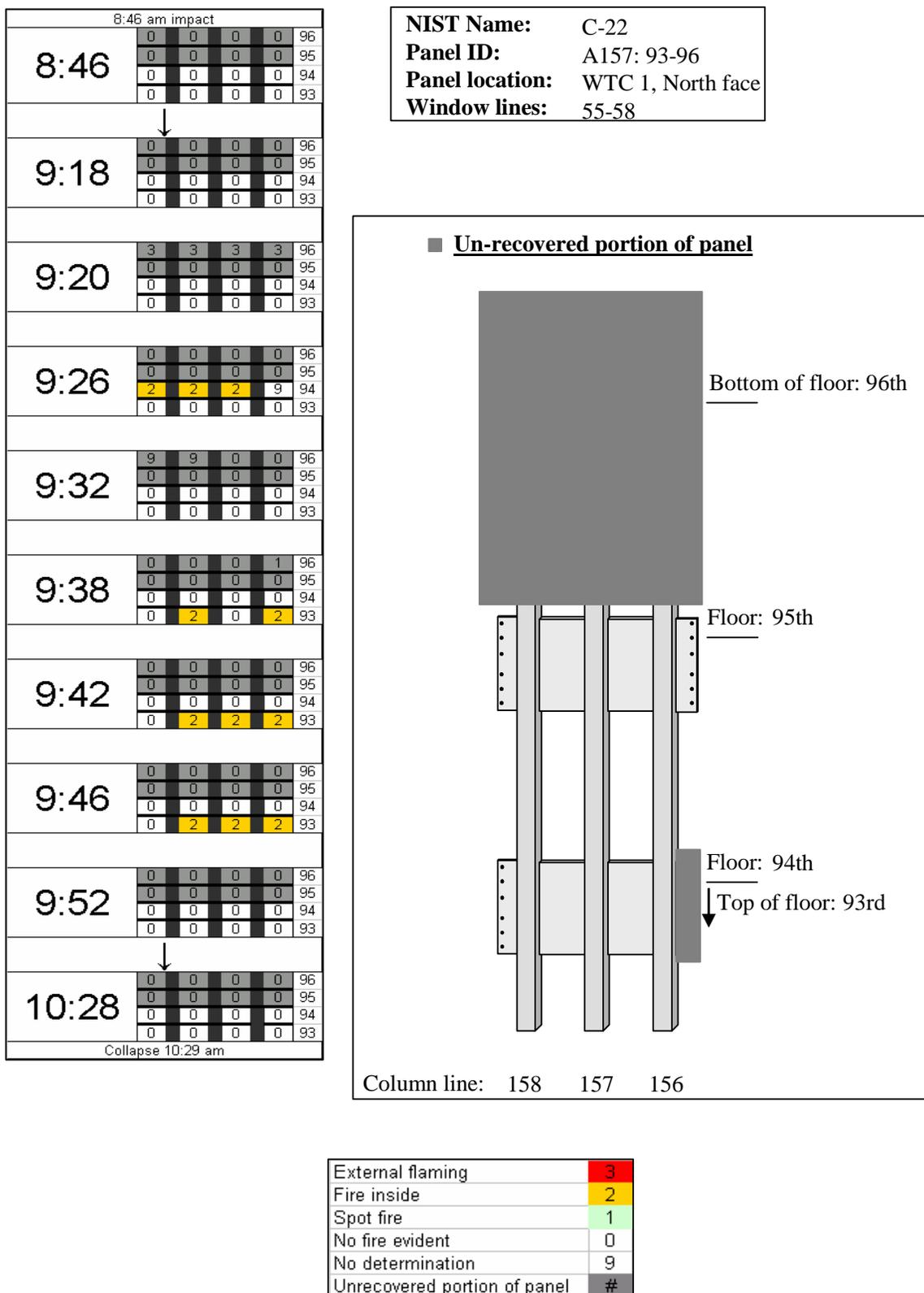
Figure 2–48. Time sequence map for WTC 1 recovered panels. j) A157: 93-96 of the north face.

Figure 2–48. Time sequence map for WTC 1 recovered panels. k) A206: 92-95 of the east face.

10:18						95
	0	0	0	0	0	94
	0	0	0	0	0	93
	0	0	0	0	0	92

↓

10:28						95
	9	9	9	9	9	94
	9	9	9	9	9	93
	9	9	9	9	9	92

Collapse 10:29 am
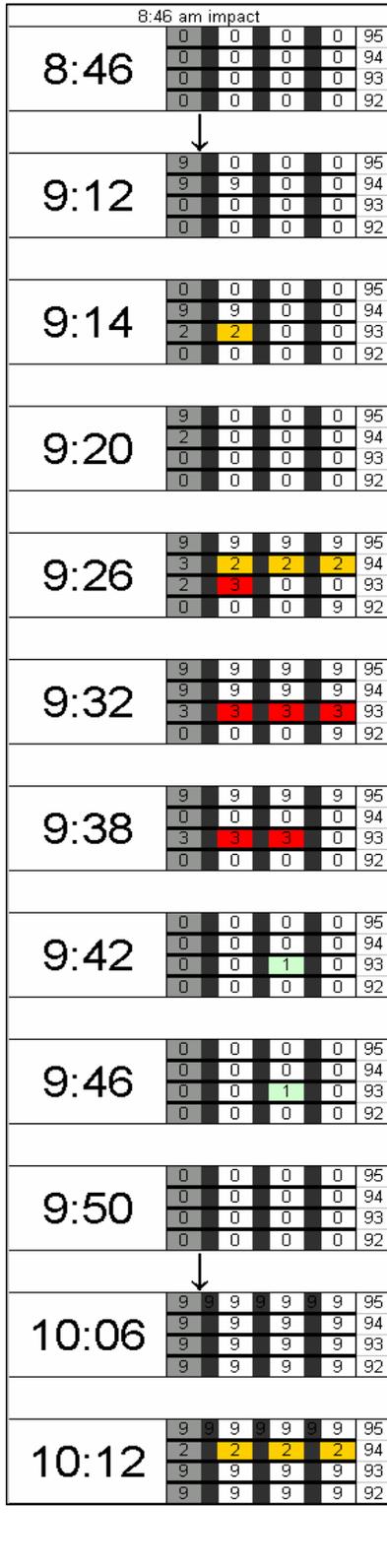
NIST Name:	N-12
Panel ID:	A206: 92-95
Panel location:	WTC 1, East face
Window lines:	4-7

■ **Un-recovered portion of panel**

Bottom of floor: 95th

Floor: 94th

Floor: 93rd

Top of floor: 92nd

Column line: 207 206 205

External flaming	3
Fire inside	2
Spot fire	1
No fire evident	0
No determination	9
Unrecovered portion of panel	#

Figure 2–48. Time sequence map for WTC 1 recovered panels. k) A206: 92-95 of the east face (cont.).

NIST Name: C-55
Panel ID: A209: 94-97
Panel location: WTC 1, East face
Window lines: 7-10

■ **Un-recovered portion of panel**

Bottom of floor: 97th

Floor: 96th

Floor: 95th

Top of floor: 94th

Column line: 210   209   208

External flaming	3
Fire inside	2
Spot fire	1
No fire evident	0
No determination	9
Unrecovered portion of panel	#

Figure 2–48. Time sequence map for WTC 1 recovered panels. l) A209: 94-97 of the east face.

NIST Name: C-55
Panel ID: A209: 94-97
Panel location: WTC 1, East face
Window lines: 7-10

■ **Un-recovered portion of panel**

Bottom of floor: 97th

Floor: 96th

Floor: 95th
↓ Top of floor: 94th

Column line: 210   209   208

External flaming	3
Fire inside	2
Spot fire	1
No fire evident	0
No determination	9
Unrecovered portion of panel	#

Figure 2–48. Time sequence map for WTC 1 recovered panels. l) A209: 94-97 of the east face (cont.).

Figure 2–48. **Time sequence map for WTC 1 recovered panels. m) A209: 97-100 of the east face.**

NIST Name:	K-1
Panel ID:	A209: 97-100
Panel location:	WTC 1, East face
Window lines:	7-10
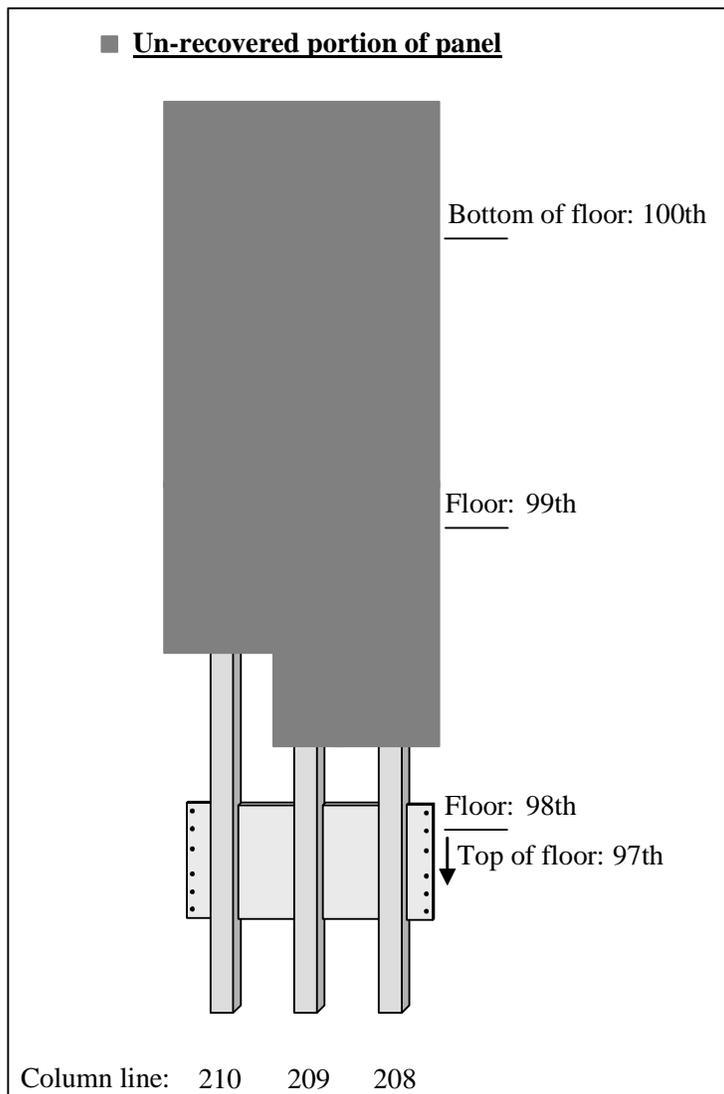
■ **Un-recovered portion of panel**

Bottom of floor: 100th

Floor: 99th

Floor: 98th

Top of floor: 97th

Column line: 210   209   208

External flaming	3
Fire inside	2
Spot fire	1
No fire evident	0
No determination	9
Unrecovered portion of panel	#
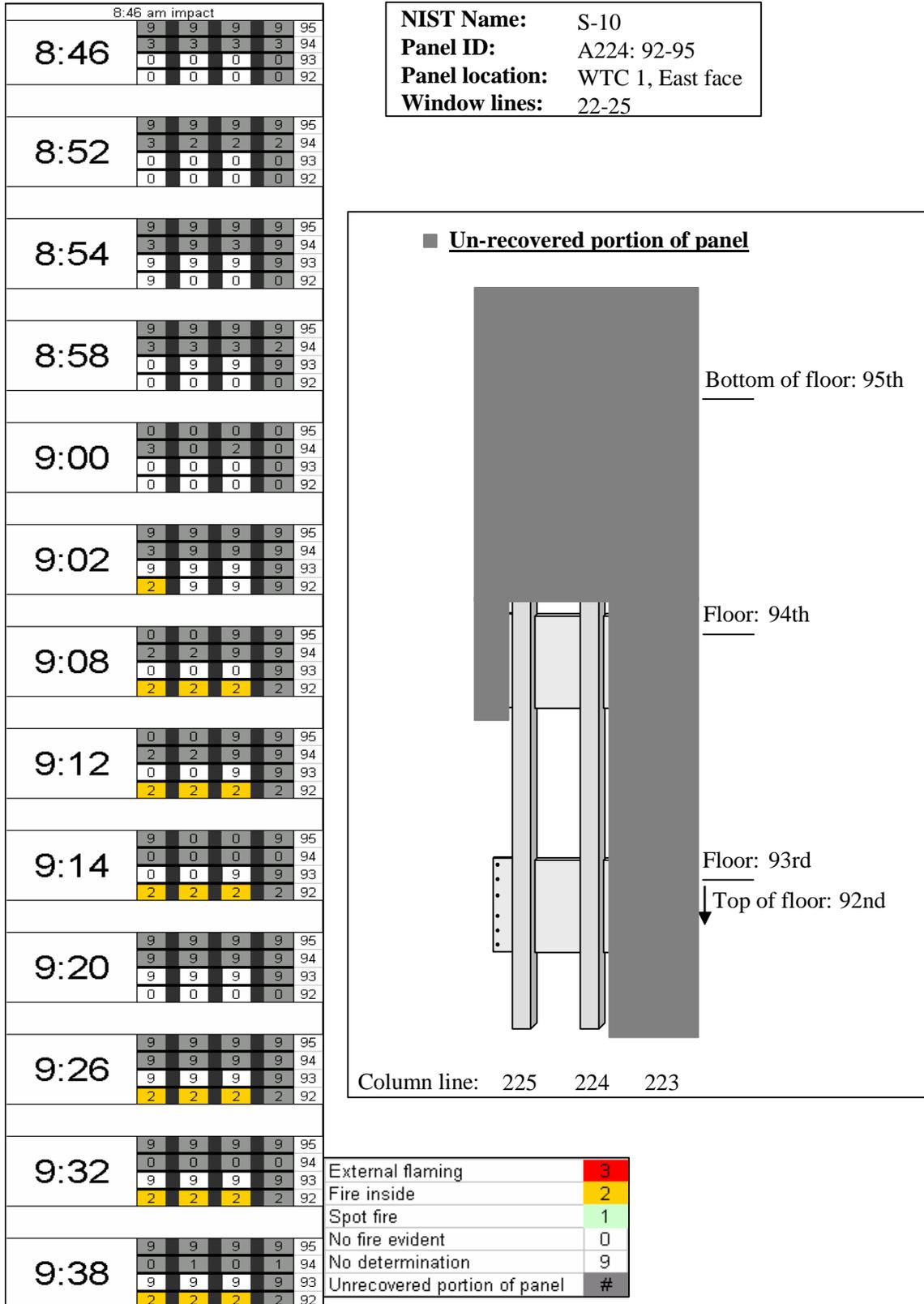
Figure 2–48. Time sequence map for WTC 1 recovered panels. m) A209: 97-100 of the east face (cont.).
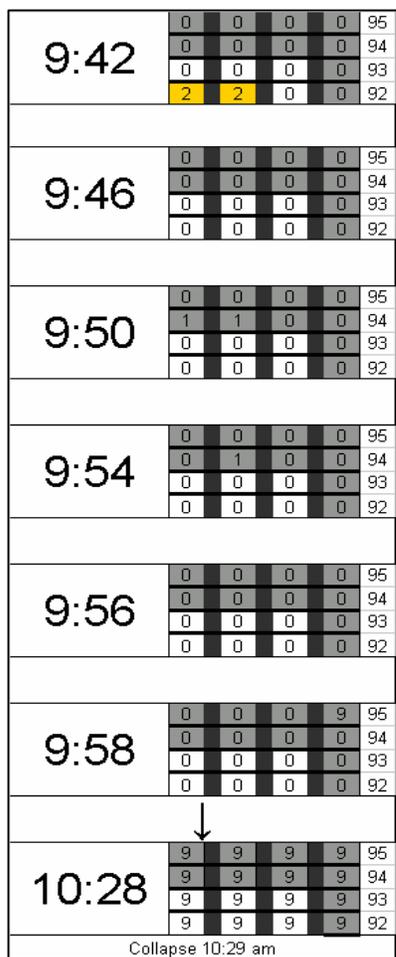
NIST Name:	S-10
Panel ID:	A224: 92-95
Panel location:	WTC 1, East face
Window lines:	22-25
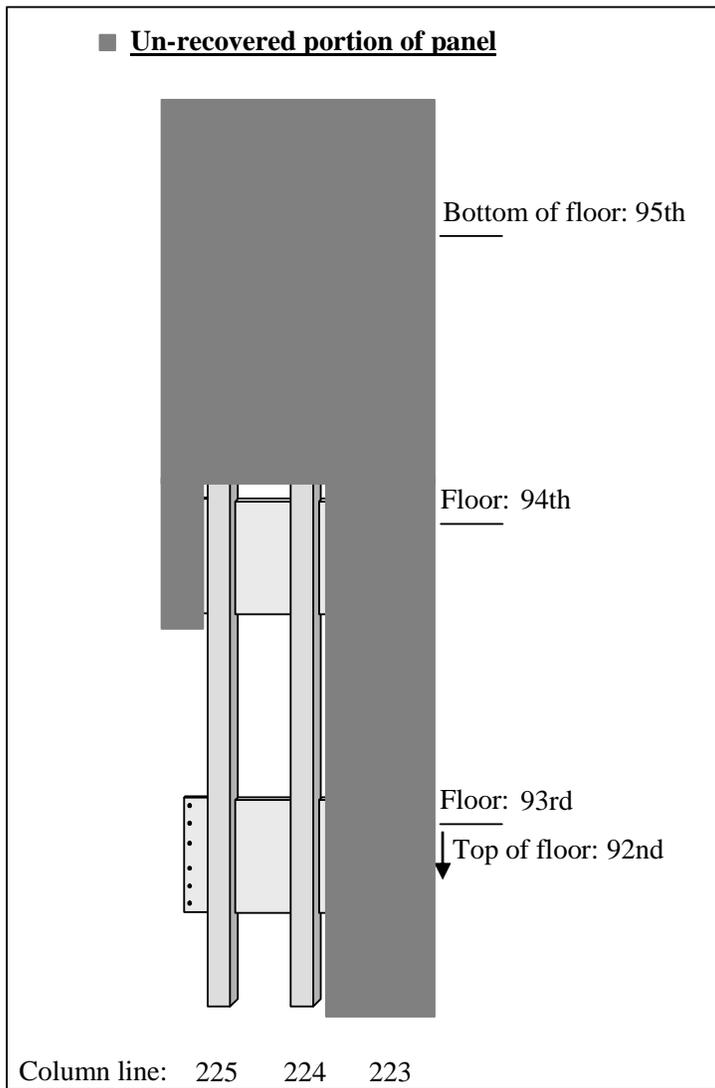
■ **Un-recovered portion of panel**

Bottom of floor: 95th

Floor: 94th

Floor: 93rd

Top of floor: 92nd

Column line: 225 224 223

External flaming	3
Fire inside	2
Spot fire	1
No fire evident	0
No determination	9
Unrecovered portion of panel	#

Figure 2–48. Time sequence map for WTC 1 recovered panels. n) A224: 92-95 of the east face.

Figure 2–48. Time sequence map for WTC 1 recovered panels. n) A224: 92-95 of the east face (cont.).

Figure 2–48. Time sequence map for WTC 1 recovered panels. o) A236: 92-95 of the east face.
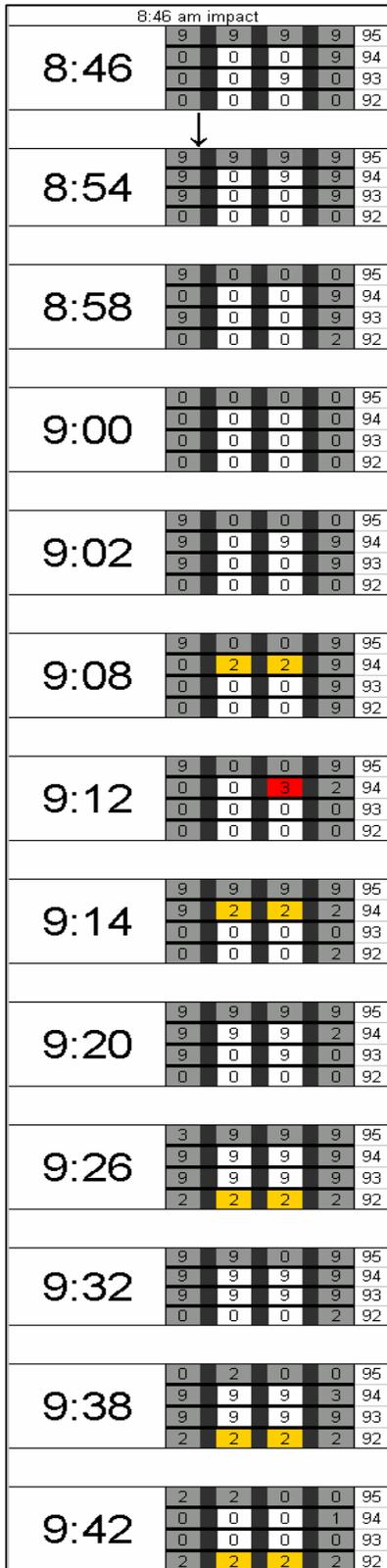
NIST Name: K-2
Panel ID: A236: 92-95
Panel location: WTC 1, East face
Window lines: 34-37
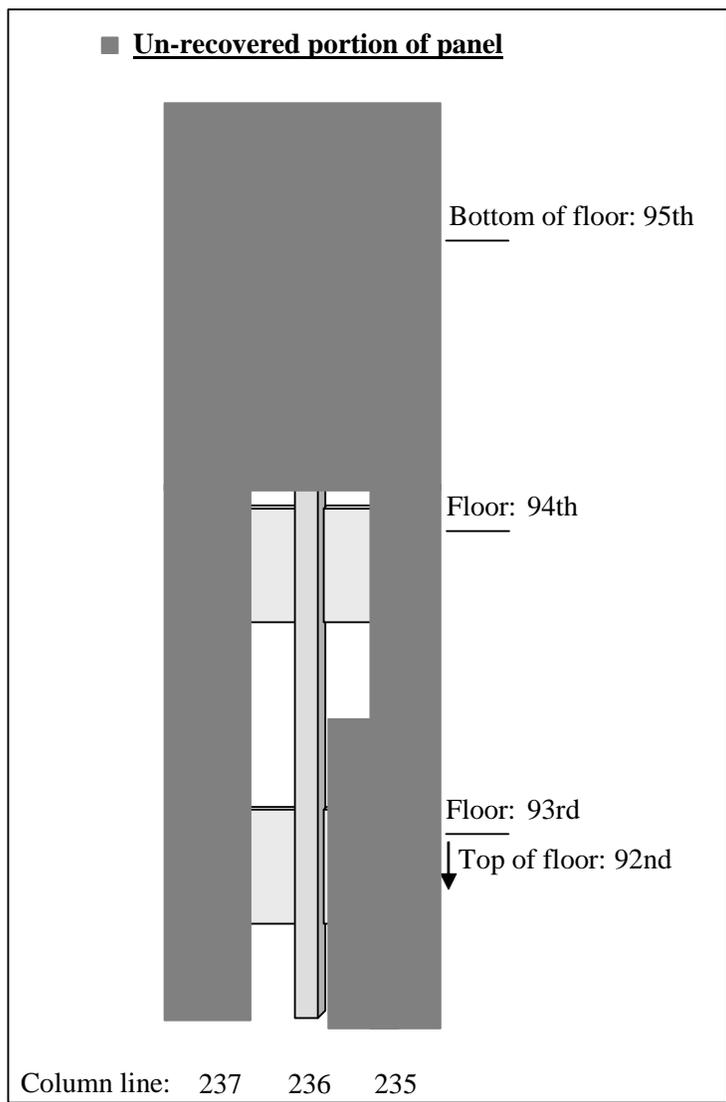
9:46 — floors 95, 94, 93, 92

9:50 — floors 95, 94, 93, 92

9:54 — floors 95, 94, 93, 92

10:28 — floors 95, 94, 93, 92
Collapse 10:29 am

■ **Un-recovered portion of panel**

Bottom of floor: 95th

Floor: 94th

Floor: 93rd
Top of floor: 92nd

Column line: 237   236   235

External flaming	3
Fire inside	2
Spot fire	1
No fire evident	0
No determination	9
Unrecovered portion of panel	#

Figure 2–48. Time sequence map for WTC 1 recovered panels. o) A236: 92-95 of the east face (cont.).
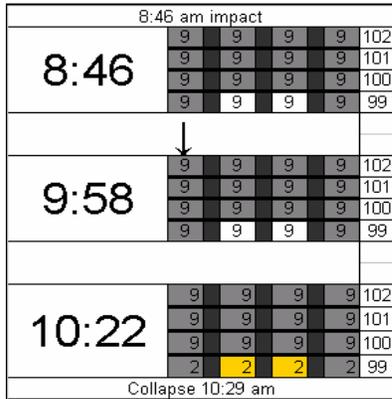
NIST Name:	C-93
Panel ID:	A339: 99-102
Panel location:	WTC 1, South face
Window lines:	37-40
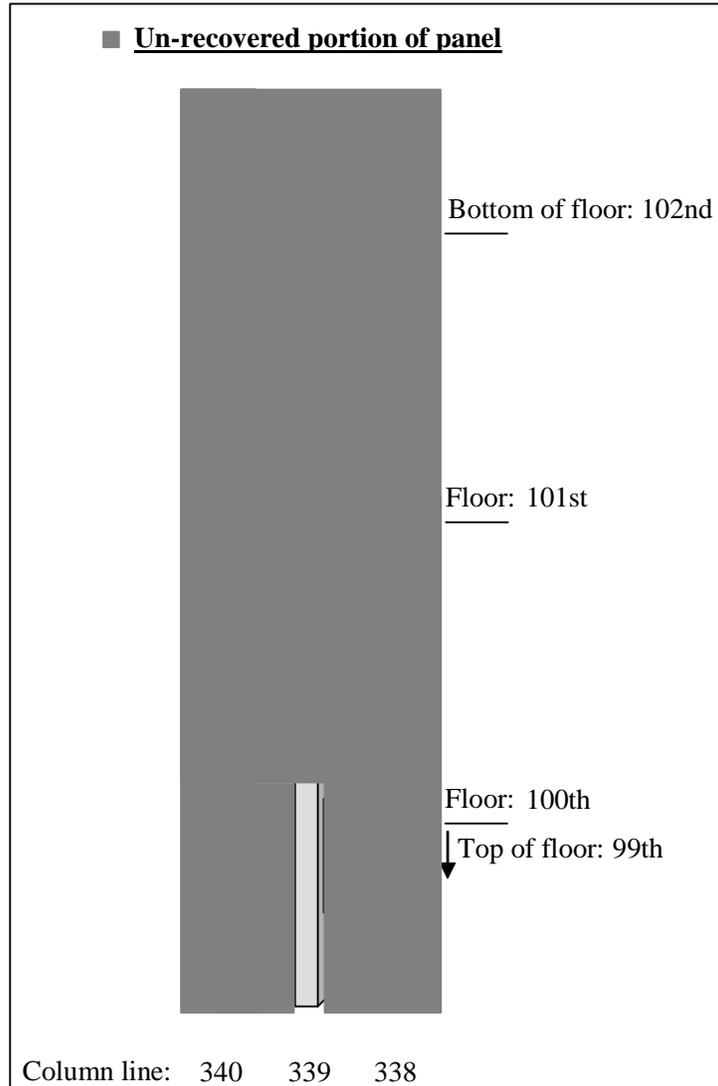
■ **Un-recovered portion of panel**

Bottom of floor: 102nd

Floor: 101st

Floor: 100th

Top of floor: 99th

Column line: 340   339   338

External flaming	3
Fire inside	2
Spot fire	1
No fire evident	0
No determination	9
Unrecovered portion of panel	#

Figure 2–48. Time sequence map for WTC 1 recovered panels. p) A339: 99-102 of the south face.

Table 2–1. Exterior panels from WTC 1 that may have experienced damage as a result of airplane impact. The column and spandrel dimensions and specified minimum yield strengths are indicated.

Panel Identification			Column 1		Column 2		Column 3		LOWER SPANDREL		MIDDLE SPANDREL		UPPER SPANDREL	
Center Column Number	Story at Splice		Column Type	F_y (ksi)	Column Type	F_y (ksi)	Column Type	F_y (ksi)	Gauge (in)	F_y (ksi)	Gauge (in)	F_y (ksi)	Gauge (in)	F_y (ksi)
	Lower	Upper												
112	96	99	121	65	121	60	121	60	3/8	36	3/8	36	3/8	36
115	95	98	122	60	122	60	122	60	3/8	36	3/8	36	3/8	36
115	98	101	120	60	120	60	120	60	3/8	42	3/8	42	3/8	42
118	94	97	122	60	122	60	122	60	3/8	45	3/8	42	3/8	45
118	97	100	121	60	121	60	121	60	3/8	42	3/8	36	3/8	42
121	93	96	123	55	123	55	123	55	3/8	42	3/8	36	3/8	42
121	96	99	121	60	121	60	121	60	3/8	42	3/8	42	3/8	42
124	92	95	123	55	123	55	123	55	3/8	36	3/8	42	3/8	42
124	95	98	122	60	122	55	122	55	3/8	36	3/8	36	3/8	36
127	91	94	124	55	124	55	124	50	3/8	42	3/8	42	3/8	36
127	94	97	122	55	122	55	123	55	3/8	42	3/8	42	3/8	42
127	97	100	121	60	121	55	121	55	3/8	42	3/8	42	3/8	42
130	93	96	123	55	123	55	124	50	3/8	42	3/8	36	3/8	42
130	96	99	122	55	122	55	122	55	3/8	36	3/8	36	3/8	42
133	91	94	125	50	125	55	125	55	3/8	42	3/8	45	3/8	45
133	94	97	123	55	123	55	123	55	3/8	42	3/8	45	3/8	45
133	97	100	122	55	122	55	122	55	3/8	42	3/8	42	3/8	42
136	92	95	124	55	124	55	124	55	3/8	36	3/8	42	3/8	42
136	95	98	123	55	123	55	123	55	3/8	36	3/8	42	3/8	36
139	93	96	124	55	124	55	123	60	3/8	42	3/8	45	3/8	42
142	91	94	124	60	124	60	124	60	3/8	42	3/8	42	3/8	42
142	94	97	123	60	123	60	122	65	3/8	42	3/8	42	3/8	42
145	92	95	123	60	123	60	123	65	3/8	36	3/8	42	3/8	36
145	95	98	122	65	122	65	122	65	3/8	42	3/8	42	3/8	42
148	93	96	123	65	123	65	123	65	3/8	42	3/8	42	3/8	42
151	91	94	124	60	123	65	123	65	3/8	36	3/8	42	3/8	36
151	94	97	122	65	122	65	122	65	3/8	42	3/8	42	3/8	42

Note: All panels were of the 300-type (i.e., 3 columns wide with uniform width, 3 stories tall). Columns are numbered from left to right when viewed from within the building.

Table 2–2. Strength/gauge combinations of columns that may have experienced damage as a result of airline impact for both WTC 1 and WTC 2. Also shown are similar data for the columns recovered by NIST.

Flange F_y (ksi)	Flange gauge (in)	Columns in airplane impact region		Number of columns recovered and IDed by NIST	Match between possible and recovered
		WTC 1	WTC 2		
45	1-3/4			1	
50	1/2	2		2	Y
50	9/16	1		2	Y
50	5/8		1	0	N
50	1-1/16			2	
50	1-13/16			1	
50	2-1/16			1	
50	2-1/8			1	
50	2-1/4			1	
50	2-1/2			1	
50	2-5/8			1	
55	1/4			12	
55	5/16	2		5	Y
55	3/8	10		6	Y
55	7/16	15	1	3	Y
55	1/2	7		0	N
55	9/16	2	7	3	Y
55	5/8		2	0	N
55	1-3/8			1	
55	1-11/16			1	
60	1/4	3		5	Y
60	5/16	9		6	Y
60	3/8	7		1	Y
60	7/16	5	3	0	N
60	1/2	4	3	1	Y
60	9/16		5	0	N
65	1/4			7	
65	5/16	1		0	N
65	3/8	7		1	Y
65	7/16	4	9	0	N
65	1/2	2	6	0	N
65	9/16		4	0	N
65	13/16			1	
70	1/4			7	
70	3/8		1	0	N
70	7/16		2	2	Y
70	3/4			1	
75	1/4			3	
75	3/8		1	0	N
75	7/16		1	2	Y
80	1/4			3	
80	3/8		1	0	N
80	5/8			1	
80	1-3/16			1	
85-100	1/4		2	12	Y
85-100	5/16		4	0	N
85-100	3/8		1	0	N
85-100	9/16			3	
85-100	1-1/8			2	
85-100	1-3/16			3	

Table 2–3. Strength/gauge combinations of spandrels that may have experienced damage as a result of airplane impact for both WTC 1 and WTC 2. Also shown are similar data for the spandrels recovered by NIST.

Spandrel F_y (ksi)	Spandrel gauge (in)	Spandrels in airplane impact region		Number of spandrels recovered by NIST	Match for impact?
		WTC 1	WTC 2		
36	3/8	23		16	Y
36	7/16		1		N
36	9/16			3	
36	1-1/4			3	
36	1-3/8			3	
42	3/8	51		24	Y
42	7/16		18		N
45	3/8	7	2	7	Y
45	7/16		14		N
46	3/8		1	4	Y
50	3/8			5	
50	7/16		1	2	Y
50	15/16			2	
55	3/8		2	2	Y
55	7/16		2		N
60	3/8		2	6	Y
60	7/16		1		N
60	15/16			1	
65	3/8			1	
65	7/16		4		N
65	9/16			1	
65	5/8			2	
65	15/16			1	
70	3/8			2	
75	3/8			1	
80	9/16			1	

Table 2–4. Exterior panels from WTC 2 that may have experienced damage as a result of airplane impact. The column and spandrel dimensions and specified minimum yield strengths are indicated.

PANEL			PANEL TYPE	COLUMN 1		COLUMN 2		COLUMN 3		LOWER SPANDREL		MIDDLE SPANDREL		UPPER SPANDREL	
Center Column Number	Story at Splice			Column Type	F_y (ksi)	Column Type	F_y (ksi)	Column Type	F_y (ksi)	Gauge (in)	F_y (ksi)	Gauge (in)	F_y (ksi)	Gauge (in)	F_y (ksi)
	Lower	Upper													
412	78	81	302	121	100	121	100	122	85	7/16	65	7/16	65	7/16	65
412	81	84	300	120	90	120	100	121	90	7/16	65	7/16	60	3/8	60
415	80	83	300	122	80	123	75	123	70	7/16	55	7/16	50	7/16	55
415	83	86	300	121	85	122	75	122	70	7/16	55	7/16	55	3/8	60
418	79	82	300	124	65	124	65	124	65	7/16	45	7/16	45	7/16	45
418	82	85	300	123	65	123	65	123	65	7/16	45	7/16	45	3/8	45
421	78	81	302	125	65	124	65	124	65	7/16	45	7/16	45	7/16	45
421	81	84	300	124	65	123	65	123	70	7/16	45	7/16	45	3/8	46
424	77	80	303	125	65	125	65	125	65	7/16	42	7/16	45	7/16	45
424	80	83	300	123	65	123	65	123	65	7/16	45	7/16	42	7/16	45
427	77	79	201	125	60	125	60	125	60	n/a	n/a	7/16	42	7/16	42
427	79	82	300	123	65	123	65	123	60	7/16	45	7/16	42	7/16	42
430	77	78	101	125	55	125	55	125	55	n/a	n/a	n/a	n/a	7/16	42
430	78	81	302	124	60	124	60	124	60	7/16	42	7/16	42	7/16	42
433	77	79	201	125	55	125	55	125	55	n/a	n/a	7/16	42	7/16	42
433	79	82	300	123	60	123	60	123	55	7/16	42	7/16	42	7/16	42
436	77	80	303	125	55	125	60	125	60	7/16	42	7/16	42	7/16	42
439	77	78	101	126	50	126	55	126	55	n/a	n/a	n/a	n/a	7/16	36

Note: Columns are numbered from left to right when viewed from within the building.

Table 2–5. Recovered exterior panel sections with known as-built locations, separated by pre-collapse location and environmental conditions.

Panel Description	Bldg	NIST Name	Brief Description	Center Column #	Story at Splice Lower	Story at Splice Upper	Location of fire observations	Relevant region of componet recovered
Exterior panel sections within impact region	WTC 1	N-7 or M-3	Full panel	127	97	100	97th and 98th	Y
	WTC 1	M-27	2 columns, lower 3/4ths	130	93	96	95th	N
	WTC 1	M-2	Full panel	130	96	99	98th	Y
	WTC 1	M-30	2 columns, lower 1/3rd	133	94	97	96th	N
	WTC 1	S-9 or C-63	Full panel	133	97	100	98th	Y
	WTC 2	None						
Exterior panels within fire exposure floors	WTC 1	N-10 or M-15	2 columns, lower 2/3rds	115	89	92	92nd	N
	WTC 1	M-20	2 columns, lower 1/3rd	121	99	102	No fire evident/unable to be determined	
	WTC 1	M-26	Full panel	130	90	93	92nd	Y
	WTC 1	N-13 or M-14	3 columns, lower 1/3rd	130	99	102	No fire evident/unable to be determined	
	WTC 1	N-101 or M-21	Full panel	133	100	103	No fire evident/unable to be determined	
	WTC 1	C-40	2 columns, lower 2/3rds	136	98	101	98th	Y
	WTC 1	N-8 or M-7	Full panel	142	97	100	97th and 98th	Y
	WTC 1	N-99 or M-16	Almost full panel, missing lower 1/3rd of 1 column	148	99	102	No fire evident/unable to be determined	
WTC 1: 89th floor and above	WTC 1	N-9 or M-8	Almost full panel, missing lower 1/3rd of 1 column	154	101	104	No fire evident/unable to be determined	
	WTC 1	C-22	3 columns, lower 1/2	157	93	96	93rd, 94th, 96th	Y
	WTC 1	C-25	1 column, lower 1/2	206	89	92	No fire evident/unable to be determined	
	WTC 1	N-12 or M-13	2 full columns	206	92	95	93rd and 94th	Y
	WTC 1	C-55	1 column, lower 1/3rd	209	94	97	94th, 95th, 96th, 97th	Y
	WTC 1	K-1 or K-13	3 columns, lower 1/3rd	209	97	100	97th and 98th	Y
	WTC 1	S-10 or C-17	2 columns, lower 1/2	224	92	95	92nd and 94th	Y
	WTC 1	K-2 or K-40	1 column, lower 2/3rds	236	92	95	92nd, 94th, 95th	Y
	WTC 1	C-93	1 column, lower 1/3rd	339	99	102	99th	Y
	WTC 2	C-92	Partial of single column	130	93	96	No fire evident/unable to be determined	
	WTC 2	C-13 or S-11 C-13a or S-19	Single rectangular column Partial of single column	200	90	92	No fire evident/unable to be determined	
	WTC 2	M-10b	3 columns, lower 1/2	206	83	86	No fire evident/unable to be determined	
	WTC 2	M-10a	3 columns, lower 1/3rd	209	82	85	No fire evident/unable to be determined	
WTC 2: 77th floor and above	WTC 2	S-14 or C-20	Full panel	218	91	94	No fire evident/unable to be determined	
	WTC 2	C-18	3 columns, bottom 2/3rds	230	93	96	No fire evident/unable to be determined	
	WTC 2	C-14 or S-18	1 column, lower 1/3rd	300	85	87	No fire evident/unable to be determined	
	WTC 2	M-28	3 columns, lower 1/4th	345	98	101	No fire evident/unable to be determined	
	WTC 2	C-48 or S-5	Nearly 2 full columns	442	91	94	No fire evident/unable to be determined	
Exterior panels outside of area analyzed for fire exposure	WTC 1	CC	2 full columns	124	70	73	Outside of area analyzed	
	WTC 1	N-1	2 full columns	218	82	85	Outside of area analyzed	
	WTC 1	S-1 or EE	2 columns, lower 1/3rd	433	79	82	Outside of area analyzed	
	WTC 1	C-10	Full panel	451	85	88	Outside of area analyzed	
	WTC 2	B-1024	Full panel	154	21	24	Outside of area analyzed	
	WTC 2	C-46	Almost full panel, missing lower 1/3rd of 1 column	157	68	71	Outside of area analyzed	
	WTC 2	C-24	3 columns, upper 1/2	203	74	77	Outside of area analyzed	
	WTC 2	C-89	2 full columns	215	12	15	Outside of area analyzed	
	WTC 2	ASCE-2	1 full column	330	40	43	Outside of area analyzed	
	WTC 2	B-1043	Mechanical floor, full panel	406	40	43	Outside of area analyzed	
	WTC 2	B-1044	Mechanical floor, full panel	409	40	43	Outside of area analyzed	

Chapter 3
PHYSICAL DAMAGE OF RECOVERED EXTERIOR WALL PANELS

This chapter of the report covers the physical damage and failure modes observed on the recovered, pre-fabricated exterior column panels. As reported in Sec. 2.1.3, there were 42 distinct panel sections that were unambiguously identified, i.e., their precise, as-built location was known, and one partially identified from the 90 panel samples recovered. Table 2–5 summarizes the identified pieces as well as comments on their pre-collapse environmental exposure.

Also reported in Sec. 2.5, the panels were divided into four groups. This chapter discusses the analysis of the samples with respect to these four categories (dictated by their as-built location in relation to the impact regions and pre-collapse exposure to fires).

While the following sections describe in detail the damage that was observed on these pieces, it should again be emphasized that the damage and failure mechanisms observed were reported in their present condition. The damage may have been a result of any one of the extreme loading conditions mentioned above (aircraft impact, the concomitant fires, the collapse of the buildings and ensuing fires, or the subsequent handling related to the recovery efforts). While in some cases the origin of damage may be evident, there are other cases in which the event that caused the damage is difficult or impossible to determine.

3.1 OVERALL DAMAGE PATTERNS OF EXTERIOR WALL PANEL SECTIONS

Only five of the recovered panels from World Trade Center (WTC) 1 were either directly hit by the airplane or sustained damage as a result of the impact, and no impact-damaged panels were retrieved for WTC 2. Therefore, physical damage incurred for a majority of the recovered exterior panel sections was a result of events that occurred during or after the collapse of the buildings. The major portion of this section focused on those five samples recovered that were from the airplane impact zone. Limited comments concerning the damage of the panels outside the impact region are also made.

3.1.1 WTC Panels Outside of Impact Region

All damage found on the panels located outside of the impact zone was ascribed to events occurring during and after the collapse, therefore, in-depth descriptions were not reported. However, one general note concerning the exterior column panels themselves was the size of the individual recovered pieces. More often, the pieces from WTC 1 were larger than those from WTC 2, and in later sections describing specific damage features or failure modes, more observations were found for elements from WTC 1 than WTC 2 for a given feature. No explanation was found for this occurrence.

3.1.2 WTC 1 Panels in Impact Region

The following five recovered panels were located in the impact region for WTC 1, Fig. 3–1. When referring to photographic images of pre-collapse damage, please see Sec. 2.2.

- **M-30:** Photographic images indicate that panel M-30 was directly hit by the wing and fuselage of the airplane, with a majority of the panel pushed into the envelope of the building. The recovered panel (Fig. 3–2a) consists of the lower portions of columns 132 and 133 at and below the 95th floor level spandrel. The columns were severed at different locations. Column 132 was severed at the stiffener plate associated with the top of the spandrel, Fig. 3–2b, while column 133 appears to have been severed at a slightly lower elevation associated with the 95th floor level concrete slab, Fig. 3–2c. This damage pattern was indicative of the inclination of the airplane impact. With the exception of the spandrel plate, the remaining portion of the recovered panel, portion of columns located in the upper 94th floor level, was relatively undeformed.

- **S-9:** This panel was located directly above M-30. From photographic evidence, it seems that the vertical tail section of the plane hit the lower portion of the columns, damaging the aluminum façade. It is unknown how much damage occurred to the underlying columns themselves as smoke obscured most views of the panel. However, the aluminum façade above the 98th floor level did not appear disrupted, indicating that the panel may not have been significantly displaced upon impact. The recovered panel (Fig. 3–3a) contained all three columns, though the panel was badly damaged (Fig. 3–3b). The columns below the 98th floor spandrel were bent in various directions. Column 132 sustained the most damage at and just above the 98th floor spandrel. The column was bent nearly 180 degrees just above the 98th floor spandrel with the spandrel completely detached from the column (Fig. 3–3c). The portion of the column near the spandrel had a "splayed" appearance as the four individual plates comprising the box column were no longer joined. Additionally, the outer web was completely severed and slightly bent inward. This damage may have been a result of the aircraft impact. Some damage was also noted on the lower portions of columns 133 and 134, though it is unknown whether this was caused by the impact.

- **M-27:** This panel was hit directly by the nose and fuselage of the plane. The photographic evidence shows that the portion below the 95th floor spandrel still appeared to be intact while the portion above this had been bent inward. The top portions of the two recovered columns (Fig. 3–4), numbers 130 and 131, were in general disarray, with portions above the 96th floor level missing. These columns also had a splayed appearance with the four individual plates making up each column deformed along their entire length. The only connection between the two columns was located at the 95th floor level as the 94th floor spandrel, while still joined to column 131, was detached from column 130.

- **M-2:** This panel, directly above M-27, was struck by the upper part of the fuselage and the vertical stabilizer of the tail. From the photographic images, it appears that the condition of this panel after recovery was remarkably similar to its condition prior to the collapse, Fig. 3–5a. Therefore, the damage observed was assumed to be a result of the impact. Inward bending of the columns was observed at numerous locations on the panel. A lower bend was directly associated with the concrete slab of the 97th floor level, Fig. 3–5b. The floor appears to have acted as a fulcrum point over which the columns and lower portion of the spandrel were bent inside the building envelope. Also, for columns 129 and 130, the lower end plates were found to be ripped off with the two columns having the splayed appearance, Fig. 3–5c. The end plate for column 131 was still intact and the lower portion of the column was relatively

undeformed. From the pre-collapse images, the lower portion of this column was also bent inward just below the 97th floor spandrel, however, it had been bent back out. The former was associated with the impact, with the latter occurring sometime during or after the collapse.

- **N-7:** From photographic images, it appears that N-7 was not struck directly by the plane and experienced relatively minor damage by having the panel below it pushed into the building. While smoke obscures most of the images, the aluminum façade on column 124 at floor 97 appears to be disturbed. No other comments can made concerning pre-collapse damage. The recovered panel consists of three, relatively intact columns that sustained limited damage (Fig. 3–6). The 98th floor spandrel between columns 126 and 127 is partially missing and completely detached between columns 126 and 127. It was not possible to determine when this damage occurred. The entire panel itself was folded inward about an axis parallel to the length of the columns with the outer web of the columns facing outward. This was believed to have happened during or after the recovery efforts.

3.1.3   Summary

From observing the pre-collapse photographs and the five recovered panels from the impact zone, two of the four directly impacted panels (M-2 and M-30) appear to be in a similar condition to that which they were in as a result of the impact. Some of the extraneous damage was attributed to the events during and after the collapse, but the general shape and appearance of the recovered pieces agree with the damage photographs. There was a lack of detailed pre-collapse visual evidence of impact damage sustained by panels M-27 and S-9, and it is not possible to make a similar statement. Finally, the lower portion of N-7 did incur some damage; however, it could not be positively correlated with pre-collapse images.

3.2   DAMAGE AND FAILURE MODES OF EXTERIOR WALL COLUMNS

A survey was conducted on the individual exterior wall columns of the recovered panels to identify and inventory the various failure modes associated with impact and collapse of the building. As most columns were not damaged by the impact, only the five samples within the impact region of WTC 1, and other special cases, were documented in detail. Other samples were separated and analyzed according to their post impact, pre-collapse environment and known/unknown as-built location.

To summarize the samples used in this portion of the analysis, there were 42 exterior panels identified, 26 from WTC 1 and 16 from WTC 2. There were 60 individual columns for observation from WTC 1. From WTC 2, only 13 of the 16 identified panels were used for the analysis. The three panels located at John F. Kennedy International Airport (B-1024, B-1043, and B-1044) were not fully analyzed during the visits to the hangar, and thus, the condition of their columns was not taken into consideration for the statistical analysis. Of the remaining 12 panels, 29 individual columns were available for inspection. Section 2.1.3 describes in detail the strength/gauge combinations for the recovered columns. Finally, there was one panel that was partially identified (C-117) and 47 exterior panels not identified as to their as-built locations. From these 48 samples, an additional 55 columns for observations were available.

3.2.1   Types of Failure Modes

Recovered exterior columns were observed to have numerous damage features and failure modes. While the columns that had heavier flange sections experienced similar damage, those columns with lighter gauges were observed to experience more severe characteristics. These damage features/modes of failure were grouped into the following categories for statistical purposes.

Type 1: Gross physical distortion of flange/web material.

> Type 1a: Crushed sections (Fig. 3–7a and 3–7b): not limited to, but typically a result of handling during the recovery effort.

> Type 1b: Punctured flanges and/or webs (Fig. 3–7c).

> Type 1c: Buckling of flange and/or webs (Fig. 3–7d): no distinction was made for possible pre-collapse environments, i.e., whether or not exposure to fire may have occurred.

Type 2: Fracture near fillet welds.

> (As discussed below in Sec. 3.2.2.1, fractures typically occurred in the heat affected zone of the base metal; fracture in the actual weld material itself was an infrequent occurrence).

> Type 2a: Localized fracture associated with welded joints (Fig. 3–8a): inches to a few feet of crack growth near one weld.

> Type 2b: Extensive fracture associated with welded joints (Fig. 3–8b): few feet to yards of crack growth near one or more welds.

> Type 2c: Columns that were splayed open (Fig. 3–8c): the fracture associated with all four welds of perimeter column in the same vicinity.

Type 3: Severing of columns.

> Type 3a: Severing associated with internal stiffener/diaphragm plate (Fig. 3–9a).

> Type 3b: Severing away from internal stiffener/diaphragm plate (Fig. 3–9b).

> Type 3c: Severing at floor level (Fig. 3–9c).

> Type 3d: Flame cut ends during recovery (Fig. 3–9d), though not a true "failure mode", was necessary to classify a fair number of columns.

While these damage features were observed and recorded for each individual column, no effort was made to quantify the frequency with which the modes occurred for each column, particularly for Type 1 and Type 2 modes.

3.2.2   WTC 1 Panels in Impact Region

Exterior panels from WTC 1 were analyzed to determine if different damage features were observed for those columns located within the impact region and those outside of this region. There were 13 observations from the 5 panels in the impact region and 47 from the 18 panels outside. From Table 3–1, for the majority of damage features or failure modes observed, those in the impact zone had a higher frequency of damage observations. It was unknown whether this was due to the violent nature of

the impact or if it was an artifact of the smaller sampling size. Regardless, the majority of columns directly hit by the airplane experienced all three types of gross deformation. The higher occurrence of the columns being crushed and/or punctured in this region may be related to the high rate of impact of the plane with the concomitant transfer of energy/momentum of the high density aircraft components to the structural elements in this region. This transfer of energy can also be translated to the weld fractures, as a higher frequency of columns experienced fracture in the vicinity of the welded joints. Severing of the column was typically related to the stiffener or diaphragm plate associated with the spandrel connection.

In NIST NCSTAR 1-3B, National Institute of Standards and Technology (NIST) labeled samples M-2, M-27, M-30, N-7, and S-9 were observed located in the impact region, with all but N-7 being directly hit by the plane. As these pieces were located in the impact area, detailed analysis of the columns may yield insights into the behavior of the material and/or components of the panel upon impact.

- **M-30:** As described above, the two columns recovered for sample M-30 were severed at different locations. Column 132 was severed at the stiffener plate associated with the top of the 95th floor spandrel plate (Fig. 3–1b). Both the outer web and spandrel plate were fractured very near the top edge of the stiffener plate, while the flanges were fractured just above. Given the constraint afforded by the stiffener plate and the concrete floor, and the fact that the column was relatively undistorted, these plates likely failed in some complicated combination of shear and tension. Column 133 appears to have been severed at a slightly lower elevation associated with the 95th floor level concrete slab (Fig. 3–1c). Portions of the outer web and spandrel plate were bent inward, nearly 90 degrees, with fractures occurring in the plates perpendicular to the rolling direction of the plate. The flanges were found to fracture at a slightly lower elevation than the web and spandrel plates. The outer web and spandrel plate of column 133 were particularly important pieces in terms of failure mode, because the combination of their proximity to the aircraft impact and the configuration of their geometry and location close to a concrete floor means that they likely experienced the highest strain rate in relatively pure tension of any of the exterior columns. Examinations were made of these fractures to determine if any brittle behavior could be found, which would indicate a transition from ductile to brittle fracture, and would have an effect on the energy balances being calculated for the impact interactions between aircraft and building. The outer web of column 133 was nominally 0.25 in. in thickness, while the spandrel plate was 0.375 in. thick. The fracture surfaces were removed from the column (Fig. 3–10) and chemically treated in an attempt to remove the rust and observe the fractography beneath. In both cases, evidence of a microscopic fracture mechanism (cleavage facets or dimpling) were obliterated by a corrosion process. However, the macrofracture features on the surface were still observable. An image of the fracture surface of the spandrel plate of column 133 is shown in Fig. 3–10c, while an overlaid schematic shows some of the details that are hard to see on another related plan view image in Fig. 3–10d. The fracture shows chevrons running along the length of the crack path, indicating crack direction and the fact that this plate failed largely in tension through the motion of a mostly mode I crack. There was a very small amount of thinning in the region of the fracture surface, and there was a small shear lip present (10 percent of the surface width), shown in the schematic illustration. From these observations, it was determined that the fracture, though certainly lower energy than would have been seen at a normal rate test, still had some ductility (formation of small shear lips). There was no evidence that this steel sample had broken in a purely brittle manner, though it was certainly low energy ductile in character. The lower portions of the columns residing in the 94th floor region were relatively undeformed.

- **S-9:** Column 132 sustained the most damage at and just above the 98th floor spandrel (Fig. 3–2c). The column was bent nearly 180 degrees just above the 98th floor spandrel, with the spandrel plate completely detached from the column. The portion of the column near the spandrel had fracture near all four welds associated with the box column, thus, resulting in a splayed appearance. Additionally, the outer web was completely severed and slightly bent inward. As this may have been a result of the airplane impact, the sample was removed for analysis (Fig. 3–11a and 3–11b). The fracture surface was badly corroded and exhibited evidence of being damaged by contact with other steel samples or pavement at some point. However, it was possible to observe some macroscopic fracture details. The fracture surface was oriented at 45 degrees with respect to the surface of the plate and oscillated between plus and minus 45 degrees at several points as the crack propagated across the plate. The edge of the fracture surface at one time was quite sharp, and significant thinning of the plate was observed within 0.5 in. of the fracture surface (Fig. 3–11c) indicating significant ductility during crack propagation. In addition, more than 10 in. from the fracture surface, the paint coating was fractured in a particular way as to indicate tensile loading of the surface (Fig. 3–11d). Although this might have been caused by localized bending, the plate at this point was nearly flat, and it was quite possible that these cracks indicate elastic/plastic stretch below a level that was measurable at these locations. This would indicate considerable energy absorption during failure of these plates as well. The additional massive damage to the remainder of the panel not observed prior to the collapse may be related to events occurring during the collapse of the building or as a result of the recovery efforts. Analysis of a weld fracture from column 133 can be found below in Sec. 3.2.3.

- **M-27:** As mentioned above, this panel was hit directly by the fuselage of the plane, which resulted in massive damage to the structural elements. Only columns 130 and 131 were recovered; the top portion had been severed at the lower stiffener plate for the 96th floor spandrel. The majority of welds between the flanges and webs have fractures in the vicinity of the welded joints, resulting in the splayed appearance and general disarray of the columns (Fig. 3–8c). The flange and web plates experienced a significant amount of deformation.

- **M-2:** Damage of lower columns was clearly associated with impact, which led to the missing endplates for columns 129 and 130. As a result, the inner and outer web plates of both columns appear to have thinned in this area (Fig. 3–12a). Similar to the behavior observed on panel S-9, the crack propagated across the inner and outer web plates as a 45 degree slant crack, oscillating between positive and negative 45 degrees with respect to the normal of the plate. The degree of necking observed in M-2 was slightly larger than that observed on S-9, as seen in the plot of the measured neck profile in the outer web, Fig. 3–12b. Large buckles were observed on both flanges for columns 129 and 130 (Fig. 3–13a) with some splitting occurring in the base material of the flanges (Fig. 3–13b) and spandrels (Fig. 3–13c). However, the welds found near this bending point remained intact (Fig. 3–13d). Analysis of fractures near welded joints from this panel associated with impact damage can be found below in Sec. 3.2.3.

- **N-7:** As the airplane did not directly impact this panel, no damage was attributed to this event. Regardless, the columns were in relatively good shape with localized fracture near the welds in some areas. As previously mentioned, the 98th floor spandrel between columns 126 and 127 was

partially missing and completely detached. As the panel below N-7 was pushed inside the building as a result of the plane impact, bolt failure between the panels occurred.

Weld Failure Analysis Associated with the Perimeter Columns

As part of the damage and failure modes of the exterior panel columns, an analysis was conducted on the damage features of the submerged arc welds found on the perimeter columns of the WTC towers. Special emphasis was placed on those panels directly hit by the airplane. Behavior of the welded joints was characterized, and the role of failure in the base metal, heat affected zone (HAZ), and weld metal were discussed.

Cross-Sectional Analysis

Panel M-2 (A130: 96-99) was struck directly by the airplane. From both pre-collapse photos and the recovered element, the lower portion of columns 129 and 130 (96th floor splice) were found to have their lower end plates ripped. The majority of welds between the flanges and webs in this area had fractures in the vicinity of the welded joints resulting in the splayed appearance. Two typical fractures associated with welds were taken from the lower portion of column 129. This column had a specified minimum yield strength of 55 ksi.

The first example was a fracture taken between the flange and the outer web, Fig. 3–14. From observations made in the field, the fracture appeared to have occurred in the outer web plate near the weld bead. It was assumed that fracture was initiated near the lower end plate of the column upon impact (when end plate was ripped out) and then ran vertically "up" the column toward the 97th floor level spandrel. The outer web was still connected to the column, but was pushed inward towards the center of the building; the inner web had been severed near the lower stiffener plate of the 97th floor level spandrel. The vertical fracture in question between the outer web and flange was found to stop short of the same lower stiffener plate of the 97th floor level spandrel. Viewing the fracture surface of the outer web plate with the naked eye, it was observed to have a fibrous and/or "woody" appearance, Fig. 3–15a. Closer examination showed that the fracture surface was stepped, Fig. 3–15b and 3–15c. Due to prior exposure to the elements of weather, the fracture surface was corroded to the point that no further information could be obtained from it.

Macroscopic investigation of the cross-section revealed that fracture did occur in the outer web plate; a portion of this plate was still visible after metallographic preparation and etching procedures, Fig. 3–16. The flange and double-pass submerged arc welds were also seen. The weld was sound with no visible flaws observed. Typically, these joints were over-welded, meaning that a 3/8 in. or 1/2 in. weld may have been deposited where only a 5/16 in. bead was specified. A slight gap existed between the plates for the outer web and flange; this was not uncommon for most weld cross-sections evaluated between these two column components. The outer face of the fracture surface was associated with the toe or root of the weld. The cross-section of the failed plate revealed a jagged, stepped fracture surface with the steps parallel and perpendicular to the rolling plane of the plate. Microscopic investigation further revealed that tearing of the outer web initiated at the toe of the weld and that the crack propagated through the HAZ of the plate, Fig. 3–17. The HAZ is a common weld feature consisting of microstructurally altered, unmelted base metal adjacent to the weld bead. It is a direct result of the heat input required for

metallurgical bonding (melting) of the two work pieces, regardless of the weld being autogeneous or made with filler material.

While the fracture features of this example had a "woody" appearance, the failure was not associated with lamellar tearing of the steel. When associated with welding, this fracture mode (lamellar tearing) typically occurs due to low ductility in the through-thickness (short-transverse) direction of the parent material in combination with employment of an improper weld joint geometry with respect to the poor through thickness properties of the plate (Kou 1987; Ludwigson et al. 1982; Sommella 1979; Porter 1976). However, the failure was not a material-related issue, as a concerted effort was made to deoxidize the steel to a relatively high degree for plates with F_y of 55 ksi or greater (NIST NCSTAR 1-3E). This was noted by the elevated levels of silicon and aluminum, with significantly low levels of phosphorous and sulfur. Additionally, the volume fraction of nonmetallic MnS inclusions was, on a qualitative basis, very low, and the inclusions were thin and well dispersed throughout the plate. Further, the banding characteristics, in terms of the pearlite constituent, of the structure were very low, particularly at the surfaces of the plate, for the 55 ksi material. Rather, the location and appearance of the fracture associated with this weld joint was most likely a result of two factors: (1) the direction of the high impact loading of fabricated columns composed of welded plates and (2) the diminished HAZ properties of a rolled plate with moderate anisotropic mechanical properties.

The weld geometry employed in manufacturing the perimeter box columns was appropriate for the building construction; sustaining a high velocity impact perpendicular to the weld bead was not considered when choosing joint geometry. However, the "geometry" of the weld, in combination with the direction of impact, did dictate where fracture would occur, that being, in the area of lowest cross-section. The plate thickness of the outer web (0.25 in.) was thinner than both the weld cross-section and flange plates. Additionally, the strength/ductility of the weld appears to be more than adequate as fracture of the weld material did not occur; this was observed throughout the majority of near-weld fractures found on perimeter columns. Location of crack initiation was found at the root of the weld observed on the outer web as this provided a stress concentrator.

Additionally, the HAZ of the material was found to have a higher hardness than the base metal and the weld (NIST NCSTAR 1-3E). This was due to microstructural changes in the base metal. As the hardness of the material increased, a concomitant decrease in the ductility of the material in the HAZ would also be implied. As a result, the macroscopic "angle" observed for fracture was related to the shape of the heat affected zone in the web plate as the crack propagated through this region of lower ductility. The stepped appearance of the fracture surface may be related to moderate anisotropic properties of the rolled plate. However, the ductile or brittle microscopic mechanism of plate failure could not be determined as corrosion of the fracture surfaces excluded definitive identification of microscopic features on the fracture surface.

The second sample removed was a fracture taken between the flange and the inner web of the same column and roughly in the same location, Fig. 3–18. The damage characteristics were quite different from the first case examined. From observations made in the field, it appeared that fracture occurred in the inner web plate near the weld bead. Initial fracture was again assumed to start near the lower end plate of the column upon impact (when end plate was ripped out) and then ran vertically "up" the column toward the 97th floor level spandrel. The inner web was then severed at the lower stiffener plate of the 97th floor level spandrel. The vertical fracture in question between the inner web and flange was found to

end near the same lower stiffener plate of the 97th floor level spandrel. Unlike the fracture between the outer web and flange, the inner web fracture surface was relatively flat with no readily observable features to the naked eye, Fig. 3–18c. Again, significant corrosion product had consumed the fracture surface; thus, further analysis would prove to be unproductive.

Macroscopic investigation of the cross-section revealed that fracture did occur in the inner web plate, Fig. 3–19. The flange and single-pass submerged arc weld were also seen. However, a few, small steps were noticeable on the fracture surface in cross-section (lower left image of Fig. 3–19). Similar to the first case discussed above, the direction of high rate impact with the joint geometry dictated that the initiation site for fracture of the inner web was associated with the stress concentrator in this area where the flange and web meet but were not metallurgically joined. It appears that the tearing initiated at the location where the weld bead intersected the surface of the inner web and then propagated through the HAZ. Microscopic investigation revealed that tearing of the inner web occurred at the juncture between the weld bead and the surface of the inner web and was restricted to the HAZ of the plate, Fig. 3–20.

Once again, the fracture associated with this WTC weld joint was not attributed to either poor material quality of the inner web or the weld joint configuration. Instead, the direction of the high impact loading of the plate in combination with the diminished properties of the HAZ of a rolled plate was believed to have led to this type of fracture. There was a differences between the two macroscopic angles of fracture; the first case having a "woody" appearance and the second case having a "flatter" fracture surface. This was most likely related to the geometry of the HAZ of the weld itself. To clarify this point, two additional cross-sections were prepared of welds that had not experienced fracture, Fig. 3–21. The first example was taken of a joint between the flange and outer web. Figure 3–22 shows the geometry of the HAZ in the outer web plate. The HAZ was angled similarly to the fracture surface observed in the first weld fracture sample. Likewise, Fig. 3–23 shows the HAZ geometry from the second example, that between a flange and an inner web. Similar to the fracture surface of the second weld fracture examined, the angle of the HAZ front had a significantly higher slope with respect to the rolling plane of the inner web. Clearly, the macroscopic angle of fracture of both plates was a result of diminished properties in the HAZ near the weld, with the difference between the HAZ geometries most likely a combination of the welding parameters and the joint geometry. Further, no microscopic information could again be obtained to define the microscopic mode of fracture.

Planar View Analysis

A third fractured weld sample was removed for investigation of crack propagation through the material. This sample was from the 96th floor level of column 133 (specified minimum yield strength of 55 ksi) on panel S-9. This panel was struck directly by the plane, in particular, the tail section. The lower portion of column 133 was found to be intact and in relatively good condition near the splice connection; however, just below the 97th floor spandrel, the column had a similarly splayed appearance as that observed for panel M-2 (Fig. 3–24a). The removal of the sample was such that the crack tip could be investigated, Fig. 3–24b. Inspection with the naked eye revealed that the crack propagated in the outer web plate along the weld bead, Fig. 3–25.

Macroscopic investigation of the cross-section revealed that fracture did occur in the outer web plate similar to the first case examined above, Fig. 3–26. This portion of the sample was taken from well behind the crack tip. Again, the flange and double-pass submerged arc welds were seen with a stepped

fracture surface in cross-section. As observed, the fracture was restricted to the HAZ material. In addition to the cross-sectional view, the sample was mounted so that propagation of the crack through the material could be viewed, Fig. 3–27. This "planar" view resulted in the rolling plane of the outer web parallel to the plane of the paper. It was seen that the crack traversed a path in the HAZ near the fusion line of the weld, Fig. 3–28. However, it was also noted from both Figs. 3–26 and 3–27 that a second crack was present. Another cross-section was prepared, with this portion of the sample taken from well in front of the original crack tip of Fig. 3–26, and analyzed. Macroscopic investigation of the cross-section revealed that the fracture of the weld occurred within the flange plate, Fig. 3–29. Microscopic analysis showed that the crack started in the HAZ of the first submerged arc weld in the flange plate and traveled into the unaffected base material, Fig. 3–30. It was believed that if this crack would have continued to propagate, it would have resulted in a weld fracture similar to that shown in Fig. 3–31.

3.2.3 Summary

Though decomposition of the perimeter columns into the four individual plates was associated with fracture through the HAZ, it should be noted that this feature is characteristic of all fusion welds of carbon steels and should not be considered a flaw in construction of the towers. Further, there was no evidence throughout this analysis to indicate that fracture associated with the welds evaluated was related to: (1) inadequate joining materials (weld strength and ductility appeared appropriate for the application), (2) inappropriate welding procedures (welds were typically oversized with no visible flaws), or (3) poor performance of the welded joint (fracture was associated with extreme loading event, i.e., impact of aircraft).

3.2.4 WTC 1 Panels Exposed to Fire

Exterior panels from WTC 1 were analyzed to determine if different damage features were observed on column panels exposed to fire and those that were not. There were 36 observations from the 16 panels exposed to fire and 24 from the remaining 10 panels. From Table 3–1, it was seen that the occurrence of buckling was greater in those columns exposed to fire. One fact not conveyed in the table was that the buckling typically occurred on the inner web plate. This was not unexpected as results from other projects of this investigation indicated that the interior web plate was prone to local buckling under certain conditions (i.e., structural response to gravity loads and fires) (NIST NCSTAR 1-5B; NIST NCSTAR 1-6C). A higher observance of punctures was also associated with the impact panels combined with the other fire exposed columns. For weld fractures, there was a slightly higher tendency for fire exposed columns to have localized fractures and splayed columns. However, both of these observations were most likely a result of these columns being located in or near the impact zone and not a direct result of the pre-collapse fires. Severing of the columns was found to occur at the stiffener plates with a higher frequency for samples located in fire exposure areas.

The observations were also correlated with the time-exposure maps (Fig. 2–48) to determine exactly which columns may have been exposed directly to fire. From this information, 30 observations were available in which fire was either located in the window (category 2) or noted with external flaming (category 3) next to the column examined. Similar results were found when the panels, as a whole, were suspected of being exposed to fire, Table 3–1.

3.2.5 Unidentified Panels

The statistics of the failure modes for the unidentified columns is presented in Table 3–1. These values differ significantly from those of the identified columns, but can be explained by the difference in the overall characteristics of the collection of columns. The unidentified columns include a large number of single very thick columns, which tended to survive the collapse relatively intact. In addition, the lengths of the unidentified columns were, on average, much shorter than the identified ones, and thus, there was also less length that had a chance to accumulate a particular type of damage. For example, crushes and buckles were more likely in long, slender members like full panels, which were more likely to have the location with the identifying stamps survive.

3.2.6 Summary

Observations of recovered panels for damage of the exterior panel columns revealed that the five panels located in the airplane impact zone had a higher tendency for damage features across the board than those outside of this region. This may be due to the high energy impact of the plane and transfer of this energy to the structural components of the building. There did not appear to be any difference in failure modes or damage characteristics whether the panels were exposed to fire or not, with the exception of the buckling phenomenon. No observations of any significance to the investigation were able to be drawn by comparing the observed failure modes on the identified and unidentified samples. Fractures of spandrels and webs were found to exhibit at least some ductile behavior, even in samples that experienced the highest tensile loading rates. For the limited number of weld fractures microstructurally analyzed, it was observed that the fracture initiated and propogated in the heat affected zone. During visual observations of all the recovered exterior panel columns, this was the dominant mode of weld fracture. In one case examined, the fracture was observed to initiate in the HAZ and subsequently propagated into the unaffected base material. There were very few examples of this type of failure observed during the visual observations of all the recovered exterior panel columns.

3.3 EXTERIOR WALL SPANDREL CONNECTIONS

A survey was conducted on the spandrel connectors of the recovered panels to identify and inventory the various failure modes associated with impact and collapse of the building. As most connections remained intact after the impact and prior to the collapse, only the five samples within the impact region of WTC 1 were documented in detail. The remaining samples were separated and analyzed according to their post impact, pre-collapse environment and known/unknown as-built location.

To summarize the samples used in this portion of the analysis, there were 42 exterior panels identified, 26 from WTC 1 and 16 from WTC 2. Of the 26 from WTC 1, only 23 panels had recovered portions with spandrel connections for inspection, yielding 82 individual observations. The remaining three panels identified that did not have observable spandrel connections were C-55, C-93, and K-2. These samples consisted of only the lower portion of the middle column of the panel. From WTC 2, only 13 of the 16 identified panels were used for the analysis. The three panels located at John F. Kennedy International Airport (B-1024, B-1043, and B-1044) were not fully analyzed during the visits to the hangar, and thus, their connections were not taken into consideration for the statistical analysis. Of the remaining 13 panels, 36 observations were possible for inspection. However, the spandrel connection between M-10a and M-10b located on the 84th floor was still intact, and thus, not tallied in the statistical analysis

of the "failures," resulting in a total of 34 observations for WTC 2. Finally, there was one panel that was partially identified (C-117) and 47 exterior panels not identified as to their as-built locations. Of these 48, 41 panels had recovered portions with spandrel connections for inspection, which yielded an addition 47 observations.

For the spandrel connection details, there were 29 specified variations in the design drawings. The differences arose from the dimensions of the splice plate and the size, number, and positioning (in terms of rows and spacing) of bolts. All bolts were ASTM International (ASTM) A325 with diameters of either 0.875 in. or 1.125 in. The bolt holes in the spandrel were aligned in a vertical fashion with the first row of bolts placed 1.5 in. on center from the outer edge of the plate. If a second row of bolts was indicated, they were 3 in. further inward from the splice on center from the first row. From the recovered panels with known as-built locations, 118 observations (including the connection between M-10a and M-10b) were available for inspection, resulting in 11 different variations of spandrel details, Table 3–2. The samples with unknown as-built locations were also inspected resulting in an additional 48 observations. Table 3–2 displays the eight variations found for these samples.

3.3.1 Types of Failure Modes

Observations of the failure modes of the spandrel plate connectors yielded five different modes.

Type 1: Bolt tear out in spandrel plate. There were three variations of this mode.

> Type 1a: The observed spandrel connection possessed the tear outs (Fig. 3–32a).

> Type 1b: The splice plate and all bolts of the observed spandrel connection remained, thus, tear out occurred in the neighboring spandrel plate to which it was attached (Fig. 3–32b).

> Type 1c: The observed spandrel connection possessed the tear out, with the additional fracture of the spandrel plate in a horizontal manner (Fig. 3–32c).

Type 2: Bolt tear out in splice plate (Fig. 3–33).

Type 3: Mixed mode (Fig. 3–34) of any of the types.

Type 4: Vertical fracture of the spandrel plate at spandrel/flange intersection. There were two variations of this mode.

> Type 4a: Fracture of observed spandrel plate (Fig. 3–35a).

> Type 4b: Fracture of the neighboring spandrel plate resulting in the observed spandrel connection retaining both the splice plate and portion of spandrel from neighboring panel (Fig. 3–35b).

Type 5: Bolt failure resulting in intact holes in spandrel or splice plate (Fig. 3–36).

Due to the storage position of the samples, some photographs were taken as if one viewed the spandrel from outside of the building looking inward toward the core and vice versa. The orientation was noted for each photograph.

3.3.2 WTC 1 Panels Located in Impact Region

Exterior panels from WTC 1 were analyzed to determine if different failure mechanisms were observed for those that were hit directly by the plane and those outside of this region. There were 21 observations from the five panels in the impact region and 61 from the 18 panels outside. As shown in Table 3–3, Type 1 and Type 4 failure modes dominated for both regions, but there does not appear to be a significant difference between the two regions. The same can be said when the two sample groups are compared to the 82 observations from WTC 1 as an individual group.

Figures 3–37 through 3–41 show the spandrel connections of the five samples located in the impact zone. The damage sustained to some of the samples did not allow for unobstructed photographs to be taken for all connections.

- **M-30:** The recovered portion of M-30 had only one spandrel connection, which was located at the 95th floor and attached to column 132. From pre-collapse photographs, it appears that this connection was intact with its neighboring recovered panel, M-27, after the impact. Reviewing the recovered connection revealed that a Type 4b failure occurred (Fig. 3–37) where the spandrel from the M-27 was still attached via the splice plate connection. This failure likely occurred upon collapse of the building and not as a result of the impact.

- **S-9:** As the entire panel of S-9 was recovered, all six spandrel connections were available for inspection. Pre-collapse photographs yielded little evidence to indicate that failure of the spandrel connections located at the 99th and 100th floors occurred upon impact, and therefore, the damage observed on these connections (Fig. 3–38) was likely sustained upon collapse of the building. The connections located on the 98th floor were obstructed by smoke, and possible damage due to impact was unable to be determined. The sample labeled M-2 was a neighbor of S-9.

- **M-27:** The recovered portion of M-27 had only two spandrel connections for observation. Both were located on column 131 at floors 94 and 95. As discussed above for M-30, the connection at floor 95 was shared between the two samples and appears to have been intact after impact, indicating that failure occurred upon collapse of the building. From the recovered portion of M-27, this specific connection failed via Type 4a mode, where the spandrel was fractured at the flange/spandrel interface (Fig. 3–39). This corresponded with the findings on sample M-30, which had a Type 4b failure mode and the remnants of the spandrel from M-27. Reviewing pre-collapse photographs for the spandrel connection located at floor 94, it also appears to have failed (Type 4a) during the collapse as there was no indication that failure occurred prior to this point.

- **M-2:** As the entire panel of M-2 was recovered, all six spandrel connections were available for inspection. From pre-collapse photographs, it appears that both connections located on floor 97 failed upon impact of the airplane. Both failures were of Type 1 (Fig. 3–40), with the connection associated with column 131 having bolt hole tear out (Type 1b), and the connection nearest column 129 still retaining the splice plate without the neighboring spandrel plate (Type 1a). The connections associated with floor 99 appeared intact, and failure may have occurred upon collapse. Those connections located on the 98th floor were obstructed by smoke and, thus, their status was unable to be determined prior to collapse. The connections on column 131 at floors 98 and 99 were shared with sample S-9. By reviewing the photographs of these two spandrel

connections, it was seen that the recovered portions were consistent with the failure modes between the two panels.

- **N-7:** As the entire panel of N-7 was recovered, all six spandrel connections were available for inspection. Reviewing pre-collapse photographs, the connections located at the 99th and 100th floors appear to be intact after the impact, thus, suggesting that failures observed were a result of collapse of the building. The connections located at the 98th floor were obstructed by smoke, and possible damage caused by impact was unable to be determined. As M-2 and N-7 were neighboring panels, they shared connections at floors 98 and 99. By reviewing the failure modes (Fig. 3–41), it was seen that the failure modes compliment each other (corresponding Type 1 failures) for the related connections on each panel.

3.3.3   WTC 1 Panels Exposed to Fire

Exterior panels from WTC 1 were analyzed to determine if different failure mechanisms were observed for those panels exposed to fire and those that were not. There were 48 observations from the 16 panels exposed to fire and 34 from the remaining 10 panels. As shown in Table 3–3, Type 1 and Type 4 failure modes dominate for both sets of samples, with panels exposed to fire slightly more inclined to fracture at the spandrel/flange interface than those not exposed to fire. However, this observation may be a result of many of these observations being from within the impact zone and not directly related to exposure to pre-collapse fires.

The observations were also correlated with the time-exposure maps (Fig. 2–48) to determine exactly which individual spandrel connections may have been exposed directly to pre-collapse fires. From this information, 19 observations were available from 10 different panels in which fire was either located in the window (category 2) or noted with external flaming (category 3). Similar results were found when the panels, as a whole, were suspected of being exposed to fire.

3.3.4   Panels Separated by Floor Locations

Exterior panels from WTC 1 were analyzed to determine if different failure mechanisms were observed for those panels above the impact region and those located below. There were 34 observations from the 12 panels at or below the 95th floor and 47 from the remaining 11 panels above the 95th floor. As shown in Table 3–3, Type 1 and Type 4 failure modes dominate for both sets of samples. However, panels above the 95th floor were more likely to have bolt hole tear out than those below the impact zone and in general more likely to have bolt hole tear out when considered versus the building as a whole. For panels below the impact zone, fracture of the spandrel panel from the column was a more dominant mechanism.

Exterior panels from WTC 2 were analyzed to determine if different failure mechanisms were observed for those panels above the impact region and those located below. There were 12 observations from the 9 panels at or below the 78th floor and 22 from the remaining 9 panels above the 78th floor. As shown in Table 3–3, panels above the impact zone behaved similarly to those from WTC 1 in that Type 1 was the more prevalent mode of failure, with Type 4 also playing a role. While a significant set of observations was not made for those samples below the impact region, splice plate fracture was found to be the dominant mode of failure.

3.3.5   Unidentified Panels

For the 41 unidentified samples with spandrel connections, there were 49 locations where connections between panels were able to be identified. The spandrel failure modes for the unidentified columns in Table 3–3 have roughly the same distribution as the identified columns with one notable exception. A large number of spandrel connections were identified as category 2, with bolt tear out in the splice plate. These were found exclusively in the columns with large thicknesses, where the weakest load bearing section of the panel spandrel connection would be the splice plates, and thus, this failure mode for these columns was as expected.

3.3.6   Summary

From the observations made on recovered panels concerning the spandrel connections, there did not appear to be a significant difference in failure mode whether the panels were exposed to fire or not. There was a statistical difference in the failure modes if the location of the individual panel was considered. For panels at or above the impact zone, bolt hole tear out was a more likely failure mode. For those samples below the impact zone, there was a higher propensity for the spandrels to be ripped off from the panels.

3.4   EXTERIOR WALL COLUMN SPLICES OR ENDPLATE/BUTT PLATE CONNECTORS

A survey was conducted on the end plate connectors of the recovered panels to identify and inventory the various failure modes associated with impact and collapse of the buildings. As most connections remained intact after the impact and prior to the collapse, only the five samples within the impact region of WTC 1 were documented in detail.

To summarize the samples used in this portion of the analysis, there were 42 exterior panels identified, 26 from WTC 1 and 16 from WTC 2. Of those 26 from WTC 1, all panels had a minimum of one end plate, resulting in 91 observations. From WTC 2, full analysis was completed on 12 of the 16 identified panels. Two panels located at John F. Kennedy International Airport (B-1043, and B-1044) were not fully analyzed during the visits to the hangar, but the tops of the columns were removed and shipped to NIST. Further, B-1024, also located at John F. Kennedy International Airport, was not analyzed at all, and M-10a did not have any end plates recovered (NIST NCSTAR 1-3B). In total, there were 40 observations from the 12 samples examined for WTC 2. Finally, there was one panel that was partially identified (C-117) and 47 exterior panels not identified as to their as-built locations. Of these 48, 27 panels had recovered portions with end plate connections for inspection, which yielded an additional 49 observations.

For the end plate splice details, there were 38 specified variations in the design drawings. The differences arose from the dimensions of the butt plate, size of the fillet weld (weld #11 between the end plate and column components), and the size, number, material type, and placing of the bolts. Further, splices located at mechanical floors were welded in addition to bolting. Bolts were either ASTM A 325 or A 490 with diameters of 0.875 in., 1 in., or 1.125 in. The type of bolt used varied according to the floor location within the buildings. From the recovered panels with known as-built locations, a total of 131 inspections were made with 11 different variations of end plate details observed, Table 3–4. For the samples with

unknown as-built locations, the failure statistics were tallied irrespective of the end plate splice details, as this information was not easily obtainable.

3.4.1   Types of Failure Modes

There were three types of failure modes associated with the end plate connectors:

Type 1: Bolt failure (Fig. 3–42).

Type 2: Fracture associated with the weld between column plates and end plate. There were two variations of this mode:

> Type 2a: Partial fracture with end plate still remaining (Fig. 3–43a).

> Type 2b: Full fracture with end plate missing (Fig. 3–43b).

Type 3: A welded connection with bolts intact, end plate of above or below adjoining column still attached (Fig. 3–44), failure occurring in flange/web material.

3.4.2   WTC Tower Panels with Known As-Built Locations

Of the 131 end plates connections inspected for the 42 panels of both buildings, nearly 90 percent had Type 1 failure where bolt breakage occurred with some deformation to the original bolt hole, Table 3–5. However, if the 11 observations from the mechanical floors, which were welded in addition to being bolted, are excluded, then 95 percent of the failures occurred via Type 1 failure, with the other 5 percent being fracture associated with the weld between the end plate and columns sides (six observations). The latter outcome resulted in the end plate being nearly or completely ripped out of the column. The breakdown for the buildings on an individual basis was similar when the mechanical floors were excluded as well.

For mechanical floor panels (ASCE-2, B-1043, B-1044, and C-24), the end plate connections were made by securing with three bolts and then subsequently welded in the field. (From the mechanical floor panels recovered and examined, it appeared to be a common practice to secure only three of the four possible bolts.) For these samples, all but ASCE-2 had failures where the connections remained (intact bolts and welds) with failure in the column flange and web plates, Type 3. Both ends of the single column recovered for panel ASCE-2 had failure of both the bolts and welds. It was unknown why these failures occurred, as both B-1043 and B-1044 were at the same floor level of WTC 2 as ASCE-2 and may have experienced similar catastrophic events related to the collapse of the building.

3.4.3   WTC 1 Panels Located in Impact Zone

From the recovered panel sections located in the impact region, there were 22 connections available for observation. Of these, 20 had bolt failures while the other two, located on sample M-2, had the end plates ripped completely out of the column base. The following describes each of the five panels separately.

- **M-30:** From photographic evidence, it was observed that the panel was fractured around the 96th floor with the portion of it below this level still visible and attached via the spandrel at the 95th floor. The failures of the lower connections were of a Type 1 mode, which corresponded with the

observations of the recovered endplates, Fig. 3–45. The chalk marks indicate deformation of the original bolt holes. It appears that the bottom of column 133 was rotated to break the bolted connection. This would be consistent with the photographic evidence showing a "twisting" of the column about the column line due to the connection to the spandrel at the 95th floor.   For column 3, it appears that the top was bent inward into the building as a result of the airplane impact.

- **S-9:** After the impact, it was observed that S-9 was still in its original position. The panel below S-9 (sample M-30) had broken away at the end plate connections due to Type 1 failures. This was correlated with the inspected bottom endplates of S-9, Fig. 3–46. A peculiar feature on this panel though, was the appearance of more damage to the bolt holes of the upper connections than those at the lower. The upper end plates have failed in the same manner (Type 1) but with significantly more deformation to the bolt holes; whether this occurred upon impact or during the collapse could not be determined. The limited deformation of the bolt holes associated with the lower connection would be consistent with a brittle failure mode of the bolts upon airplane impact. The bolts at the top of the panel would have been more slowly loaded in tension as the panel was pushed into the building, and likely did not immediately fail but deformed the holes as they stretched.

- **M-27:** For M-27, only the lower end plates of two columns were available for inspection. From pre-collapse photographs, it appears that the connections between M-27 and the panel directly below it were intact. Therefore, failure occurred upon collapse of the building. From the deformation of the bolt holes, it appears that the connection was broken through inward collapse of the top of the columns. The 1 3/8 in. end plate of column 131 was bent along a diagonal axis, Fig. 3–47; however, failure of the welds was not observed.

- **M-2:** M-2 was the panel located directly above M-27. It appears that the state of the recovered bottom portion of columns 129 and 130 was nearly identical to the condition after the impact, a Type 2b failure where the end plates were ripped completely out of the column, Fig. 3–48. Failure was found to be a mixture of fracture in the base metal (portion of the flange/web still attached to the end plate) and clean separation of the end plate from the flange/web (complete flange/web recovered with internal weld bead visible). Section 3.2.1 discussed the deformation of the flange/web plates associated with this failure. Bolt hole deformation for column 131 indicated that the connection was broken by bending inward of the lower column of the connection. Lastly, while bolt failure was observed for the top of column 129, it was noted that separation existed between the four components of the column and the endplate.

- **N-7:** N-7 was located just above one of the panels that was pushed inside the envelope of the building upon impact. From photographic evidence, it appears that the panel was still intact. Reviewing the deformation of the bolt holes on the lower endplates (Fig. 3–49) indicated that connections of columns 127 and 128 failed in a similar manner, that being, the connection was pushed in toward the building. Evidence also suggested that the bottom of column 126 broke due to torquing of the column.

3.4.4   Unidentified Panels

The overwhelming majority of the end connection failures of the unidentified columns (94 percent) were bolt failures (Table 3–5). One column had a plate attached from an adjacent column, and three total, including this one, exhibited weld failure. However, it was important to note that the two other weld failures were of very thick columns, in which case the load bearing area of the weld was much less than the webs and flanges, and weld failure was to be expected.

In addition to the examination of unidentified pieces in our possession, another source of evidence available was the extensive collection of photographs taken at both the WTC site during salvage operations, as well as photographs taken by the Building Performance Assessment Team (BPAT) at the salvage yards. These images show hundreds of columns and panels that have failed at the bolts during building collapse. The distribution of panel thicknesses, as well as the number of bolt holes in the end plates, suggests that the images cover a large distribution of panels from various heights on the buildings. These images also clearly indicate that the overwhelming failure mode of exterior panel vertical column connections was bolt fracture.

3.4.5   Summary

From the observations made on recovered panels concerning the end plate connectors, the major failure mechanism was fracture of the bolts. This was also observed for the unidentified panels. When considering the 120 connections that were exclusively bolted, there were only six examples where the end plate was ripped either partially or wholly out from the column, with two of these as a direct result of the impact. For samples where the connections were welded as well as bolted (mechanical floors), failure was dominated by fracture of the column plates (flanges/webs) near the weld of the columns.

3.5   EXTERIOR WALL SEATS OR FLOOR TRUSS CONNECTORS

A survey was conducted on the exterior wall seats (or floor truss connectors) of the recovered panels to identify and inventory the various failure modes associated with impact and collapse of the buildings. These connectors were not visible in pre-collapse photographs, and thus, the analysis must rely solely on the observations of the recovered components.

To summarize the samples used in this portion of the analysis, of the 26 panels from WTC 1, all panels had a minimum of one floor truss connection for inspection, allowing for 137 observations. From WTC 2, only 13 of the 16 identified panels were used for the analysis. The three panels located at John F. Kennedy International Airport (B-1024, B-1043, and B-1044) were not fully analyzed during the visits to the hangar, and thus, their connections were not taken into consideration for the statistical analysis. Of the remaining 13 panels, 56 observations were possible for inspection. Finally, there was one panel that was partially identified (C-117) and 47 exterior panels not identified as to their as-built locations. Of these 48 panels, 33 had recovered portions with floor truss connections for inspection, which yielded an additional 65 observations.

For the seat details, there were 84 specified variations in the design drawings. The differences arose from the type of connections used (seat versus support), the location and dimensions of the seat, placement of bolt holes on the seat, dimensions of the stand-off plates, location of stiffener plates inside column, and

location of the damping unit. From the recovered panels with known as-built locations, a total of
193 inspections were made with 21 different variations of seat details observed, Table 3–6. For the
samples with unknown as-built locations, the failure statistics were collected irrespective of the specific
detail, as this information was not feasibly attainable.

The floor trusses were connected to the perimeter panels at the interior intersection of the columns and
spandrels. The labeling system used by NIST to identify the specific intersection can be seen in
Fig. 3–50. It should be noted that this view was from the outside of the building looking inward toward
the core. For statistical purposes, the seats were separated into four groups based upon their
characteristics, Table 3–6. They are briefly described here with regard to the examples available for
inspection on the recovered elements. Photographic examples shown in Appendix A.

- *Type A*: This type of seat detail included those that belonged to the 1xxx, 2xxx, 3xxx, 4xxx, and
  7xxx series. They were found along all faces of the exterior wall, typically **supporting the main
  double trusses and continuous traverse bridging trusses**. Two standoff plates were welded
  directly to the spandrel plate in a vertical manner, with beads observed only on the outer side of
  the plates. An angle, hereafter referred to as the seat, was welded to these plates on both sides.
  The location of the welds indicated that the standoff plate/seat assemblies were first prefabricated
  and then welded to the spandrel. For the 7xxx series seats, the standoff plates were omitted, and
  the angle was welded directly to the column. On the seats, there were two slotted holes for
  attachment of the trusses. Directly below the bottom of the seat assembly was a gusset plate used
  to attach the damper unit from the lower chord of the floor truss to the exterior walls. This plate
  was welded to the spandrel on all sides and also contained two bolt holes. Once the truss was
  lowered into place and fastened to the seat by two bolts, a gusset plate, with backing bar, was
  used to further secure the joint. This was welded in the field to both the top chord of the truss and
  the column. The damping unit was then bolted both to the spandrel/gusset plate and truss.

- *Type B*: This type of connector was specific for seat details 5010 and 5510. These seats were
  observed only on the 200 and 400 series faces of the exterior walls for columns x04, x08, x12,
  x48, x52, and x56, where "x" was either 2 or 4. These were the columns that bore **the
  intermediate deck support angles**. This connector consisted of a single, triangular stiffener
  plate (3.5 in. right angle, isosceles triangle with 0.375 in. thickness) welded vertically to the
  column on all sides. A second plate (8 in. by 5 in. by 0.375 in.) placed on the top edge of the
  stiffener was subsequently welded to complete the seat. The single plate was completely welded
  on all sides to the spandrel. Like the seats of Type A, there were two slotted holes in the
  horizontal plate and a gusset plate with backing bar. Damper units were not specified for this
  detail.

- *Type C*: This type of connector was used primarily as a support for the flooring system and
  included seat details in the 5xxx and 6xxx series. These connectors were observed along all four
  exterior faces of the buildings and used in conjunction with Type A truss seats almost
  exclusively. Typically, a single gusset plate was welded on all sides. The shape of the plate was
  found to vary from a full rectangular plate to two separate tabs of 4 in. lengths to a combination
  of the two. Regardless of the shape, two flat bars, hereafter referred to as **diagonal bracing
  straps**, with shear studs were welded to the plate and attached to the top chord of the trusses.
  These diagonal bracing straps were attached to provide horizontal shear transfer between the floor

slab and exterior wall, as well as out-of-plane bracing for the perimeter columns not directly supporting the floor trusses.

A final variation of the gusset plate support of this type was found solely on column numbers 100, 200, 300, and 400; these were the columns located in the center of the chamfered corner wall section. This entailed a structural tee member welded directly to the interior face of the column. A single **diagonal bracing strap** was then welded to the horizontal of this support and attached to the truss.

- *Type D***:** This type of connector was also used as a support for the flooring system and included seat details in the 5xxx series. These supports were used solely to brace **the intermediate support angles** and **continuous transverse bridging trusses**. Thus, they were located only on the 200 and 400 series faces of the buildings, within the first 14 columns from each corner, and on alternating columns without Type B connectors. Two **diagonal bracing straps**, similar to those found on Type C floor truss connectors, were completely welded on all sides to the spandrel and attached to the trusses and angles.

Appendix B displays images of the spandrel/column intersections for all 42 recovered and identified panels.

3.5.1   WTC 1 Panels Located in Impact Region

Exterior panels from WTC 1 were analyzed to determine if different failure mechanisms were observed for those that were hit directly by the plane and those outside of this region. There were 33 observations from the 5 panels in the impact region and 90 from the 18 panels outside. As the impact region of WTC 1 was located on the north face of the building (100 series columns), there were only Type A and Type C connectors were found in this region. Damage statistics for Type A seats are found in Table 3–7. Table 3–8 displays this data for Type C supports. A minor difference between the two areas analyzed for the Type A seats is that more seats had their middle portions bent towards the columns in the impact zone. This was a direct result of the impact as the columns were being pushed towards the core before the truss chords gave or broke loose from the seat. However, failure of the gusset plate welded to the top truss chord and column was almost exclusively observed regardless of location. Fracture in the toe of the weld on the plate was the major failure associated with the Type C floor truss connectors for both areas.

3.5.2   WTC 1 Panels Exposed to Fire

Exterior panels from WTC 1 were analyzed to determine if different failure mechanisms were observed for those panels exposed to fire, regardless of location of fire, and those that were not. There were 82 observations from the 16 panels exposed to fire and 55 from the remaining 10 panels. Damage statistics for Type A seats are again found in Table 3–7. Table 3–8 displays this data for Type C supports. Information regarding Type B and Type D connectors is located in Tables 3–9 and 3–10, respectively. The observations were also correlated with the time-exposure maps (Fig. 2–48) to determine exactly which connections may have been exposed directly to fire. From this information, 39 observations were available from 13 different panels in which fire was either located in the window (category 2) or noted with external flaming (category 3). This information was also found in the tables listed above.

For Type A and Type C connectors, there were negligible changes to the damage patterns for these floor truss connectors regardless of whether or not the connector may or may not have had fire exposure. Failure of the gusset plate welded to the top truss chord was almost exclusively observed regardless of exposure. For Type B and Type D floor truss connectors, the sampling group was too limited to make any significant conclusions, but the data was shown for completeness.

3.5.3   Panels Separated by Floor

Exterior panels from WTC 1 were analyzed to determine if different failure mechanisms were observed for those panels above the impact region and those located below. There were 63 observations from the 12 panels at or below the 95th floor and 74 from the remaining 11 panels above the 95th floor. Figure 3–51 spatially displays this information for WTC 1 near the impact region of the north face. Both pictorially and statistically, below the impact zone, the majority of floor truss connectors were observed to be either bent down or completely missing. Failure of the gusset plate welded to the top truss chord was again almost exclusively observed regardless of location. This may be a result of overloading the lower floors as the floors above were "pan-caking." Again, the data for Type B and Type D floor truss connectors was too limited to define any sort of pattern.

For WTC 2, there were 30 examples of Type A floor truss connectors and 18 examples of Type C floor truss connectors. Again, the sample size for Type B and Type D floor truss connectors was limited, but the data was shown. There were 48 observations from the Type A and C floor truss connectors, with 32 observations from at or above the impact region and 16 below. Similar to WTC 1, the floor truss connectors had a higher tendency to be bent downward or were missing below the impact floors than above, with concomitant failure of the gusset plates. This data was not shown spatially, as an image similar to Fig. 3–51 with a high concentration of samples was not available; recovered panels from WTC 2 were more randomly distributed through the building.

The number of bolts found remaining in the Type A floor truss connectors differed significantly by floor. In total, there were 35 bolts remaining for WTC 1 and 8 for WTC 2. All but one bolt was found at or above the impact floors. This was considered disproportionate, as the number of seats remaining was not as unequally distributed.

3.5.4   Unidentified Exterior Column Panels

The data for the seat connections on the unidentified panels are presented in Tables 3–7 and 3–8. For the Type A seats, there appears to be no significant difference in the observed failure modes in the unidentified columns and those seen on the columns with identified locations on the building. For Type C seats, there was an observed decrease in the number of plates that remained intact and were bent down, and an increase in the number of plates that fractured away from the panels at the toe of the weld on the plate. This can be understood by considering the population of unidentified columns as a whole. These samples were missing identifying marks on specific parts of the panel due to that panel being torn off during the building collapse or the subsequent salvage operations. Thus, in general, the unidentified columns were more likely than the identified ones to be significantly damaged or in smaller pieces and would have had a higher likelihood of having protruding parts like floor seats damaged or torn off.

3.5.5 Weld Failures Associated with the Floor Truss Connectors of the Perimeter Wall

As part of the investigation of the damage and failure modes of the floor truss connectors of the WTC towers, an analysis was conducted on the damage features of the arc welds associated with these connectors. Two example joints were analyzed; the connection between the spandrel plate and standoff plates and the connection between the standoff plates and the seat (Fig. 3–52). Both undamaged and damaged welds were investigated and the behavior of the failed joints characterized with respect to the base metal, HAZ, and weld metal.

Welded Joints Between Spandrel and Standoff Plates of Type A Connectors

As stated above, the two standoff plates were fillet welded directly to the spandrel plate with multiple pass beads observed only on the outer side of the plates. The specific arc welding process was not found within the design drawings, but due to the short welding length, shielded metal arc welding (SMAW) or flux cored arc welding (FCAW) was most likely used. Typically, these joints were over-welded, meaning that a 3/8 in. or 1/2 in. weld may have been deposited where only a 5/16 in. bead was specified. Figure 3–53a shows one of the undamaged welds in cross-section. The standoff plate was a 42 ksi ferrite-pearlite steel, and the specific spandrel shown in the images was a 65 ksi plate. The HAZ in the standoff plate was seen extending through the entire thickness, while a shallower penetration was observed in the spandrel plate. This difference is related to welding procedures and angle of the heat source with respect to the two plates. As shown in Table 3–7, nearly one-fourth of the observed Type A connectors outside of the impact zone had at least one of the standoff plates "ripped" from the spandrel. As these connectors were probably intact prior to collapse, it was assumed that the plates were detached via a shear mechanism as the buildings came down. Figure 3–53b shows the cross-section of one of these failed joints. Failure was observed to occur almost exclusively within the HAZ of the standoff plate. This would be expected as the fracture path would be shorter in the plate as opposed to traversing through the stronger weld material. Additionally, the standoff plate had the lowest cross-sectional area with respect to the high loading forces of the collapse. Thus, failure here would not be unreasonable.

Welded Joint Between Standoff Plates and Type A Connectors

Removal of the seat from the spandrel revealed that a double fillet weld was used to join the seat to the standoff plates. This clearly indicated that the standoff plate/seat assemblies were first prefabricated and then welded to the spandrel. Again, SMAW or FCAW were assumed to be the processes used. Figure 3–54a shows one of the undamaged welds in cross-section. The HAZ from both fillet welds spans the entire standoff plate. Again, a shallower penetration was observed in the seat angle. As shown in Table 3–7, it was seen that nearly one-third of the observed Type A connectors outside of the impact zone had the seats ripped off with at least one of the standoff plates remaining. Similar to the premise used above for the joint between the spandrel and standoff plate, it was assumed that the plates were detached via a shear mechanism as the buildings collapsed. Figure 3–54b shows the failed cross-section of one of these joints. Failure in this case was observed to occur within the weld metal at the weld-seat interface. While this would seem unexpected, closer inspection of the intact weld revealed these areas have the lowest cross-sectional area. As seen in Fig. 3–54a, the fillet weld between the standoff plate and the seat does not metallurgically join the portion of the standoff plate in contact with the seat. Thus, with the

lowest cross-sectional area with respect to the high loading forces of the collapse, failure here would not be unanticipated.

3.5.6   Summary

From the observations made on recovered panels concerning the floor truss connectors, the most significant data was observed when the panels were separated by floor elevation. Of the 28 floor truss connectors at or below the impact floors for WTC 1, 93 percent were either missing or bent downward; only 37 percent of the 38 floor truss connectors above the impact floors. Similar results were found for WTC 2, where 88 percent of the floor truss connectors below the impact floors were bent down or missing, while only 55 percent of the floor truss connectors above the this region experienced analogous damage characteristics. This occurrence was most likely a result of the overloading of the lower floors ("pancaking" mechanism) during collapse of the building. When the seats were observed missing, it was typically a result of fracture near a welded joint associated with the standoff plates. Inspection of the welded failures associated with the floor truss connectors showed that failure typically occurred in the location with the lowest cross-sectional area. However, there was no evidence throughout this analysis to indicate that fracture associated with the welds evaluated was related to: 1) inadequate joining materials (weld strength and ductility appeared appropriate for the application), 2) inappropriate welding procedures (welds were typically oversized with no visible flaws), or 3) poor performance of the welded joint (fracture was associated with extreme loading event, i.e., overloading of the floors upon collapse).

Source: Original photograph copyright Roberto Rabanne 2001.

Figure 3–1. Image showing impact damage to the north face of WTC 1. The as-built location of the five recovered panels from the impact zone were highlighted: S-9 (pink), M-30 (blue), M-2 (orange), M-27 (green), and N-7 (yellow).

Source: NIST.

Figure 3–2. a) Overall image of panel M-30 (A133: 94-97), b) severing of column 132 at the stiffener plate associated with the top of the spandrel, and c) severing of column 133 at a slightly lower elevation associated with the 95th floor level concrete slab.

Source: NIST.

Figure 3–3. a) Overall image of panel S-9 (A133: 97-100) and b) lower portion of panel showing possible damage from airplane impact, bottoms of columns 133 and 134 shown, and c) column 132 that sustained a fair amount of damage.

Source: NIST.

Figure 3–4. Overall view of panel M-27 (A130: 93-96). This panel was from the north face of WTC 1 and struck directly by the nose and fuselage of the plane.
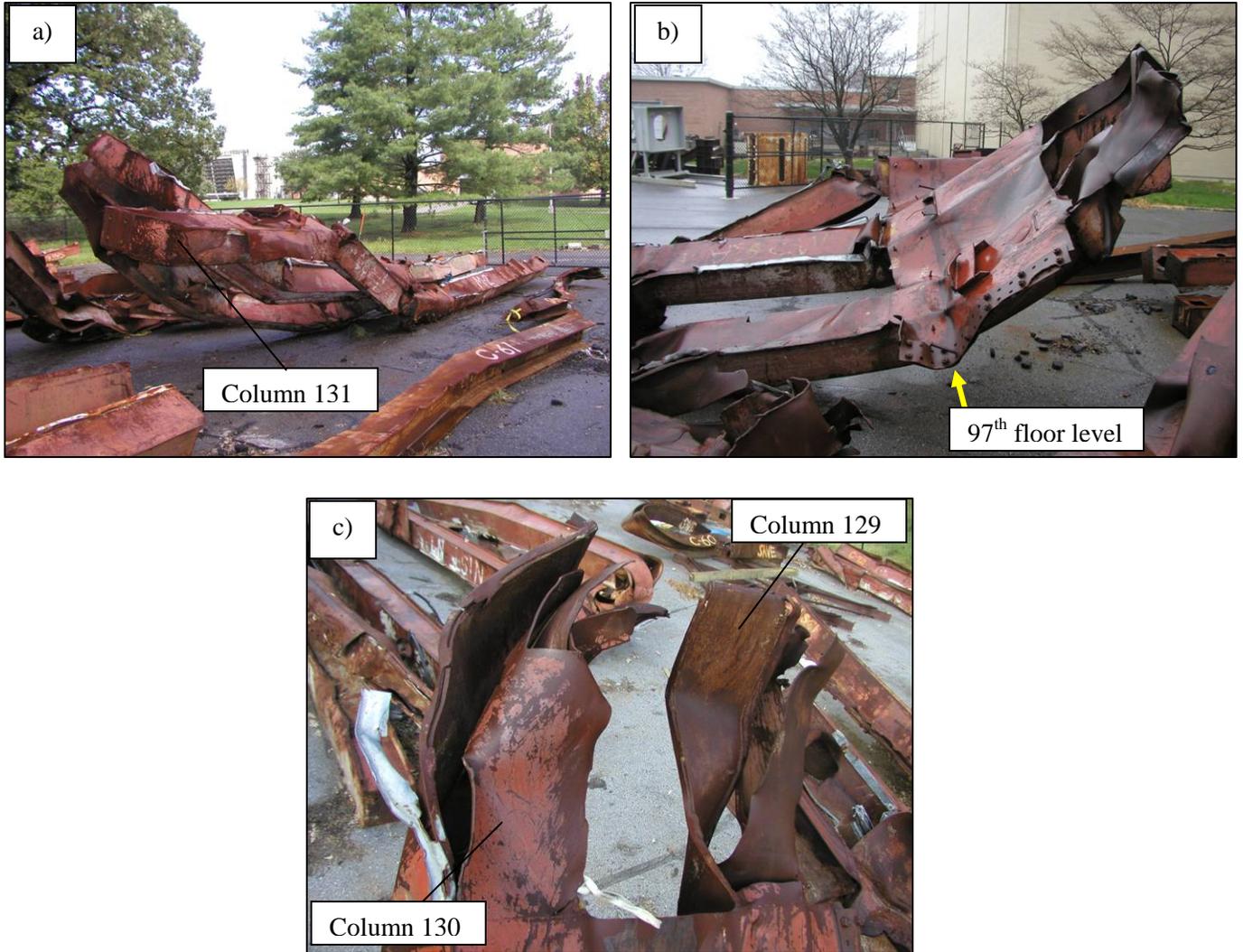
Source: NIST.

Figure 3–5. Panel M-2 (A130: 94-97). This panel was from the north face of WTC 1. The lower portion of the panel was struck by the fuselage of the airplane. General shape of panel is due to airplane impact and bending about the 97th floor slab. a) Overall view, bottom of panel is on the left-hand side of the picture and the outside of the panel is facing down, b) major bend in panel located at the 97th floor level, and c) splayed bottoms of columns 129 and 130.

Source: NIST.

Figure 3–6. Overall image of sample N-7 (A127: 97-100). Panel was in relatively good shape besides being folded inward about an axis parallel to the length of the columns with the outer web of the columns facing outward. This was believed to have happened during the collapse or recovery efforts. The three columns were relatively intact with limited damage.
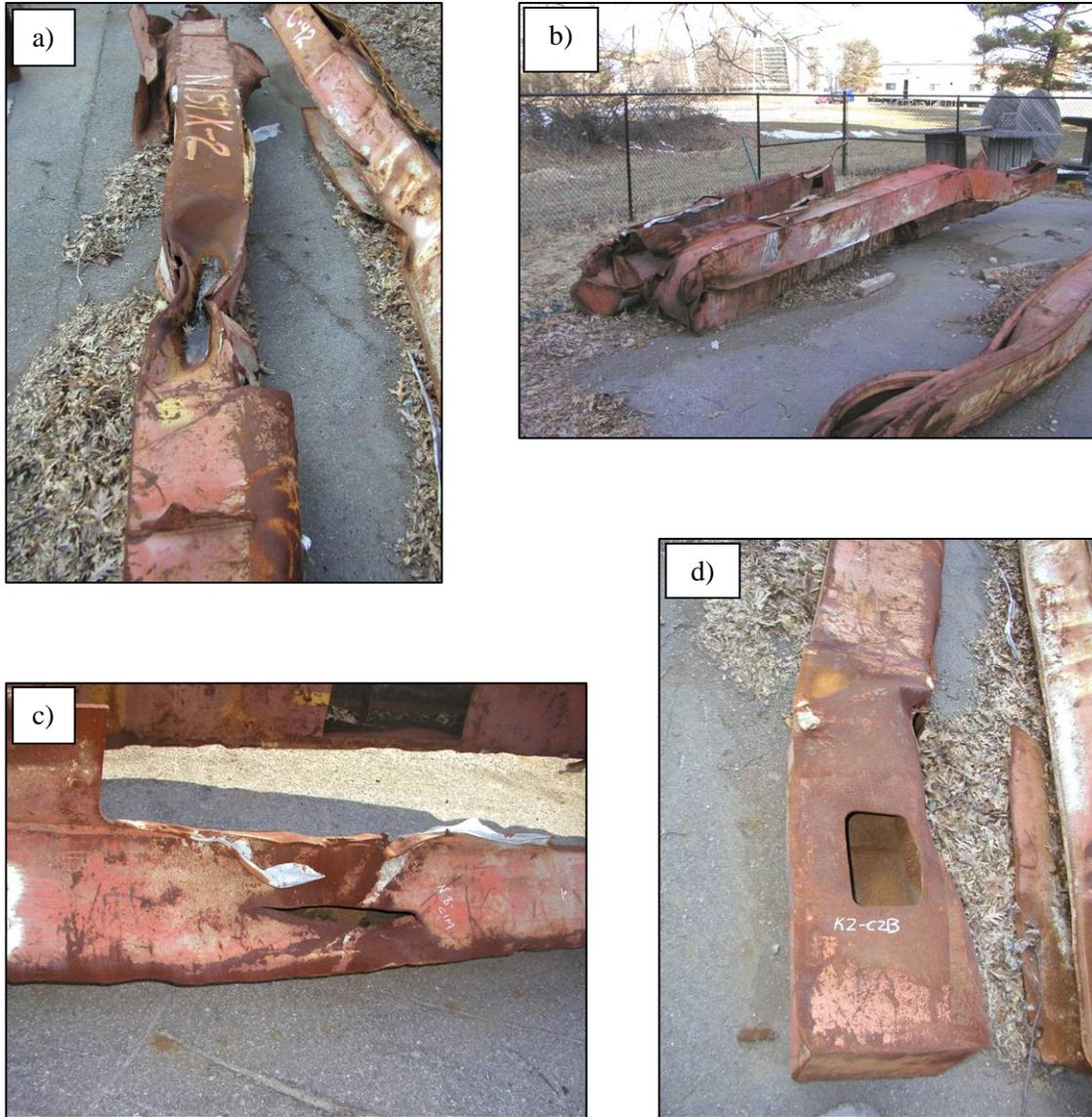
Source: NIST.

Figure 3–7. Photographic examples of Type 1 damage feature for exterior panel columns, gross physical distortion of flanges and webs. a) Type 1a, crushed columns from K-2 (A236: 92-95), b) Type 1a, crushed column from N-12 (A206: 92-95), c) Type 1b, punctured column from N-8 (A142: 97-100), and d) Type 1c, buckling of column from K-2.
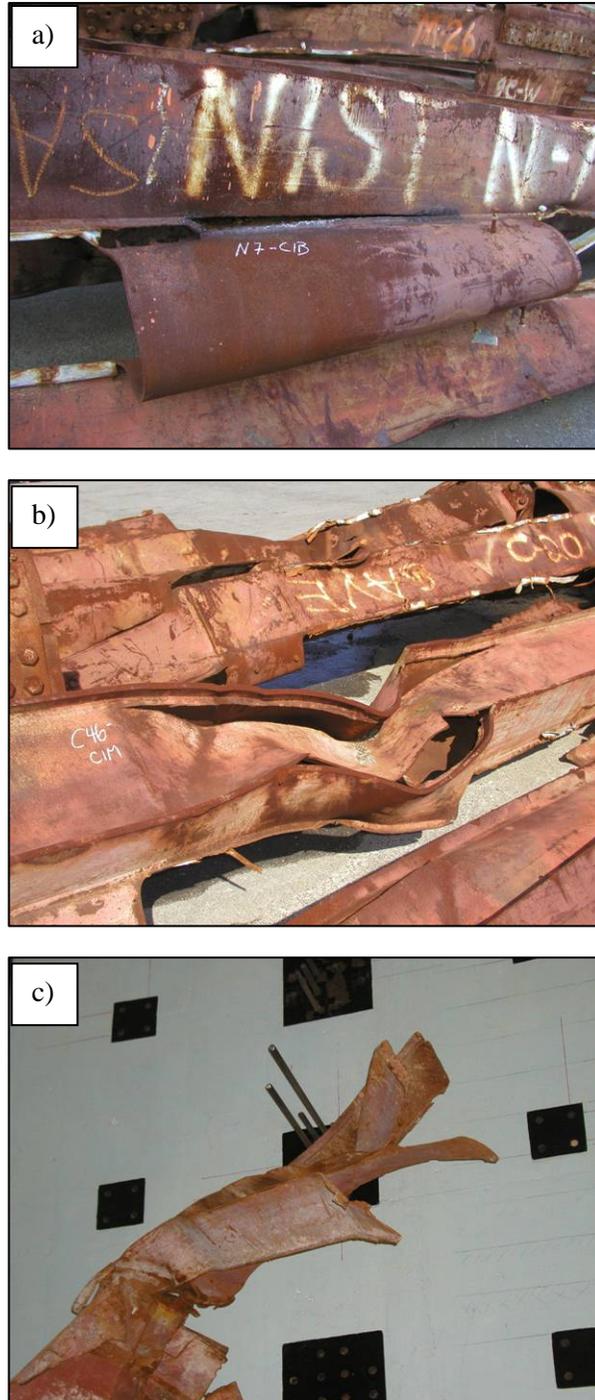
Source: NIST.

Figure 3–8. Photographic examples of Type 2 damage feature for exterior panel columns, fracture in base plate near fillet welds. a) Type 2a, localized fracture from N-7 (A127: 97-100), b) Type 2b, extensive fracture from C-46 (B157: 68-71), and c) Type 2c, extensive fracture resulting in "splaying" of column from M-27 (A130: 93-96).
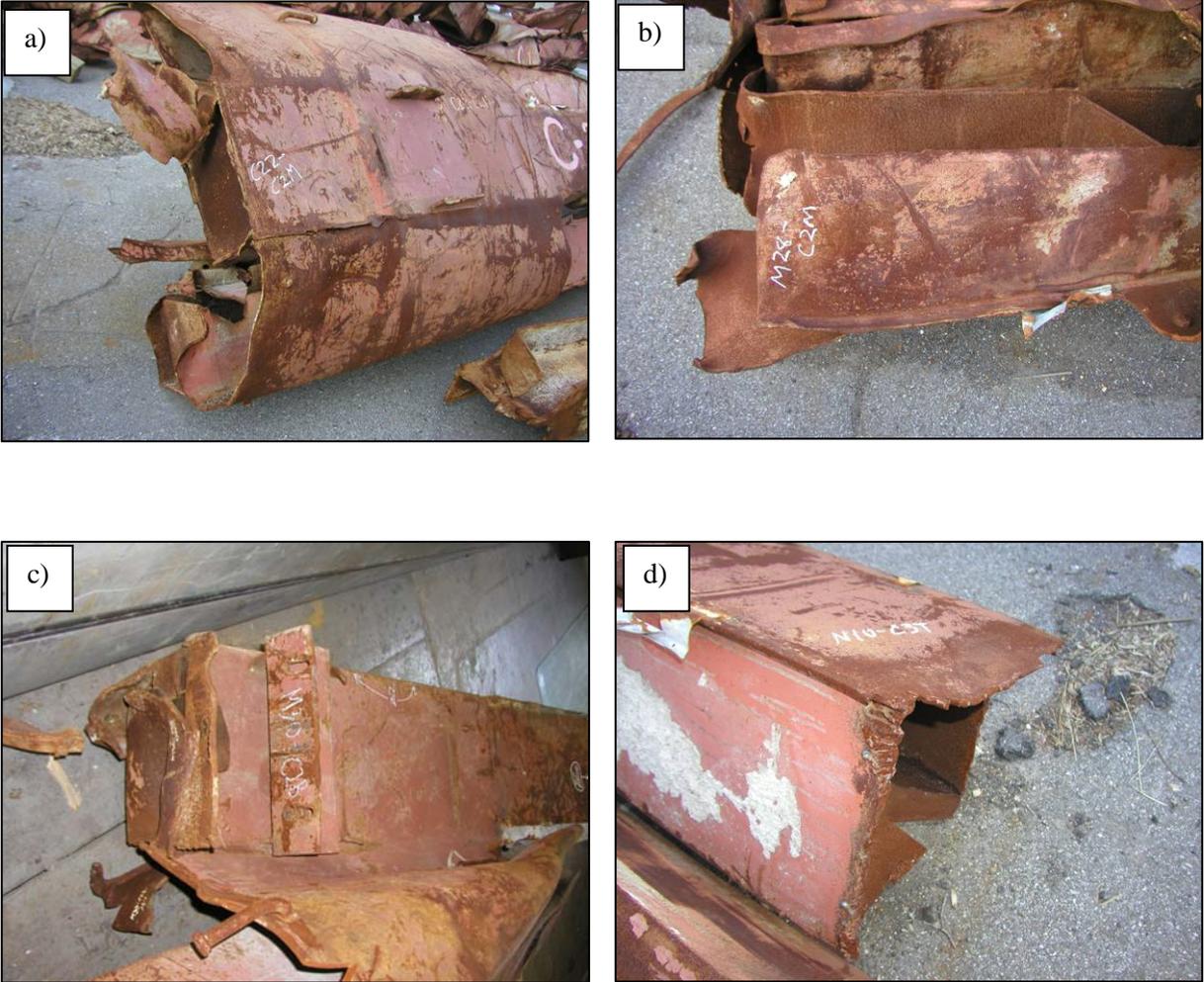
Source: NIST.

Figure 3–9. Photographic examples of Type 3 damage feature for exterior panel columns, severing of columns. a) Type 3a, sever associated with stiffener or diaphragm plate from C-22 (A157: 93-96), b) Type 3b, sever occurred away from stiffener or diaphragm plate from M-28 (B345: 98-101), c) Type 3c, sever occurred at concrete slab of floor from M-30 (A133: 94-97), and d) end was flame cut during recovery from N-10 (A115: 89-92).
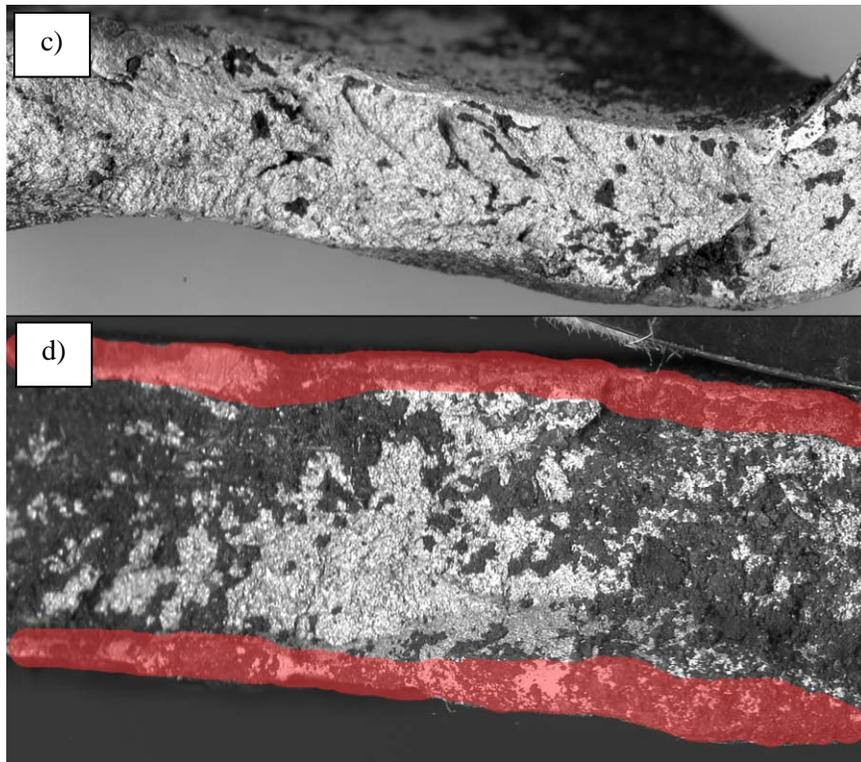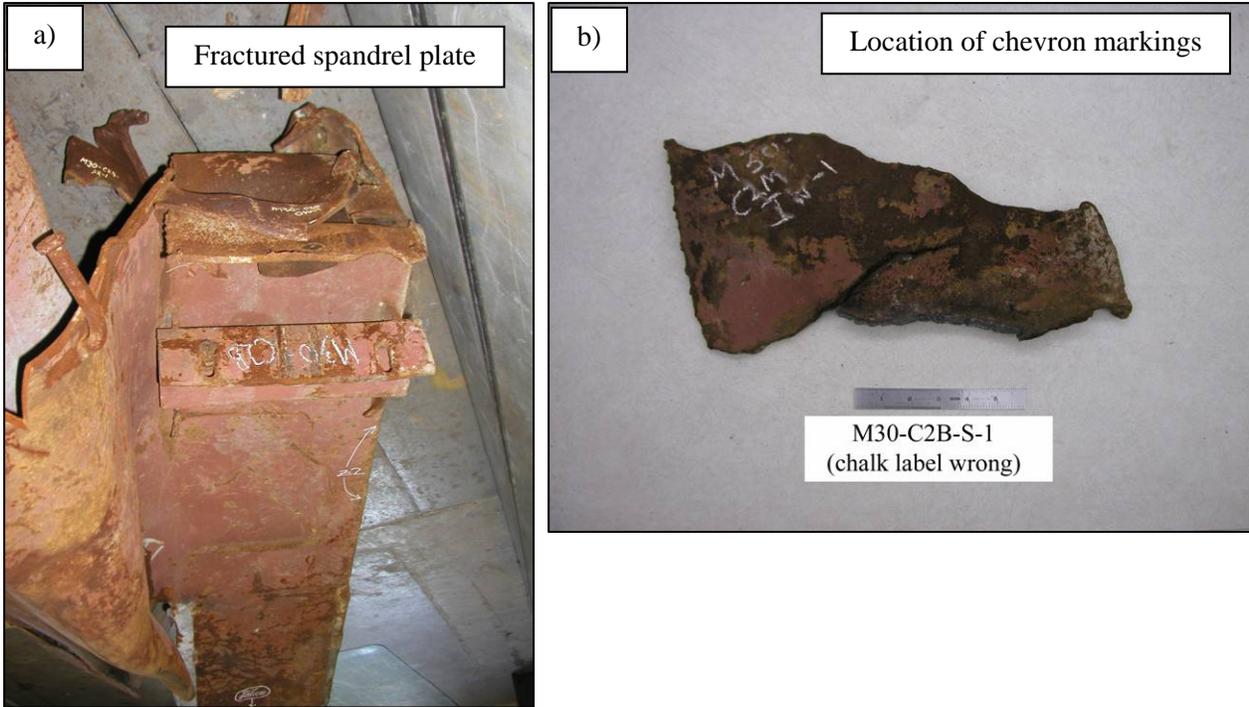
Source: NIST.

Figure 3–10. Fracture surface of sample M-30 (A133: 94-97), spandrel plate of column 133. Fracture was due to airplane impact of WTC 1. a) Location of sample removed, b) laboratory image showing sample removed, c) fracture shows chevrons running along the length of the crack path, and d) red highlighted area showing the location of small shear lips.
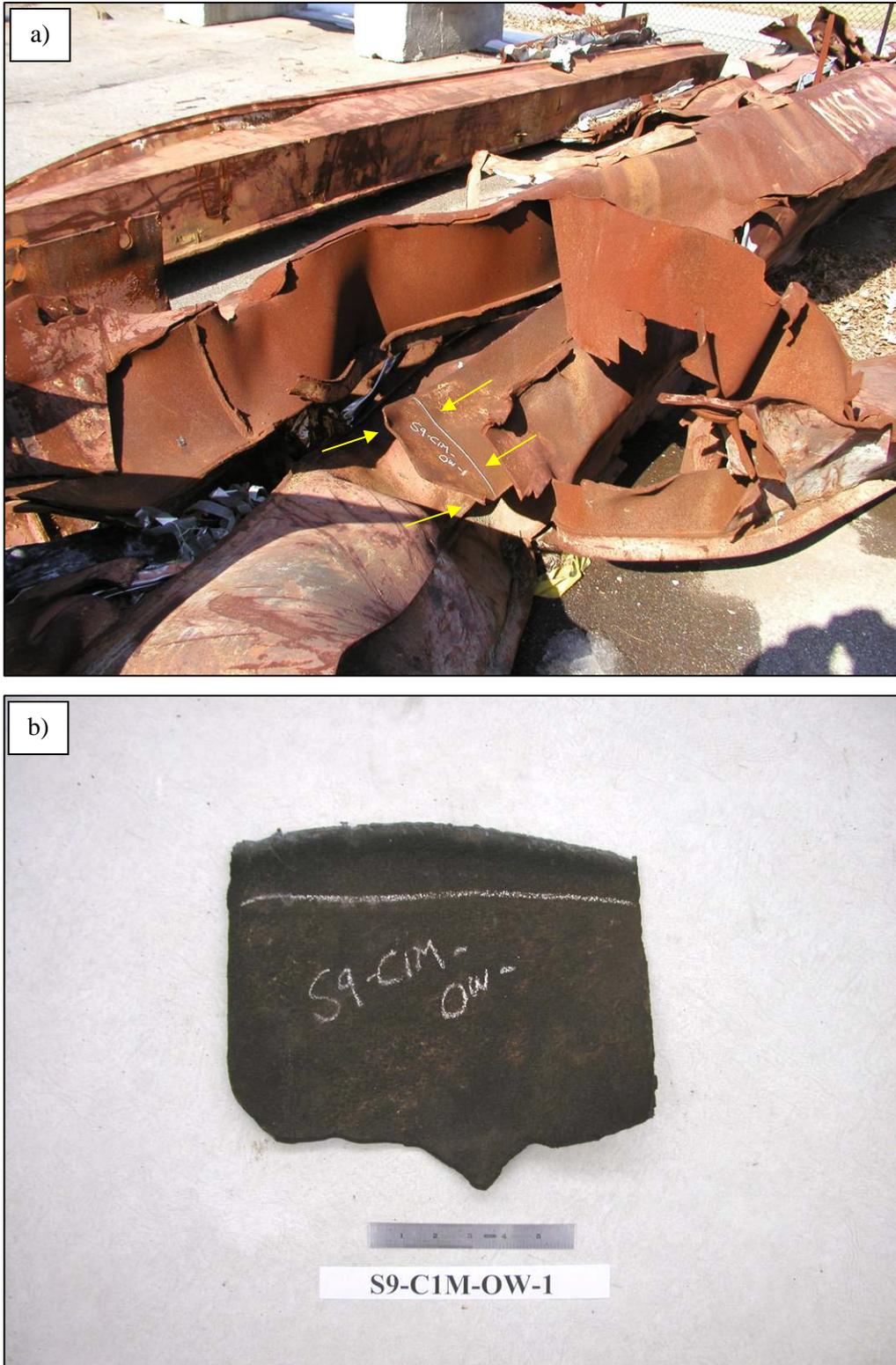
Source: NIST.
Figure 3–11. Analysis of fractured plate from sample S-9 (A133: 97-100), outer web of column 132. This panel from WTC 1 was struck by the vertical tail assembly. a) Location of sample removed, b) laboratory image showing sample removed.
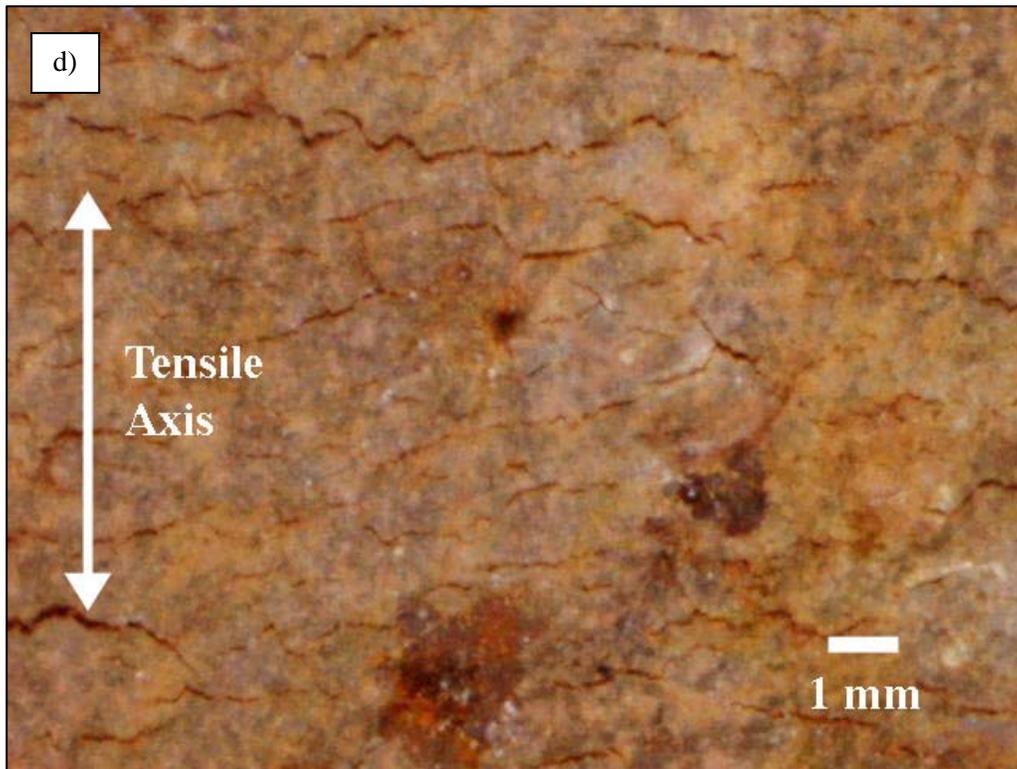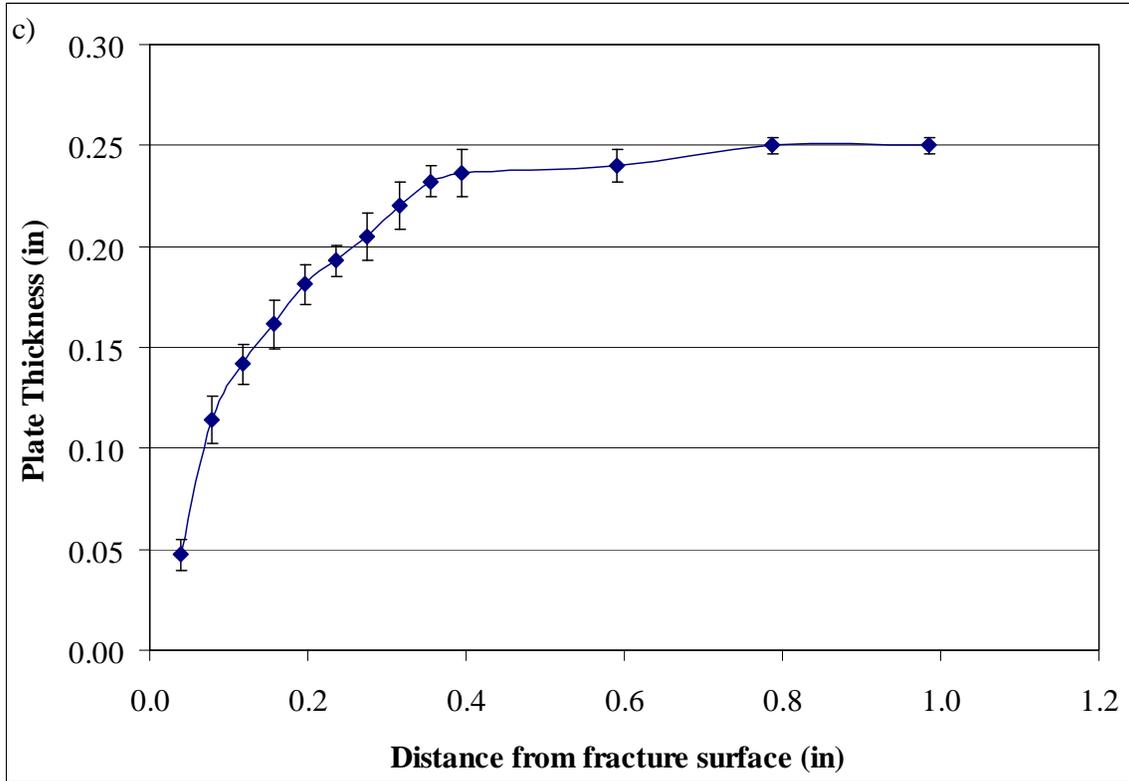
Source: NIST.

Figure 3–11. Analysis of fractured plate from sample S-9 (A133: 97-100), outer web of column 132. c) graph indicating plate thinning near fracture surface, d) image showing paint cracking as a result of tensile loading of the plate.

Source: NIST.
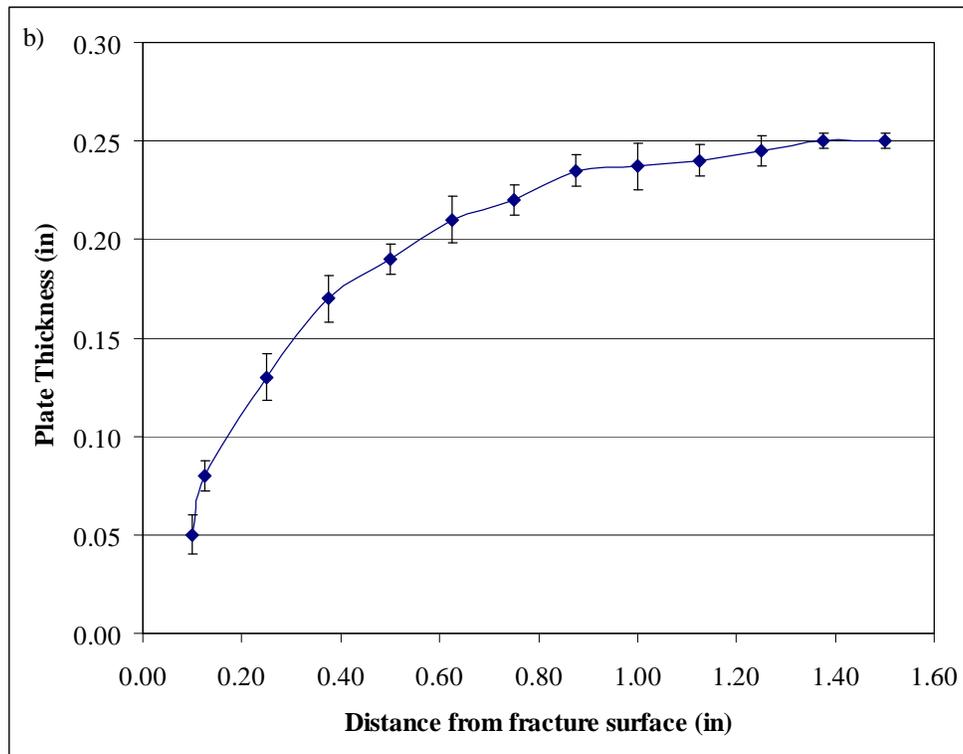
Figure 3–12. Thinning of outer web from column 130 of panel M-2 (A130: 96-99). Tensile failure of the plate was a result of airplane impact into WTC 1. a) photograph showing thinning, b) graph indicating plate thinning near fracture surface.

a)

Cracking of flange

b)

Cracking of flange

c)

Cracking of spandrel at 97th floor

d)

Welds intact
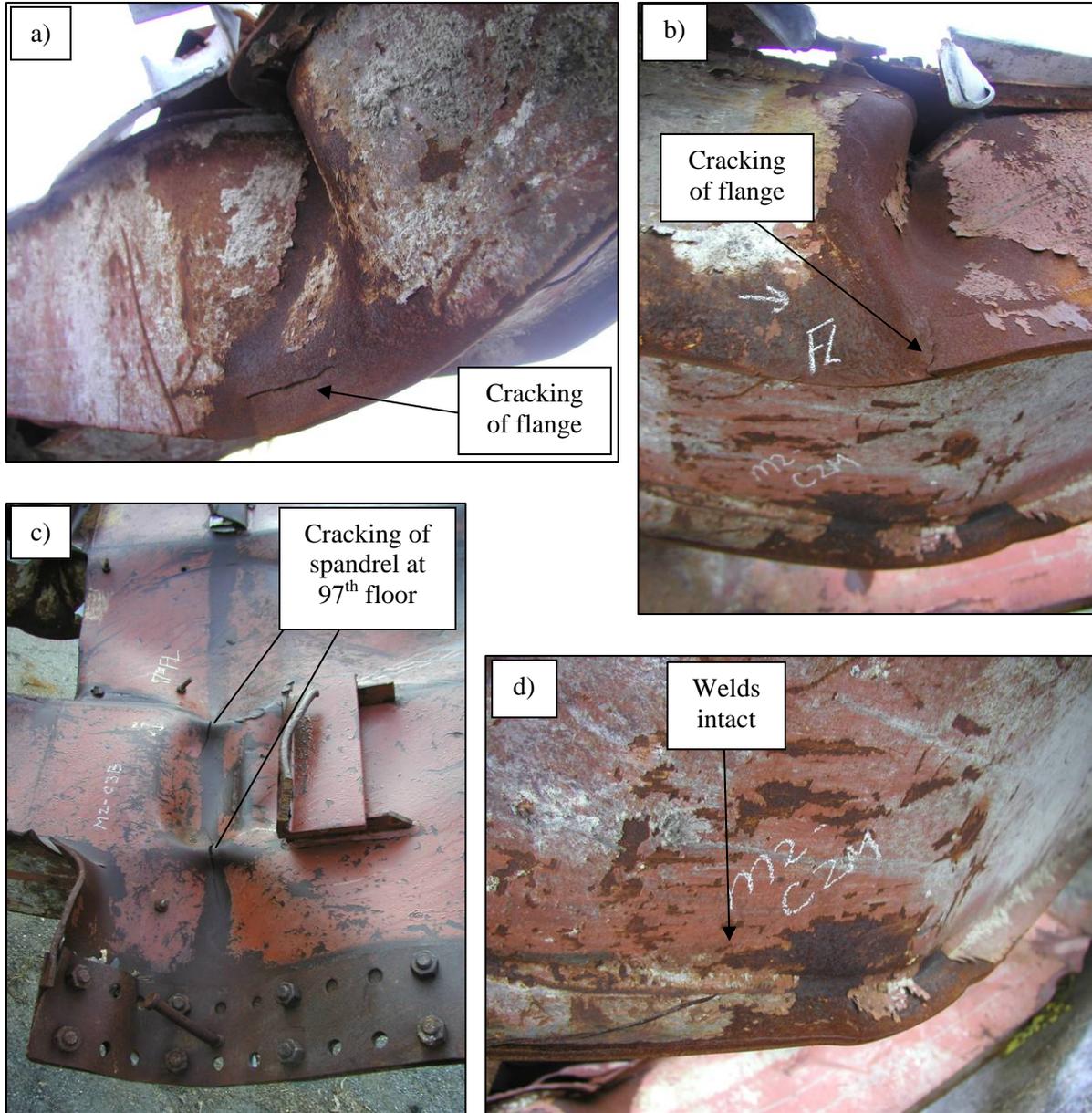
Source: NIST.

Figure 3–13. Damage images from sample M-2 (A130: 96-99). Panel from WTC 1 was struck by fuselage of airplane and bent about the 97th floor. a) Large buckles observed on the flange plates of column 130, b) cracking of the flange plates on column 130, c) cracking of spandrel at 97th floor level, and d) no cracking near the welds in this area on column 130.
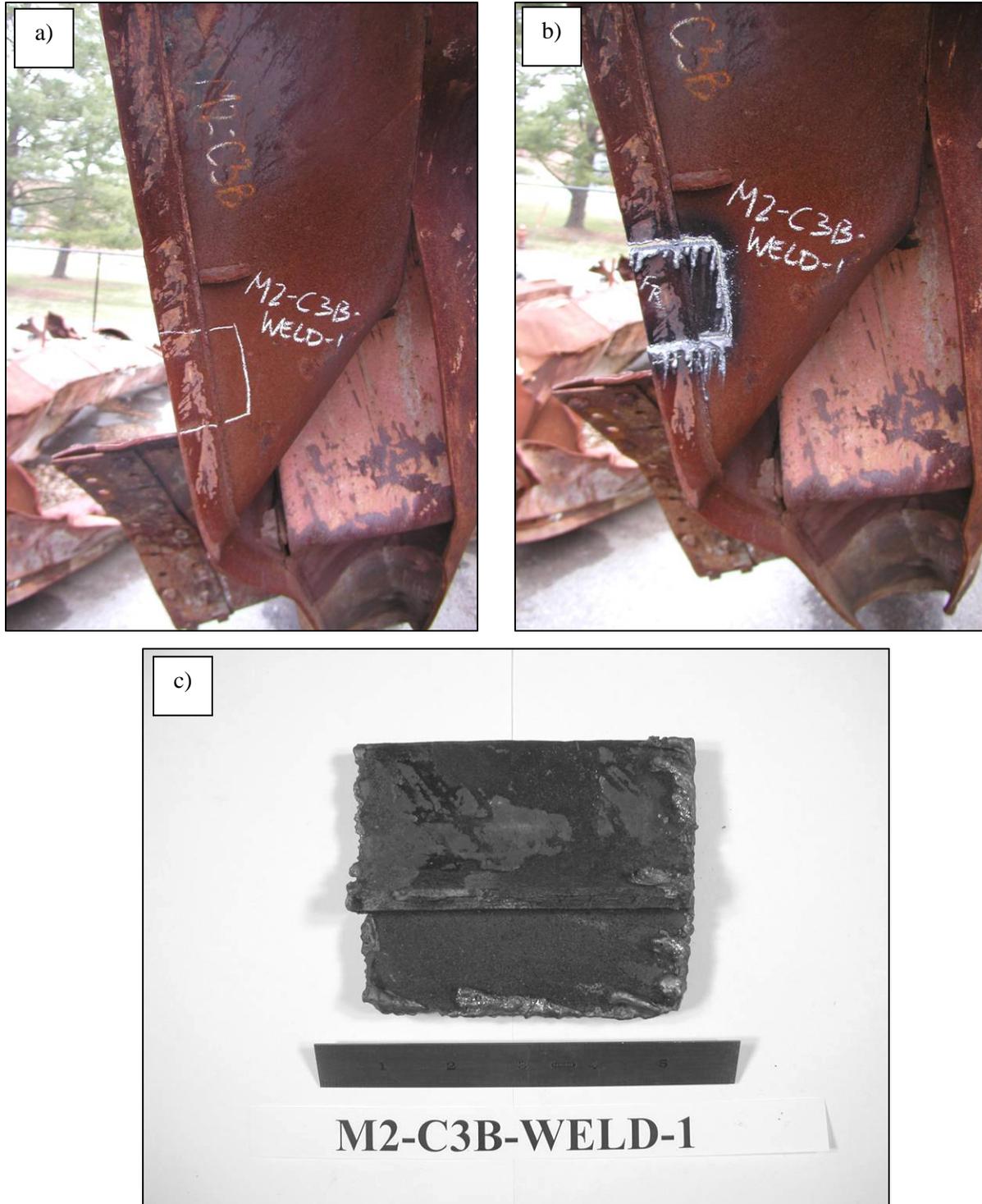
Source: NIST.

Figure 3–14. Example of fracture near weld of a perimeter column as a result of airplane impact, sample M2-C3B-Weld-1 (A130: 96-99, column 129), images taken a) prior to sample removal, b) after flame cutting, and c) in the laboratory.
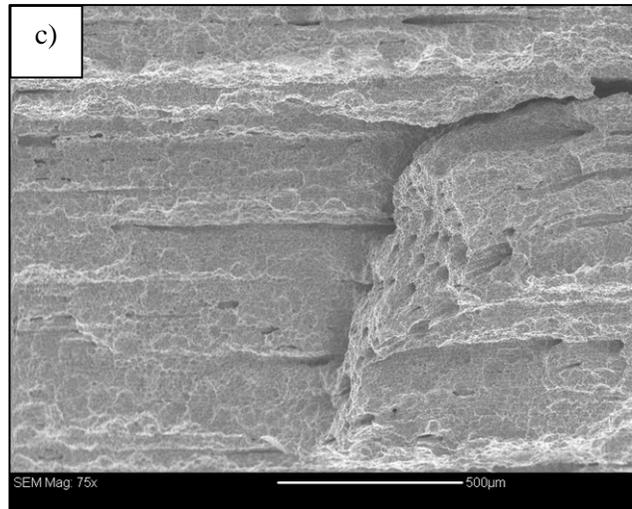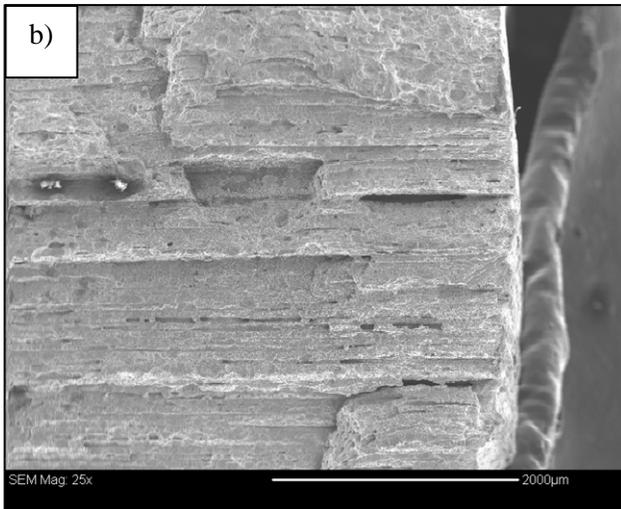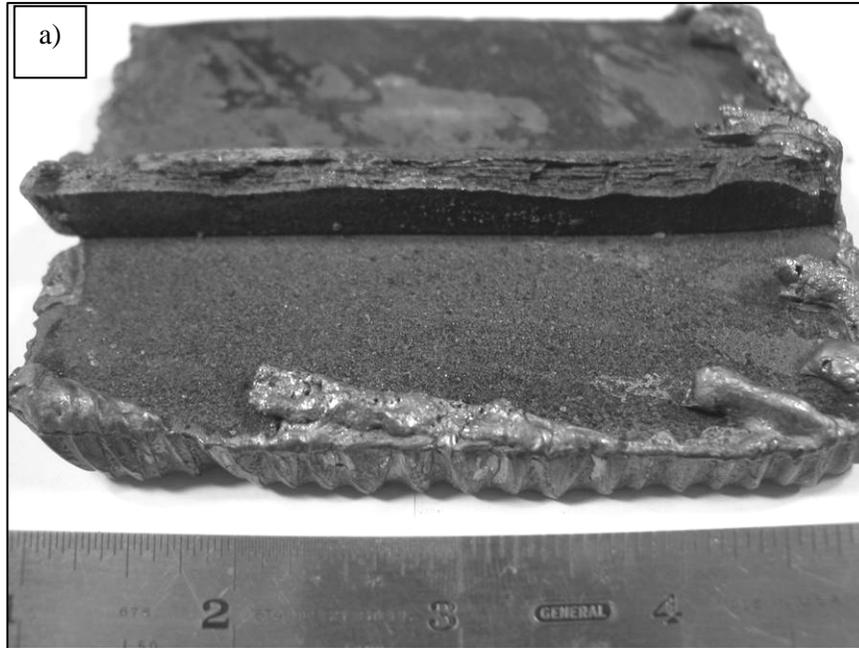
Source: NIST.

Figure 3–15. Fracture surface for sample M2-C3B-Weld-1 (A130: 96-99, column 129) shown in Fig. 3–14. Fracture features of outer web have "lamellar tearing" type fracture characteristics. a) Light micrograph, b) and c) scanning electron micrographs.
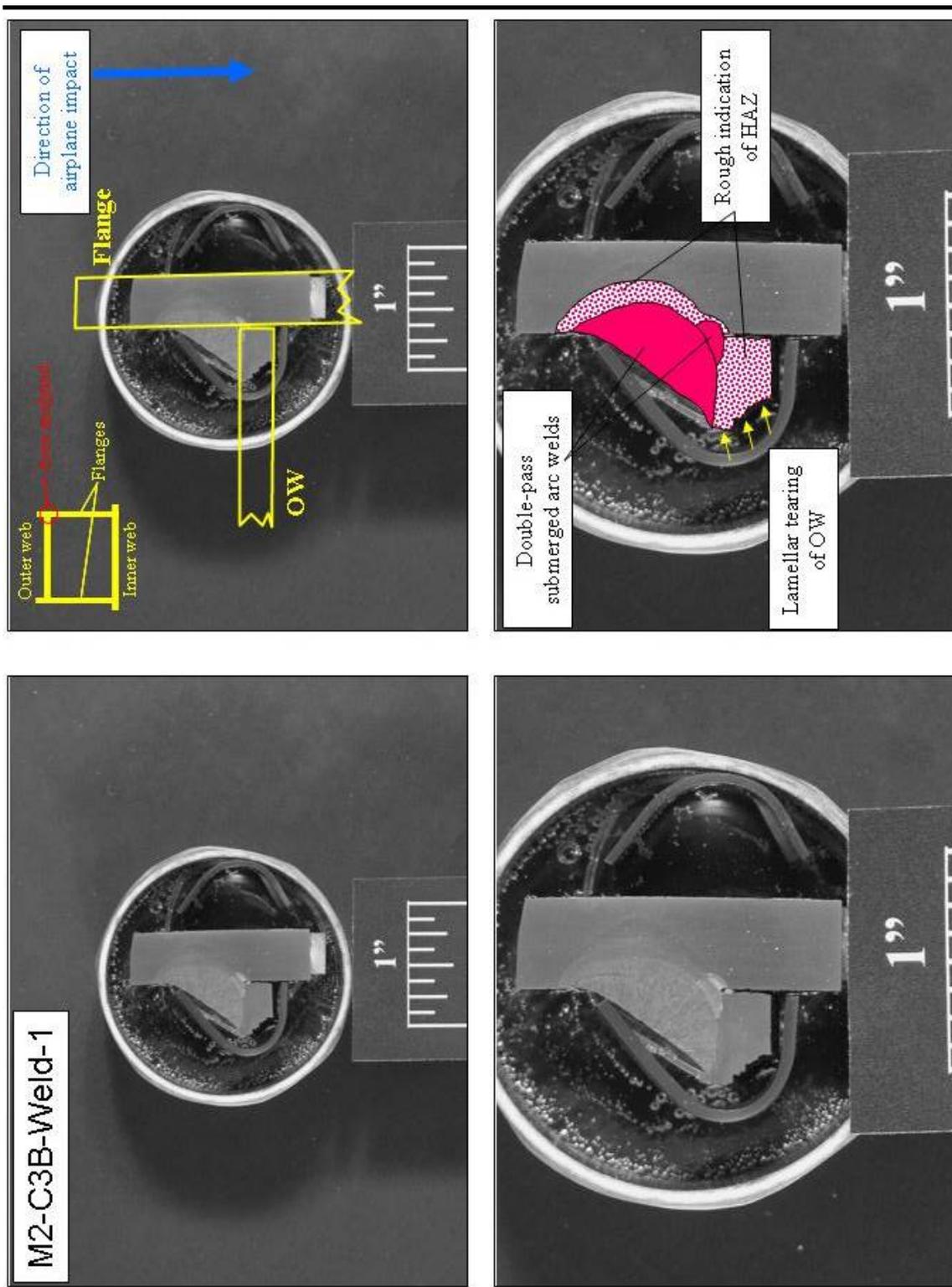
Figure 3–16. Polished and etched cross-section of fracture near weld between outer web and flange as seen in Fig. 3–14. Sample was from panel M-2 (A130: 96-99, column 129) that was directly hit by the plane. Fracture occurred in web plate; weld was intact. Two percent nital and 4 percent picral etch.
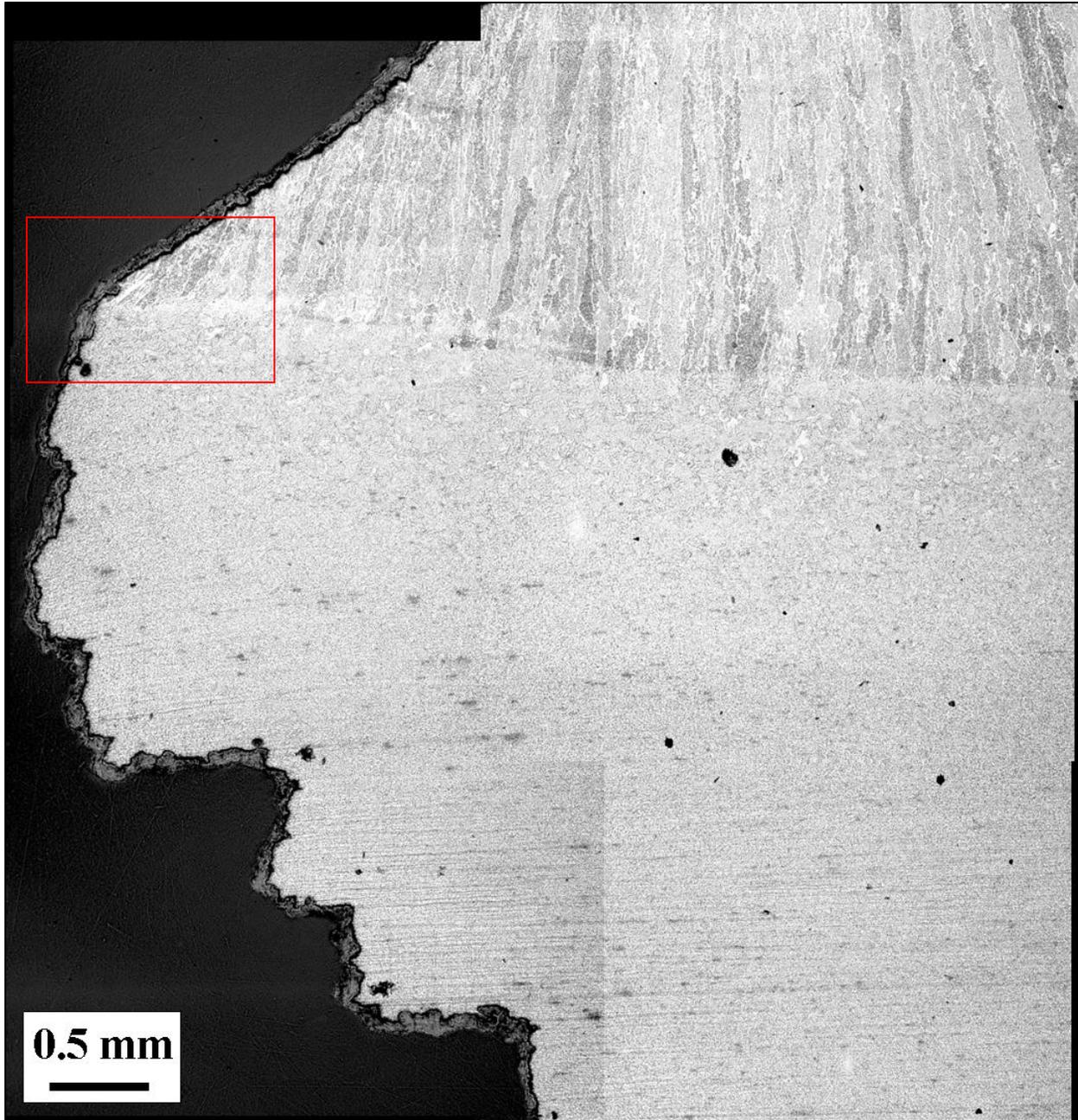
Source: NIST.

Source: NIST.

Figure 3–17. Light optical micrograph a) showing fracture of the outer web plate as a result of airplane impact (seen in Fig. 3–14). Fracture initiated at the toe of the weld and traveled through the HAZ of the plate. Two percent nital and 4 percent picral etch. (panel M-2, A130: 96-99, column 129)
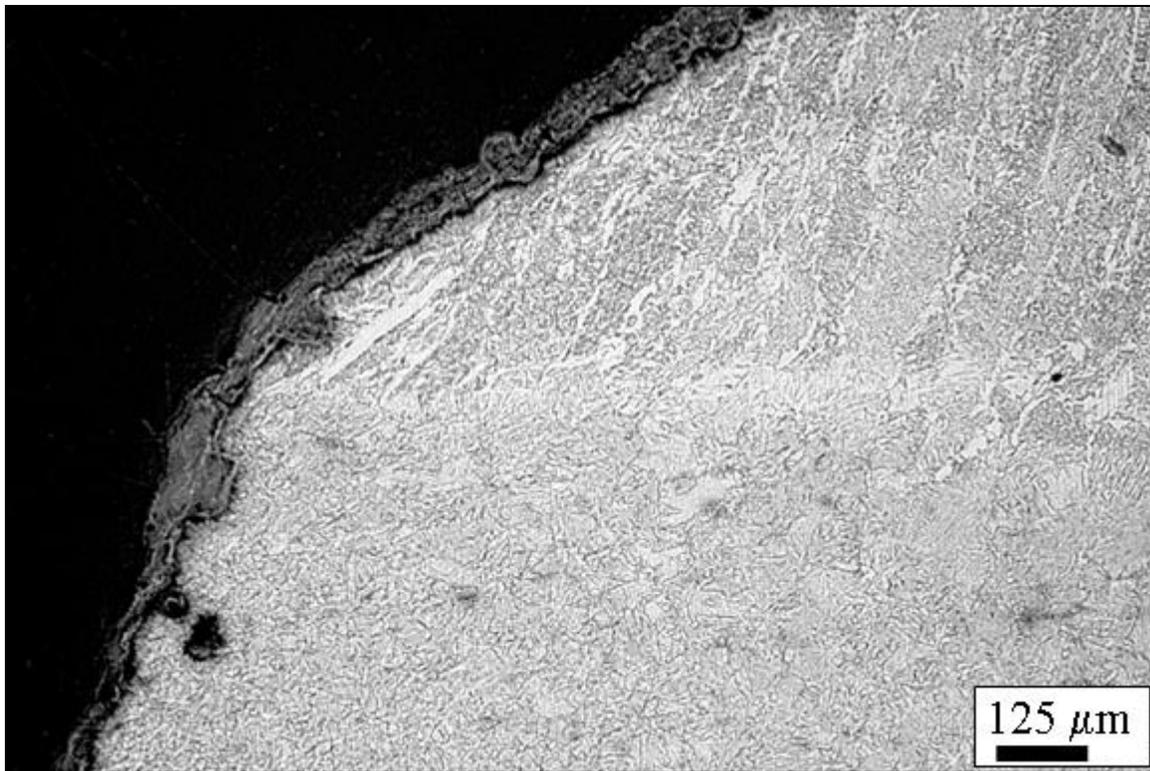
Source: NIST.

Figure 3–17. Light optical micrograph b) at higher magnification (red box in [a]) showing initiation of fracture at the toe of the weld and traveling through the HAZ of the plate. Two percent nital and 4 percent picral etch. (A130: 96-99, column 129)
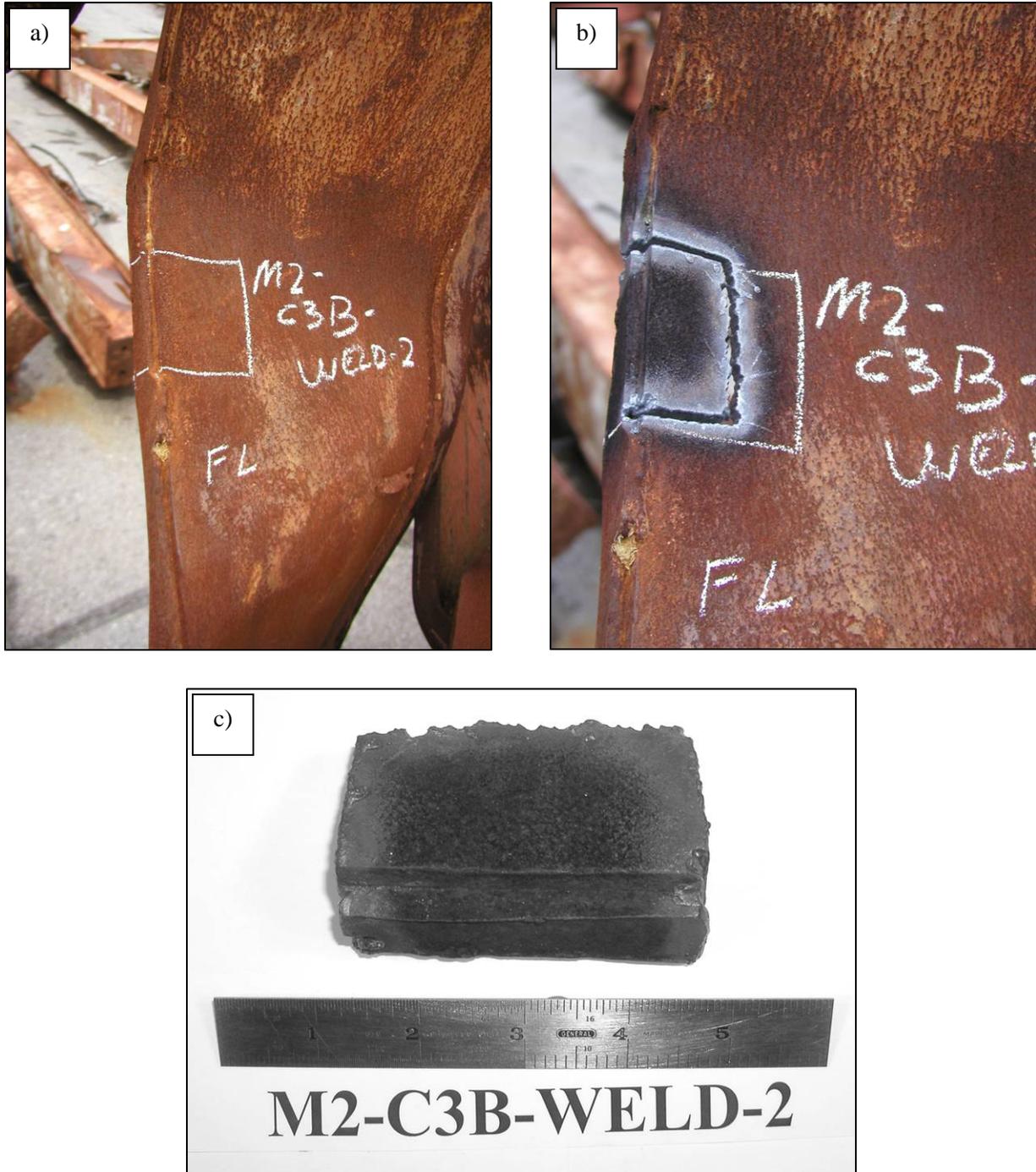
Source: NIST.

Figure 3–18. Example of fracture near weld of a perimeter column, sample M2-C3B-Weld-2 (A130: 96-99, column 129), images taken a) prior to sample removal, b) after flame cutting, and c) in the laboratory. Fracture was a result of airplane impact.
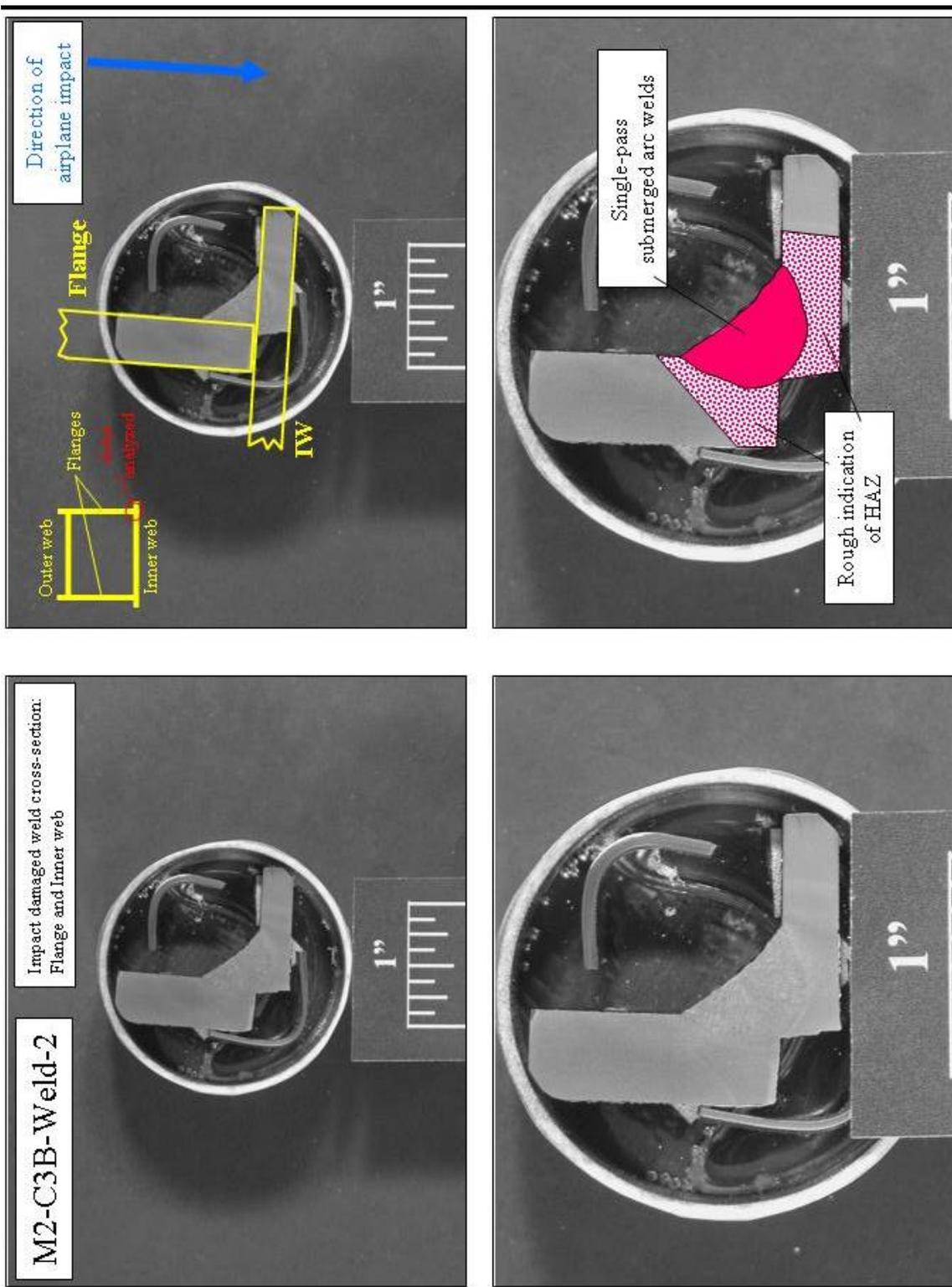
Figure 3–19. Polished and etched cross-section of fracture near weld between inner web and flange as seen in Fig. 3–18. Sample was from panel M-2 (A130: 96-99, column 129) that was directly hit by the plane. Fracture occurred in inner web plate; weld was intact. Two percent nital and 4 percent picral etch.
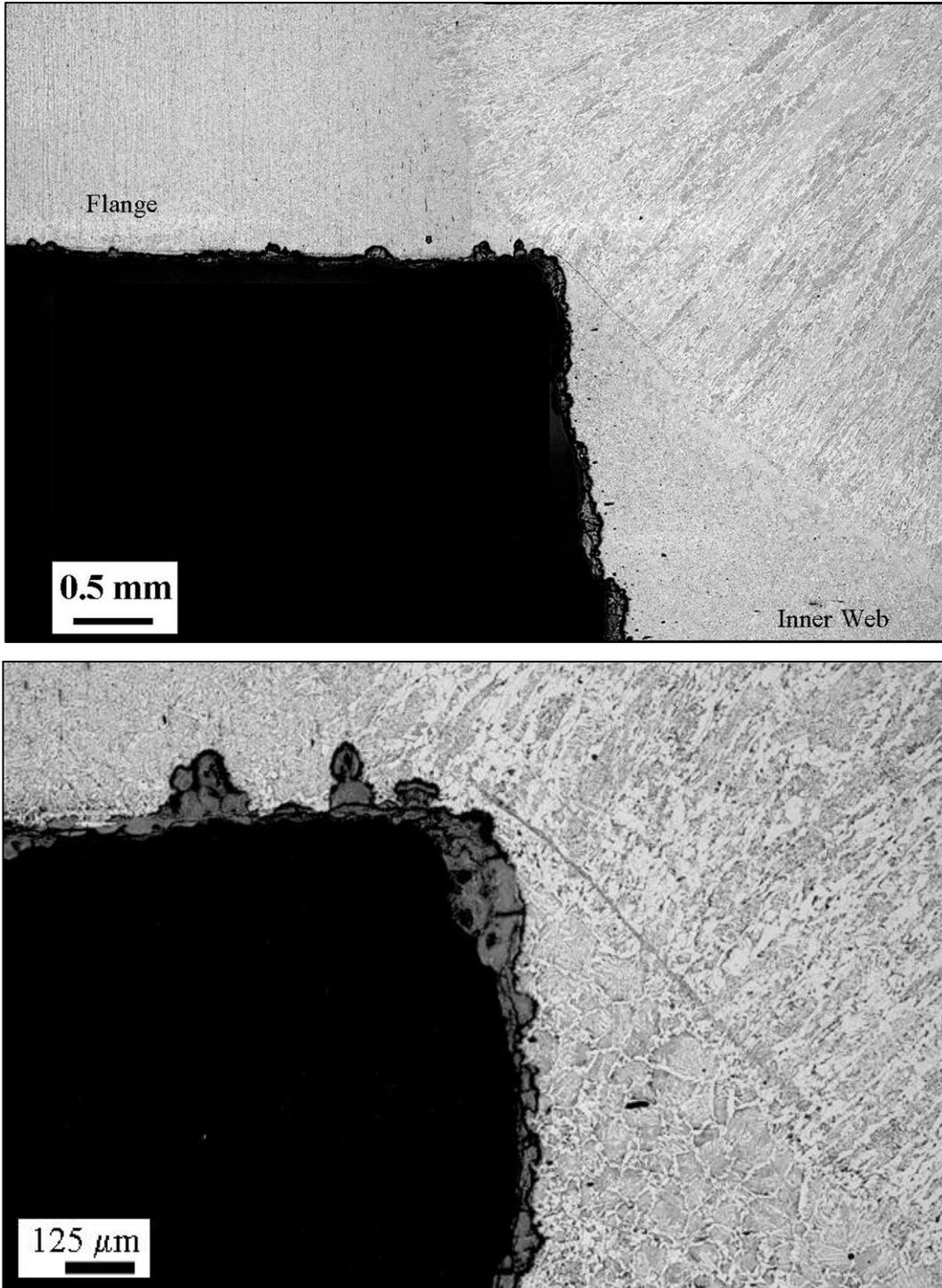
Source: NIST.

Figure 3–20. Light optical micrograph showing fracture of the inner web (from Fig. 3–18) initiating near the fusion line in the HAZ of the plate. Two percent nital and 4 percent picral etch. (A130: 96-99, column 129).
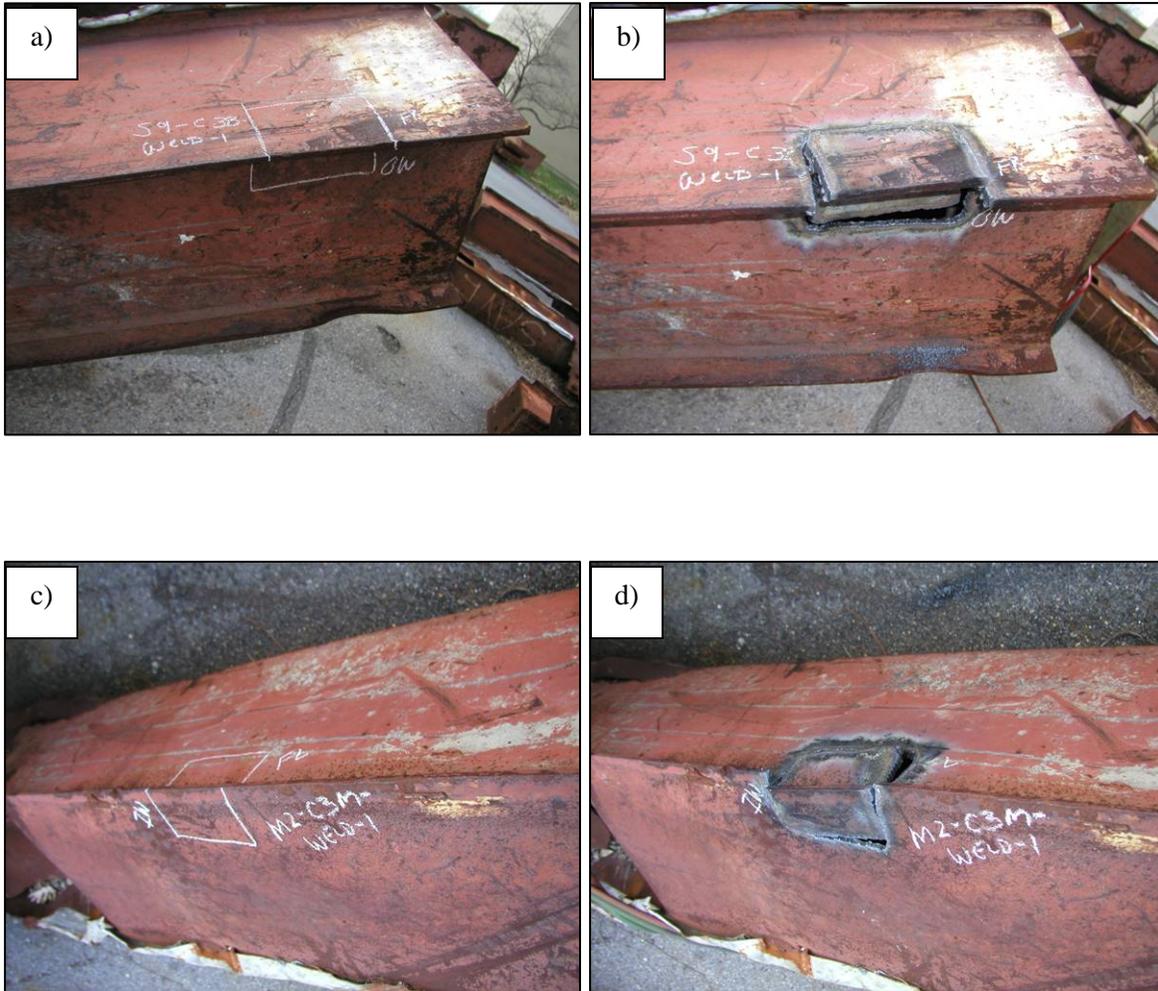
Source: NIST.

Figure 3–21. Removal of undamaged weld samples. a) Uncut sample labeled S9-C3B-Weld-1 (A133: 97-100, column 132) of a welded joint between a flange and outer web, b) cut sample, c) uncut sample labeled M2-C3M-Weld-1 (A130: 96-99, column 129) of a welded joint between a flange and inner web, and d) cut sample.
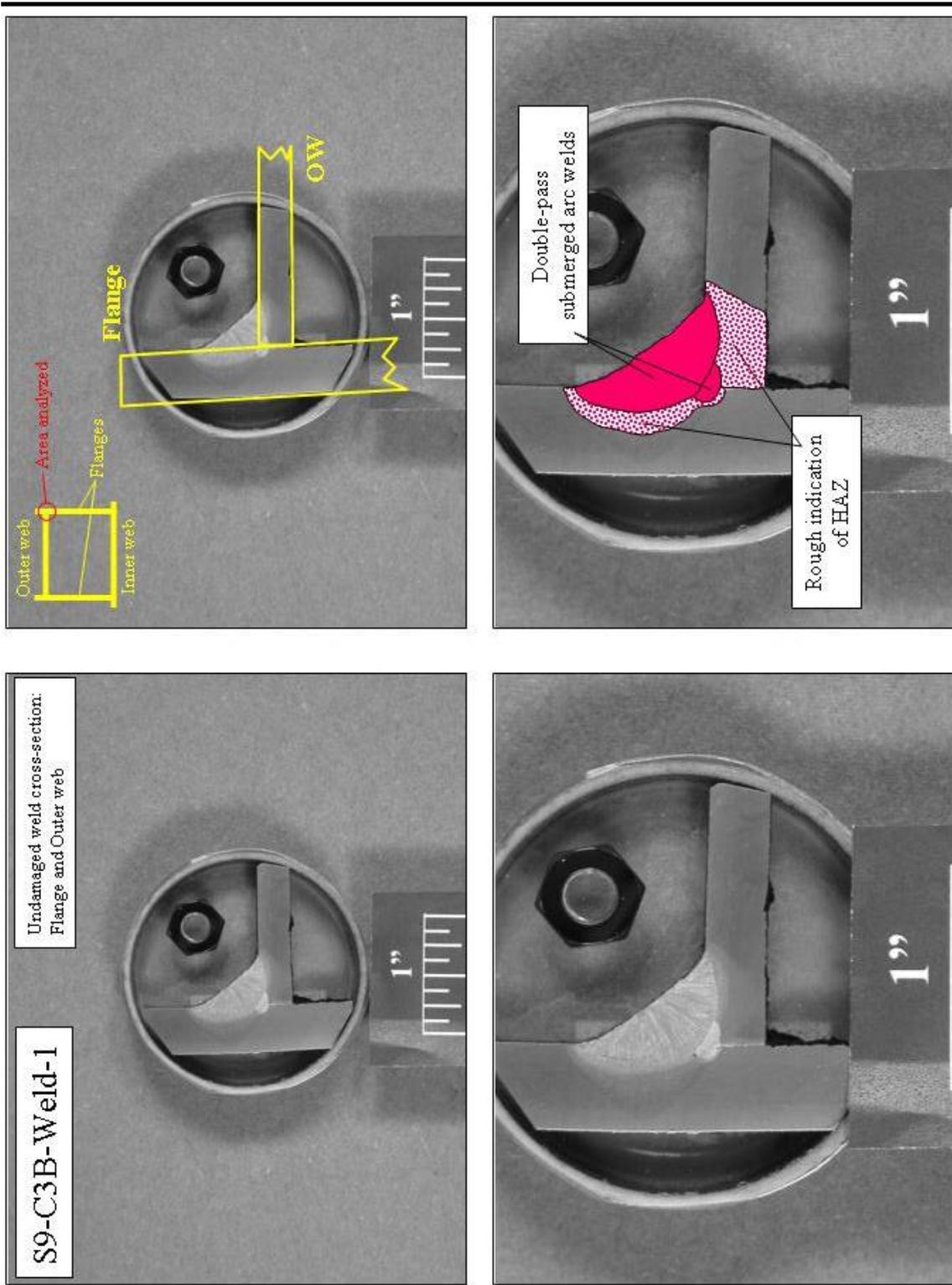
Figure 3–22. Polished and etched cross-section of intact weld between outer web and flange (same as shown in Fig. 3–21a and 3–21b). The sample was removed from an undamaged portion of column of panel S-9 (A133: 97-100, column 132) that was directly hit by the plane. Note the geometry of the HAZ in the outer web base plate. Two percent nital and 4 percent picral etch.
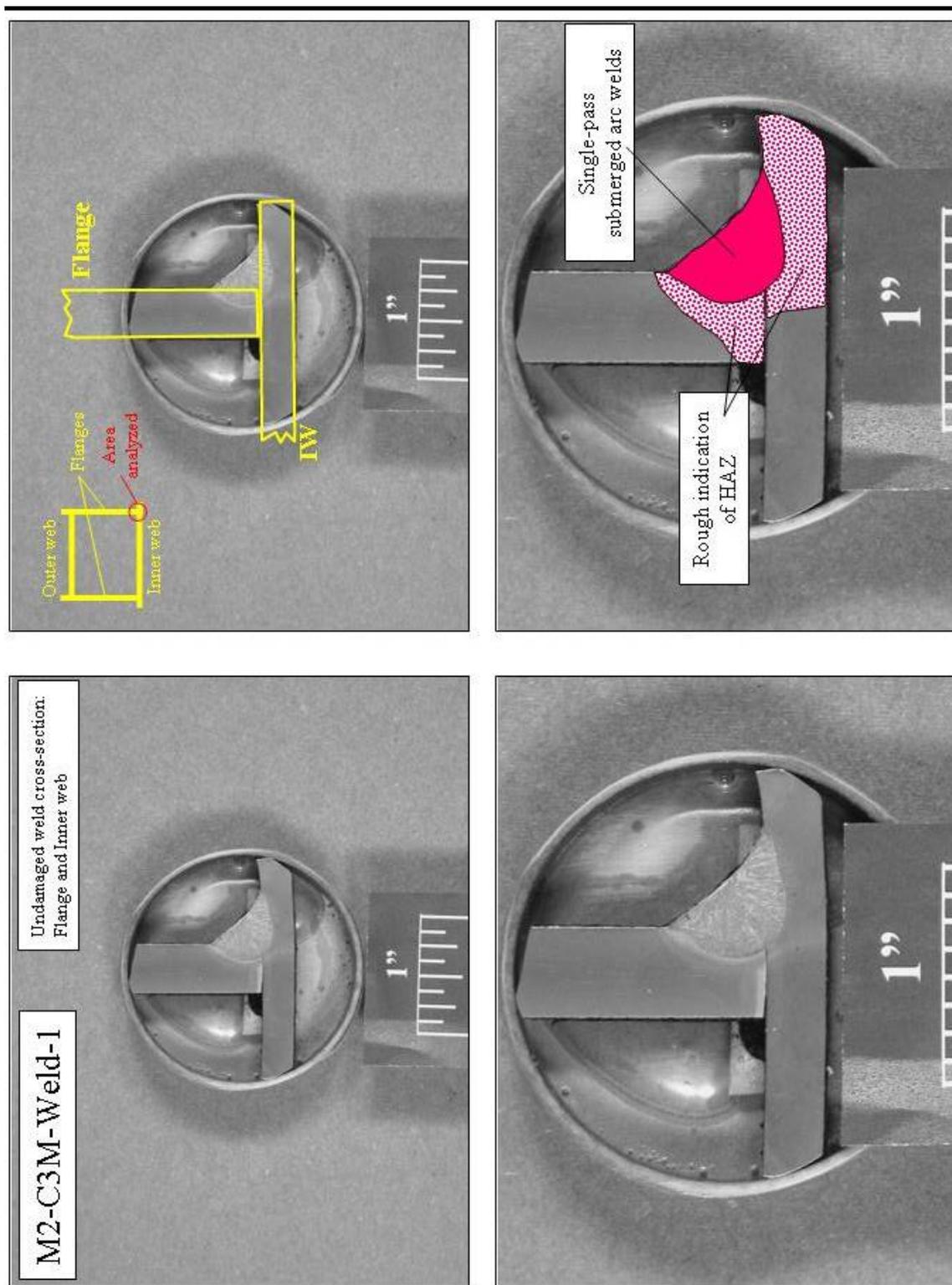
Source: NIST.

Figure 3–23. Polished and etched cross-section of intact weld between inner web and flange (same as shown in Fig. 3–21c and 3–21d). The sample was removed from an undamaged portion of column of panel M-2 (A130: 96-99, column 129) that was directly hit by the plane. Note the geometry of the HAZ in the inner web base plate. Two percent nital and 4 percent picral etch.

Source: NIST.

Figure 3–24. Weld fracture sample S9-C2B-Weld-1 (A133: 97-100, column 133), images taken a) prior to sample removal and b) after flame cutting. Panel S-9 was struck by the vertical tail assembly of the airplane.
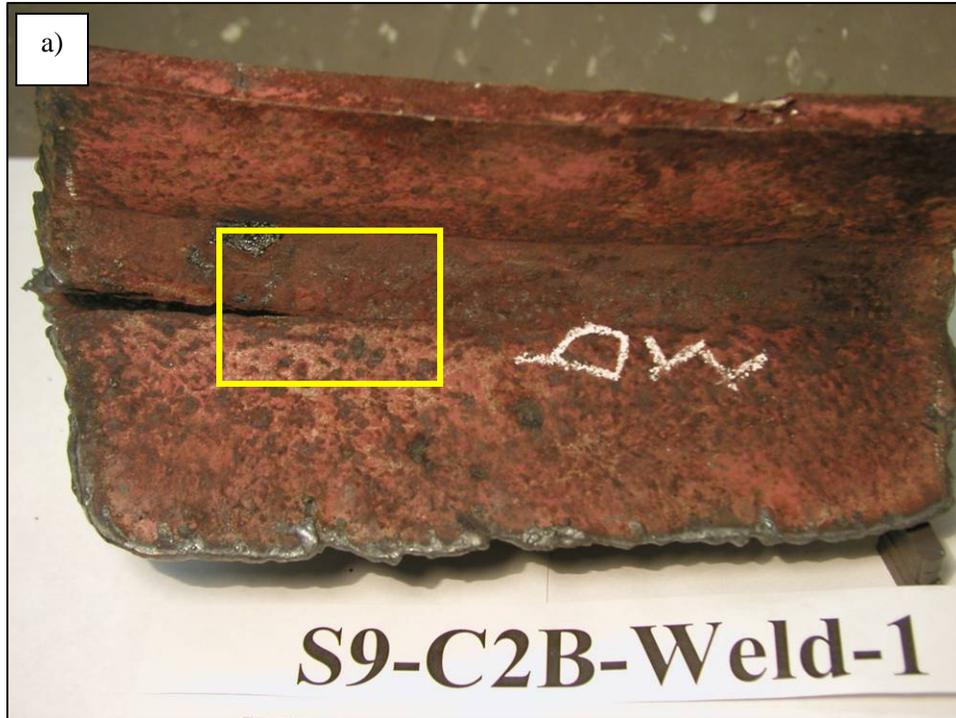
Source: NIST.

Figure 3–25. Fracture near a weld on a perimeter panel, sample S9-C2B-Weld-1 (A133: 97-100, column 133), laboratory images a) overall and b) close-up of crack and crack front propagating through the outer web. Fracture may be a result of airplane impact (vertical tail assembly) with removal shown in Fig. 3–24.
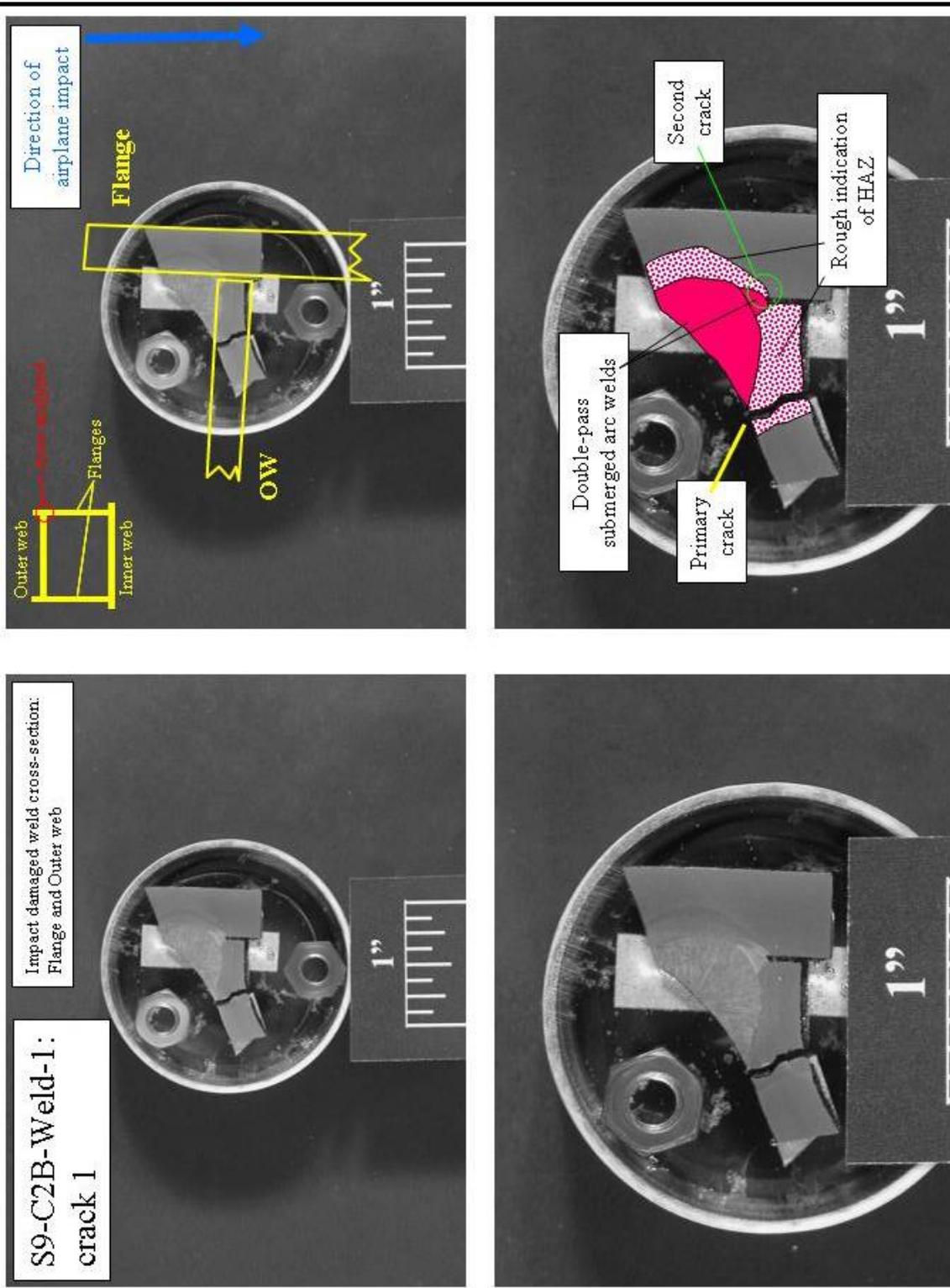
Figure 3–26. Polished and etched cross-section of fracture near weld between outer web and flange (as seen in Fig. 3–24). Sample was from panel S-9 that was directly hit by the vertical tail assembly of the plane. Yellow arrow indicates viewing direction of "planar" sample seen in Fig. 3–27. Two percent nital and 4 percent picral etch. (A133: 97-100, column 133)
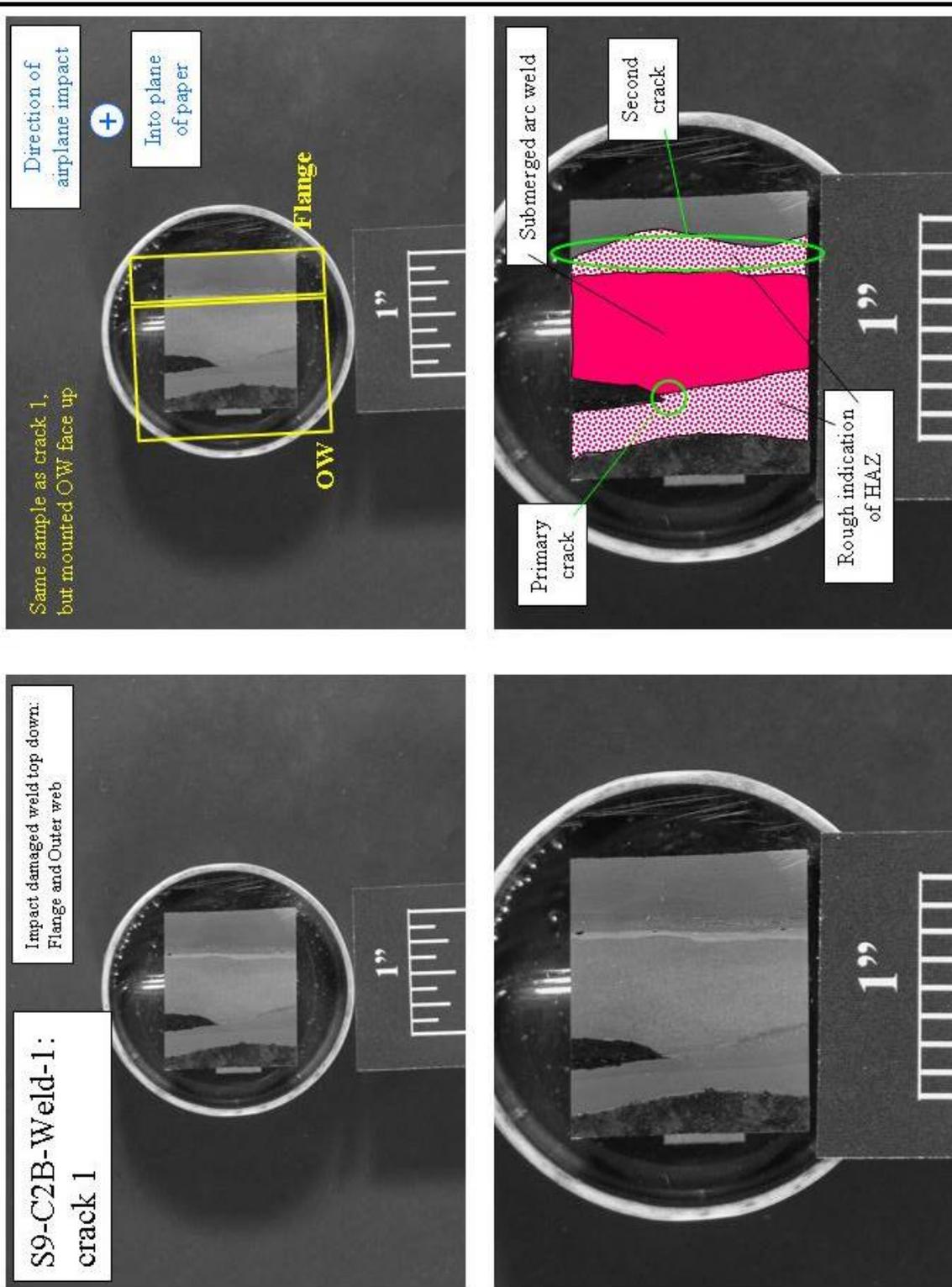
Source: NIST.

Figure 3–27. Polished and etched "planar" view of fracture near weld between outer web and flange (as seen in Fig. 3–24). The rolling plane of the outer web is parallel to the plane of the paper. Sample was from panel S-9 that was directly hit by the vertical tail assembly of the plane. Two percent nital and 4 percent picral etch. (A133: 97-100, column 133)
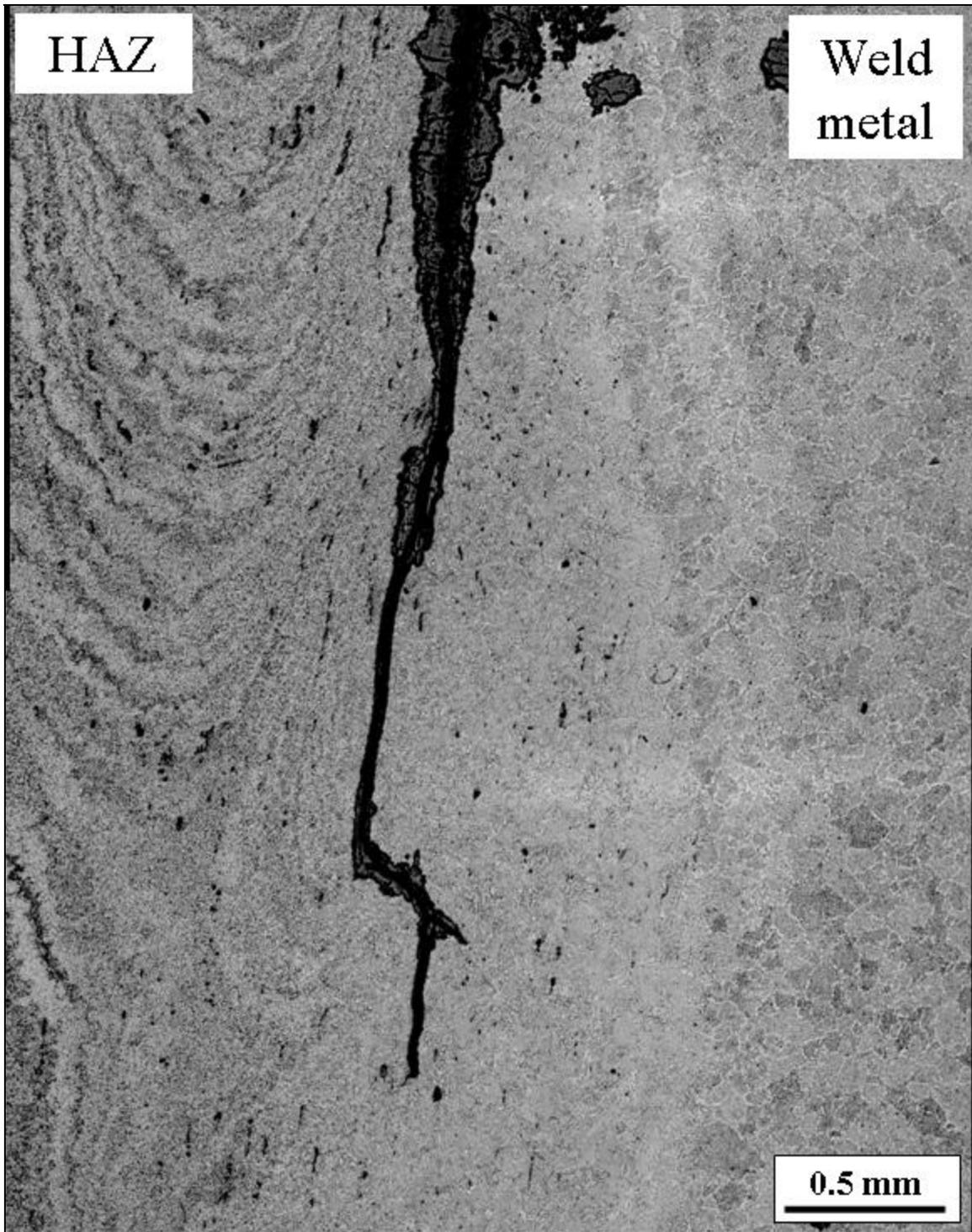
Source: NIST.

Figure 3–28. Light optical micrograph showing fracture of the outer web (from Fig. 3–27) occurring solely in the HAZ of the plate along the fusion line of the weld. Fracture may have been a result of airplane impact. Two percent nital and 4 percent picral etch. (panel S-9, A133: 97-100, column 133)
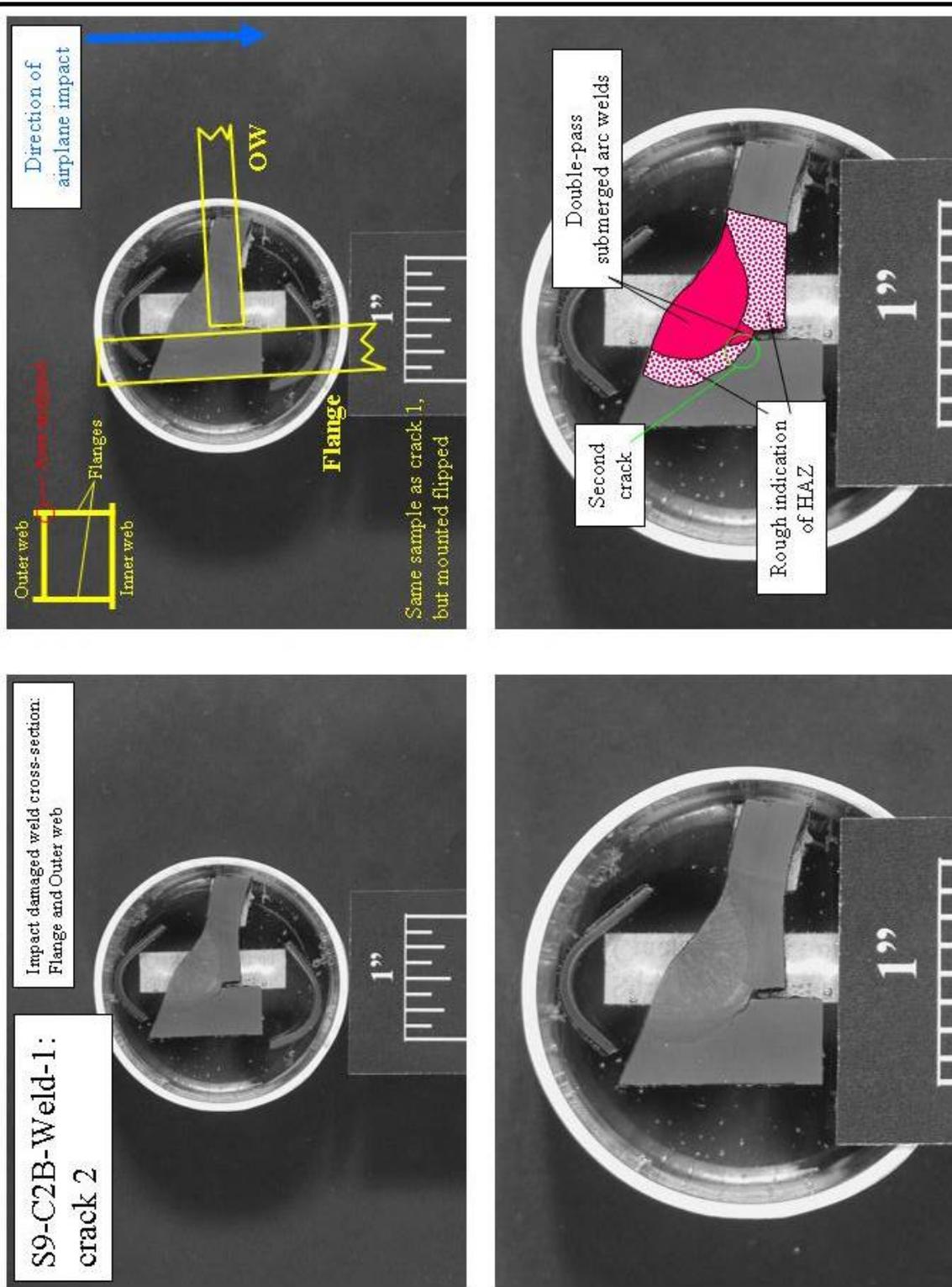
Source: NIST.

Figure 3–29. Polished and etched cross-section of fracture near weld between outer web and flange. Sample was the same as Fig. 3–25, but from well ahead of the original crack tip and mounted 180 degrees reversed so that viewed from the opposite direction as Fig. 3–26. Note that the crack started in the HAZ of the weld, but traveled into the flange plate. Two percent nital and 4 percent picral etch. (A133: 97-100, column 133)
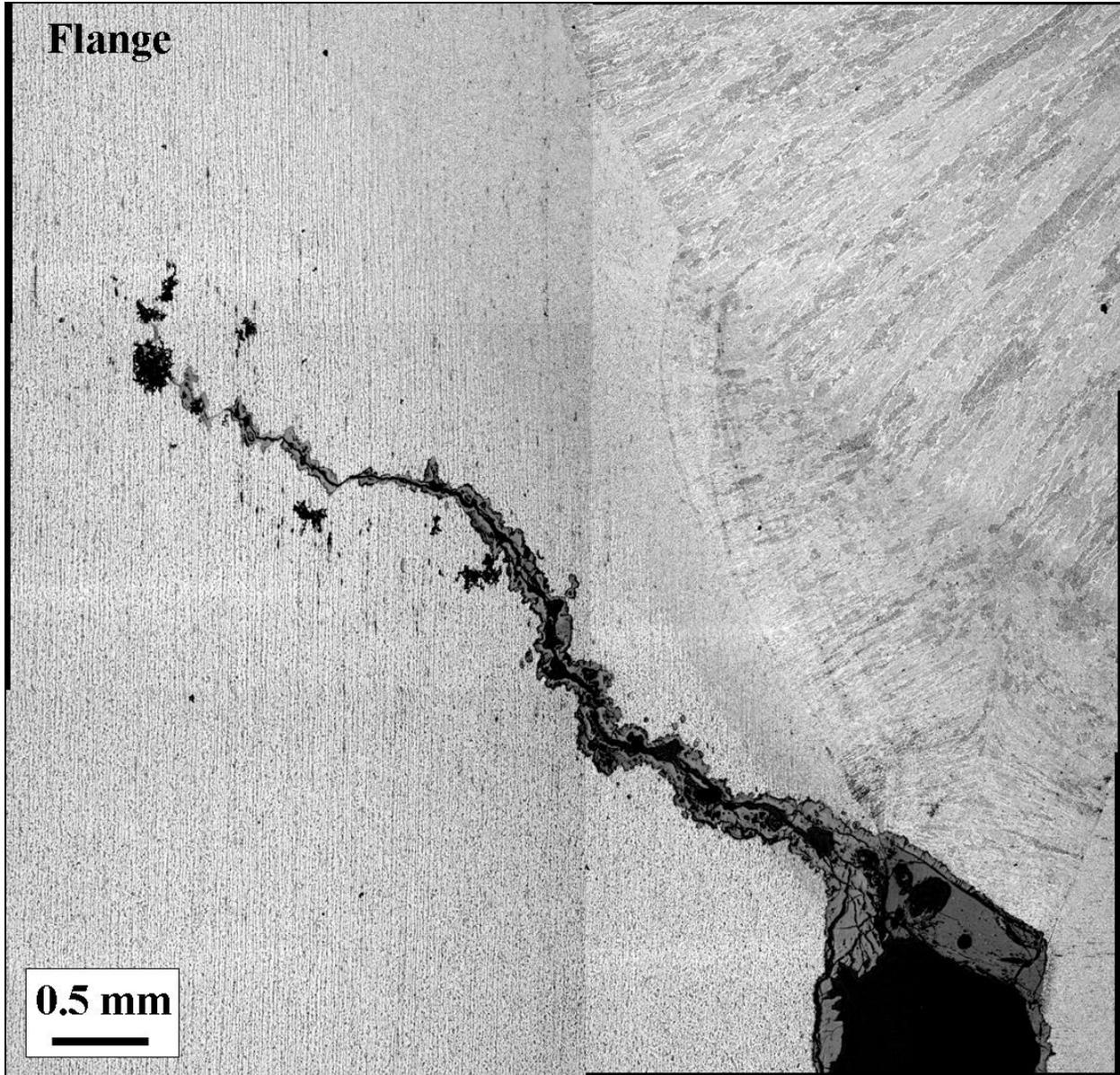
Source: NIST.

Figure 3–30. Light optical micrograph showing fracture of the flange plate (as seen in Fig. 3–29) initiating in the HAZ of the first submerged arc weld and then propagating into the unaffected base material. Two percent nital and 4 percent picral etch. (A133: 97-100, column 133)

Source: NIST.

Figure 3–31. Most-likely scenario for fracture associated with weld if second crack of sample S9-C2B-Weld-1 had continued to propagate through the flange plate. Sample shown is from N-1 (A218: 82-85). Damage most likely occurred during the collapse of WTC 1.
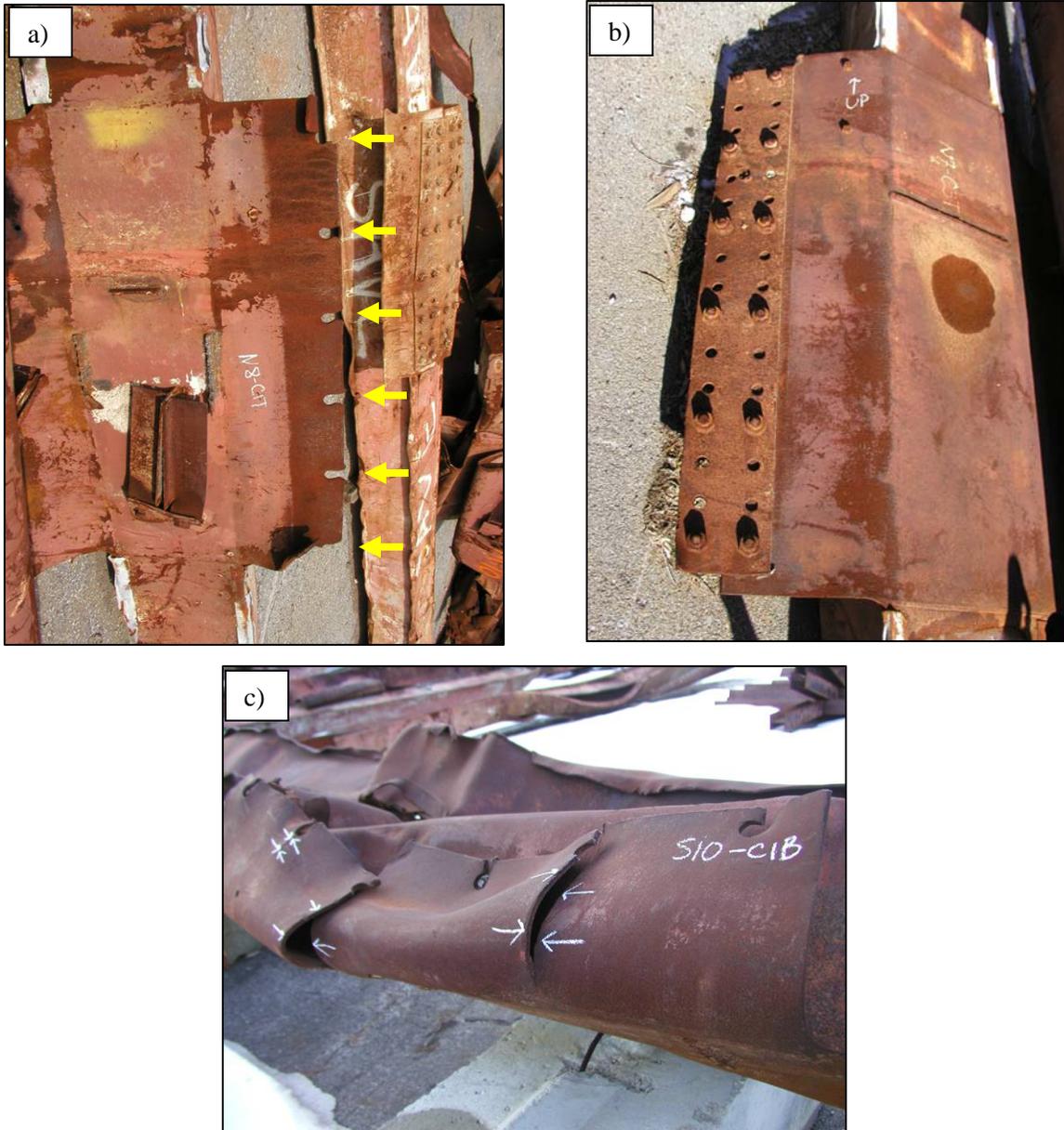
Source: NIST.

**Figure 3–32. Photographic examples of Type 1 failure mode for spandrel connections.
a) Type 1a, the observed spandrel connection possessed the tear outs (arrows) from N-8
(A142: 97-100), b) Type 1b, the splice plate and all bolts of the observed spandrel
connection remained, thus, tear out occurred in the neighboring spandrel plate to which
it was attached from N-7 (A127: 97-100), and c) Type 1c, the observed spandrel
connection possessed the tear out, with the additional fracture of the spandrel plate in a
horizontal manner from S-10 (A224: 92-95). All orientations are from the inside of the
buildings looking out. Damage of this type may be due to any one of the extreme
loading events.**

Source: NIST.

Figure 3–33. Photographic example of Type 2 failure mode for spandrel connections, bolt tear out in splice plate from C-46 (B157: 68-71). Orientation was from the outside of the building looking in. Damage of this type may be due to any one of the extreme loading events.

Source: NIST.

Figure 3–34. Photographic examples of Type 3 failure mode for spandrel connections, mixed mode. Left image orientation was from the inside of the buildings looking out from N-9 (A154: 101-104), right image orientation was from the outside of the building looking in from C-89 (B215: 12-15). Damage of this type may be due to any one of the extreme loading events.
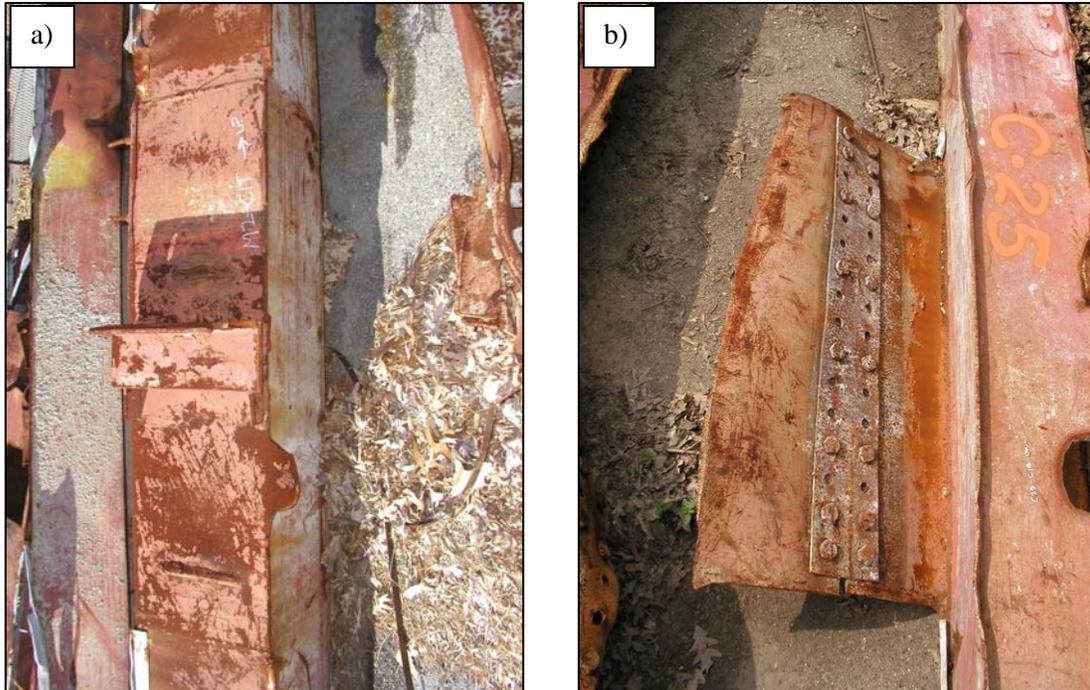
Source: NIST.

Figure 3–35. Photographic examples of Type 4 failure mode for spandrel connections. a) Type 4a, vertical fracture of observed spandrel plate (observed from inside the building looking out) from M-2 (A130: 96-99) and b) Type 4b, vertical fracture of the neighboring spandrel plate resulting in the observed spandrel connection retaining both the splice plate and portion of spandrel from neighboring panel (observed from outside the building looking in) from C-25 (A206: 89-92). Damage of this type may be due to any one of the extreme loading events.

Source: NIST.

**Figure 3–36. Photographic example of
Type 5 failure mode for spandrel
connections, bolt failure resulting in intact
holes in spandrel or splice plate (observed
from outside the building looking in) from
C-89 (B215: 12-15). Damage of this type may
be due to any one of the extreme
loading events.**

Splice Plate

M30-C3B
Column 132, 95th floor

Spandrel Detail: 101
Failure mode: Type 4b, portion of spandrel from M27-C1M still attached.
Orientation of image: From inside building looking out.
Probable cause of damage: collapse

Portion of spandrel from M-27

Source: NIST.

Figure 3–37. Photographs of the recovered spandrel connections from M-30 (A133: 94-97).

S9-C1T
Column 134, 100th floor

Spandrel Detail: 101
Failure mode: Type 3
Orientation of image: From inside building looking out.
Probable cause of damage: Collapse

S9-C1M
Column 134, 99th floor

Spandrel Detail: 101
Failure mode: Type 4a
Orientation of image: From inside building looking out.
Probable cause of damage: Collapse
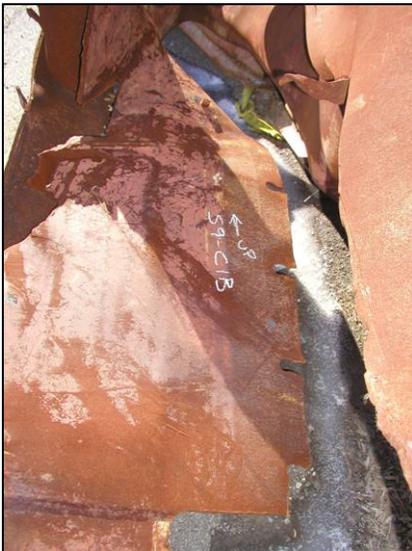
S9-C1B
Column 134, 98th floor

Spandrel Detail: 101
Failure mode: Type 1a
Orientation of image: From inside building looking out.
Probable cause of damage: Impact or Collapse

Source: NIST.

Figure 3–38. Photographs of recovered spandrel connections from sample S-9 (A133: 97-100).

S9-C3T
Column 132, 100th floor

<u>Spandrel Detail</u>: 101
<u>Failure mode</u>: Type 1a
<u>Orientation of image</u>: From inside building looking out.
<u>Probable cause of damage</u>: Collapse

S9-C3M
Column 132, 99th floor

<u>Spandrel Detail</u>: 101
<u>Failure mode</u>: Type 4b, portion of spandrel from M2-C1T still attached.
<u>Orientation of image</u>: From outside building looking in.
<u>Probable cause of damage</u>: Collapse

Splice plate

Portion of spandrel from M-2
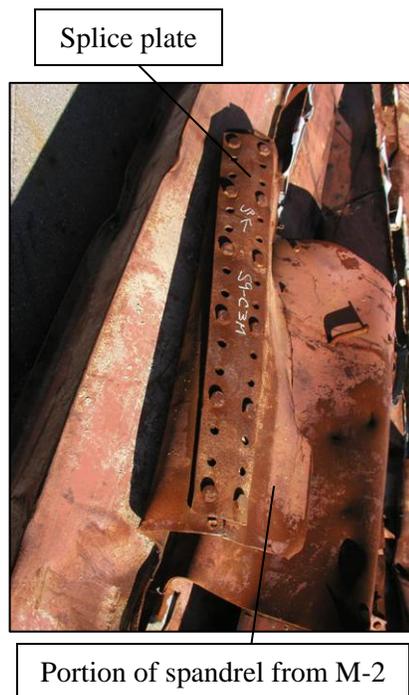
S9-C3B
Column 132, 98th floor

<u>Spandrel Detail</u>: 101
<u>Failure mode</u>: Type 3
<u>Orientation of image</u>: From outside building looking in.
<u>Probable cause of damage</u>: Impact or collapse

Source: NIST.

Figure 3–38. Photographs of recovered spandrel connections from sample S-9 (A133: 97-100) (cont.).

M27-C1M
Column 131, 95th floor

Spandrel Detail: 101
Failure mode: Type 4a
Orientation of image: From inside building looking out.
Probable cause of damage: Collapse

M27-C1B
Column 131, 94th floor

Spandrel Detail: 102
Failure mode: Type 4a
Orientation of image: From inside building looking out.
Probable cause of damage: Impact or collapse

Source: NIST.

Figure 3–39. Photographs of recovered spandrel connections from sample M-27 (A130: 93-96).

M2-C1T
Column 131, 99th floor

Spandrel Detail: 101
Failure mode: Type 4a
Orientation of image: From inside building looking out.
Probable cause of damage: Collapse

M2-C1M
Column 131, 98th floor

Spandrel Detail: 101
Failure mode: Type 3, portion of spandrel from S9-C3B still attached
Orientation of image: From inside building looking out.
Probable cause of damage: Impact or collapse

M2-C1B
Column 131, 97th floor

Spandrel Detail: 101
Failure mode: Type 1a
Orientation of image: From inside building looking out.
Probable cause of damage: Impact

Source: NIST.

Figure 3–40. Photographs of recovered spandrel connections from sample M-2 (A130: 96-99).

M2-C3T
Column 129, 99th floor

Spandrel Detail: 101
Failure mode: Type 1b
Orientation of image: From inside building looking out.
Probable cause of damage: Collapse

M2-C3M
Column 129, 98th floor

Spandrel Detail: 101
Failure mode: Type 1a
Orientation of image: From inside building looking out.
Probable cause of damage: Impact or collapse

M2-C3B
Column 129, 97th floor

Spandrel Detail: 101
Failure mode: Type 1b
Orientation of image: From intside building looking out.
Probable cause of damage: Impact

Source: NIST.

Figure 3–40. Photographs of recovered spandrel connections from sample M-2 (A130: 96-99) (cont.)

N7-C1T
Column 128, 100th floor

<u>Spandrel Detail</u>: 101
<u>Failure mode</u>: Type 4a
<u>Orientation of image</u>: From outside building looking in.
<u>Probable cause of damage</u>: Collapse

N7-C1M
Column 128, 99th floor

<u>Spandrel Detail</u>: 101
<u>Failure mode</u>: Type 1c
<u>Orientation of image</u>: From outside building looking in.
<u>Probable cause of damage</u>: Collapse

N7-C1B
Column 128, 98th floor

<u>Spandrel Detail</u>: 101
<u>Failure mode</u>: Type 1b
<u>Orientation of image</u>: From outside building looking in.
<u>Probable cause of damage</u>: Impact or collapse

Source: NIST.
Figure 3–41. Photographs of recovered spandrel connections from sample N-7 (A127: 97-100).

N7-C3T
Column 126, 100th floor

<u>Spandrel Detail</u>: 101
<u>Failure mode</u>: Type 1b
<u>Orientation of image</u>: From inside building looking out.
<u>Probable cause of damage</u>: Collapse

N7-C3M
Column 126, 99th floor

<u>Spandrel Detail</u>: 101
<u>Failure mode</u>: Type 1c
<u>Orientation of image</u>: From inside building looking out.
<u>Probable cause of damage</u>: Collapse

N7-C3B
Column 126, 98th floor

<u>Spandrel Detail</u>: 101
<u>Failure mode</u>: Type 3
<u>Orientation of image</u>: From inside building looking out.
<u>Probable cause of damage</u>: Impact or collapse

Source: NIST.

Figure 3–41. Photographs of recovered spandrel connections from sample N-7 (A127: 97-100) (cont.).

Source: NIST.

Figure 3–42. Photographic example of Type 1 failure mode for end plate connections, bolt failure. Column on right (M26-C3B) has two failed bolts remaining (arrows). Sample shown is M-26 (A130: 90-93). Damage of this type may be due to any one of the extreme loading events.

Source: NIST.

Figure 3–43. Photographic example of Type 2 failure mode for end plate connections. a) Type 2a, partial failure with end plate still remaining (arrows) from M-28 (B345: 98-101) and b) Type 2b, full failure with end plate missing from N-9 (A154: 101-104). Damage of this type may be due to any one of the extreme loading events.

Source: NIST.

Figure 3–44. Photographic example of Type 3 failure mode for end plate connections, a welded connection with bolts intact, end plate of above or below adjoining column still attached. Sample shown is C-24 (B203: 74-77). Damage of this type may be due to any one of the extreme loading events.

M30-C2B
WTC1
Col 133
Fl 94

Torque direction

M30-C3B
WTC1
Col 132
Fl 94

Source: NIST.

Figure 3–45. Photographs of recovered end plate connections from sample M-30 (A133: 94-97). Both connection failures were due to airplane impact.

S9-C1T
WTC1
Col 134
Fl 100

No change in bolt
hole shape

S9-C1B
WTC1
Col 134
Fl 97

Source: NIST.

**Figure 3–46. Photographs of recovered end plate connections from sample S-9
(A127: 97-100). Lower connection failed upon airplane impact, upper connection failed as
a result of either airplane impact or collapse.**

S9-C2T
WTC1
Col 133
Fl 100

No change in bolt
hole shape

S9-C2B
WTC1
Col 133
Fl 97

Source: NIST.

**Figure 3–46. Photographs of recovered end plate connections from sample S-9
(A127: 97-100). Lower connection failed upon airplane impact, upper connection failed
as a result of either airplane impact or collapse (cont.).**

S9-C3T
WTC1
Col 132
Fl 100

S9-C3B
WTC1
Col 132
Fl 97

Source: NIST.

Figure 3–46. Photographs of recovered end plate connections from sample S-9 (A127: 97-100). Lower connection failed upon airplane impact, upper connection failed as a result of either airplane impact or collapse (cont.).

**Endplate is bent, no weld
failures observed**

**M27-C1B
WTC1
Col 131
Fl 93**

Source: NIST.

**Figure 3–47. Photographs of recovered end plate connections from sample M-27
(A130: 93-96). Probable cause of connection failure was collapse.**

M27-C2B
WTC1
Col 130
Fl 93

Source: NIST.

Figure 3–47. Photographs of recovered end plate connections from sample M-27 (A130: 93-96). Probable cause of connection failure was collapse (cont.).

M2-C1T
WTC1
Col 131
Fl 99

M2-C1B
WTC1
Col 131
Fl 96

Source: NIST.

Figure 3–48. Photographs of recovered end plate connections from sample M-2 (A127: 97-100). Lower connection failed upon airplane impact, upper connection failed as a result of either airplane impact or collapse.

No change in bolt
hole shape

M2-C2T
WTC1
Col 130
Fl 99

Internal weld
bead on OW

Fracture of
flange
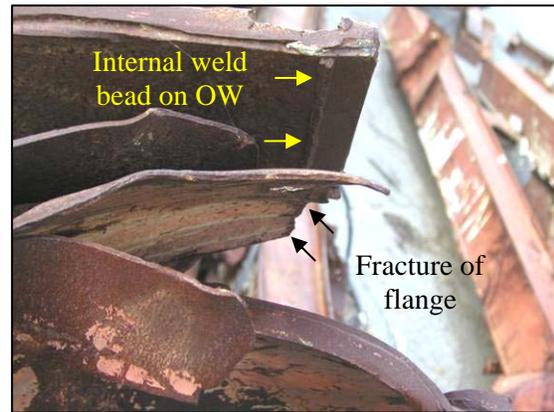
M2-C2B
WTC1
Col 130
Fl 96

Source: NIST.

**Figure 3–48. Photographs of recovered end plate connections from sample M-2
(A127: 97-100). Lower connection failed upon airplane impact, upper connection failed
as a result of either airplane impact or collapse (cont.).**

Separation between flange plates and butt plate

M2-C3T
WTC1
Col 129
Fl 99

M2-C3B
WTC1
Col 129
Fl 96

Source: NIST.

Figure 3–48. Photographs of recovered end plate connections from sample M-2 (A127: 97-100). Lower connection failed upon airplane impact, upper connection failed as a result of either airplane impact or collapse (cont.).

N7-C1T
WTC1
Col 128
Fl 100

N7-C1B
WTC1
Col 128
Fl 97

Source: NIST.

Figure 3–49. Photographs of recovered end plate connections from sample N-7 (A127: 97-100). Lower connection failed upon airplane impact, upper connection most likely failed as a result of collapse.

N7-C2T
WTC1
Col 127
Fl 100
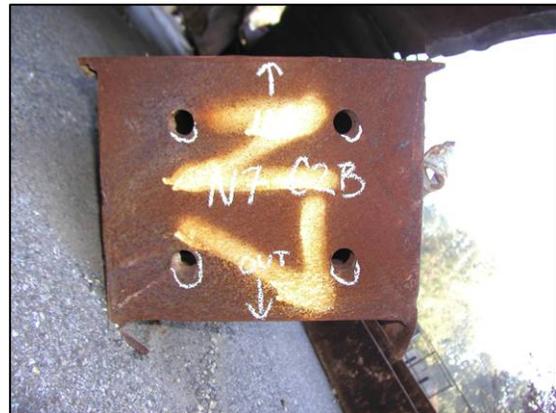
N7-C2B
WTC1
Col 127
Fl 97

Source: NIST.

Figure 3–49. Photographs of recovered end plate connections from sample N-7 (A127: 97-100). Lower connection failed upon airplane impact, upper connection most likely failed as a result of collapse (cont.).

N7-C3T
WTC1
Col 126
Fl 100

N7-C3B
WTC1
Col 126
Fl 97

Torque direction

Source: NIST.

Figure 3–49. Photographs of recovered end plate connections from sample N-7 (A127: 97-100). Lower connection failed upon airplane impact, upper connection most likely failed as a result of collapse (cont.).

Outside of building looking in at panel

Column

Top

C1T

Spandrel

C3T

C2T

Middle

C1M

C3M

C2M

Bottom

C1B

C3B

C1   C2   C3

C2B
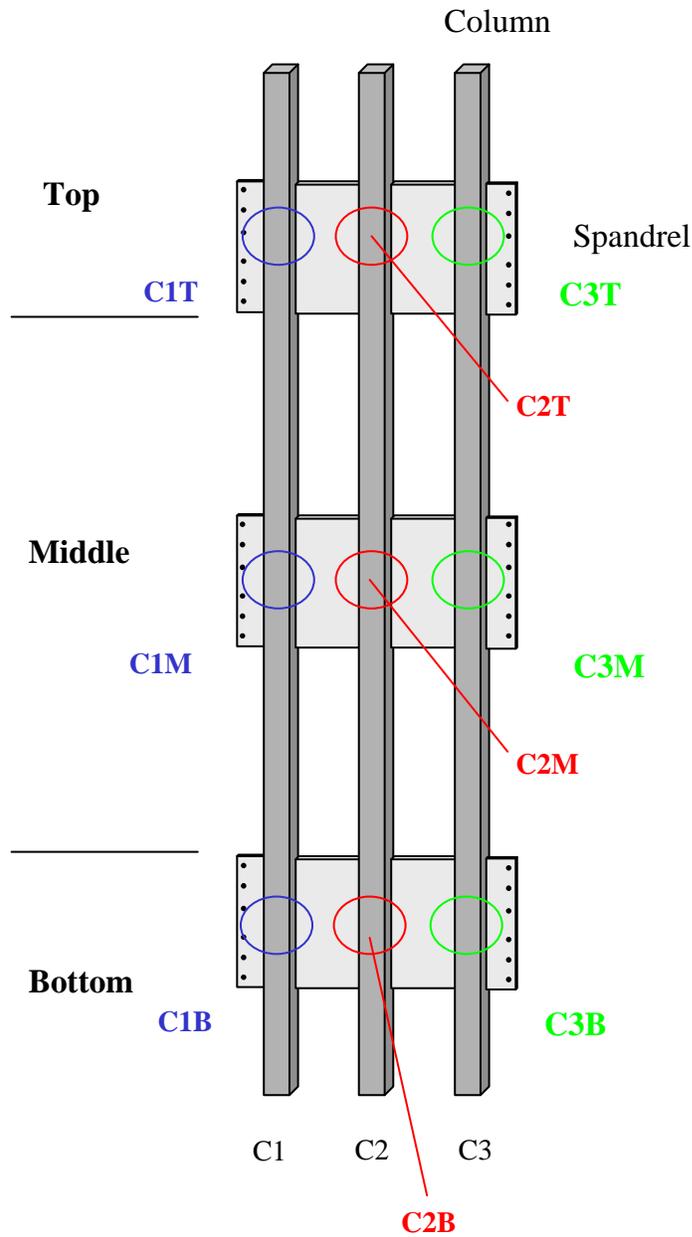
Figure 3–50. Labeling system used by NIST to identify the specific intersections of columns and spandrels of the exterior wall panels.
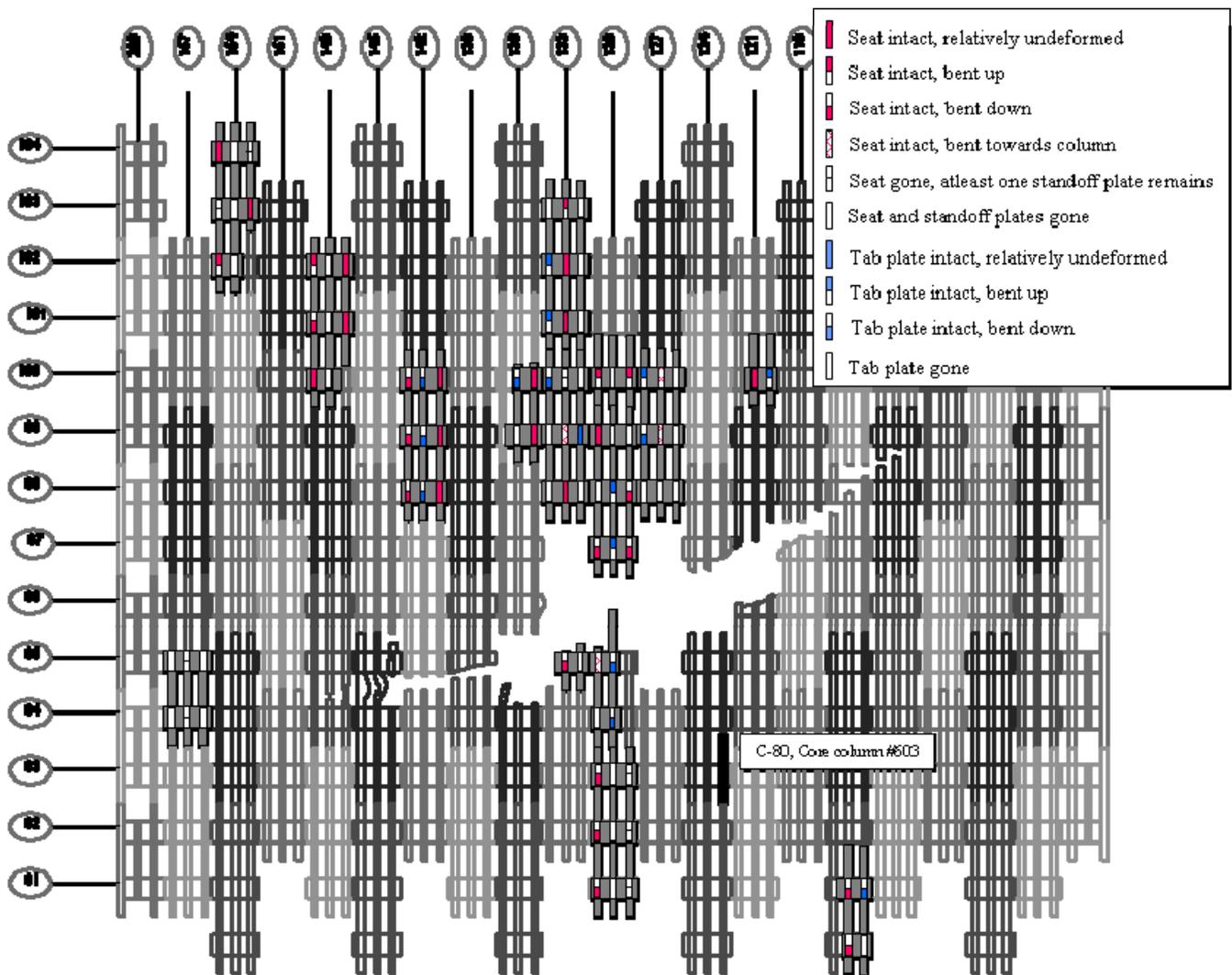
Figure 3–51a. WTC 1, damage diagram overlaid with recovered samples and damage of connectors.
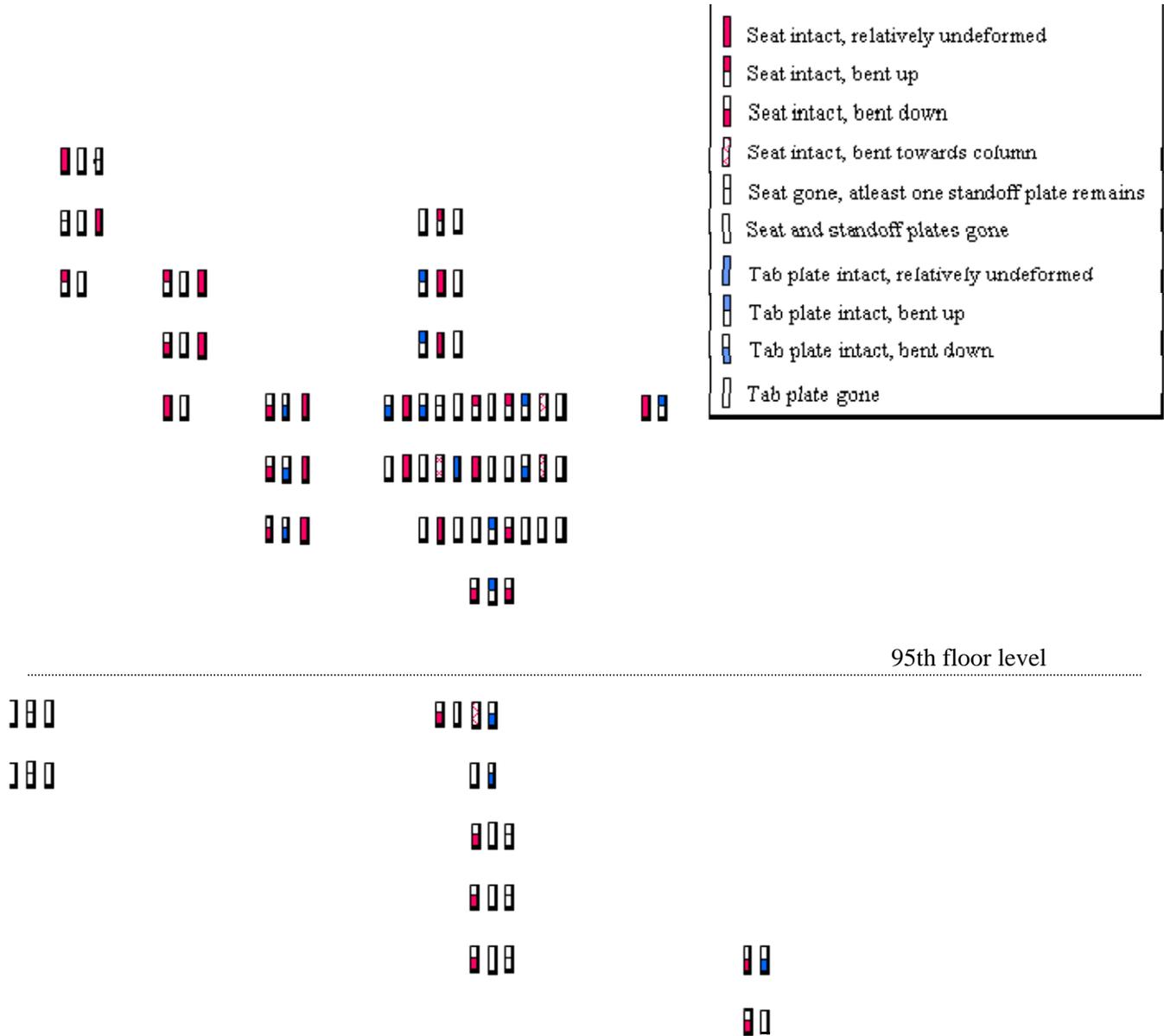
Figure 3–51b. WTC 1, damage of connectors. At or below the 95th floor, all connectors are either bent down or missing.
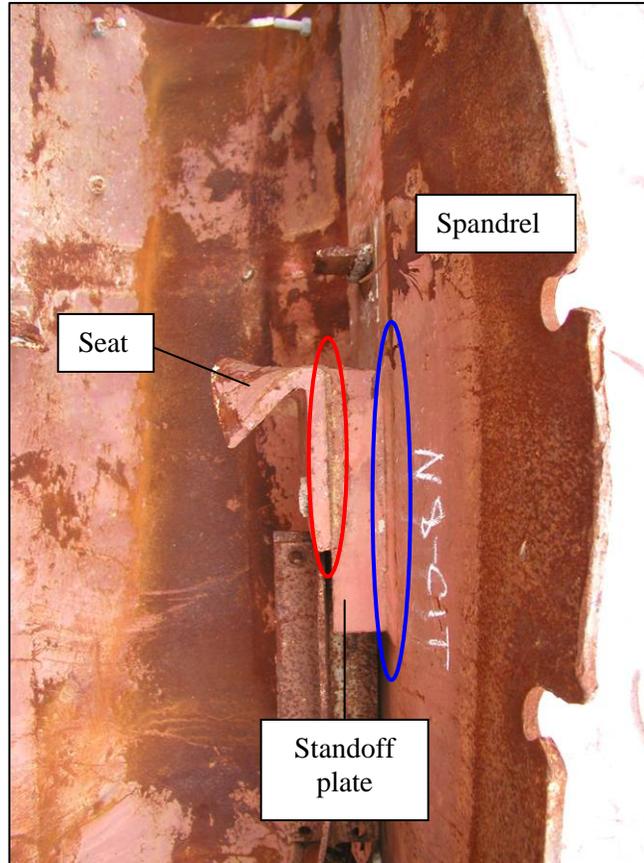
Source: NIST.

Figure 3–52. Photograph indicating location of welds between the spandrel and standoff plate (blue indicator) and between the standoff plate and seat (red indicator).
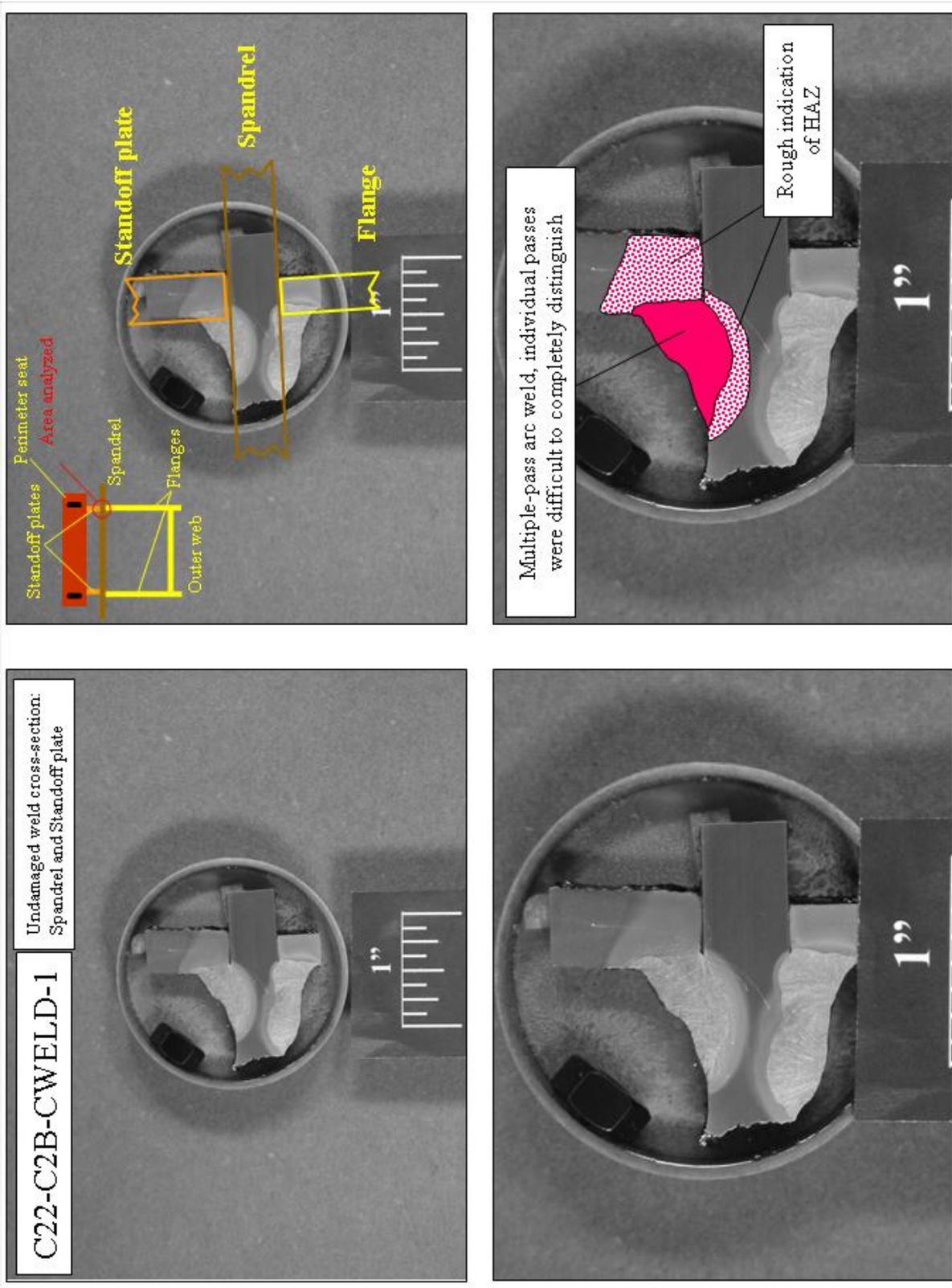
Figure 3–53a. Etched cross-section of intact weld between spandrel plate (65 ksi) and standoff plate (42 ksi). Sample was from panel C-22 (A157: 93-96, column 157, 94th floor). Two percent nital and 4 percent picral etch.

Source: NIST.

The following labels appear on the figure:

M2-C3T-WELD-1

Damaged weld cross-section: Spandrel and Standoff plate

Standoff plate

Spandrel

Flange

Perimeter seat

Area analyzed

Standoff plates

Spandrel

Flanges

Outer web

Multiple-pass arc weld, individual passes were difficult to completely distinguish

Rough indication of HAZ

1"
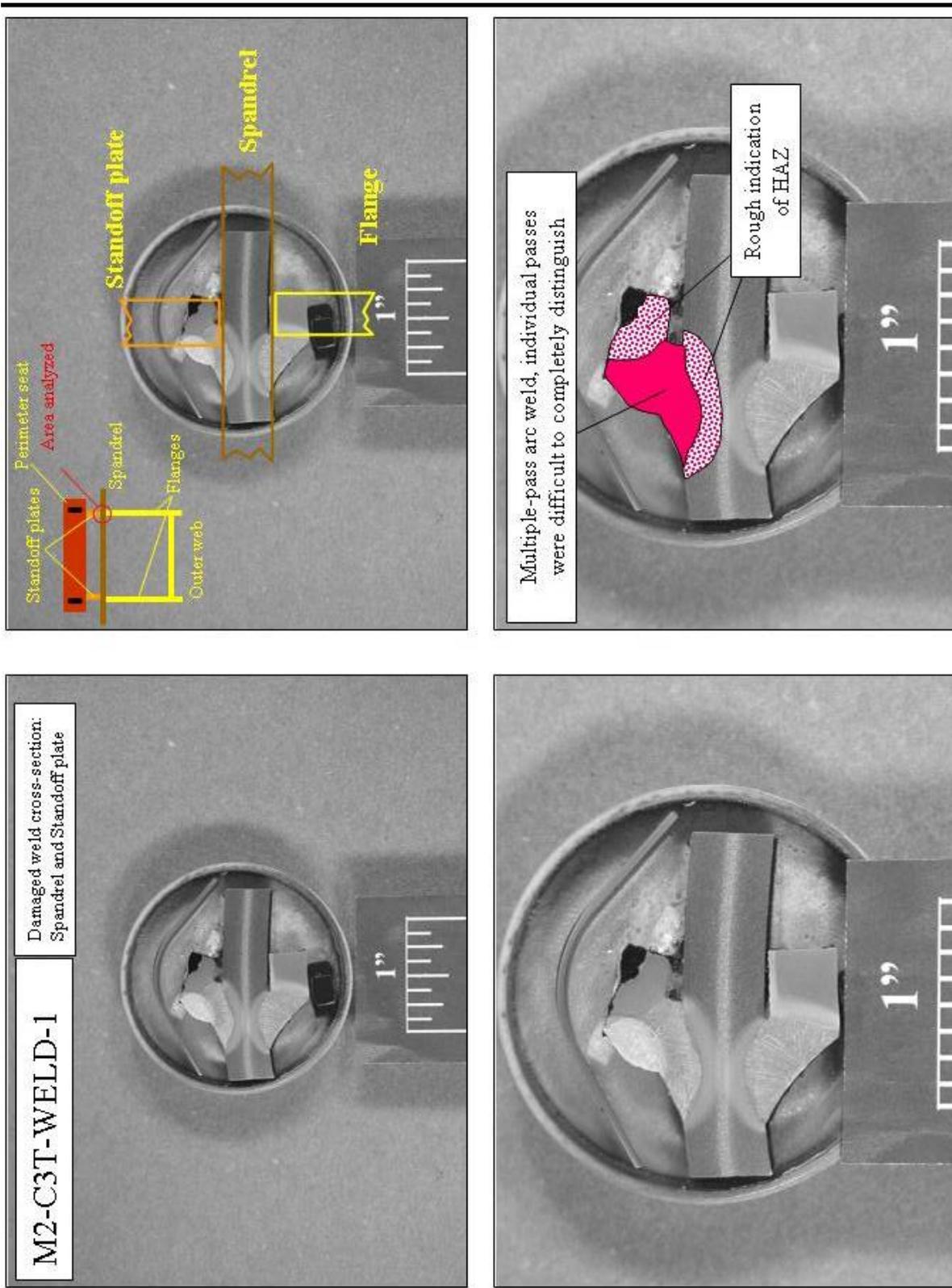
Source: NIST.

Figure 3–53b. Etched cross-section of fracture near weld between spandrel plate (36 ksi) and standoff plate (42 ksi). Sample was from panel M-2 (A130: 96-99, column 129, 99th floor). Two percent nital and 4 percent picral etch (cont.).
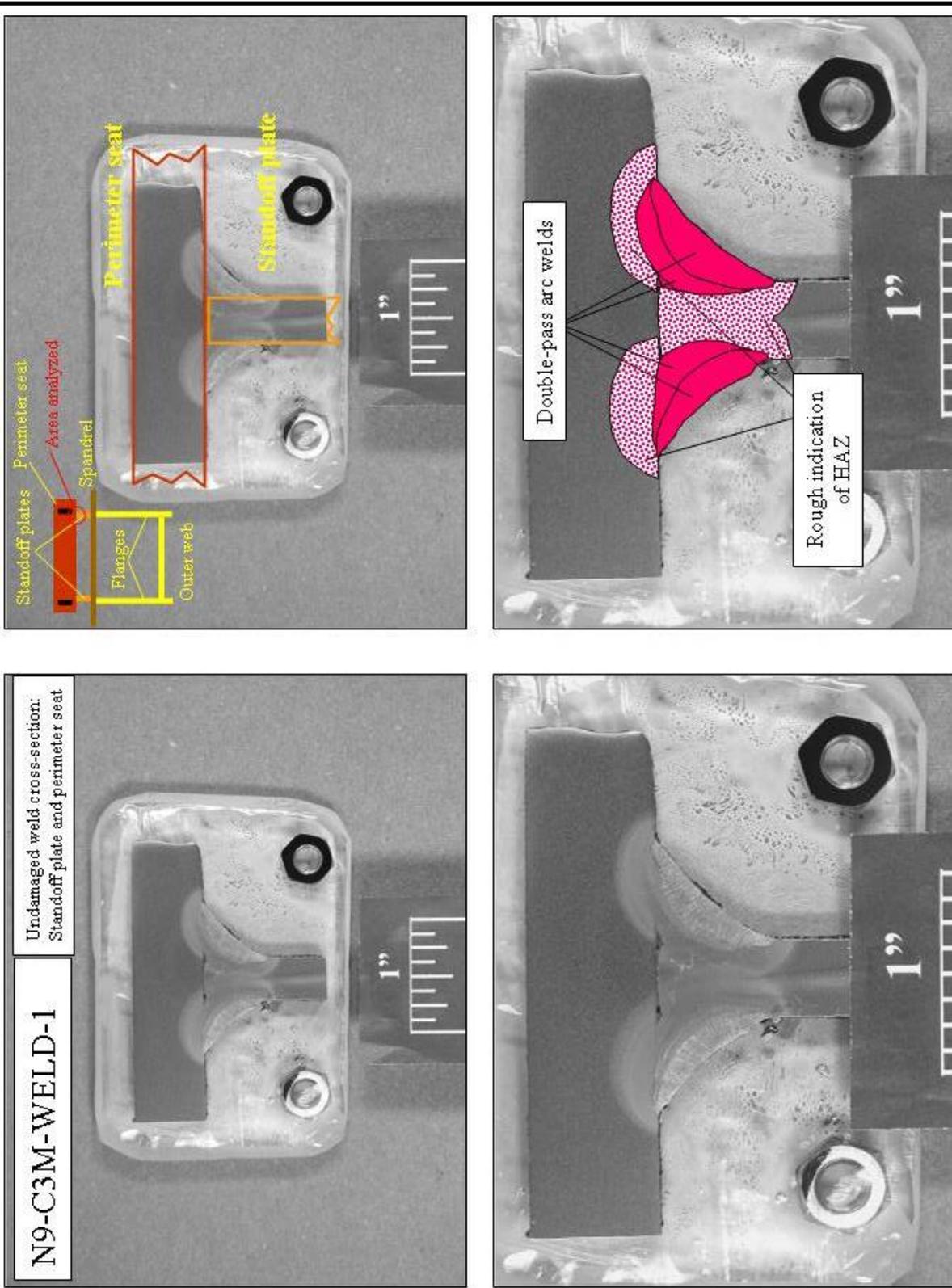
Figure 3–54a. Etched cross-section of intact weld between a standoff plate and truss seat. Sample was from panel N-9 (A154: 101-104, column 153, 103rd floor). Two percent nital and 4 percent picral etch.
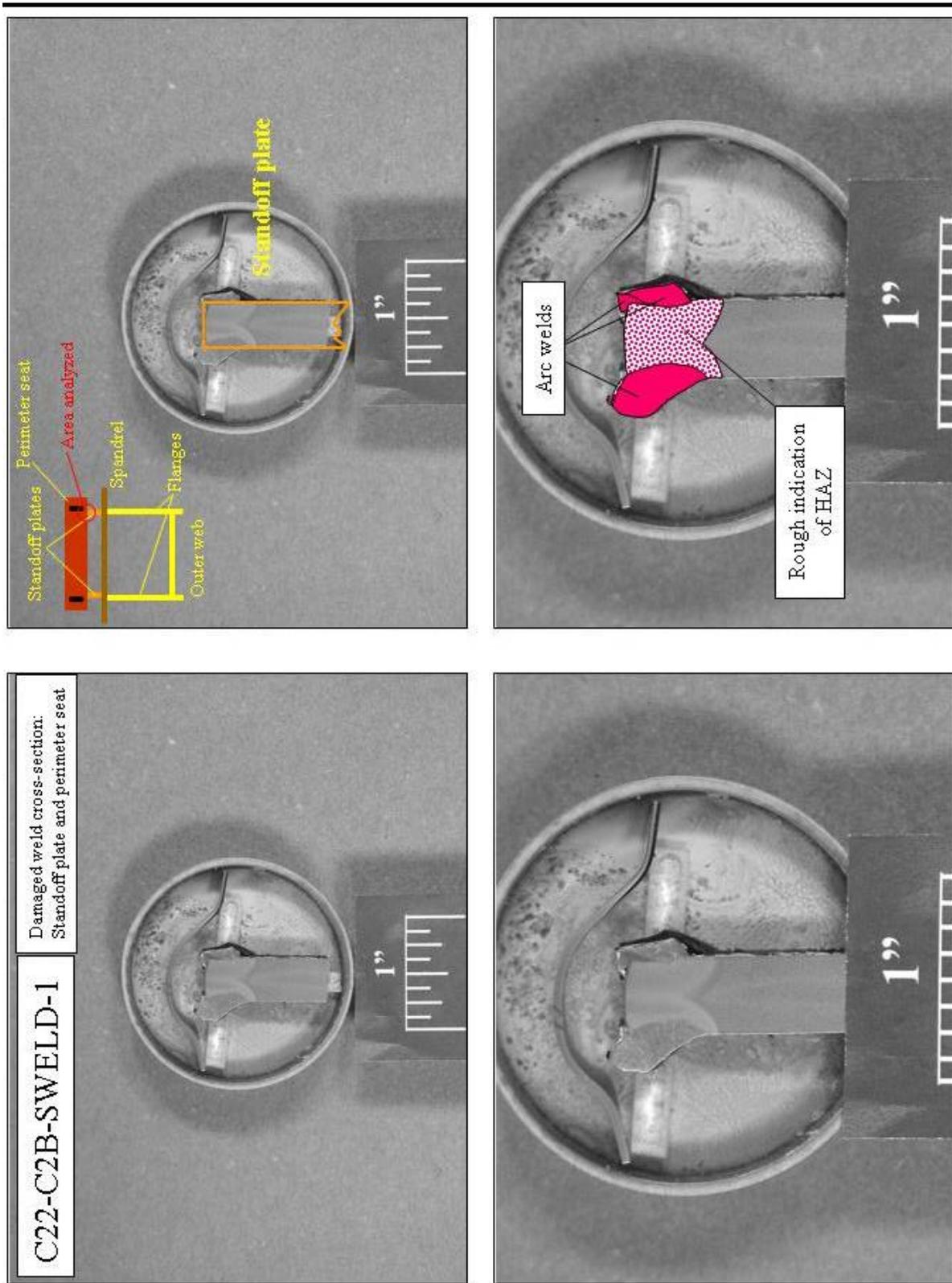
Figure 3–54b. Etched cross-section of fracture near weld between standoff plate and truss seat. Sample was from panel C-22 (A157: 93-96, column 156, 94th floor). Two percent nital and 4 percent picral etch.

Table 3–1. Statistical data of damage and failure modes for recovered exterior columns. Unless otherwise noted, values are in percentages of observations.

Panel Description	Panels Considered	Number of Observations	Gross deformation of column			Weld ruptures			Severing of column			
			Crushed	Punctured	Buckling	Localized	Extensive	Splaid column	At stiffener	Away from stiffener	At floor level	Flame cut
WTC 1	All panels	60	55	42	75	88	60	22	27	12	3	12
WTC1 panels in impact region	Panels in impact region	13	69	62	85	92	62	38	23	0	8	0
	Panels outside of impact region	47	51	36	72	87	60	17	28	15	2	15
WTC 1 panels exposed to fire	Panels exposed to fire	36	56	53	92	92	61	28	39	6	3	6
	Panels not exposed to fire	24	54	25	50	83	58	13	8	21	4	21
	Columns exposed to fire	30	53	57	97	93	63	23	37	7	0	0
	Columns not exposed to fire	30	57	27	53	83	57	20	17	17	7	23
WTC 1 panels separated by floor	Panels above 95th floor	35	49	43	83	89	60	20	26	11	3	9
	Panels at and below 95th floor	25	64	40	64	88	60	24	28	12	4	16
WTC 2	All panels	29	54	39	82	93	89	46	43	18	0	4
WTC 2 panels separated by floor	Panels above 78th floor	20	60	40	85	100	90	45	55	10	0	5
	Panels at and below 78th floor	9	38	38	75	75	88	50	13	38	0	0
Unidentified panels	All panels	56	16	21	14	18	18	36	15	29	0	9

Table 3–2. Spandrel connection details for recovered and identified panels.

Detail Number	Number of Observations		Bolts, A325			Splice Plate (F_y 36)		
	Identified panels	Un-identified panels	Number in row	Size (in)	Number of rows	Width (in)	Thickness (in)	Length (in)
101	67	24	6	7/8	1	6-3/4	1/4	49
102	26	7	8	7/8	1	6-3/4	1/4	49
103	5	3	10	7/8	1	6-3/4	1/4	49
112	5	1	16	7/8	2	12-3/4	1/4	49
122	3	1	8	1-1/8	1	8-3/4	3/8	49
123	2	6	10	1-1/8	1	8-3/4	3/8	49
124	3	5	12	1-1/8	1	8-3/4	3/8	49
131	3	0	16	1-1/8	2	14-3/4	3/8	49
222	0	1	12	1-1/8	1	8-3/4	3/8	61
401	1	0	11	1-1/8	1	8-3/4	3/8	96
412	1	0	13	1-1/8	1	8-3/4	3/8	96
414	2	0	17	1-1/8	1	8-3/4	3/8	96

Table 3–3. Statistical data of damage and failure modes for recovered spandrel connections. Unless otherwise noted, values are in percentages of observations.

Panel Description	Panels Considered	Number of Observations	Type 1	Type 2	Type 3	Type 4	Type 5
WTC 1	All panels	82	52	0	12	36	0
WTC1 panels in impact region	Panels in impact region	21	48	0	19	33	0
	Panels outside of impact region	61	54	0	10	36	0
WTC 1 panels exposed to fire	Panels exposed to fire	48	50	0	12	38	0
	Panels not exposed to fire	34	56	0	12	32	0
	Spandrels exposed to fire	19	47	0	11	42	0
	Spandrels not exposed to fire	63	54	0	13	33	0
WTC 1 panels separated by floor	Panels above 95th floor	47	64	0	13	23	0
	Panels at and below 95th floor	35	37	0	11	52	0
WTC 2[a]	All panels	34	35[a]	18	15	29	3
WTC 2 panels separated by floor	Panels above 78th floor	22	50	0	14	36	0
	Panels at and below 78th floor	12	8	50	17	17	8
Unidentified Panels	All panels	92	42	3	22	32	1

a. Spandrel connection between M-10a and M-10b located at the 48th floor is still connected and not counted.

Table 3–4. Column splice details for recovered and identified panels.

Splice Detail	Number of Observations	Butt Plate Thickness (in)	Inner Fillet Weld #11 (in)	Bolts				Additional Comments
				Number	Size (in)	Grade	Gage (in)	
101	9	1-3/8	5/16	4	7/8	A 325	3-1/2	Mechanical floor splice, field welded
102	1	1-3/8	5/16	4	7/8	A 325	2-1/2	Mechanical floor splice, field welded
103	1	1-3/8	5/16	4	7/8	A 325	1-1/2	Mechanical floor splice, field welded
411	75	1-3/8	5/16	4	7/8	A 325	3-1/2	
421	26	1-5/8	3/8	4	7/8	A 325	3-1/2	
431	6	1-7/8	7/16	4	1	A 325	3-1/2	
432	3	1-7/8	7/16	4	1	A 325	2-1/2	
441	1	2-1/8	1/2	4	1-1/8	A 325	3-1/2	
442	1	2-1/8	1/2	4	1-1/8	A 325	2-1/2	
491	4	2-3/8	11/16	4	1-1/8	A 490	3-1/2	Floor at splice: 68th
682	4	2-5/8	13/16	6	1	A 490	2-1/2	Floor at splice: 12th and 15th

Table 3–5. Statistical data of damage and failure modes for recovered column connections. Unless otherwise noted, values are in percentages of observations.

Panels Considered	Number of observations	Type 1	Type 2	Type 3
All Panels	131	89	4	7
All panels, non-mechanical floors	120	95	5	0
Panels from WTC 1[a]	91	96	4	0
Panels from WTC 2	40	73	5	23
Panels from WTC 2, non mechanical floors	29	93	7	0
Panels from WTC 2, mechanical floors only	11	18	0	82
Unidentified Panels	51	94	4	2

a. No mechanical floors were recovered from WTC 1.
Note: Unless otherwise noted, values are in percentages of observations.

Table 3–6. Exterior wall seat details observed on recovered and identified panels.

Exterior Wall Seat Detail Number	Number of Observations	NIST Type	Seat					Standoff Plate		Gusset plate			
			Piece A	Horizontal length (in)	Thickness (in)	Distance between centerline of holes (in)	Distance between floor level and seat (in)	Vertical length (in)	Thickness (in)	Dimensions (in)	Thickness (in)	Distance between floor level and plate (in)	Optional stiffener (in)
1111	14	Type A	L 4 x 4	16	1/2	9	8-1/2	8	5/16	na	na	na	na
1113	1	Type A	L 6 x 4	16	3/8	9	10	8	3/8	na	na	na	na
1212	11	Type A	L 6 x 4	16	3/8	3-1/4	8-3/4	8	3/8	na	na	na	na
1311	8	Type A	L 4 x 4	16	1/2	10-1/2	8-1/2	8	5/16	na	na	na	na
1313	2	Type A	L 4 x 4	16	1/2	3-1/4	8-1/2	8	5/16	na	na	na	na
1411	46	Type A	L 6 x 4	16	5/8	10-1/2	8-1/2	9	3/8	na	na	na	na
1511	3	Type A	L 6 x 4	16	5/8	10-1/2	8-1/2	10	3/8	na	na	na	na
1611	2	Type A	L 6 x 4	16	3/4	10-1/2	8-1/2	11	3/8	na	na	na	na
2110	1	Type A	L 6 x 4	16	5/8	8-1/2	14-5/8	9	3/8	na	na	na	na
2310	1	Type A	L 6 x 4	16	5/8	10-1/2	14-5/8	9	3/8	na	na	na	na
2410	2	Type A	L 6 x 4	16	5/8	10-1/2	14-5/8	10	3/8	na	na	na	na
2610	1	Type A	L 7 x 4	16	3/4	10-1/4	14-5/8	12	3/8	na	na	na	na
4120	1	Type A	P 9X	16	1/2	5-1/2	18-1/2	9	3/8	na	na	na	na
4424	2	Type A	P 11x	19	7/8	2-3/4	22-3/4	17	3/8	na	na	na	na
5010	7	Type B/Type C	na	na	na	na	na	na	na	8 x 5	3/8	8-7/8	5/16
5110	37	Type C/Type D	na	na	na	na	na	na	na	14 x 4	3/8	4	5/16
5210	48	Type C/Type D	na	na	na	na	na	na	na	14 x 4	3/8	4	5/16
5510	3	Type B	na	na	na	na	na	na	na	8 x 5	3/8	8-7/8	5/16
6220	1	Type C	na	na	na	na	na	na	na	14 x 4	3/8	13-9/16	5/16
7010	1	Type A	4 x 6	9	5/8	2-1/4	13-9/16	na	na	na	na	na	na
7494	1	Type A	8 x 6	16	7/8	3-1/2	23-3/4	na	na	na	na	na	na

Table 3–7. Statistical data of damage and failure modes for recovered Type A connections (1 of 3).

Panel Category	Panel Category	Number of Observations Of Type A Connectors	Description of Gusset Plate Welded to Top Chord and Column			
			Partial remains, rip away from weld	Fracture in plate at toe of weld	Fracture in spandrel at toe of weld	No evidence of gusset plate
WTC 1	All panels	66	47	29	23	2
WTC1 panels in impact region	Panels in impact region	15	53	33	13	0
	Panels outside of impact region	51	45	27	25	2
WTC 1 panels exposed to fire	Panels exposed to fire	40	50	30	20	0
	Panels not exposed to fire	26	42	27	27	4
	Connectors exposed to fire	18	56	33	11	0
	Connectors not exposed to fire	48	44	27	27	2
WTC 1 panels separated by floor	Panels above 95th floor	38	58	24	18	0
	Panels at and below 95th floor	28	32	36	29	4
WTC 2	All panels	28	64	11	21	4
WTC 2 panels separated by floor	Panels above 78th floor	20	70	5	25	0
	Panels at and below 78th floor	8	50	25	13	13
Unidentified Panels	All panels	35	63	17	17	3

Note: Unless otherwise noted, values are in percentages of observations.

Table 3–7. Statistical data of damage and failure modes for recovered Type A connections (2 of 3).

Panel Category	Panel Category	Number of Observations Of Type A Connectors	Description of Seat						Description of bolt holes in seat				
			Intact, relatively undeformed	Intact, bent upwards	Intact, bent downwards	Intact, bent inwards	Seat missing, both standoff plates remain	Seat missing, one or both standoff plates missing	Number of seats remaining	Both intact	Both torn	Half and half	# of bolts remaining
WTC 1	All panels	66	23	9	27	8	11	23	44	39	16	45	35
WTC1 panels in impact region	Panels in impact region	15	13	0	27	27	7	27	10	30	10	60	7
	Panels outside of impact region	51	25	12	27	2	12	22	34	41	18	41	28
WTC 1 panels exposed to fire	Panels exposed to fire	40	18	3	35	10	13	23	26	31	15	54	16
	Panels not exposed to fire	26	31	19	15	4	8	23	18	50	17	33	19
	Connectors exposed to fire	18	17	5	28	11	17	22	11	27	27	45	6
	Connectors not exposed to fire	48	25	10	27	6	8	23	33	42	12	45	29
WTC 1 panels separated by floor	Panels above 95th floor	38	37	16	21	11	5	11	32	41	16	44	34
	Panels at and below 95th floor	28	4	0	36	4	18	39	12	33	17	50	1
WTC 2	All panels	28	25	7	29	4	14	21	18	50	28	22	8
WTC 2 panels separated by floor	Panels above 78th floor	20	35	5	30	5	10	15	15	53	27	20	8
	Panels at and below 78th floor	8	0	13	25	0	25	38	3	33	33	33	0
Unidentified Panels	All panels	35	29	31	6	0	11	40	14	50	14	36	9

Note: Unless otherwise noted, values are in percentages of observations.

Table 3–7. Statistical data of damage and failure modes for recovered Type A connections (3 of 3).

Panel Description	Panels Considered	Number of Observations Of Type A Connectors	Description of damper unit				
			Intact, bent upward	Intact, bent downward	Partial remains, rip away from weld	Fracture in plate at toe of weld	No evidence of plate for damper unit
WTC 1	All panels	66	21	12	2	61	5
WTC1 panels in impact region	Panels in impact region	15	33	7	7	53	0
	Panels outside of impact region	51	18	14	0	63	6
WTC 1 panels exposed to fire	Panels exposed to fire	40	15	13	3	65	5
	Panels not exposed to fire	26	31	12	0	54	4
	Connectors exposed to fire	18	0	11	6	83	0
	Connectors not exposed to fire	48	29	13	0	52	6
WTC 1 panels separated by floor	Panels above 95th floor	38	37	11	3	50	0
	Panels at and below 95th floor	28	0	14	0	75	11
WTC 2	All panels	28	29	18	4	39	11
WTC 2 panels separated by floor	Panels above 78th floor	20	40	15	0	35	10
	Panels at and below 78th floor	8	0	25	13	50	13
Unidentified Panels	All panels	35	20	6	3	54	17

Note: Unless otherwise noted, values are in percentages of observations.

Table 3–8. Statistical data of damage and failure modes for recovered Type C connections.

Panel Description	Panels Considered	Number of Observations Of Type C Connectors	Description of Gusset Plate			
			Intact, bent upward	Intact, bent downward	Partial remain, fracture in plate	Fracture in plate at toe of weld
WTC 1	All panels	57	18	18	9	56
WTC1 panels in impact region	Panels in impact region	18	28	17	0	56
	Panels outside of impact region	39	13	18	13	56
WTC 1 panels exposed to fire	Panels exposed to fire	36	19	19	8	53
	Panels not exposed to fire	21	14	14	10	62
	Connectors exposed to fire	16	13	13	19	56
	Connectors not exposed to fire	41	20	20	5	56
WTC 1 panels separated by floor	Panels above 95th floor	34	26	12	0	62
	Panels at and below 95th floor	23	4	26	22	48
WTC 2	All panels	18	17	44	0	39
WTC 2 panels separated by floor	Panels above 78th floor	12	25	17	0	58
	Panels at and below 78th floor	6	0	100	0	0
Unidentified panels	All panels	30	10	3	0	87

Note: Unless otherwise noted, values are in percentages of observations.

Table 3–9. Statistical data of damage and failure modes for recovered Type B connections.

Panel Description	Panels Considered	Number of Observations Of Type B Connectors	Description of Gusset Plate Welded to Top Chord and Column			Description of Support				
			Partial remains, fracture away from weld	Fracture in plate at toe of weld	Fracture in spandrel at toe of weld	Intact, relatively undeformed	Intact, bent upwards	Intact, bent downwards	Intact, bent inwards	Support missing
WTC 1	All panels	4	50	0	50	25	0	75	0	0
WTC1 panels in impact region	Panels in impact region	0	0	0	0	0	0	0	0	0
	Panels outside of impact region	4	50	0	50	25	0	75	0	0
WTC 1 panels exposed to fire	Panels exposed to fire	1	100	0	0	100	0	0	0	0
	Panels not exposed to fire	3	33	0	67	0	0	100	0	0
	Connectors exposed to fire	1	100	0	0	100	0	0	0	0
	Connectors not exposed to fire	3	33	0	67	0	0	100	0	0
WTC 1 panels separated by floor	Panels above 95th floor	1	100	0	0	100	0	0	0	0
	Panels at and below 95th floor	3	33	0	67	0	0	100	0	0
WTC 2	All panels	5	40	40	20	60	0	20	0	20
WTC 2 panels separated by floor	Panels above 78th floor	2	50	0	50	50	0	50	0	0
	Panels at and below 78th floor	3	33	67	0	67	0	0	0	33
Unidentified panels	All panels	0	0	0	0	0	0	0	0	0

Note: Unless otherwise noted, values are in percentages of observations.

Table 3–10. Statistical data of damage and failure modes for recovered Type D connections.

Panel Description	Panels Considered	Number of Observations Of Type D Connectors	Description of Diagonal Bracing Straps		
			Remains of both, fracture in strap	Half and half	Both fractures in strap at toe of weld
WTC 1	All panels	10	50	30	20
WTC1 panels in impact region	Panels in impact region	0	0	0	0
	Panels outside of impact region	10	50	30	20
WTC 1 panels exposed to fire	Panels exposed to fire	5	60	20	20
	Panels not exposed to fire	5	40	40	20
	Connectors exposed to fire	4	50	25	25
	Connectors not exposed to fire	6	50	33	17
WTC 1 panels separated by floor	Panels above 95th floor	1	0	0	100
	Panels at and below 95th floor	9	56	33	11
WTC 2	All panels	3	0	33	67
WTC 2 panels separated by floor	Panels above 78th floor	3	0	33	67
	Panels at and below 78th floor	0	0	0	0
Unidentified panels	All panels	0	0	0	0

Note: Unless otherwise noted, values are in percentages of observations.

Chapter 4
PHYSICAL DAMAGE OF CORE ELEMENTS (COLUMNS AND CHANNELS)

This chapter of the report covers the physical damage and failure modes observed on the recovered core columns and channel elements used to connect the floor trusses to the core. The damage may have been a result of any one of the extreme loading conditions mentioned above (aircraft impact, the concomitant fires, the ensuing collapse of the buildings, or the subsequent handling related to the recovery efforts). While in some cases the origin of damage may be evident, there may be cases in which the event that caused the damage to occur may be difficult or impossible to resolve.

4.1   CORE COLUMNS

There were 55 wide flange and built-up box beam elements recovered (NIST NCSTAR 1-3B). Of these, 12 columns were unambiguously identified as core columns with their as-built location known, 12 wide flange sections were found to have markings that were not interpretable, and 31 columns were without any markings at all. Due to the ambiguous nature of the last two groups, only the first group of samples were analyzed.

Table 4–1 displays the 12 identified core columns, their as-built locations, and the possible conditions to which they may have been exposed prior to the collapse of the buildings. Due to the small number of samples, statistical data of the various damage features and failure modes would be irrelevant. Therefore, in depth descriptions of the four significant pieces (C-80, C-88a, C-88b, and HH) that were located within the fire zone floors were made. For reference, Figs. 1–7 and 1–8 display the horizontal and vertical positioning of the recovered core columns within the buildings with respect to the location of the perimeter panel damage as a result of the impacts for World Trade Center (WTC) 1 and WTC 2, respectively.

In the two buildings, there were 329 core columns, each three stories tall, traversing floors involved in the impact and pre-collapse fires. NIST has portions of four of these columns, which represents about 1 percent of all core columns intersecting floors with damage from the impact or fires. Thus, while these pieces allow for some assessment of damage, the following forensic analysis does not, and cannot, give a full and accurate picture of the type and amount of damage sustained by the vast majority of core columns.

4.1.1   Core Columns Located in Impact Region

Sample C-80 (Fig. 4–1a), from WTC 1, was a 36 ksi wide flange, located in the middle of the second row of core columns along the north face. Only the lower third of the column was recovered (approximately 13 ft). The location of the column line in the core would place it squarely in the path of the airplane (Fig. 1–7), however, its elevation within the building (ending just below the 93rd floor) may indicate that it did not sustain impact damage. Different failure modes were observed for each end (Fig. 4–1b and 4–1c). Bolt fracture occurred at the lower portion of the column (92nd floor region), while the upper portion was torn through the material (near the 93rd floor region). No visible necking (reduction in area)

was observed on the plate in the immediate vicinity of the fracture. Again, as perimeter panel damage in this area occurred in the 95th floor region, damage of this column most likely occurred during collapse of the building. This result was consistent with the aircraft impact damage analysis of the NIST investigation (NIST NCSTAR 1-2A).

Core columns C-88a and C-88b, from WTC 2, were unique among the recovered core elements in that the columns were still connected at the welded column splice, Fig. 4–2. Both columns were 42 ksi built-up box columns with their shared splice in the 80th floor level. The as-built location of C-88a was above that of C-88b. The lower 16 ft of C-88a was recovered (floors 80 through 82), whereas the upper 8 ft of C-88b was still attached (primarily within the 80th floor). The location of the column line, in the middle of the first row on the south face of WTC 2 (Fig. 1–8), would place the columns very close to the direct path of the plane. The failed portion of C-88a shows that the upper part of the column was bent downward near the 81st floor level, Fig. 4–3. The flanges and webs were bent toward the south-southwest direction with the plates ending in fractured surfaces. (The south flange was subsequently separated from the rest of the column during recovery and was labeled "C-88c".) The fracture surfaces were too corroded for a macroscopic inspection, but they were relatively flat with no noticeable necking. The damage characteristics of this column suggest that deformation occurred during collapse of the building. This was based upon (1) the damage (81st floor level) was above the floors of impact in this region (79th floor level), (2) the columns were bent downward indicating overloading of the column from above, and (3) the bending direction of the plates was opposite to the direction of the travel of the plane. This result was consistent with the aircraft impact damage analysis of the NIST investigation (NIST NCSTAR 1-2A).

The failed portion of C-88b was quite different. Both webs and the "south" flange were severely bent to the east and had flame cut ends (prior to arrival at NIST), Fig. 4–4. The bends appeared to occur just below the connector for the channel associated with the 80th floor. The "north" flange had a less significant bend toward the north, with approximately 80 percent of the failed end of the plate as a fracture. There was no visible necking of the plate in the area of failure with the remaining portion of the plate being flame cut (again, prior to arrival at NIST). This flange was fractured roughly 2 ft below the splice in the 80th floor level. The fracture surfaces were not available for analysis as they were significantly corroded. As with the upper portion of C-88a, the bending of the south flange and the webs likely occurred during the collapse of the building as the direction of bending was not consistent with the travel of the airplane. However, the damage to the north flange may have been a result of impact damage, as the severity and location of the plate failure was different than the other three plates of the column and the direction of the bend was consistent with the travel of the airplane. Base case simulations indicated that impact damage would not have occurred to this column, however, another analysis with parameters set to represent a more severe case indicated that the column may have sustained damage (NIST NCSTAR 1-2A).

4.1.2   Core Columns Located in Fire Region

In addition to the three columns discussed above, there was only one other column recovered from within the fire region. This was sample HH from WTC 1, Fig. 4–5. This was a 42 ksi wide flange positioned near the middle of the second row of core columns along the north face. The bottom half of the column was recovered (approximately 16 ft). The location of the column line number in the core would put it directly in the path of the airplane (Fig. 1–7), however, its elevation within the building may have been

high enough (starting within the 98th floor) that it was not damaged during the impact. The failure mode of each end was different (Fig. 4–5a). Fracture of the plates used in the bolted connection occurred at the lower portion of the column (98th floor region), while the upper portion was torn through the material (100th floor region). Additionally, the sample was nearly bent in half (99th floor region) with fracturing of the wide flange taking place. Figure 4–5b shows that the flanges became separated from the web in the region of the bend. As the deformation of this column occurred above the impact damage sustained by the perimeter panels, this separation likely occurred during collapse of the building. This result was consistent with the aircraft impact damage analysis of the NIST investigation (NIST NCSTAR 1-2A).

4.1.3 Other Identified Core Columns

As none of the remaining columns were within the impact or fire floors, no further analysis was conducted as damage was assumed to be a result of the collapse and subsequent handling during the recovery.

4.1.4 Unidentified Core Columns

Due to the unknown location of these columns, and the small overall population of the core columns, no further analysis was conducted.

4.2 CORE CHANNELS AND SEATS

There were 25 pieces of channel material retrieved from the WTC towers. Twenty-four of these pieces had truss seats welded directly to the channel and varied in length between 2 ft and 12 ft. An example of one of these elements can be seen in Fig. 4–6. The other piece, labeled C-124, appears to have been a support for a stairwell, Fig. 4–7, as brackets for the risers and runs were observable. While some markings were observed on a limited number of pieces (Fig. 4–8), the code was ambiguous and the as-built location of the channels could not be determined.

An analysis was conducted to evaluate the failure modes of the channels and the condition of the core seats. Observations concerning these elements can be found in Table 4–2. Of the 24 channels used to support the floor trusses, half of the samples were observed to have both ends fail within the channel itself, Fig. 4–9a, while the other half were observed to have failure at one or both of the end connectors, Fig. 4–9b. Only 21 pieces of channel were found to have seats or remnants of them. As mentioned above, sample C-124 appears to have come from a stairwell, while samples C-97, C-99, and C-105 have no indication that seats were attached to the recovered portions of the channels. From the 21 channels with seats, a total of 31 seats were available for inspection and can be observed in Appendix C. Over 90 percent of the seats were still intact with the majority of these somewhat deformed. Only two seats were observed to be ripped completely from the channel at the welded joint between the seat and the channel, Fig. 4–9c. Half of the retained seats were observed to have both bolt holes still intact, while the other half had a minimum of one bolt hole ripped out.

4.3 SUMMARY

Unlike the exterior panels, relatively few samples of identified core columns were recovered and available for inspection. In addition, photographic evidence indicating their condition prior to collapse

was not available. Further, 25 pieces of core channel material were recovered; however, none of the pieces were able to be identified as to their as-built location. Therefore, analysis of these core elements could only be conducted in their present state without regard to direct visual evidence of damage occurring as a result of the airplane impacts. From this analysis, the following were concluded:

- Two columns of significance were recovered from WTC 1; one was located within the impact floors (C-80, 603A: 92-95), and the other was located within floors exposed to fire (HH, 605A: 98-101). Evidence suggested that damage observed on these pieces occurred during the building collapse and not a result of impact.

- Two columns of significance were recovered from WTC 2; they were both located within the impact floors (C-88a, 801B: 80-83, and C-88b, 801B: 77-80). Evidence suggested that damage found on C-88a was a result of building collapse. However, C-88b may have been damaged directly by the airplane impact.

- Failure of core columns occurred both at the splice connections and fracture of the columns themselves. Of particular note was the unbroken weld splice between core columns C-88a and C-88b.

- Of the 31 core seats recovered, 90 percent were still intact though some had extensive damage. Only two were observed to have been completely torn from the channel.

NIST has documented approximately 1 percent of all core columns intersecting floors with damage from the impact or fire floors. Thus, the preceding forensic analysis does not, and cannot, give a full and accurate picture of the type and amount of impact damage sustained by the vast majority of core columns.

Source: NIST.

Figure 4–1. Core column C-80 (603A: 92-95) located in the impact zone for WTC 1. Damage believed to be due to collapse. a) Overall view of recovered column, b) view of connection in the 92nd floor region, failure as a result of bolt fracture, and c) torn end of column near the 94th floor region.
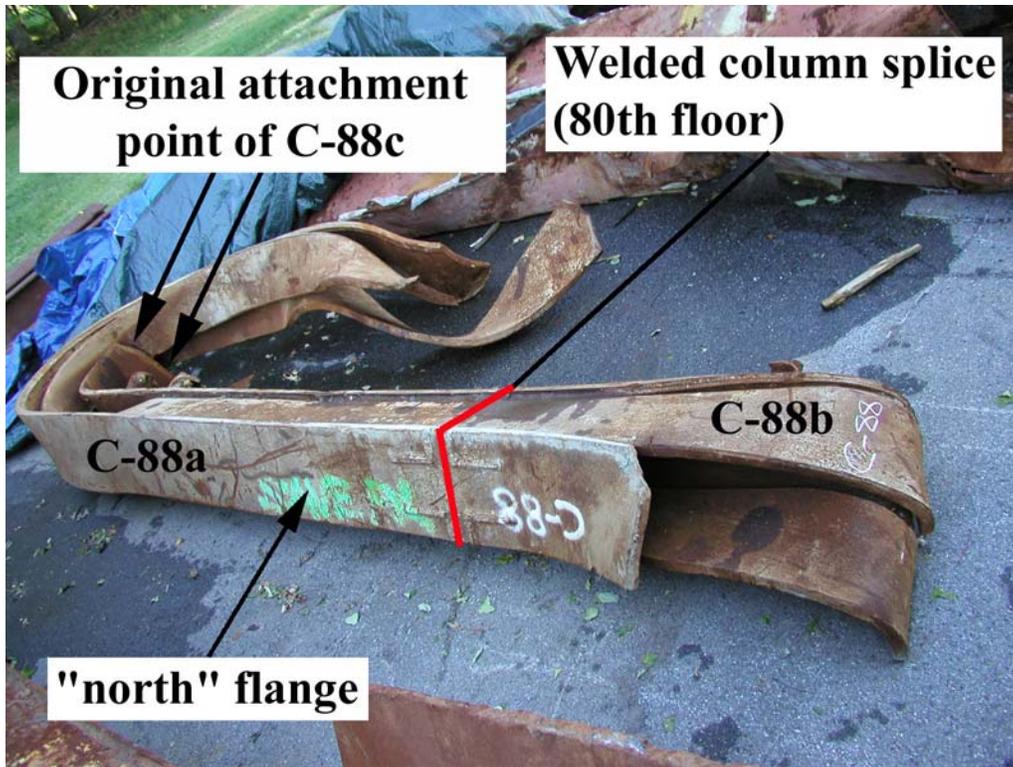
Source: NIST.

Figure 4–2. Overall view of recovered core columns C-88a (801B: 80-83) and C-88b (801B: 77-80) that were located in the impact zone of WTC 2. The north flange of C-88b may have sustained impact damage. Note that the welded column splice was still intact though the airplane may have struck a portion of this column.

Source: NIST.

Figure 4–3. Damage associated with core column C-88a (801B: 80-83) from the impact zone of WTC 2.
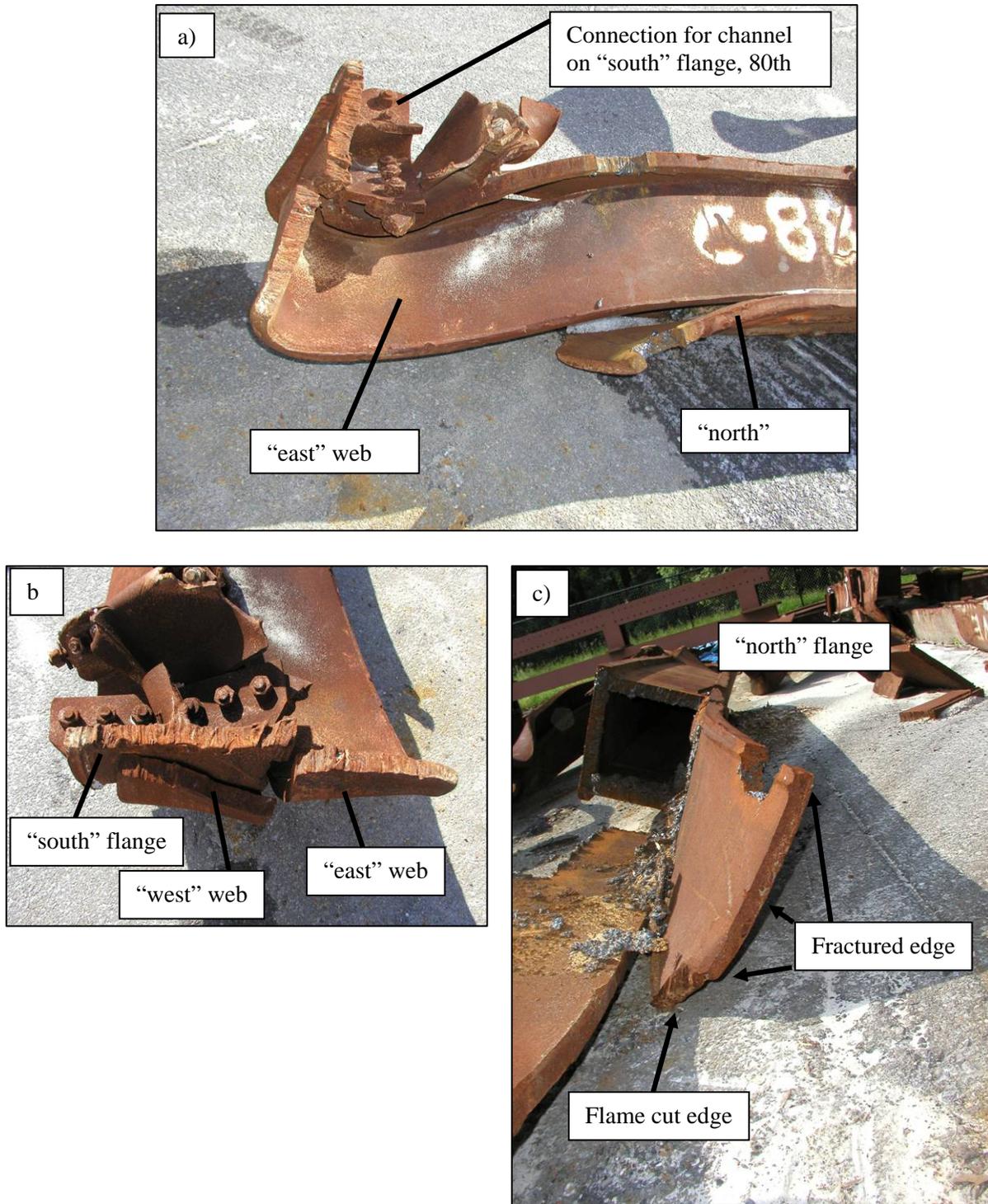
Source: NIST.

Figure 4–4. Damage associated with core column C-88b (801B: 77-80) from the impact zone of WTC 2. a) Overall view of fractured end, b) bottoms of "south" flange and both webs bent toward the east just below the 80th floor level, ends were flame cut prior to arrival at NIST, and c) "north" flange bent toward the north, majority of plate was fractured with some flame cutting (prior to arrival at NIST).
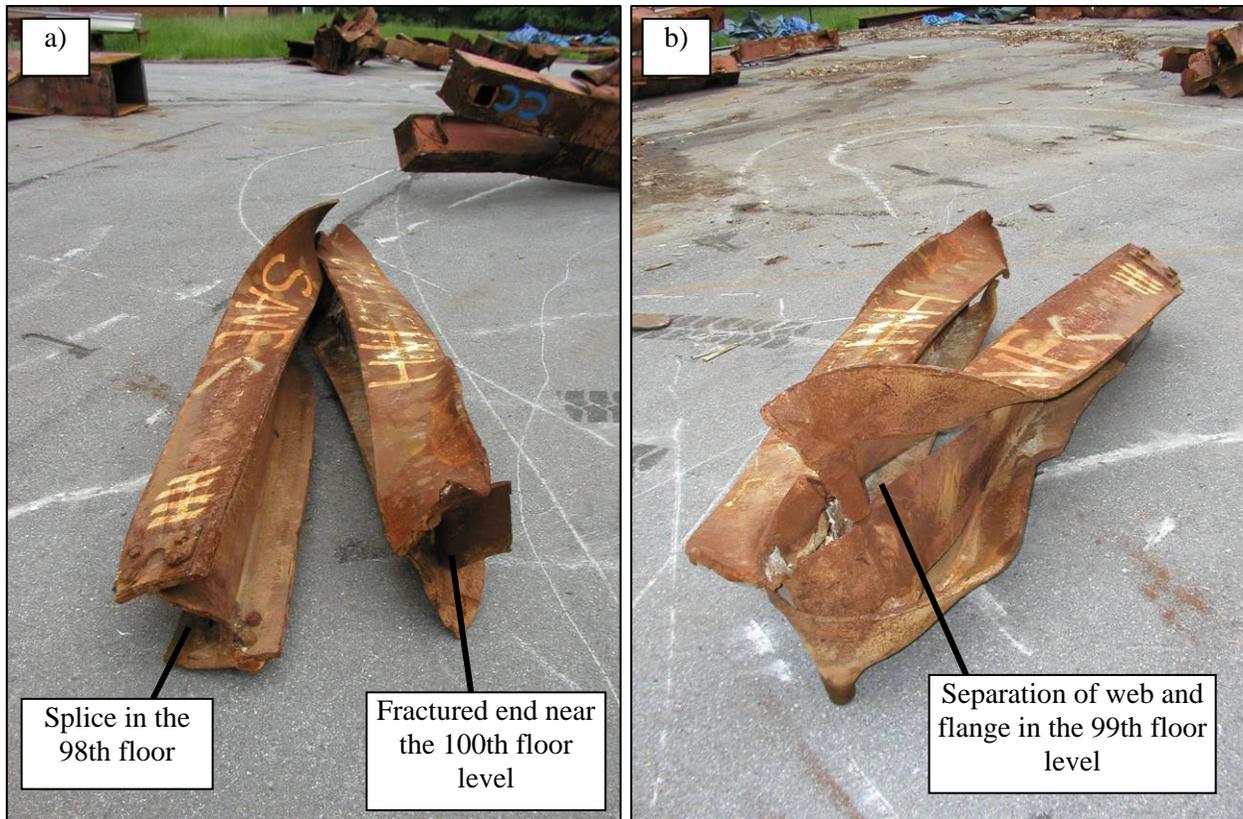
Source: NIST.

Figure 4–5. Core column HH (605A: 98-101) from the fire floors of WTC 1. a) Failure at both ends and b) separation between flange and web in the 99th floor region.

Source: NIST.

Figure 4–6. Example of a recovered core channel. Arrows indicate seats used to attach the floor trusses to the channel (core columns).

Source: NIST.

Figure 4–7. Sample C-124 from the core area, apparently used to support stairs as brackets for runs and riser were observable.

Source: NIST.

**Figure 4–8. Channel with ambiguous code stamped on it.
The stampings read: "35 21 – 35   27   55".**
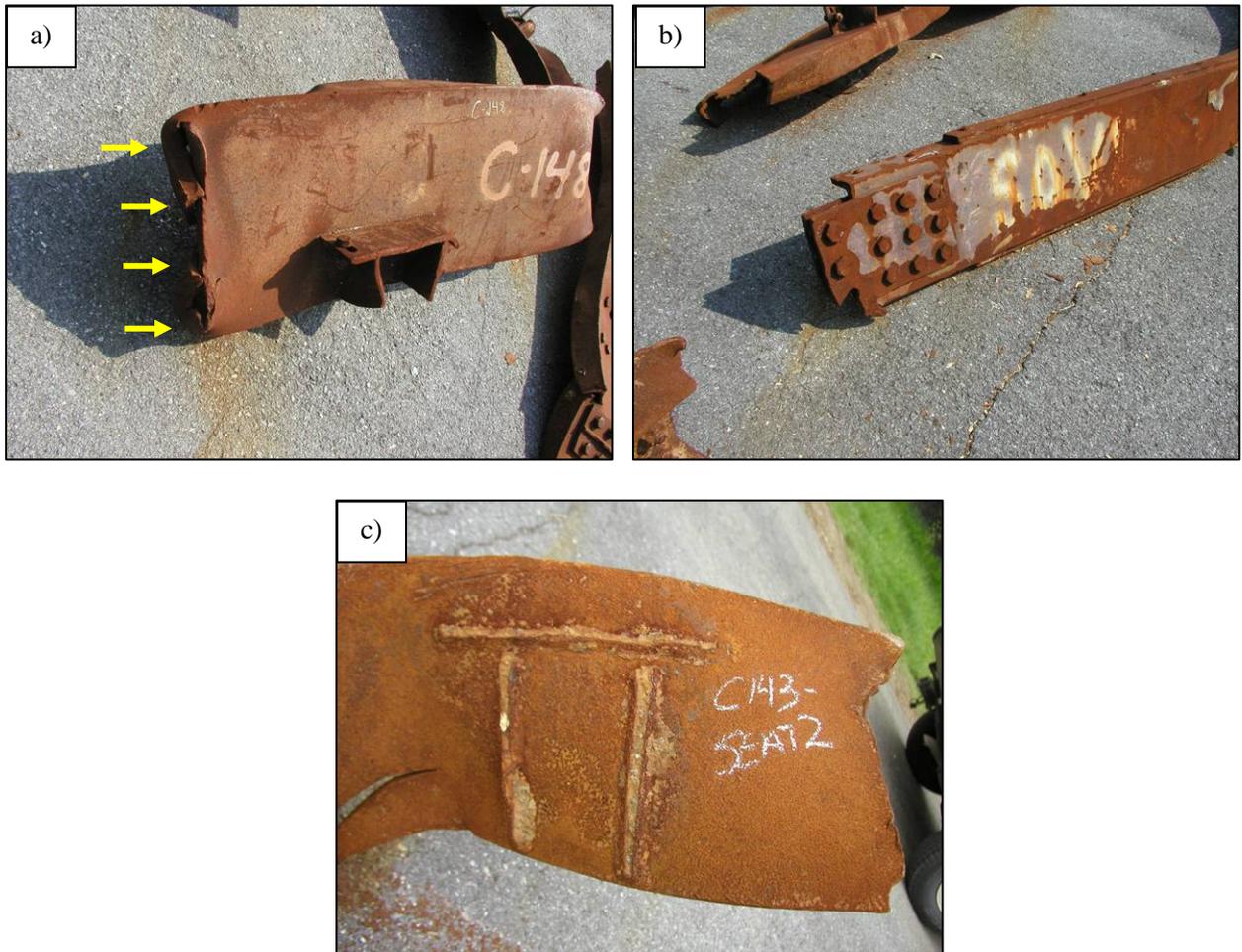
Source: NIST.

Figure 4–9. Failure modes of core channels. a) Fracture through channel as indicated by arrows, b) failure associated with end connector, and c) seat ripped off at welded connection to channel.

Table 4–1. Recovered core columns with known as-built locations, grouped by pre-collapse conditions.

Column Description	Bldg	NIST Name	Brief Description	Column #	Story at Splice Lower	Story at Splice Upper	F_y (ksi)
Core columns within impact region	WTC 1	C-80	Wide flange	603	92	95	36
Core columns within impact region	WTC 2	C-88b	Built-up box beam	801	77	80	42
Core columns within impact region	WTC 2	C-88a	Built-up box beam	801	80	83	42
Core columns within fire exposure zone	WTC 1	HH or S-2	Wide flange	605	98	101	42
Core columns within fire exposure zone	WTC 2	none					
Core columns outside of fire exposure zone	WTC 1	B-6152-2	Built-up box beam	504	33	36	36
Core columns outside of fire exposure zone	WTC 1	B-1011	Built-up box beam	508	51	54	36
Core columns outside of fire exposure zone	WTC 1	B-6152-1	Built-up box beam	803	15	18	36
Core columns outside of fire exposure zone	WTC 1	C-71	Wide flange	904	77	80	36
Core columns outside of fire exposure zone	WTC 1	C-155	Wide flange	904	83	86	36
Core columns outside of fire exposure zone	WTC 1	C-65 or S-8	Wide flange	904	86	89	36
Core columns outside of fire exposure zone	WTC 2	C-90	Built-up box beam	701	12	15	36
Core columns outside of fire exposure zone	WTC 2	C-30 or S-12	Wide flange	1008	104	106	36

Table 4–2. Statistical data of damage and failure modes for recovered channels and core truss seats.

Channel Description				Core Truss Seat Description				Seat hole description			
Number of observations	Failure solely at connections	Connection failure/ channel failure	Failure solely in channel	Number of observations	Intact, undeformed	Intact, deformed	Ripped off at weld	Both intact	Both torn	Half and half	# of bolts remaining
24	4	46	50	31	19	74	7	52	27	21	21

Note: Unless otherwise noted, values are in percentages of observations.

This page intentionally left blank.

Chapter 5
PHYSICAL DAMAGE OF FLOOR TRUSS MATERIAL

5.1   RECOVERED TRUSS MATERIAL

This chapter of the report covers the physical damage observed on the recovered, pre-fabricated floor trusses that spanned the distance between the exterior wall and core columns. Samples received at National Institute of Standards and Technology (NIST) were either very small sections (less than 3 ft to 4 ft in length) of chord and rod material (Fig. 5–1a) or large entangled masses in the form seen in Fig. 5–1b. According to Structural Engineers Association of New York (SEAoNY) volunteer members involved in the recovery effort, it was necessary to "ball up" any truss pieces of significant size to facilitate removal and subsequent handling in the recovery yards. This was required as the primary and bridging trusses for a given floor were welded together into huge grids. During the collapse, these lightweight floor sections were severely damaged and could not be easily removed. Thus, it was unknown when the observed specific damage features occurred. Further, it was likely that sections of multiple trusses were "balled" together rather than labeled samples consisting of just one pre-fabricated truss unit.

Attempts were made to identify the truss material, but unlike most of the other major structural elements, identifying marks could not be found on the trusses to establish their as-built location. Difficulty was also encountered in trying to measure the length of the truss members to determine if they were of the 35 ft or 60 ft variety. It appears that no whole length sections were recovered. A large majority of the compressive resistance welds between the chords and rods were observed to have failed. This was evident from the large amount of chord material recovered without rods attached and vice versa. It was unknown when these failures occurred and what caused them.

A number of floor truss ends (bolted portion of chord material for attaching the trusses to the seats, Fig. 1–6b) were recovered for both upper and lower supports, typically intertwined within the balled sample. The majority of upper chord connectors (Fig. 5–2a) were found to have bolt failures, i.e., the bolt holes on the connectors were still intact. In addition, portions of the gusset plates, welded to the top truss chord in the field after the truss was put into its as-built location, remained (Fig. 5–2b). For the lower chord connections, failure typically involved failure of the bolts associated with the viscoelastic dampers (Figs. 5–2c and 5–2d). Portions of diagonal bracing straps were also found within the truss material, as well as separately. These straps were welded in the field and provided horizontal shear transfer between the floor slab and the exterior wall, as well as out of plane bracing for perimeter columns not directly supporting floor trusses. Typically these straps were found attached to the upper chords and entangled within the piles of twisted steel bars and rods that made up the floor truss.

5.2   SUMMARY

Floor truss material was recovered from the World Trade Center (WTC) towers; however, the as-built location of the elements could not be determined. In addition, due to their light-weight construction, they were easily damaged during events associated with the collapse of the building as well as during the

recovery and subsequent handling phases. Thus, there was no determination of when damage occurred. From the restricted number of samples available, the following general statements were made:

- Failure of the connection between the floor truss and seats was typically a result of bolt failure.

- Failure of a large majority of the compression resistance welds was observed.

Source: NIST.

Figure 5–1. Examples of recovered floor truss material. a) Small sections of rod and chord (sample C-53) and b) "balled-up" sections of rod and chord. (C-137f).
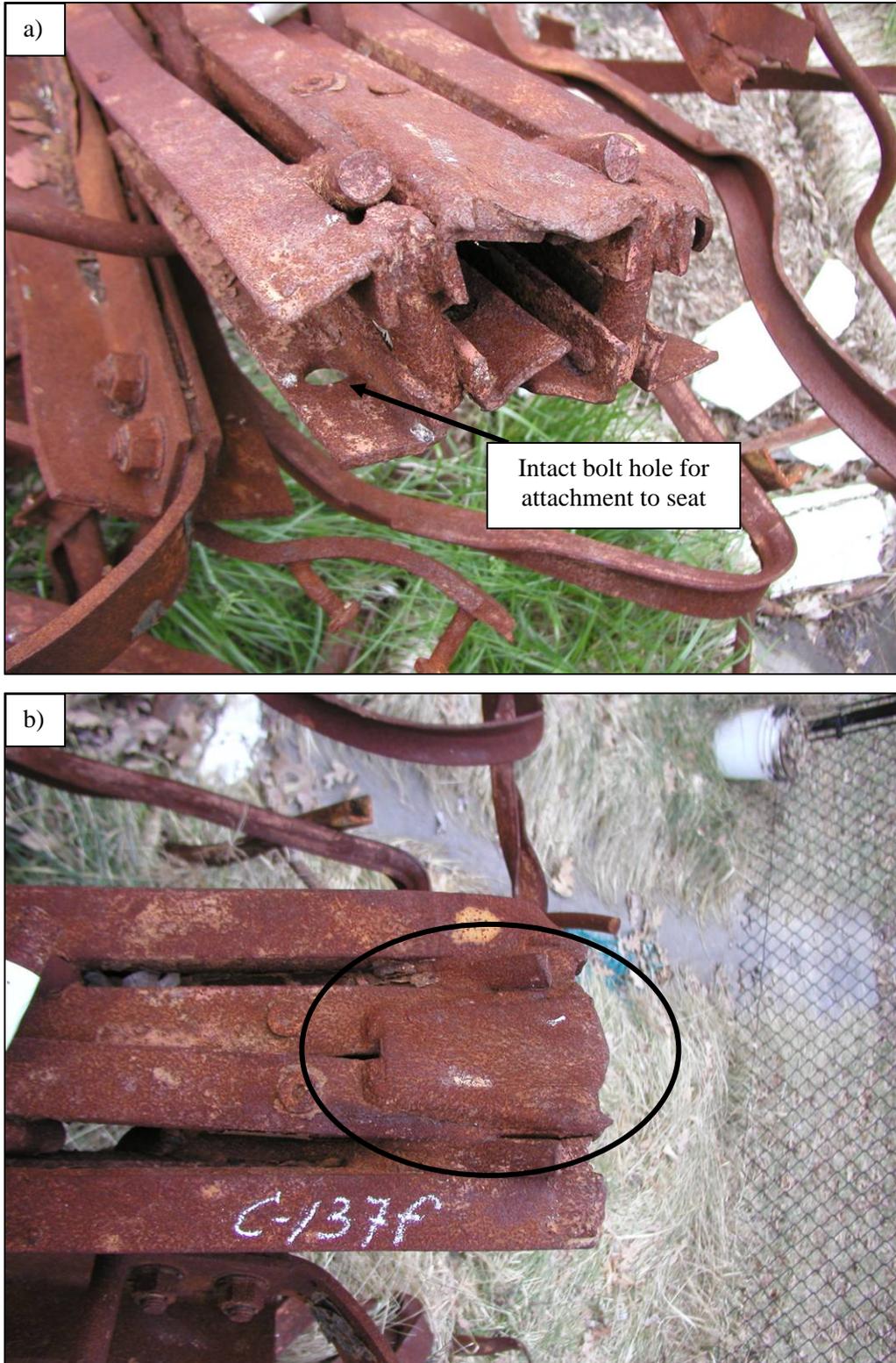
Source: NIST.

Figure 5–2. Recovered floor truss connectors from sample C-137f. a) Upper support and b) remnants of gusset plate (as indicated) welded to top chord of truss during construction.
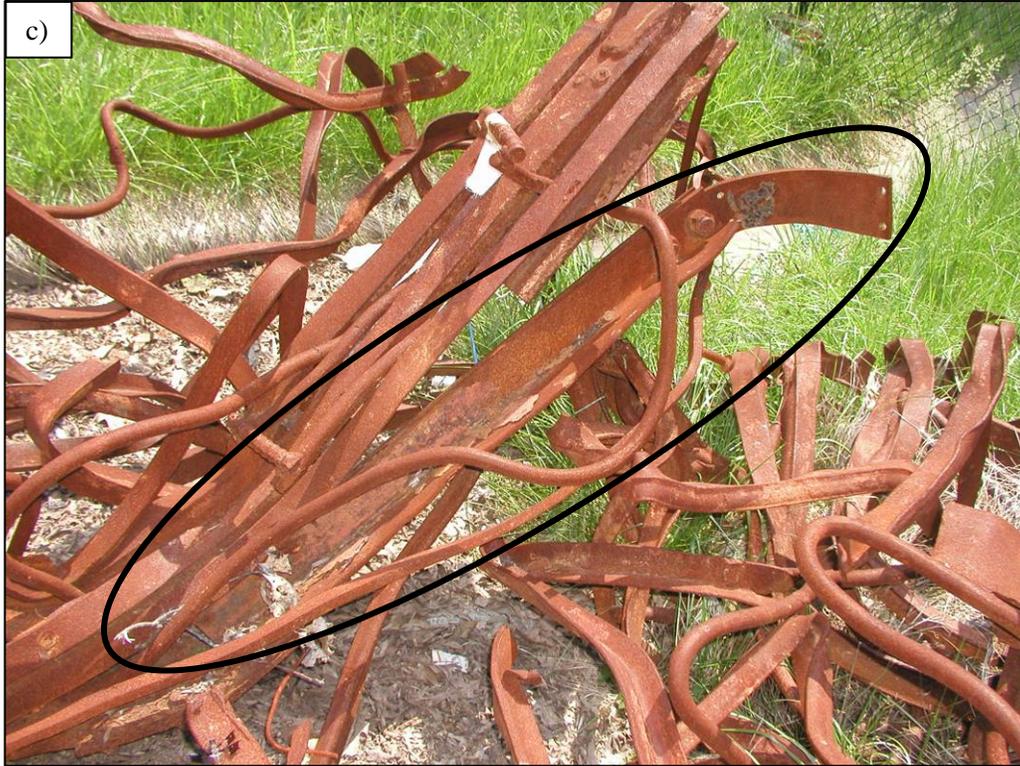
Source: NIST.

Figure 5–2. Recovered floor truss connectors. c) lower support with attached remnant of viscoelastic damper (as indicated) and d) close-up of remnants of viscoelastic damper showing intact bolt holes (indicating bolt failure) (cont.).

This page intentionally left blank.

Chapter 6
FIRE EXPOSURE OF THE STRUCTURAL ELEMENTS

Examination of the structural steel components for indications of fire damage was an important aspect of this investigation. This chapter of the report attempts to (1) determine the temperature excursions experienced by the steel components, (2) determine when the excursion occurred (pre- or post-collapse), (3) determine if pre-collapse fires significantly affected the mechanical properties of the structural elements such that the structural integrity (load bearing capabilities) of the component may have been compromised, and (4) provide this information for input/validation of the fire and thermal models of the project entitled "Reconstruction of Thermal and Tenability Environment" (NIST NCSTAR 1-5). Analytical techniques used to meet these tasks involved assessment of the present condition of the primer paint and metallurgical evaluation of the recovered structural steel elements.

6.1 BACKGROUND OF FIRE EXPOSURE STUDY

In addition to structural damage incurred by the World Trade Center (WTC) towers as a result of the airplane strikes, fires initiated soon after the impacts and continued up to the collapse of both towers (103 min for WTC 1 and 56 min for WTC 2). The location of the fires was not contained to the impact area, as fuel from the airplanes was dispersed inside the buildings, igniting the office contents of numerous floors. In the project entitled "Reconstruction of Thermal and Tenability Environment" (NIST NCSTAR 1-5A), a detailed time line for the growth and spread of fires for both buildings was constructed. Fires were observed on floors 92 through 100 and the 104th floor of WTC 1 and floors 78 through 83 of WTC 2. This information was subsequently used in Sec. 2.3 of this report, where the recovered perimeter panels were correlated with the pre-collapse environmental conditions. Sixteen panels recovered from WTC 1 were known to have been exposed to fire prior to collapse, with 13 of them having recovered portions exposed to pre-collapse fires (Table 2–5 and Fig. 2–48). No similar panels were recovered for WTC 2. As conditions within the building core could not be determined from the photographic database, it was unknown what environment the recovered core columns may have experienced. However, all four core columns discussed in Sec. 4.1 (C-80, C-88a, C-88b, and HH) had as-built locations within the fire affected floors.

In the two buildings, there were 1,950 perimeter columns and 329 core columns traversing floors involved in pre-collapse fires. NIST has portions of 54 of the perimeter columns and four of the core columns, which represents about 3 percent and 1 percent, respectively, of the columns intersecting floors with pre-collapse fires. Thus, while these pieces allow some comparison of metal and paint condition with the predications of the fire model, the following forensic analysis does not, and cannot, give a picture of temperatures seen by the vast majority of perimeter and core columns.

A number of methods were available to assess fire exposure and its effects on the steel, ranging from non-destructive evaluation (e.g., visual observations and measurements of the pieces, surface hardness) to destructive testing (e.g., residual stress measurements, metallographic analysis, chemical and physical analyses). Some of these methods are reviewed in Tide (1998). However, since the building collapsed, some of these techniques were unemployable, while the availability and importance of others were

augmented. For example, the structural elements could not be evaluated in their as-built location, with surrounding evidence, to determine the extent and duration of fire exposure and document physical damage as a result of the fires in combination with structural loading conditions. In addition, the components most likely experienced secondary physical damage during the collapse that could accentuate or mask the actual damage incurred as a result of the pre-collapse fires. Further, the collapse resulted in the pieces being exposed to both post collapse fires (some pieces for nearly four months) and many months of ambient degradation. These events may obscure the origin of the degradation features observed.

Taking this knowledge in to account, a visual inspection and metallurgical evaluation of the recovered steel were conducted to determine the extent and effect of fire exposure of the various structural elements. Four features were analyzed (when appropriate): (1) condition of the primer paint, (2) microstructure, (3) chemistry, and (4) hardness. To aid in the study, National Institute of Standards and Technology (NIST) developed a novel approach to evaluating the primer paint for exposure to high temperature excursions (see Appendix D). This method was relatively easy to implement and robust enough to examine the entire component in the field. The other three techniques were chosen based upon their relative ease of implementation and analysis.

Again, it was difficult to separate visual evidence of fire and/or degradation of the microstructure as a result of fire exposure from the 1 h to 2 h experienced prior to the collapse of the buildings compared to that caused by the fire exposure in the debris pile at the WTC site (for some samples, possibly up to four months).

6.2   VISUAL INSPECTION OF RECOVERED STRUCTURAL COMPONENTS

Visual inspection for the fire effects on recovered steel was conducted solely on the perimeter panels and core columns, as these were the only structural elements that had known as-built locations. For the perimeter panels, the analysis initiated with the correlation of the time-fire exposure maps (Sec. 2.3) and mapping of the condition of the primer paint on these samples. (This procedure is described below.) To summarize, 16 of the 26 exterior panels from WTC 1, and none of the 16 panels from WTC 2, were observed to be exposed to fire at some point prior to the collapse. However, two samples from WTC 2 (M-10a and M-10b) were chosen to be analyzed as they were located within the fire zone floors, and three other panels were also examined (panel N-9 (A154: 101-104) and C-11 and M-14, both unidentified) based upon an outside contractor's analysis of pieces possibly exposed to pre-collapse fires (Wiss, Janney, Elstner Associates, Inc. report found in Appendix F). On each of the 21 panels selected, numerous locations on the inner webs, flanges, spandrels, and floor truss connectors for each floor level were analyzed, providing that sufficient paint was available for the analysis. Core columns C-80 and HH were examined from WTC 1, and samples C-88a and C-88b were tested from WTC 2; these columns resided within the fire floors for their respective buildings. The entire length of each core column was examined, and evaluations of the primer paint were made when sufficient paint was available for inspection.

As shown in Appendix D, the procedure developed for evaluating the condition of the primer paint on the structural elements was relatively easy to implement and robust enough to examine the entire component in order to determine possible fire exposure of the WTC steels. Calibration tests showed that the paint used on the WTC steels that reached temperatures over 250 °C cracked from the difference in thermal

expansion between the paint and the steel. This approach had the singular advantage of requiring no sample preparation, could be used in the field, and was feasible for mapping exposure on entire structural sections. The paint coating was not a paint in the traditional sense, but was actually a ceramic coating (Tnemic) containing no organic binders. Thus, when the coating was exposed to high temperatures, the coating did not burn as no organic binder exists to combust.

The difference in thermal expansion coefficients between the base metal and the coating creates tensile stresses that are applied to the coating at high temperatures. This causes the coating to crack, generally along faint cracks that pre-exist after the original low temperature baking of the paint. The pattern formed is generally termed "mud cracking." Images of the paint exposed to high temperature and in the unexposed condition can be seen in Fig. 6–1. The cracking pattern has no directionality, and exhibits a characteristic length scale of the islands that were quickly identified using a 50X microscope. Laboratory tests, as explained in Appendix D, have shown that the pattern becomes visible once the painted steel has reached approximately 250 °C.

The presence of cracking of the paint does not necessarily mean that the base metal reached 250 °C. Cracking of the paint, which was brittle, can occur due to mechanical damage, such as impact, abrasion, or deformation of the steel. Also, corrosion can work apart the same pre-existing drying cracks in the coating and give an appearance similar to that produced by high temperature exposure. In many of these cases, the cracking pattern exhibited a directionality, as seen in Fig. 3–11d of Sec. 3.2.1, and was dismissed. However, an unambiguous determination as to the source of the cracking was generally not possible, and the observations herein should be considered "definite negative," i.e., if the mud cracking pattern was absent, the particular material did not experience a temperature excursion in excess of about 250 °C.

6.2.1   Exterior Panels Exposed to Fire

The analysis locations, time-fire exposure data, and visual inspection results for each individual component can be found in Appendix E. Over 170 areas associated with the 21 exterior panels were analyzed with the results shown in Table 6–1. For all panels exposed to fire, whether external flaming, fires observed inside the window, or spot fires, over 90 percent of the paint results showed a "negative" conclusion indicating that these areas were not exposed to temperatures excursions above 250 °C. As shown in Appendix E, seven areas were deemed "no conclusion", as sufficient paint was not available for the analysis. Five locations had paint available for inspection, but due to such confounding factors as corrosion products or residual cement, a definitive conclusion could not be made, and thus, these locations were labeled "inconclusive." Finally, three locations were observed to have a "positive" finding. The "positive" finding indicated that the original primer paint developed mud cracking. Areas where mud cracking occurred were:

1. Panel K-1, WTC 1, column 210, flange and inner web of 98th floor region. Prior to the collapse of WTC 1, the sample was observed to have experienced varying degrees of fire exposure for a minimum of 31 cumulative minutes. The upper portion of the recovered column was crushed, while generally maintaining concentric axial alignment with the lower portion of the column, Fig. 6–2. Metallographic analysis of this sample can be found in Sec. 6.3.4.

2. Panel K-2, WTC 1, column 236, 93rd floor spandrel. This area was observed to have fire exposure for 9 cumulative minutes prior to collapse. A positive reading was made directly below the floor truss connector while above the connector, in the same location a negative result was obtained, Fig. 6–3. Metallographic analysis of this sample can be found in Sec. 6.3.4.

3. Panel N-8, WTC 1, column 143, seat and standoff plates supporting the 99th floor. This seat (Fig. 6–4) was exposed to fire for a minimum of 18 cumulative minutes before collapse. In viewing the seat, it appears that a plastic note paper binder (based upon melted black plastic with imbedded papers) settled and melted on the seat. According to the drip pattern of the binder (Fig. 6–4b), it appears that the panel was in a horizontal position when this occurred. Mud cracking was not observed on the spandrel plate to which the seat was welded. Metallographic analysis of this sample can be found in Sec. 6.3.3.

6.2.2   Core Columns Exposed to Fire

Four of the core columns with known as-built locations were examined for mud cracking of the paint. Appendix E also lists these results. For columns C-88a and C-88b, sufficient paint for analysis was not available. The loss of paint may be due to one of numerous reasons (pre-or post-collapse exposure to high temperature excursions, ambient corrosion subsequent to collapse, or mechanical damage) and was not determined during this investigation.

For columns HH and C-80, very minimal paint was observed (three to five spots per column) with "negative" conclusions for these areas.

6.3   METALLOGRAPHIC ANALYSIS OF ELEMENTS EXPOSED TO FIRE

Some aspects of the thermo-mechanical history of a structural steel element may be revealed through a careful assessment of the component's microstructure. Identification of phases, whether stable or metastable, and their characteristics (e.g., size, morphology, distribution) can help lead to an understanding of the possible rolling conditions and/or cooling rates used during fabrication. These factors are directly related to the room temperature mechanical properties of the component. Likewise, high temperature excursions due to fire can also lead to alterations in the microstructure and the mechanical properties. Therefore, if knowledge of the "as-fabricated" microstructural characteristics of the member is available, then a review of the "affected" microstructure may give an indication of the level of elevated temperature exposure while in service.

As part of the metallographic analysis of the recovered steel, an assessment was made to determine if information could be compiled on the extent and effect of fire exposure to the perimeter panels that experienced pre-collapse fires. Chemical analysis and hardness evaluations were used to supplement the results when appropriate. Samples for analysis were chosen based upon the pre-collapse exposure to fire that was reported in Sec. 2.3. These included floor truss connectors (seats) and the lower portion of spandrels where external flaming was observed in the window directly beneath the location of sample removal, Table 6–2. These results were compared with the paint mapping analysis reported in Sec. 6.2. Almost all of the areas exposed to pre-collapse fires (from Sec. 2.3) did not display mud cracking characteristics. An example of this can be seen for the spandrel located at the 99th floor level of sample

M-2 (Fig. 2–48e of Sec. 2.3). The 98th floor was observed to have external flaming and fires inside for a minimum of 18 cumulative minutes, yet there was no mud cracking of the paint either on the columns near the window openings of the 98th floor or the spandrel for the 99th floor. Therefore, samples were chosen from areas where severe fire was observed prior to the collapse of buildings and were analyzed to determine if these exposures affected the microstructure. In addition to the samples listed in Table 6–2, examples of unique, heat-related damage to perimeter columns (from panels K-1 and K-16) and truss material (from samples C-115 and C-131) are discussed in a separate section.

This portion of the study had a disadvantage in that the analysis had to rely solely upon the recovered material for the "representative" microstructures and properties for comparison. The "as-fabricated" microstructure cannot be assumed based upon a single observation from a component with similar F_y (yield strength), as physical damage sustained from the impact/collapse and exposure to both pre- and post-collapse fires may have previously altered the microstructure of the component. In addition, components with identical specified F_y may exhibit variations in microstructure, even when produced at the same mill. Therefore, representative, as-fabricated microstructures and properties were selected only after careful evaluation of all the plates for a given component (e.g., perimeter column flange, web of a wide-flange section, top chord of a floor truss) with a specified minimum F_y and similar gauge. (For representative microstructures for all the steels see NIST NCSTAR 1-3E (2005) where over 400 metallographic samples from distinct structural components were evaluated.) Care was taken to disregard any specimen from a given group that may have had visual evidence indicating that a microstructure-altering event occurred (e.g., significant deformation of the plate, indications of high temperature exposure based upon pre-collapse evaluation of fire exposure of the component [Sec. 2.3] or mud cracking of the primer paint in the area where the sample was removed [Sec. 6.2]). Additionally, the controlled rolling and cooling rate schedules for the steels could not be obtained as they were proprietary, and the documents were not presently obtainable. Thus, the as-rolled microstructures for the plates can not be "hypothetically characterized" and compared with the "representative" microstructures decided upon.

Material from core columns was not evaluated based upon two reasons. First, the exposure to pre-collapse fires could not be determined as elements within the core could not be visually assessed prior to collapse. Second, only 12 core columns with known as-built locations were recovered. This severely limited the population from which an "as-fabricated" microstructure could be chosen as the size and shape of the columns recovered for a given F_y varied.

6.3.1   Examples of Microstructural Features Possibly Related to Fire Exposure

Steels in the WTC towers were classified as either hot-rolled or quenched-and-tempered (NIST NCSTAR 1-3E). To help understand possible phase changes from high temperature exposure, a portion of the Fe-C phase diagram is shown in Fig. 6–5. It is important to note the two phases of iron, ferrite (alpha, low temperature bcc phase) and austenite (gamma, high temperature fcc phase), the iron carbide phase (Fe_3C, also known as cementite), and the lines indicating various phase changes at equilibrium. The A_1 line is the temperature, independent of composition, at which austenite begins to form during heating; it is also known as the lower critical temperature and occurs at 727 °C. The A_3 line is the composition-dependent temperature where the transformation of ferrite to austenite is completed. Knowledge of this diagram was important through out the rest of this section.

There are numerous examples of microstructural features that can be used to indicate if steels experienced high temperature exposure subsequent to being produced. Detailed comparison between "as-fabricated" and "exposed" microstructures was required. A few of these examples are briefly described below with respect to possible observances found during the analysis of the WTC steels. Some microstructural examples shown were taken from (NIST NCSTAR 1-3E) where plates from various structural components were furnace exposed to 625°C for up to 2 h.

- **Spheroidizing of the iron carbide (Fe_3C, cementite) in ferrite-pearlite steels:** If an as-rolled, plate containing pearlite was exposed to temperatures near the A_1 line and held for an extended period of time, the carbide lamellae could dissolve, and upon cooling, re-precipitate in the form of spheroidal or globular morphologies of the carbide in the steel. However, the plates do not have to completely dissolve, but can break up to form spherical carbides in the microstructure. The extent of spheriodization depends upon time at temperature and both the composition and prior amount of cold working of the steel. An example of spheroidization is shown for a 60 ksi flange plate, Fig. 6–6. After 15 min of exposure at 625 °C, spherical carbides can be observed in the prior pearlite colony in place of the plates. However, steels with different thermo-mechanical histories behave differently, and thus, there was no general rule relating time-temperature exposures to degree of spheroidization. If the pearlite distribution was initially banded and then exposed to temperatures below the A_1 line, the spheroidized carbide distribution will most likely be non-uniform as well (Bramfitt and Benscoter 2002). This can be seen in the example shown for short times where carbides primarily reside in the location of the original pearlite bands. The same steel exposed for longer times or to temperatures just above the A_1 line and then slow cooled can result in a more uniform distribution of the carbide particles in the structure.

- **Formation of carbides in the grain boundaries of ferrite-pearlite steels:** Analogous to the case of non-uniform distribution of spheroidization, carbides could also form in the ferrite grain boundaries.

- **Change in constituent size or morphology of ferrite-pearlite steels:** The size and/or morphology of constituents (ferrite grains or pearlite colonies) could be altered through many different processes. One example would be to expose a steel with these constituents to temperatures above the A_3 line and then cool at a much slower/faster rate than the original cooling rate used during fabrication. This could produce a much large/smaller ferrite grain size and cementite lamellar spacing than the parent material before exposure.

- **Post-fabrication tempering of quenched-and-tempered steels:** Production of a quenched-and-tempered structure typically starts with the plate at a temperature above the A_3 line so that the entire structure consists of austenite. Rapid cooling restricts carbon diffusion and traps the carbon in solution to form the metastable phase of martensite. The body center tetragonal (bct) lattice, as a result of trapped carbon in the body center cubic (bcc) structure, is highly strained and results in a material with high hardness and strength levels. Tempering is the process by which the steel can be softened by reheating to below the A_1 line to allow carbon to diffuse out of solution and form spheroidized carbides in a matrix of ferrite. The repositioning of carbon results in a decrease in strength but increase in toughness. Tempering of the structure could continue if the sample was further exposed to temperatures below the A_1 line. An example is shown in

Fig. 6–7 for a 100 ksi quenched-and-tempered flange plate. With increased exposure at 625 °C, the sharpness of the lath boundaries decrease while the carbides become more distinct.

- **Decarburization:** A decarburization zone in a steel structure is the loss of carbon and associated C-rich phases (e.g., iron carbide), near the surface layer of a component. This transpires when carbon at the surface reacts with a medium (typically oxygen) to form a reaction product (in the case of oxygen, carbon oxidizes to either CO or CO_2 gas). This loss of carbon establishes a concentration gradient between the surface layer and the unaffected base material that acts as the driving force for continuing carbon diffusion. This process typically occurs when exposures are above the A_1 line (i.e., above 727 °C), as ferrite below the A_1 line is saturated with carbon so that the carbon concentration gradient necessary for subsequent diffusion may not be established. Therefore, decarburization may not occur or may be very slow below these temperatures (Samuels 1980). The overall depth of the layer is dependent upon time, temperature, and composition of the steel.

- **Development of external corrosion scale:** The surface of structural steel is readily reactive with its conventional environment. The formation of a corrosion scale typically occurs as a result of (1) high temperature exposure, (2) atmospheric degradation, or (3) a combination of the two corrosion processes. Many different corrosion products can form (e.g., oxides, sulfides) depending upon the sort of corrosive species in the vicinity of the surface (e.g., oxygen, sulfur) with their stoichiometry and morphology dependent upon time, temperature, and environmental conditions. Iron sulfides are typically formed at elevated temperatures with sulfur present and do not tend to form continuous scales when significant levels of oxygen are present. Similarly, iron oxide scales (Fig. 6–8) formed at high temperatures are generally denser and more uniform, with columnar grains, than those formed by ambient processes. The diffusional kinetics at elevated temperatures allow for continued and regular growth via transport through the scale. Iron oxides formed at ambient temperatures (rust) are typically less dense, compositionally layered, and friable as continued scale growth relies upon exposure of fresh material subsequent to spallation.

- **Development of internal corrosion phases:** Internal attack of an alloy can also take place as the corroding species diffuses into the material to form corrosion phases not physically connected to the externally developed corrosion scale. This usually occurs when the metal has some solubility for the corrosive species in amounts such that its activity in the alloy is sufficient to form a compound with the less noble metal (i.e., the metal contains alloying elements with a higher affinity for the corroding specie than the matrix material). Preferential attack of individual alloy constituents in the steel by the inward diffusion of the corroding specie is commonly observed as precipitates ahead of a metal/oxide scale interface.

All these microstructural features may also be a direct result of the processing of the plate or component itself. It was very possible that a specific combination of rolling schedules and cooling rates can produce many of the features discussed above. Therefore, it was again important to carefully select the representative microstructures to be used as comparison against samples believed to have been exposed to fire.

6.3.2   Spandrel Plates Exposed to Severe Fire Conditions

Table 6–2 displays information about the four locations of sample removal for the spandrel material. The samples were removed from the bottom portion of spandrel plates located at window openings where severe fire exposure conditions were observed prior to the collapse of WTC 1 (i.e., if external flaming was observed on the 97th floor, then the sample was removed from the bottom portion of the 98th floor spandrel). The minimum duration of exposure ranged from 16 min to 32 min. As reported in Sec. 6.2, visual observations for mud cracking of the paint were either negative or inconclusive (as paint was not available for inspection). The samples had a plate thickness of 0.375 in., were relatively undeformed, and had specified minimum yield strengths of 36, 42, and 50 ksi.

In comparing microstructures from both the "exposed" and "representative" samples of equivalent strength spandrel material, the following microstructural features were observed to be similar for both cases:

- Ferrite grain size and pearlite distribution (Fig. 6–9a)

- Absence of a decarburization zone near the surface of the plate (Fig. 6–9a)

- Limited decoration of the ferrite grain boundaries with carbides (Fig. 6–9b)

- Similar appearance of pearlite (typically distinct lamella observed)

- Thin, non-uniform, cracked oxide scales (Fig. 6–9a)

Again, these features were observed on all samples regardless of exposure history or specified minimum F_y. As reported in NIST NCSTAR 1-3E (2005), a 42 ksi spandrel plate was isothermally exposed at temperatures ranging from 200 °C to 625 °C for up to 2 h. Figure 6–10 shows the change in microstructure that occurred with time for the samples exposed to 625 °C; below this temperature, no apparent change to the microstructure was observed via light optical microscopy. After only 15 min of exposure at 625 °C, the pearlite showed signs of spheroidization. As this feature was not observed in any of the four spandrel materials evaluated, it was believed that the spandrels were not exposed to this temperature or that if they were, it was for significantly less time than 15 min.

In addition to the microstructural results, the hardness evaluation suggested that there was no deterioration of the mechanical properties of the materials as a result of exposure to pre-collapse fires (Table 6–2).

Based upon these results, it was concluded that none of the four portions of spandrel material visually observed in severe pre-collapse fire exposure experienced temperatures severe enough to alter the microstructure or mechanical properties of the plates when compared to samples of similar F_y that did not experience fire conditions. Further, a dense and continuous oxide scale was not observed on these samples from exposure to post-fabrication elevated temperatures. As shown in Fig. 6–9a, the oxide scale was non-uniform and relatively porous; thus, it was most likely a result of environment degradation subsequent to the collapse of the buildings and not a result of exposure to elevated temperatures. These conclusions agree with the findings of Sec. 6.2.

The lack of high temperature exposure evidence for the fire exposed spandrels may be related to the possible temperature experienced and the duration of the exposure. Tide (1998) reviewed fire research on the exposure of structural steel to fire conditions and summarized the following points that should be considered when evaluating possible temperature excursions experienced by steel structures:

- The steel temperature is significantly reduced as the distance from the center of the fire increases.

- Ventilation of a fire compartment greatly reduces the temperature of steel at distances away from the center of the fire.

- The temperature of fire-protected steel in the vicinity of the fire is significantly less than unprotected steel at the same location.

Consideration of these points may lead to a possible explanation for a lack of microstructural change.

The longest duration of exposure evaluated was for panel S-10, which was exposed for just over 30 min (this was the longest exposure time for the recovered perimeter panels [Appendix E]). However, after 15 min of exposure to 625 °C, the 42 ksi spandrel exhibited spheroidization of the pearlite. It would be expected that the 50 ksi plate would behave similarly. If the exposure temperatures were somewhat below this, then kinetically, it may not have been possible to produce a microstructural change within this time frame. Additionally, the windows were consistently breaking out as the fire advanced, allowing for ventilation of the fire compartment to occur. Thus, the temperatures of the spandrel steel may not have been as high as if there was no ventilation of the floors. Finally, a majority of the perimeter panels that burned out were most likely undamaged after the impact. The sprayed fire-resistive material applied to the columns and spandrels may well have been intact and would have provided some protection from the high temperatures of the fire. Thus, it was plausible to conclude that the maximum temperature the steel may have attained was below that which would have allowed for microstructural changes, despite severe fire exposure observed photographically.

6.3.3 Perimeter Floor Truss Seats Exposed to Severe Fire Conditions

In addition to the spandrel plates, portions from four perimeter floor truss seats were also removed for a similar metallographic analysis. It was believed that these connectors may not have been well protected during the fires, as the photographs that were obtained of both the original application of sprayed fire-resistive material (SFRM) and upgrades that took place in the 1990s showed that while fire protection was indeed applied to the seats, the thickness of the originally applied sprayed fire-resistive material appeared marginal (NIST NCSTAR 1-6A). The four seats examined supported floors that had severe fire conditions directly below them (i.e., if fire was observed on floor 97, then the seat supporting floor 98 was analyzed). The seats chosen were all of similar size (type 1212 or 1411, see Table 3–6). Conclusions for three of the four seats examined for mud cracking of the paint were either negative or inconclusive. The fourth seat, which supported the 99th floor of sample N-8, was found to have mud cracking on both the seat and the standoff plates; the spandrel to which the seat was attached did not have mud cracking of the paint.

Microstructures of the fire exposed seats showed a partially decarburized zone near the surface with a depth ranging from 400 μm to 500 μm, Fig. 6–11. Spandrel material adjacent to these locations was also examined, and decarburization zones were not observed. The pearlite within the seat material had plates

that were not clearly distinguishable, in addition to the overall mottled appearance. Seats for panels C-40, M-2, and N-12 had a thin, non-uniform, and cracked oxide scale. The fourth seat, from panel N-8, had two corrosion features that were unique to this sample. The first was a continuous, uniform, and dense scale of iron oxide (Fig. 6–12a), with the second being internal penetration of the iron oxide phase and decarburization fronts (Fig. 6–12b) surrounding an oxidized crack.

Microstructures from comparable non-exposed samples showed specimens both with and without the decarburized zone. Additionally, they all appeared to contain the mottled pearlite to some degree, and had a thin, non-uniform oxide scale. Further, coupons from a truss seat were isothermally exposed at temperatures in the range from 200 °C to 625 °C for up to 2 h (NIST NCSTAR 1-3E). After 15 min of exposure, the pearlite had begun spheroidization (Fig. 6–13) at 625 °C. Below this temperature, there was no apparent change in the microstructure via light optical microscopy techniques.

Vickers microhardness results indicated that all four of the seats had lower hardnesses when compared to other seats of similar size, Table 6–2. However, the results of Rockwell hardness testing B scale (HRB) were slightly more ambiguous. All of the samples had decreased HRB values relative to other seats of similar size with the exception of the sample that tested positive for mud cracking (N-8). In this case, it was determined that using hardness as an analytical tool was unreliable as the results were extremely variable.

As no major change to the microstructural features was observed in seats from panels C-40, M-2, and N-12, it is likely that the pre-collapse fire exposure was not severe enough to have a significant effect on the microstructure. Results from the seat taken from panel N-8 indicate that this seat may have been exposed to elevated temperatures. While vast changes in the microstructure and hardness were not observed, the continuous oxide scale seen, as well as the internal oxidation, was believed to have formed as a result of a high temperature excursion. It was unclear when this exposure may have occurred. These findings were in agreement with those of Sec. 6.2.

6.3.4 Unique Cases of Damage Possibly Related to Elevated Temperature Exposure

Five samples of the NIST inventory were identified from visual inspection as having unique physical damage that may have been related to elevated temperature exposure. Three were perimeter columns (from panels K-1 and K-2 and single column K-16), and two were floor truss materials (C-115 and C-131). As these samples were distinctive among the entire group, an in-depth investigation of their damage features was conducted with the results discussed in detail below.

Perimeter Panel K-1

This exterior panel was located on the east face near the north corner of WTC 1, at floor levels 97 through 100. A portion of one column (column 210 in the vicinity of the 98th floor) was crushed, while the lower portion was relatively undistorted, Fig. 6–14a. The crushed segment had roughly concentric axial alignment with the lower portion of the column. This would suggest that the lower portion of the column was constrained axially while the 98th floor section collapsed, most likely during the collapse of the building. Additionally, columns 208 and 209 appear to have been severed at the upper stiffener plate of the 98th floor spandrel, with portions of the flanges and outer web "peeled down like a banana peel." All three columns from the panel had 60 ksi flange plates with a 0.25 in. thickness.

Pre-collapse images indicated that immediately after the impact, there was no disruption in the aluminum façade of this panel (column 210 in the 98th floor region), Fig. 6–15a. This would suggest that the sprayed fire-resistive material of this panel, at least the exterior portion, was still intact at this time. The impact models verified that the sprayed fire-resistive material was most likely intact on this panel (NIST NCSTAR 1-2A). There was no fire or smoke evident from any of the 98th floor windows at this time, though there was external flaming of the 97th floor near the panel. Table 6–2 summarizes the time-fire exposure data obtained from Fig. 2–48m for this area, as well as other essential data related to the analysis of this sample. Significant external flaming was visually observed in the windows adjacent to column 210 on the 98th floor from 9:46 a.m. to 10:22 a.m. The extent of this external flaming can be observed in Fig. 6–15b. However, after 10:22 a.m., photographic evidence suggests that the fire had retreated to within the building and appeared to have completely receded from this area closer to the time of collapse. Smoke inhibits the view of this panel at these later times. However, evidence showed that at 10:17 a.m., the fire had already begun to subside in this area (Fig. 6–15c) and commenced its movement toward the southern face of the building. At times shortly thereafter, external flaming was concentrated at the middle of the west face of the building and toward the southern end of the 98th floor. As stated above, a fair amount of smoke from other locations of the building obscured the view of the panel near the time of collapse. However, at the initiation of collapse, external flaming was observed coming out the windows on the 98th floor near the southeast corner where fire was observed at slightly earlier times. No external flaming was associated with the northeast corner at the moment of collapse. Evidence shows that collapse was initiated on or very near the 98th floor level for WTC 1 (NIST NCSTAR 1-6).

In order to determine if fire damage of the steel occurred due to external flaming, microstructural examination and hardness measurements were conducted on the flange in both the undeformed and crushed portions of the column. Figure 6–14 shows the location from which the metallographic samples were removed; red circle in (c) was from the flange plate above the 98th floor spandrel, and blue circle in (d) was from the same flange plate below this spandrel. These samples were removed at a distance of approximately 10 ft apart. The sample taken from the lower portion of the column had paint that was in good condition (i.e., no mud cracking of paint, no sooting), even though it experienced 12 min of continuous external flaming. There were minor scratches and gouges in the material, but cracking and/or sooting of the paint was not observed. In contrast, a majority of the paint was missing, with a fair amount of corrosion product on the surface, from the column located in the 98th floor. However, there were a few localized areas of remaining paint available that indicated mud cracking did occur, as shown in Appendix E.

Both samples were mounted and prepared using standard metallographic practices. The etched microstructure of the bent plate in the 98th floor region was observed to vary across the transverse section (Fig. 6–16). Figure 6–16a indicates the micrograph locations of (b), (c), and (d). As the plate was bent, the outer surface (which was the outer face of the flange on the column) was in tension while the inner face was in compression. This fact was visually observed through the appearance of the microstructural constituents in the two locations. The outer face (in tension) contained elongated grains of ferrite and pearlite colonies (Fig. 6–16b), while these features were distorted in compression at the inner surface (Fig. 6–16d). The ferrite grains at the neutral axis (centerline of the plate) appeared to be relatively coarse grained with the development of a faint Widmanstätten morphology (Fig. 6–16c). Banding of the pearlite was found primarily at the centerline of the plate, but with the tensile deformation at the outer face of the plate, the stretching of the ferrite and pearlite lent the appearance that the microstructure was also banded in this region. Correspondingly, the microstructure at the centerline of the plate located in the 97th floor

contained a banded microstructure with similar sized microstructural constituents. Widmanstätten ferrite was observed in addition to the blocky ferrite (Fig. 6–17b). However, the edges of the plate had a relatively uniform distribution of pearlite (Fig. 6–17a). Decarburization zones were not observed in either case (97th or 98th floor locations).

Both microstructures from K-1 were compared to microstructures from the centerline of other 60 ksi plates known not to have been exposed to elevated temperatures prior to the collapse. As no other 60 ksi flange plates with 0.25 in. thickness were recovered, outer web plates of similar thickness and F_y were used as comparison as the plates were found to be chemically and microstructurally similar (NIST NCSTAR 1-3E). A representative micrograph of 0.25 in. 60 ksi outer web plate is shown in Fig. 6–18. The microstructural features were similar in appearance.

An oxide scale was also observed on the sample from the 98th floor region (Figs. 6–16b and 6–19). This scale was somewhat dense and continuous, but non-uniform in thicknesses (ranging on the order of 25 μm to 250 μm). The latter characteristic was a result of localized scale penetration into the flange material, resulting in nodular oxide structures when viewed in cross-section (Fig. 6–19). The scales were composed of gray colored phases of varying shades when examined using a light optical microscope. Energy dispersive spectroscopy (EDS) concluded that the two lighter gray phases contained Fe with traces of Mn (oxygen was not detectable with the system utilized). Table 6–3 displays the qualitative results of the EDS probed areas on Fig. 6–19. In addition to Fe, the darkest gray phase was found to have relatively high amounts of Ca, though it was unclear from where this elemental component originated. Another scale observed was orange in color and found to contain Ti, most likely contributed by the primer paint. When viewed using polarized light, the scale was optically active, resulting in a red-orange shading throughout the scale (Fig. 6–19b).

Contrasting the scale development on the plate at the 98th floor level was the absence of scale development on the sample removed from the lower portion of the column, Fig. 6–17. It was observed that a majority of the primer paint in this area was still intact and in relatively good shape prior to removing the specimen. However, optical microscopy revealed that there were localized regions where isolated scale growth occurred; these areas were optically inactive under polarized light and were few and far between. The corrosion product may have been there prior to application of the paint.

Hardness measurements were conducted to determine if the intensity and duration of the heat from the external flaming altered the room temperature properties of the steel in the area where crumpling occurred. Vickers microhardness testing was performed on the material from the crushed portion of the column as it was difficult to prepare a flat sample from the highly deformed material for Rockwell testing. Table 6–2 shows the results and compares them to the average for other 0.25 in. 60 ksi plate material known not to have been exposed to fire prior to the collapse of the building. The results showed that the material from the 98th floor region was higher in hardness than steel from both below the 98th floor spandrel and the average for similar materials. The higher hardness value was attributed to the high amount of deformation (work hardening) in the material as a result of the "folding" of the flange.

Based upon the information above, it was concluded that the flange plate analyzed from column 210 of panel K-1 did not experience a temperature excursion significant enough to alter the microstructure of the mechanical properties. Additionally, the oxide scales observed on the "fire affected" flange were similar in nature to those formed by ambient processes. Therefore, the temperature excursion may not have been severe enough to develop a high temperature oxide scale. This was in agreement with the results of NIST

NCSTAR 1-3E, which indicated that temperatures at or lower than 500 °C did not produce metallographic changes for this material.

Perimeter Panel K-2

This exterior panel was located in the middle of the east face of WTC 1 at floor levels 92 through 95. Only the lower 24 ft of column 236 were recovered. Unique to this panel was the observance of mud cracking of the paint on the spandrel below the 93rd floor slab, while no mud cracking was found just above the floor level. As shown in the time-fire exposure map (Fig. 2–48o) of this panel, fires were observed inside for roughly 10 min, discontinuously, on the 92nd floor. No pre-collapse fires were seen on the 93rd floor.

In order to determine if fire damage of the steel occurred, microstructural examination and hardness measurements were conducted on spandrel material removed from just below the floor slab (area where mud cracking was observed), Fig. 6–3. These results were compared with samples of 42 ksi spandrel that were known not to have been exposed to fire prior to collapse.

Metallographic analysis did not reveal any changes present in the microstructure from the representative micrographs of Sec. 5.1.2 of NIST NCSTAR 1-3E. No spheroidization of the pearlite was observed, nor did an oxide scale develop that would be indicative of high temperature exposure.

Hardness measurements were also conducted and displayed in Table 6–2. Comparison with other 42 ksi spandrel plate known not to have been exposed to fire prior to the collapse of the building showed that averages were similar.

Based upon this information, it was concluded that the spandrel plate did not experience a temperature excursion high enough to alter the microstructure. From the heat treatment studies of Sec. 5.4 of NIST NCSTAR, it was observe that this exposure was most likely less than or equal to 500 °C.

Single Column K-16

The third example of a unique damage feature of a perimeter column was found on sample K-16. (As discussed below, a piece sectioned from this column prior to arrival at NIST was studied and reported on in the Federal Emergency Management Agency [FEMA]/Building Performance Assessment Team [BPAT] [McAllister 2002] report, Appendix C.) This was a single, unidentified column that experienced what appeared to be a large amount of material degradation as a consequence of erosion/corrosion processes, Fig. 6–20. Of all the recovered steel examined, this was the only case where this type of degradation was observed on a perimeter or core column. The damage consisted of localized thinning in the outer and inner web plates in this area, leading to significant perforations in the outer and inner webs. The stampings at the base of the column on the flange indicated that it was a 50 ksi column with column type 143. The database of all columns showed that columns matching this description were no higher than the 52nd floor level in WTC 1 and the 53rd floor level in WTC 2. Therefore, it was unlikely that this column experienced degradation prior to the collapse of the towers. The attrition appearance of the column, in terms of the two webs experiencing the highest degree of degradation with minimal attack observed on the flange sections, also indicates that the column was in a horizontal position while the attack occurred.

Three samples were removed from the column, analyzed metallographically and chemically, and tested for hardness. The samples consisted of one each from the inner and outer webs in the corroded region and one from the outer web at the base of the column where corrosion did not occur. Both samples removed from the corroded area had thinned down to a knife edge after initially starting at a thickness of 9/16 in. Corrosion product was observable on the surface, and no paint was available for analysis. The sample removed from the base of the column did not have a significant amount of corrosion product on the surface and had maintained the original thickness of the web plate. However, paint was not available on this section either. All samples were mounted and prepared using standard metallographic practices.

As both corroded samples had similar characteristics, only the description of the outer web material was detailed. The etched microstructure can be seen in Fig. 6–21a and 6–21b. Compared to other 50 ksi outer webs not exposed to fire prior to collapse, the ferritic grain and pearlite colony size of these microstructures were nearly an order of magnitude larger (NIST NCSTAR 1-3E). In addition, strong banding of the pearlite was observed, with the lamellar features clearly distinguishable. The banding made it difficult to determine if a decarburized zone was present near the metal-oxide interface. However, the spacing of the pearlite bands indicated that decarburization of the structure occurred since pearlite was not observed within nearly 200 μm from the metal-scale interface (Fig. 6–21a and 6–21b). In contrast to the corroded samples, the sample removed from the lower portion of the column was significantly different (Fig. 6–22a). The grain size and pearlite distribution were more in accordance with that from other samples of 50 ksi material; however, spheroidization of iron carbide (Fe_3C) in the pearlite that had begun, Fig. 6–22b.

The corrosion scales on the outer web can be observed in all three images of Fig. 6–21. Viewed optically, the scales were a complex mixture of varying gray-shaded scales, gold-colored phases, and dark grain boundary precipitates. Table 6–3 shows the results of the EDS probed areas in Fig. 6–21c. Again, the lighter gray phases at the scale-environment interface appeared to be iron oxides. The darker gray phases in the scale interior appeared to be iron oxides containing high levels of Ca, as well as minor quantities of Cl, Si, and S. The bulk gold-colored phases, as well as the majority of phases in the grain boundaries, were iron sulfides. The corrosion scale observed on the un-corroded web (Fig. 6–22a) were found to be all oxides that had a similar morphology to the scales observed on sample K-1 (Figs. 6–16a and 6–19). Further, corroding elements (e.g., S, Cl), as found in the scale observed in the eroded/corroded regions, were not detected.

Hardness of the samples was also evaluated using Vickers microhardness testing. Results, shown in Table 6–2, indicate that both samples were softer than representative 50 ksi flange material of similar thickness. For the corroded regions, this would be expected as the constituent size was much larger than that found in typical 50 ksi plate. However, the hardness was also significantly less for the lower portion of the web where corrosion did not occur, even though the microstructural features were similar. One possible reason for this drop may be related to the spheroidization of iron carbide (Fe_3C) in the pearlite that had begun (Fig. 6–22b), thus, reducing the effectiveness of inhibiting dislocation movement through the structure.

The wasting of the web plates most likely resulted from a high temperature, corrosion process that was exacerbated by the presence of sulfur. While not enough evidence was available to indicate whether corrosion occurred through gaseous, liquid, or solid attack (in addition to varied conditions possible in the rubble pile and lack of information associated with the recovery of this column at the WTC site), it was

likely that the degradation process was most likely a complex combination of these three. As sulfur was not readily available in large amounts in the steel (0.02 weight percent max.), an external source must have supplied this specie (e.g., plastic, rubber). Viewing the column, this external source was in all probability burning directly on top of the outer web while the column lay in a prone position. With the knowledge that there exist many different corrosion paths that could be taken to achieve similar microstructures, the following hypothesis was presented as a possible explanation for the observed features in the microstructure. The corrosion process began with sulfur ingression into the material, diffusing along the grain boundaries, and forming large sulfide phases within the matrix. With continued lateral and inward growth of the sulfides, probable changes in the local environment may have led to the oxidation of the outer layers of the sulfide phases, thus freeing up sulfur to travel further into the base material for continued attack of the steel. The internal sulfide deposits in the grain boundaries were classical morphologies that identified sulfur penetration via a solid state diffusion mechanism. As a result of sulfide-oxide phase changes, as well as the initial porous nature of the developed sulfide scales, the outer oxide scales would be friable and spall, exposing fresh sulfide phases for oxidation. Given the proper time-temperature-environment conditions, this process would continue until the outer web material was completely wasted, allowing the corroding material to fall through the hollow column and settle on the interior web where attack of this plate began. This latter statement was supported by the fact that the outer web sustained more degradation than the inner web and that pattern of material attrition would be consistent with corrosion beginning first at the outer web. Again, it was noted that degradation of the column occurred following the collapse of the building. Therefore, it was unknown what specific items (e.g., office furniture, office supplies, carpeting) were the sources of the corroding elements found in the scale, how long this process occurred, or at what temperature.

While analysis of sample K-16 yielded no revelations on the collapse mechanism for the buildings, the changes in the web material as a result of high temperature corrosion exposure were interesting. The original 50 ksi plate contained ferrite and pearlite, contained about 0.16 weight percent carbon, and had an average ASTM International grain size number near 12 (average grain diameter around 6 μm) for the ferrite. The distribution of the pearlite throughout the plate was varied depending upon the component (e.g., perimeter column plate was normalized for good pearlite distribution, while spandrel material was moderately banded). The microstructure observed from the lower portion of the column was closely representative of the original plate, with the exception of the spheroidization of the cementite phase. The spheroidization was most likely a result of extended exposure of the steel in this region to temperatures just below the lower critical temperature (A_1, ~727 °C).

However, the microstructure for the material in the corroded regions was quite different. With the knowledge that there exist many different thermal processing paths that could be taken to achieve similar microstructures, the following hypothesis was presented as a possible explanation for the observed features in the microstructure. Assuming that the original microstructure in this area was similar to that found in Fig. 6–22a, the re-distribution of pearlite and larger ferrite grain size would imply significant changes in the microstructure that could have only been achieved through austenitizing of the steel. Concomitantly, this would suggest that temperatures were much higher in this portion of the plate than found at the base of the column. With the average weight percent carbon in the material at 0.16, the plate temperature would have to exceed 830 °C (above the upper critical temperature [A_3]) to enter the fully austenitic region. In this region, both the original ferrite and pearlite have completely transformed. The exact excursion above this line and the time within the field were difficult to determine. However, it did not appear that normalization (heat treatment designed to produce a uniform microstructure) nor

homogenization (heat treated designed to eliminate or minimize compositional segregation) of the material occurred. If normalization had been completed, the ferrite grain size would be far more uniform throughout the plate than observed in Fig. 6–21a. Further, the fact that the pearlite was heavily banded indicated that homogenization did not occur. This heat treatment requires relatively high temperatures (typically well above A_3) for extended periods (tens of hours). In fully achieving this heat treatment, the alloying elements, such as Mn, Si, or Cr, could diffuse uniformly throughout the structure. As seen by the present banding in the material, this was not the case. Instead, it appears that at some point in this sample's history, it reached a relatively high temperature (above the A_3 line) in which the original microstructure was eliminated, but did not remain for an extended period of time in the austenite region in order to obtain an equilibrium ferrite grain size or to reduce the chemical segregation within the structure.

A final clue to the history was in the heavy banding itself. While the chemical segregation of the structure did not change from the as-rolled plate to the exposed column, the cooling rate at these two "stages" of the plate's history must have been different. During processing of the plate, the cooling rate was sufficiently fast that a nearly homogeneous distribution of pearlite occurred due to the lack of time for carbon to diffuse. However, in the present structure, it appears that once the elevated temperature was reached, there was ample time for carbon to diffuse back to the alloy element-rich bands in the microstructure, and thus, the heavy banding occurred within the material. This latter premise was reasonable as the steel in the debris pile at the WTC site had a relatively long time to cool down when compared to typical processing cooling rates.

As a final note concerning K-16, a preliminary metallurgical examination was conducted on a portion of this column and reported in Appendix C of the FEMA/BPAT study (McAllister 2002). The sample (specified as Sample #2 in the appendix) consisted of a portion of the flange and outer web in the heavily corroded/eroded area of the column. The image in Fig. 6–23 was taken of column K-16 on the NIST campus showing that the size, shape, and orientation of the sample was identical to the coupon removed at the recovery yard by one of the FEMA/BPAT team members. The samples evaluated in the FEMA study and this investigation originated from the same outer web plate at a distance no further than 0.5 m apart. In the FEMA study, the following findings were reported:

1. The steel was a high strength low-alloy (HSLA) steel containing copper.

2. Thinning of the steel occurred by high temperature corrosion as a result of combined oxidation/sulfidation processes.

3. The rate of corrosion/erosion of the columns, while unknown, was found to be accelerated by the sulfidation attack via a solid state diffusion mechanism.

4. The high concentration of sulfides in the grain boundaries of the corroded regions of the steel occurred due to copper diffusing from the HSLA steel combining with Fe and S, thus making both discrete and continuous sulfides in the steel grain boundaries.

5. Temperatures in the corroded region of the steel were likely to be in the range of 700 °C to 800 °C.

6. No source for the sulfur was identified.

7. Two possible explanations for the corrosion events: the result of long-term heating in the ground following the collapse of the buildings or start of corrosion phenomenon prior to collapse of the buildings that accelerated the weakening of the steel structure.

The present analysis led to different conclusions regarding items 4, 5, and 7 above, in part, due to the opportunity to examine the condition of the entire column as a whole instead of just an isolated portion.

The FEMA study reported the formation of (Fe,Cu) sulfides in the grain boundaries (Finding #4). These results were also presented at the International Metallographic Society conference in San Antonio, TX, in August of 2003, where significantly large copper sulfide phases (on the order of 10s of microns) were observed in the outer scale (Vander Voort 2003). The outer web plate analyzed had copper additions of approximately 0.05, based upon the chemical results obtained in this study. Given this low value of copper in the steel, it would seem unlikely that enough copper could diffuse to form the amount of (Fe,Cu) sulfides observed in the FEMA/BPAT analysis. In addition, copper containing sulfides were not found during the present analysis. Therefore, it was more likely that a localized, external source of copper was available to form these phases in the sample analyzed in the FEMA/BPAT report.

The study further states that temperatures were in the range from 700 °C to 800 °C (Finding #5). However, very limited supporting evidence was given for this claim. Unlike the analysis of the steel from WTC 7 (Sample #1 of Appendix C, FEMA/BPAT study) where corrosion phases and morphologies were able to determine a possible temperature region, no comments were made concerning the microstructure observed in the corroded regions which may have yielded addition information in which to make the assertion of the temperature range for Sample #2. The present analysis found, through a microstructural evaluation, that the temperature excursion was much higher than the range stated.

Finally, as this piece was clearly in a prone position during the corrosive attack and was located no higher than the 53rd floor of the building, this degradation phenomenon had no bearing on the weakening of the steel structure or the collapse of the building (Finding #7).

Floor Truss Material C-115 and C-131

There were two unique pieces of truss rod identified as having possibly experienced high temperature exposure based upon the sort of damage characteristics observed. These were samples C-115 and C-131, which had portions of truss rods with significantly reduced cross-sections. The as-built location and exposure history of these two pieces were unknown. Thus, the results of this metallurgical analysis did not aid in determining possible impact damage to the floor truss sections or help to ascertain possible collapse mechanisms for the towers.

As both rods appeared to have similar damage characteristics, only one sample (C-115) is discussed below. Sample C-115 arrived at NIST as shown in Fig. 6–24. The entire length of the sample (roughly 2.5 ft) was non-uniform in thickness. Sections of maximum and minimum thickness are indicated on Fig. 6–24. There were two areas where the diameter appeared to be a maximum of approximately 1.10 in. These areas were located at what appears to be a knuckle of the truss design and the opposite end of the reduced section of the rod; this end was flame cut prior to arriving at NIST. The opposite end of the rod had a reduced area measuring approximately 0.25 in. This tip was severely deformed, as if it had been dragged. The entire sample appeared corroded, though the remaining scale was not friable.

Figure 6–24 indicates the location of samples removed for analysis. One was taken from the significantly reduced area (hereafter referred to as "reduced section") and the other from the opposite end of the rod where the diameter was slightly greater than 1 in. (hereafter referred to as "1 in. section"). Chemical analysis of the two sections of rod indicated a slight difference in carbon levels (0.16 weight percent for the 1 in. section and 0.18 weight percent for the reduced section). The Mn contents were similar (~0.8 weight percent), with additions of V also observed (0.038 weight percent for the 1 in. section and 0.028 weight percent for the reduced section). Based upon these results, the rod met chemistry specifications for A 242 and most likely had an original diameter of 1.14 in. (NIST NCSTAR 1-3A).

Microstructural evaluation of both ends revealed a ferrite-pearlite structure with fairly coarse constituents, Fig. 6–25. The ferrite grains were relatively equiaxed with no banding of the pearlite. Additionally, there were no indications that spheroidization of the pearlite had occurred. In contrast, other (undeformed) rods of A 242 examined revealed a different structure, Fig. 6–26. In addition to the significantly smaller ferrite grain size (and size of pearlite colonies), in general, a Widmanstätten morphology was widely observed throughout the structure. Development of ferrite in this morphology typically occurs when the steel is austenitized at a relatively high temperature, above the A_3 line, and then cools at a relatively fast rate (Samuels 1980). Some banding of the pearlite was locally observed.

The corrosion product at the surface of the rod from the reduced section was also investigated. There was some evidence that decarburization did occur near the surface, Fig. 6–27. A close-up of the scale is shown in Fig. 6–28 with four regions of interest noted. The first was the actual corrosion scale itself. Numerous gray-colored and gold-colored phases, when viewed light optically, were present in the scale. Figure 6–28a shows a secondary electron image of this region and the location of EDS analysis. Table 6–3 displays the results of the EDS analysis. From these results, it appears that a mixture of oxide and sulfides were present (points 1-4 and 9-11). These scales were similar to those observed on corroded samples from panel K-16. The second region of interest was the matrix directly surrounding the advancing corrosion product, Fig. 6–28b. This region appeared to be free of any internal oxidation or grain boundaries and, according to EDS analysis (points 5, 8, and 12), contained iron with nickel in solution. Within this region were two other phases; one needle-like and the other with a "feathery" appearance. These two phases can be seen in Fig. 6–28c. Both of these contained iron and nickel, with the nickel concentrations higher than that found in the surrounding matrix (points 6, 7, 13, 16-18). The next region was an internal oxidation region of varying thickness and depth into the sample, also observed in Fig. 6–28c. The final area was the matrix itself.

Two facts have led to the conclusion that this floor truss rod was heated above the A_3 line: 1) the high ductility displayed by the material under load and 2) the constituents observed in the microstructure were significantly larger than observed for other A 242 rods. Exposure to this high a temperature explains how the extent of deformation observed on the sample was obtained without the concomitant microstructural indications of deformation (e.g., elongated ferrite grains). At these temperatures, and under the applied tensile load, the rod was extremely ductile, which allowed it to thin down to the dimensions observed. Deformation of the microstructure was eliminated through dynamic recrystallization of the austenite grains and upon cooling, no indication of deformation was observable in the microstructure. Additionally, it is likely that (1) this rod was not at high temperature for an extended period of time as a decarburization zone at the surface of the rod was not found or (2) the cooling rate of the rod was such that the carbon was able to uniformly redistribute after exposure. While review of the evidence does not give any indication as to when the temperature excursion and subsequent deformation occurred, it is

likely that the piece was in the debris pile at the WTC site when the corrosion products developed, as external sources for sulfur and nickel were necessary to obtain the corrosion phases observed.

6.4   SUMMARY

Twenty-one exterior panels and four core columns were visually inspected to determine the extent of fire exposure of the various structural elements. From this analysis, the following were concluded:

- The majority of areas examined using the paint cracking technique had "negative" results, indicating that temperatures of the elements did not exceed 250 °C, even though photographic evidence indicated that several locations experienced severe fire exposure, up to 15 min of direct flaming, prior to collapse.

- There were three "positive" findings from the areas analyzed, indicating that mud cracking of the paint occurred.

    - Panel K-1 (A209: 97-100): Located on the flanges of the crushed portion of column (note: the spandrel directly below this area was "negative"),

    - Panel K-2 (A236: 92-95): Located on the spandrel just below the floor level (note: spandrel above the floor level and column plates below spandrel were "negative"),

    - Panel N-8 (A142: 97-100): Located on a seat and its standoff plates, the spandrel was "negative" both above and below floor levels.

- The selected spandrel steels that were identified to have been exposed to severe fire events prior to the collapse of the building did not experience material degradation due to the exposure.

- Results indicated that three of the four seats observed to be exposed to severe pre-collapse fire conditions did not experience significant degradation as a result of the exposure. Results from the seat taken from panel N-8 indicate that this seat may have been exposed to elevated temperatures.

- From the limited number of recovered structural steel elements, no conclusive evidence was found to indicate that pre-collapse fires were severe enough to have a significant effect on the microstructure that would have resulted in weakening of the steel structure.

NIST has documented approximately 3 percent of all perimeter columns and 1 percent of all core columns intersecting floors with pre-collapse fires. Thus, the preceding forensic analysis does not, and cannot, give a picture of temperatures seen by the vast majority of perimeter and core columns.
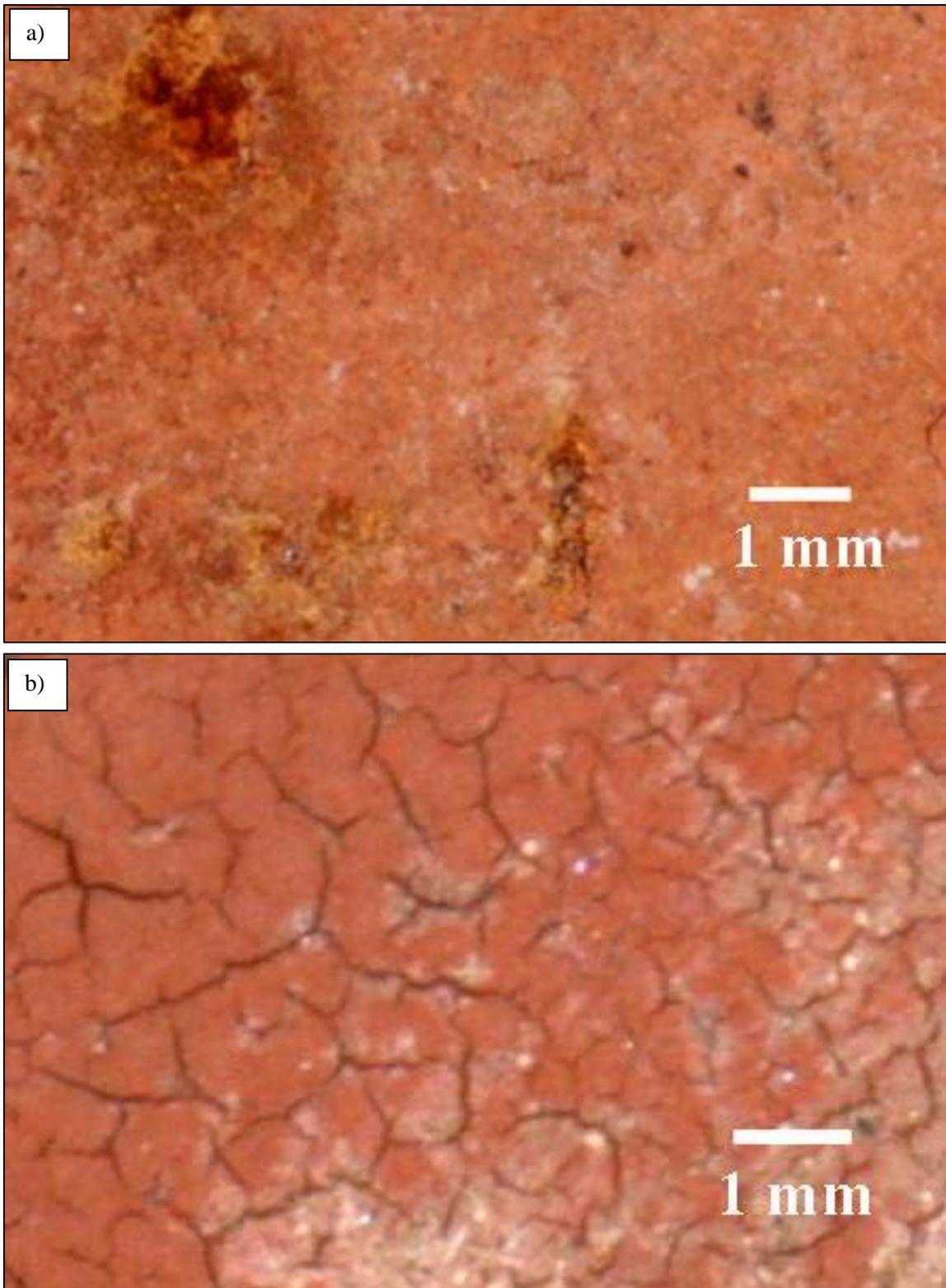
Source: NIST.

Figure 6–1. Photographic images of the primer paint. a) paint in its original condition and b) mud cracking of paint after exposure at 250 °C for 1 h.
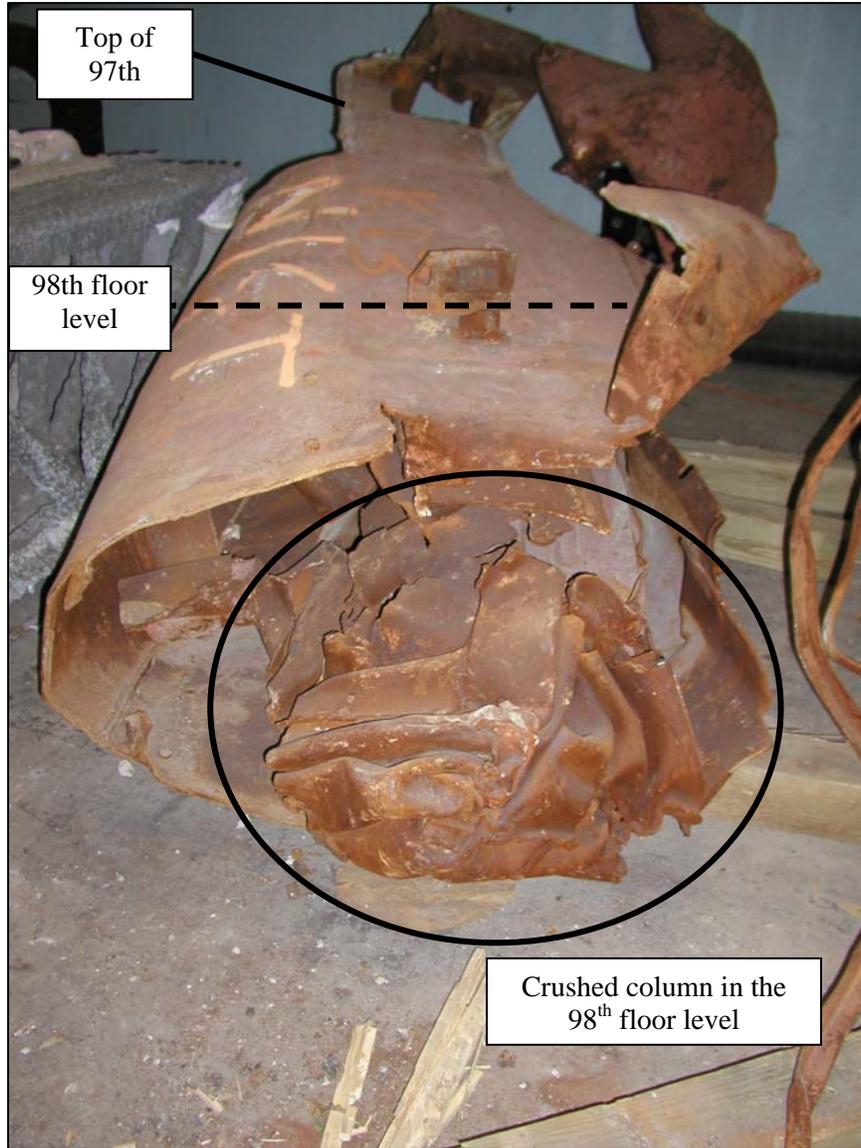
Source: NIST.

Figure 6–2. Crushed portion of column 210 in the area of the 98th floor of WTC 1 (panel K-1, A209: 97-100). Mud cracking of the paint was observed in crushed portion of this column. The cracking of the paint was a result of either temperature exposure over 250 °C, mechanical deformation, or environmental degradation.
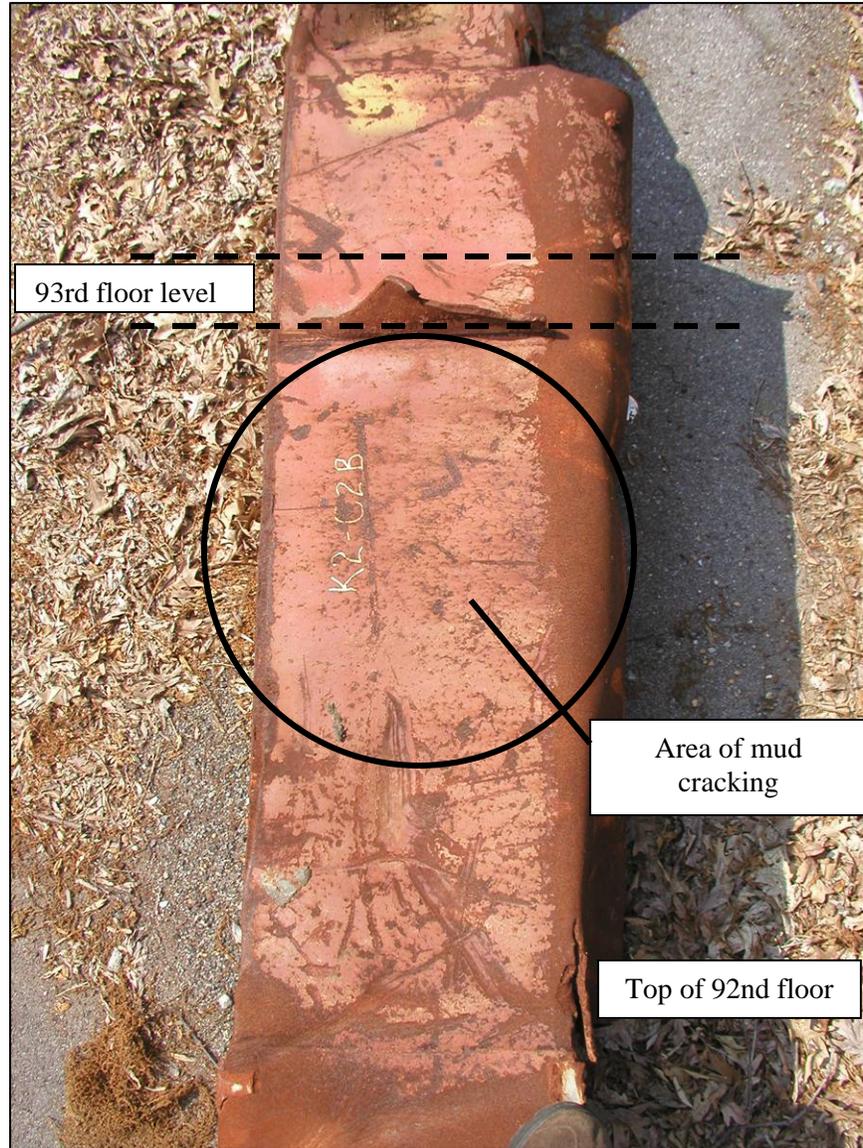
Source: NIST.

Figure 6–3. Spandrel at the 93rd floor of column 236 of WTC 1 from panel K-2 (A236: 92-95). Mud cracking of the paint occurred below the 93rd floor line. No evidence of mud cracking was observed above the floor line.
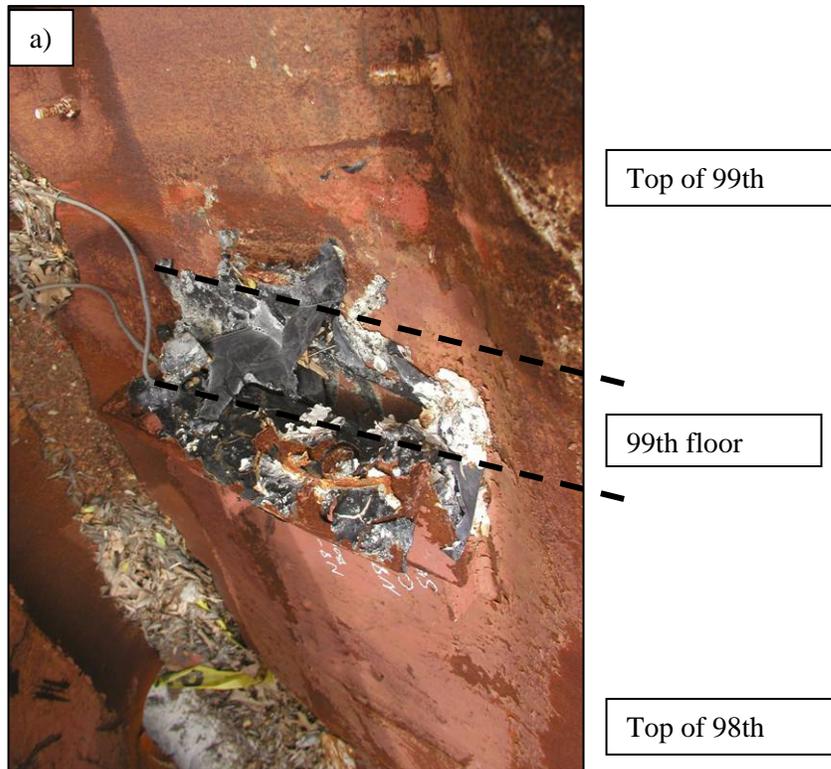
Source: NIST.

Figure 6–4. Truss seat of the 99th floor on column 143 of WTC 1 from panel N-8 (A142: 97-100). Mud cracking was observed only on the truss seat and standoff plates. a) Top view showing the re-solidified black plastic with imbedded papers, most likely a binder of some type and b) bottom view showing the drip pattern.
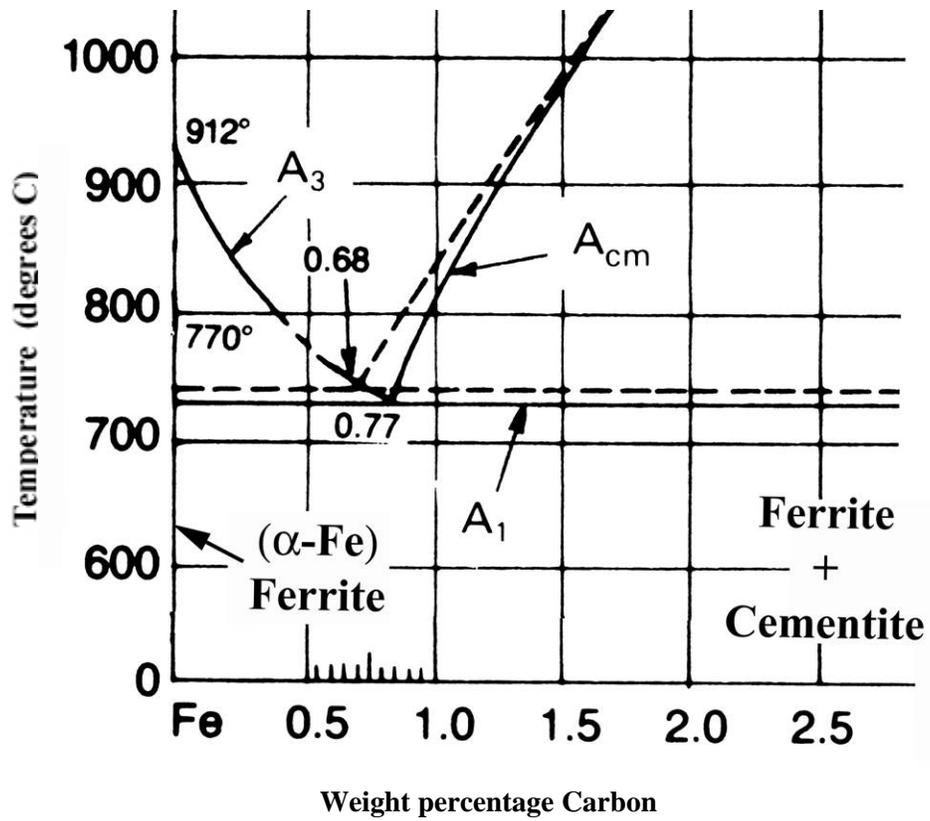
Figure 6–5. Portion of the iron-carbon (Fe-C) phase diagram.

<div style="text-align:center">t = 0 h   t = 0.25 h   t = 0.5 h   t = 1 h   t = 2 h</div>
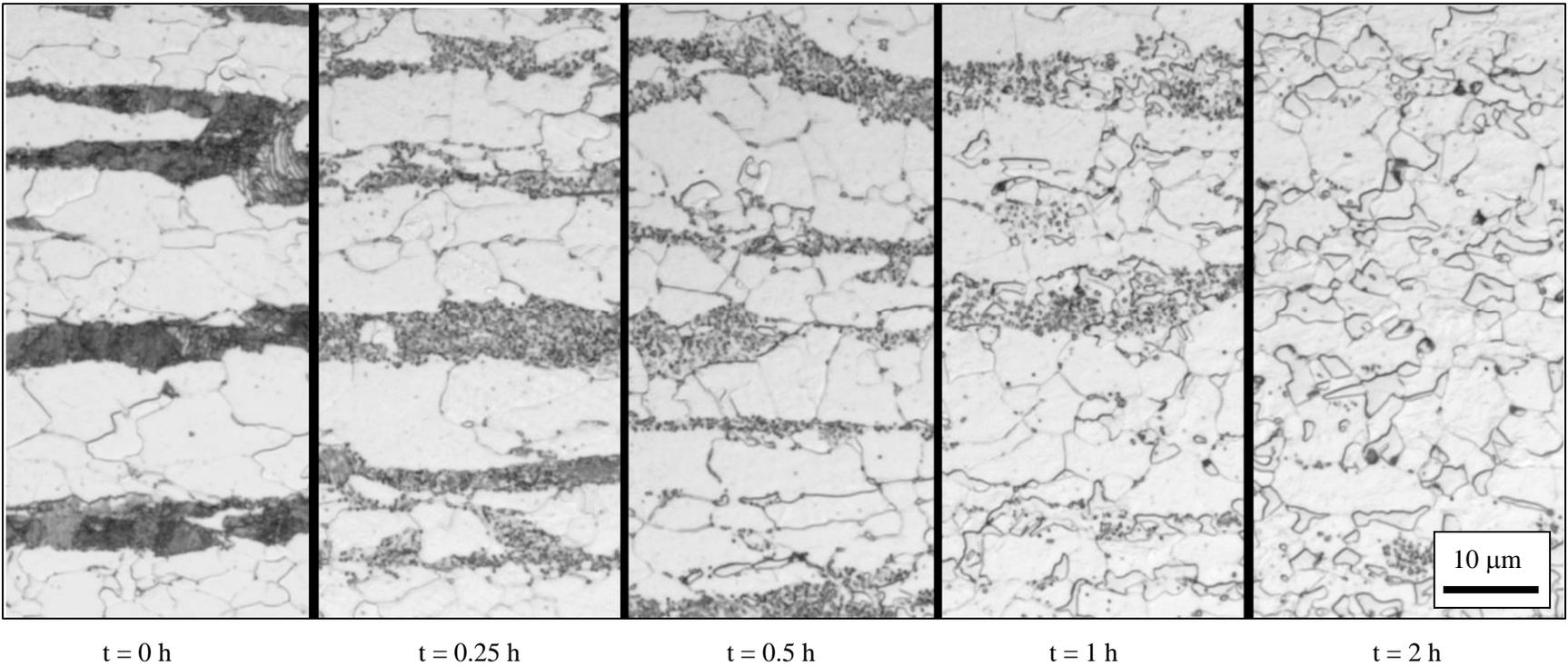
Source: NIST.

Figure 6–6. Change in microstructure of a 60 ksi flange plate that was heat treated in a laboratory furnace at 625 °C for various times. Pearlite was observed to spheroidize. Sample shown was from panel N-7 (WTC 1, column 126, 97th floor). Two percent nital and 4 percent picral etch.

t = 0 h   t = 0.25 h   t = 0.5 h   t = 1 h   t = 2 h

10 μm
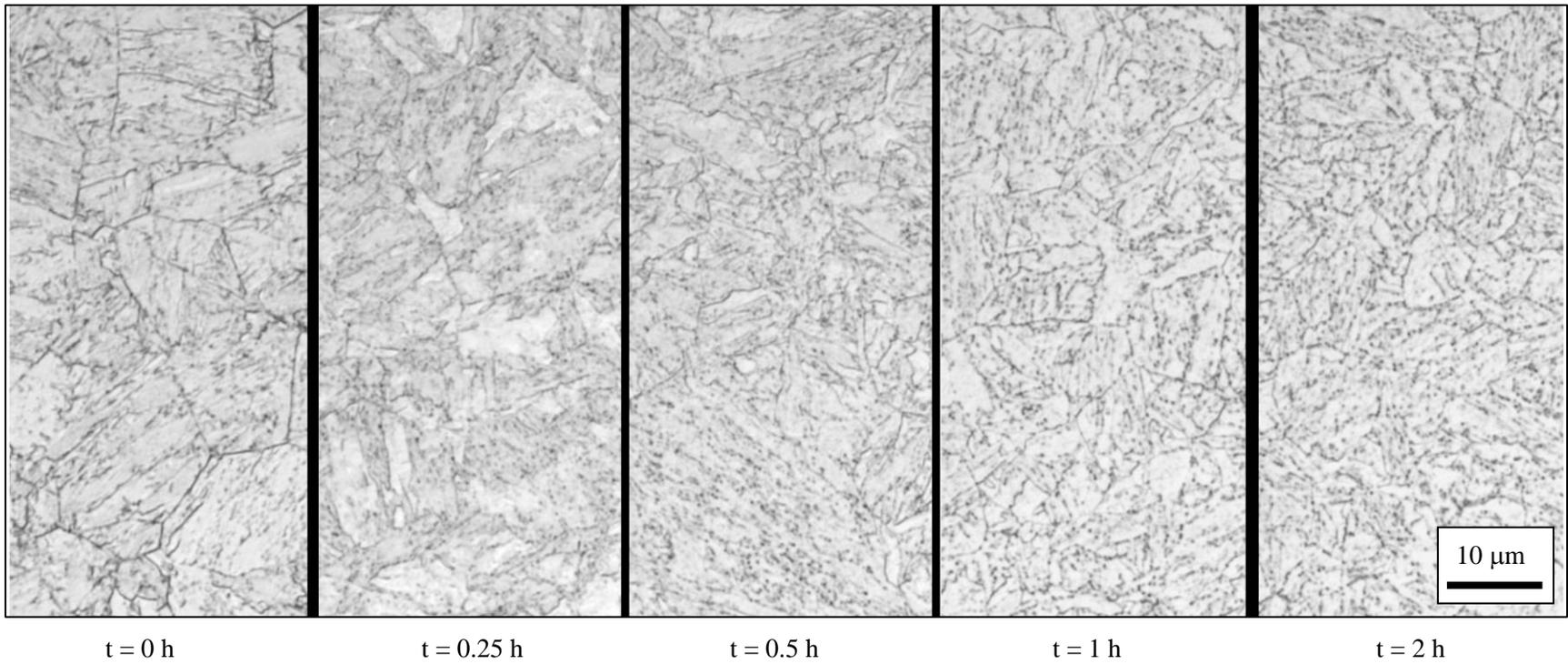
Source: NIST.

Figure 6–7. Change in microstructure of a 100 ksi flange plate that was heat treated in a laboratory furnace at 625 °C for various times (t). Sharpness of lath boundaries was observed to decrease while the carbide precipitates became more discernable. Sample was from panel C-10 (WTC 1, column 451, 88th floor). Two percent nital and 4 percent picral etch.
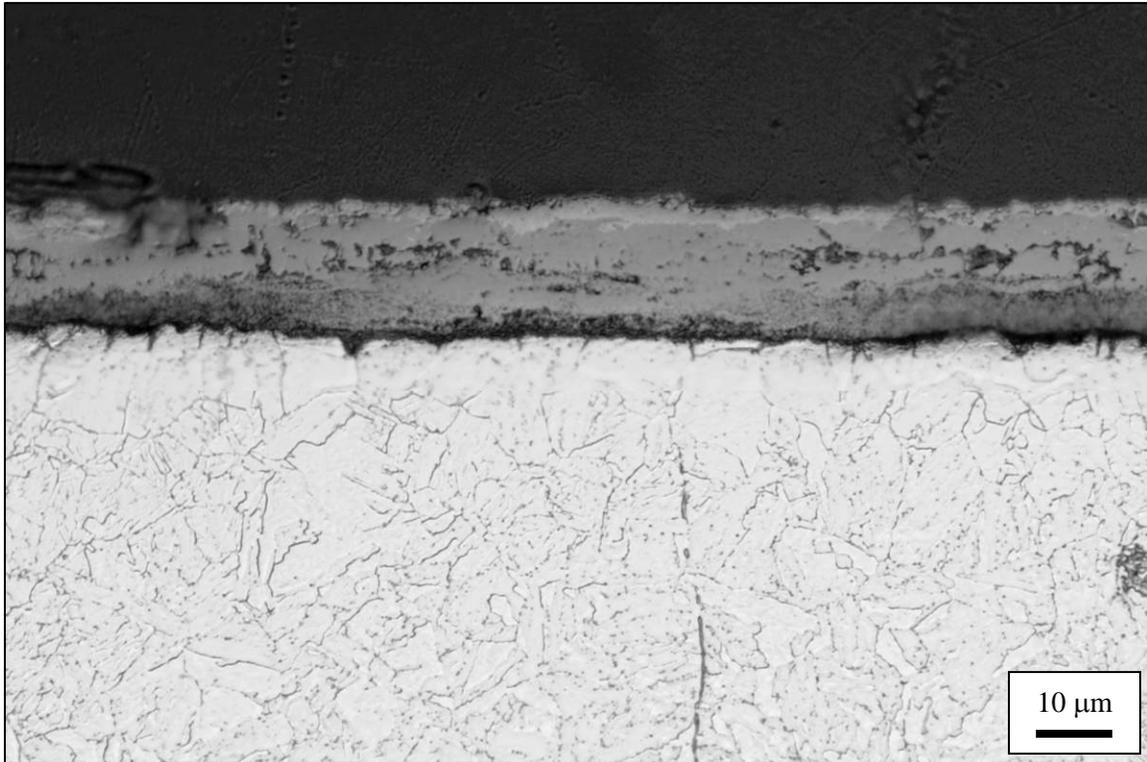
Source: NIST.

Figure 6–8. Iron oxide scale that developed on a 100 ksi quenched-and-tempered flange plate after isothermal exposure at 625 °C for 2 h. Sample was from panel C-10 (WTC 1, column 451, 88th floor). Two percent nital and 4 percent picral etch.
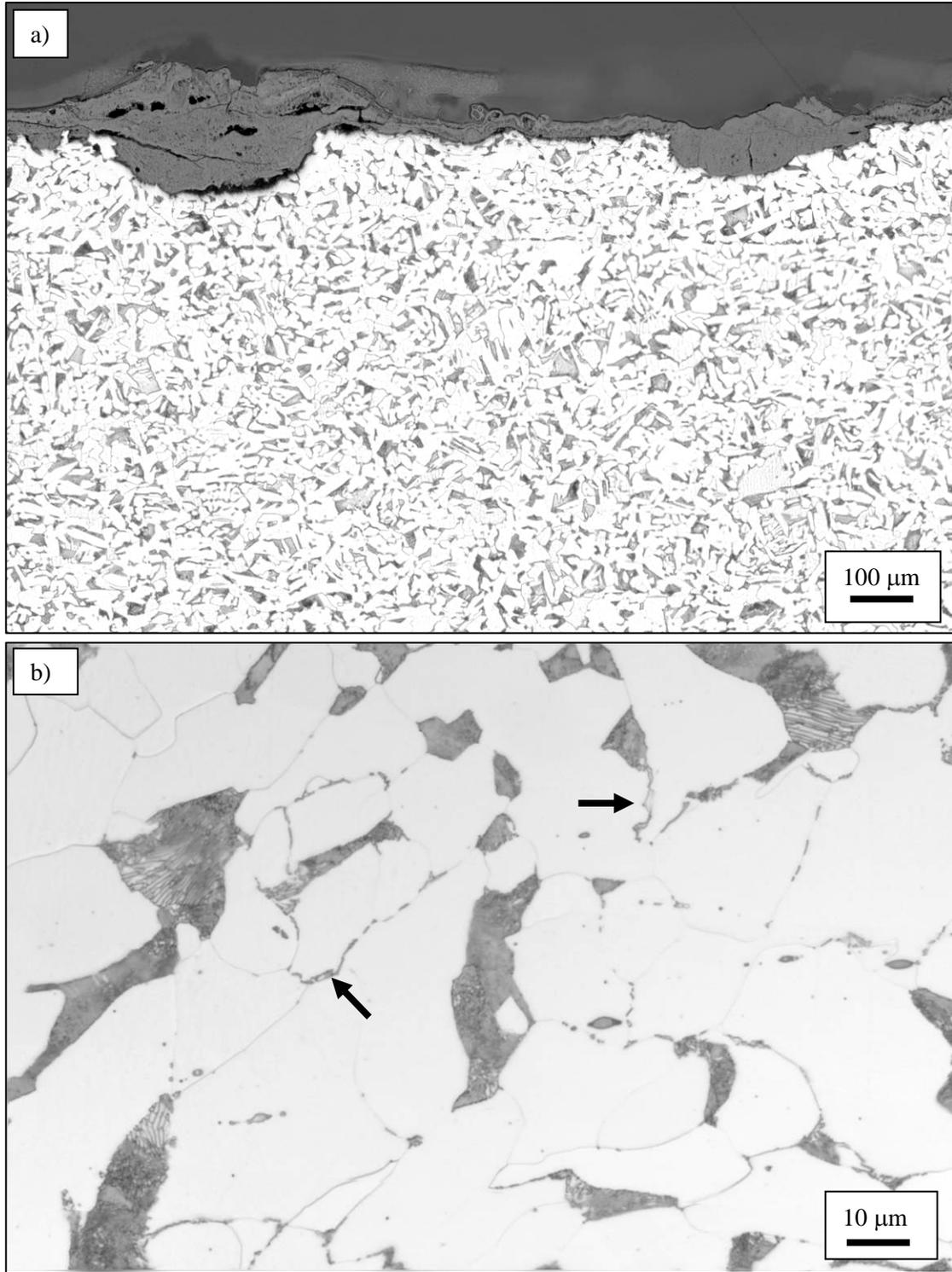
Source: NIST.

Figure 6–9. Light optical micrographs showing the microstructures from "fire exposed" spandrels. a) Ferrite-pearlite structure and developed oxide scale, b) lamellae were observable in pearlite, carbides (indicated by arrows) decorating ferrite grain boundaries. Both images taken from the 99th floor spandrel of WTC 1, panel M-2 (A130: 96-99). Two percent nital and 4 percent picral etch.

| t = 0 h | t = 0.25 h | t = 0.5 h | t = 1 h | t = 2 h |
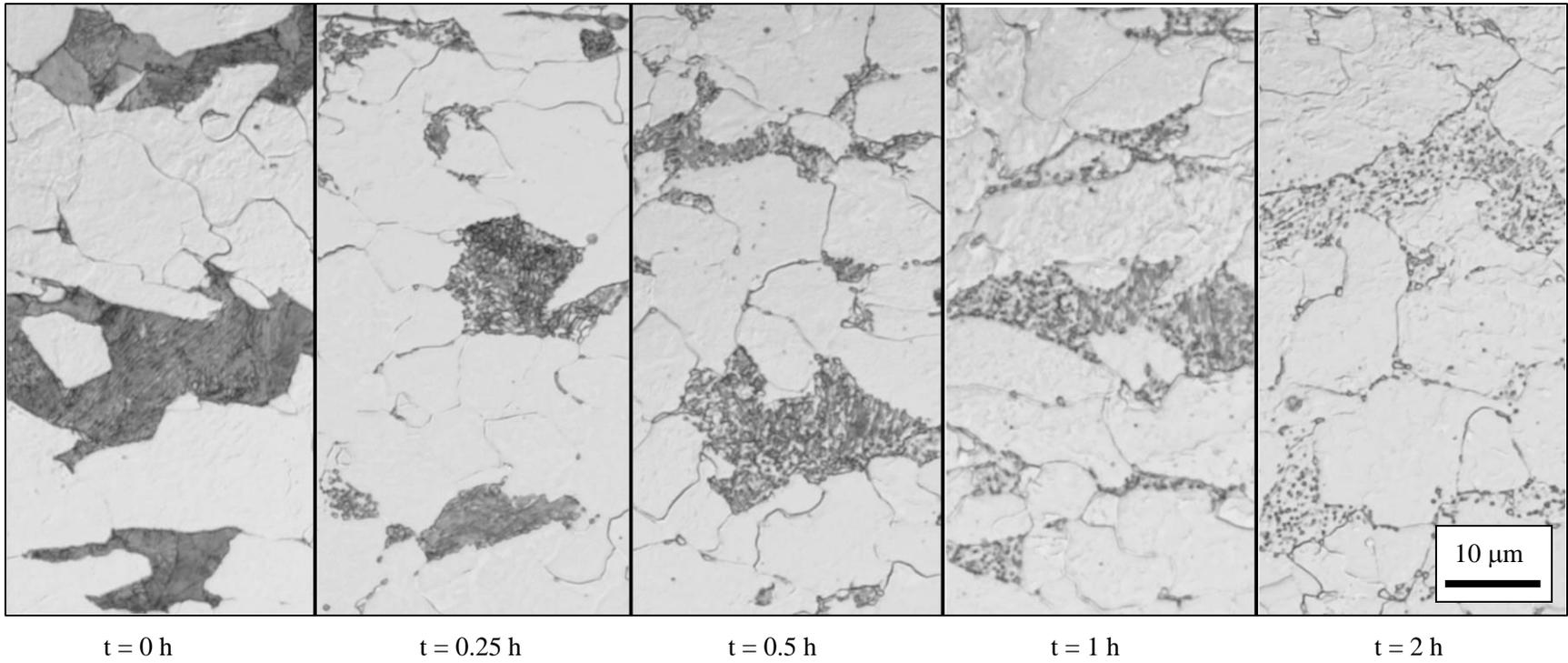
Source: NIST.

Figure 6–10. Change in microstructure of a 42 ksi spandrel plate that was heat treated in a laboratory furnace at 625 °C for various times. Pearlite was observed to spheroidize. Sample shown was from panel N-9 (WTC 1, 102nd floor spandrel, near column 154). Two percent nital and 4 percent picral etch.
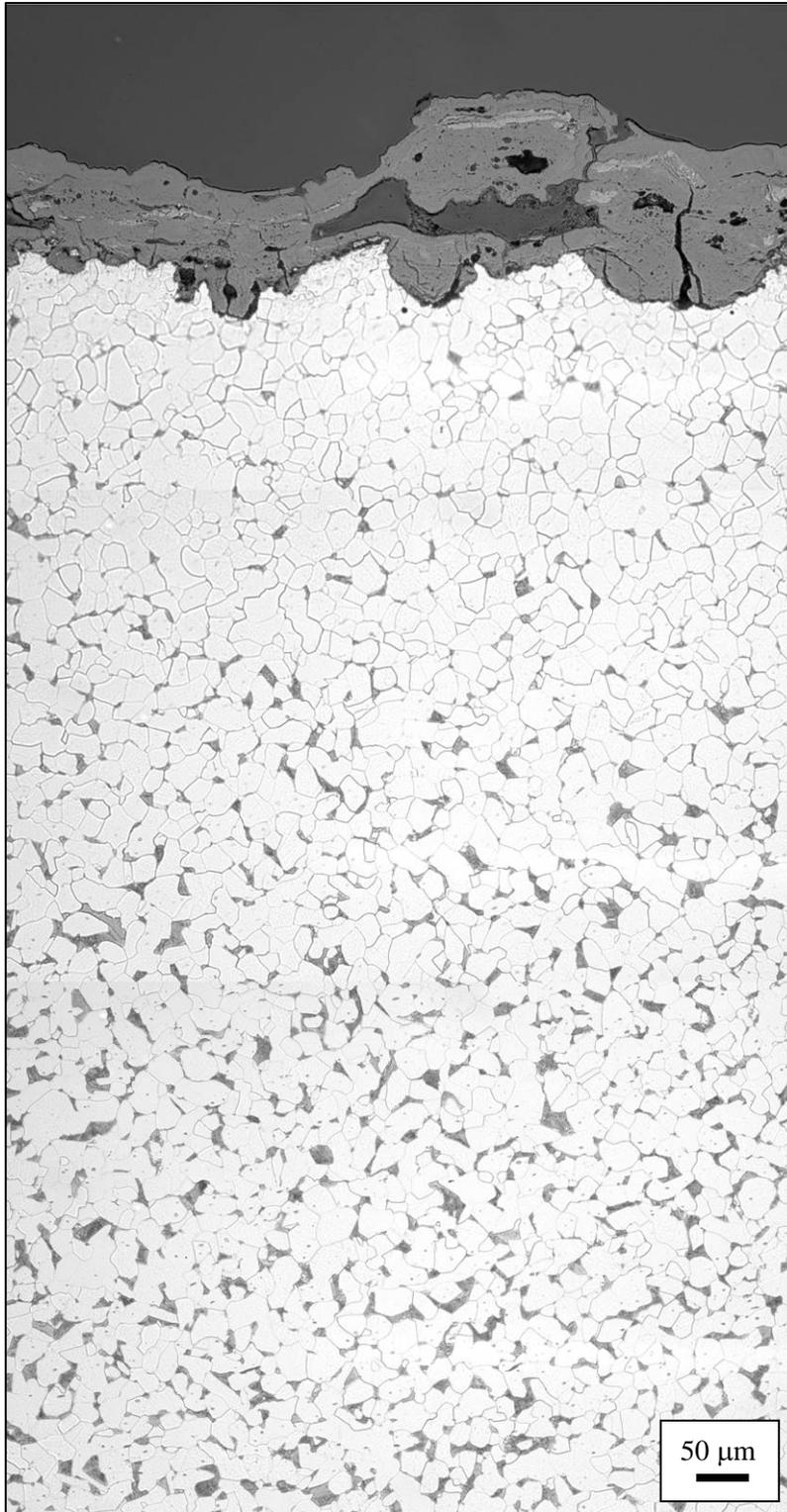
Source: NIST.

Figure 6–11. Light optical micrograph showing the partially decarburized zone found near the surface of a perimeter floor truss seat from directly above the airplane impact on the 99th floor of WTC 1, panel M-2 (A130: 96-99). Two percent nital and 4 percent picral etch.
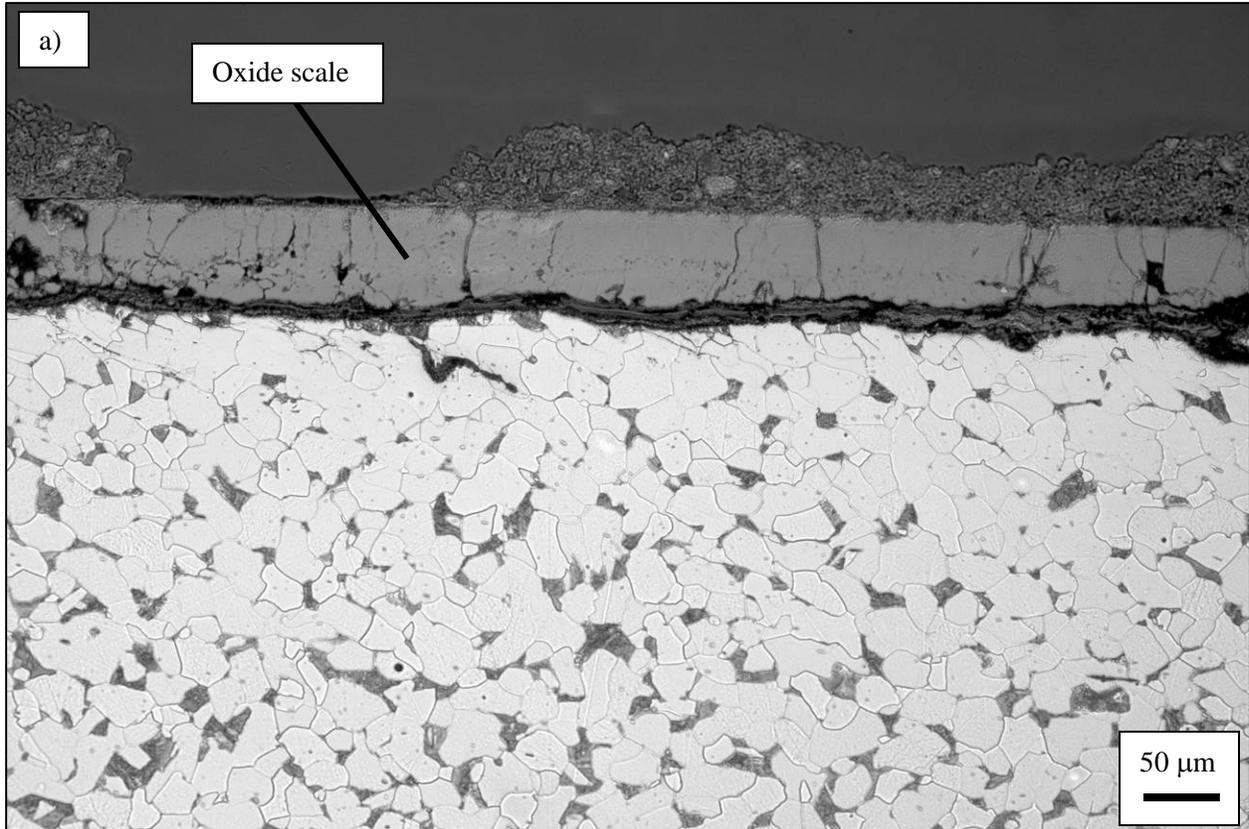
Source: NIST.

Figure 6–12. Light optical micrographs of the microstructure of a perimeter floor truss seat from the 99th floor of WTC 1, panel N-8 (A142: 97-100). a) Ferrite-pearlite microstructure and developed oxide scale. Two percent nital and 4 percent picral etch.
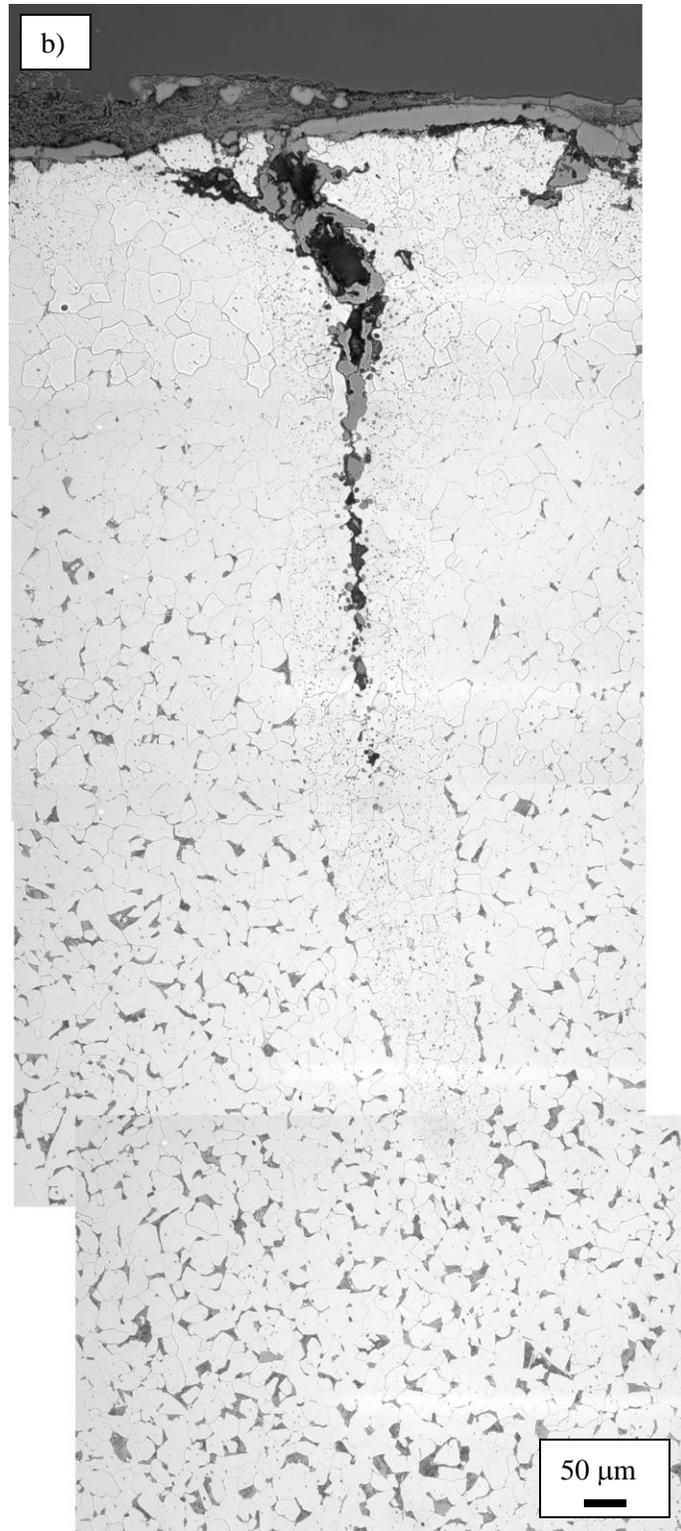
b)

50 μm

Source: NIST.

Figure 6–12. Light optical micrographs of the microstructure of a perimeter floor truss seat from the 99th floor of WTC 1, panel N-8 (A142: 97-100). b) penetration of the iron oxide phase with internal oxidation and decarburization fronts possibly due to elevated temperature exposure. Two percent nital and 4 percent picral etch (cont.).

t = 0 h   t = 0.25 h   t = 0.5 h   t = 1 h   t = 2 h
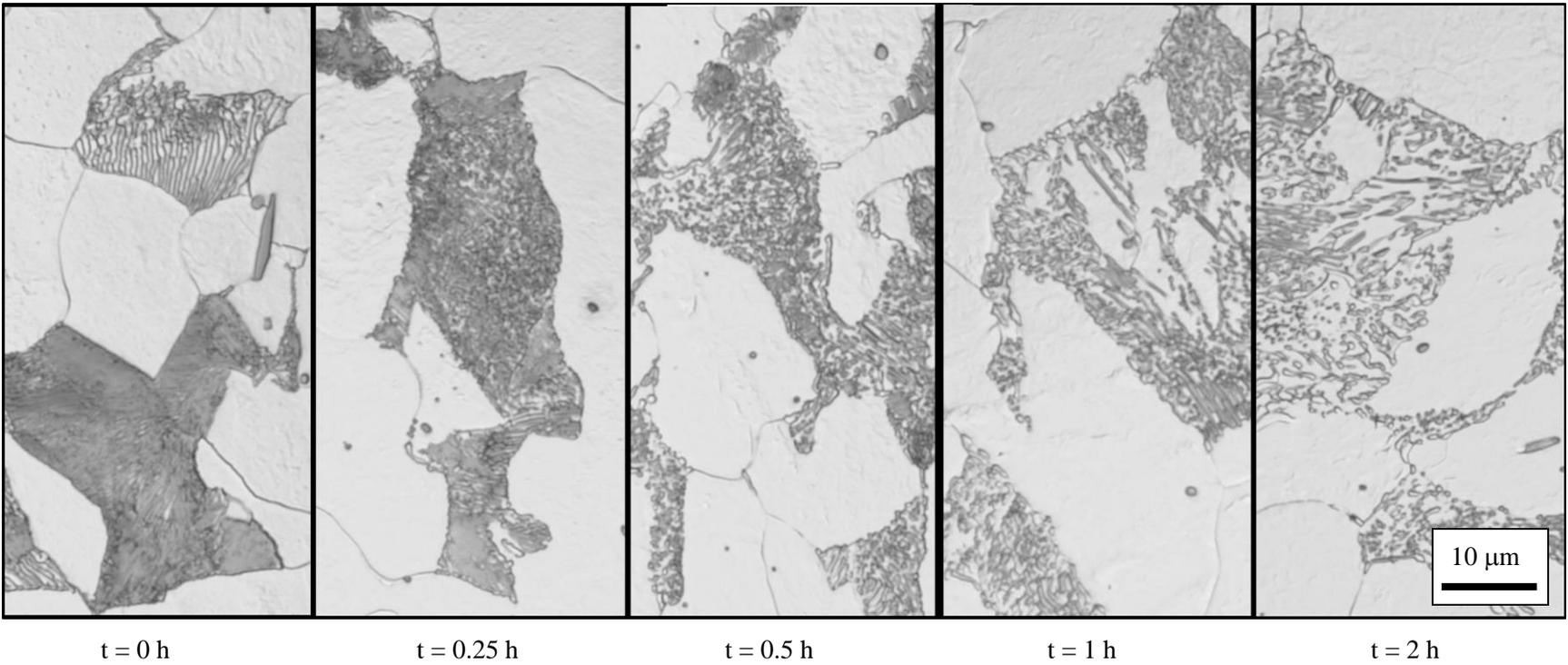
Source: NIST.

Figure 6–13. Change in microstructure of a truss seat that was heat treated in a laboratory furnace at 625 °C for various times. Pearlite was observed to spheroidize. Sample shown was from panel C-18 (WTC 2, column 231, 95th floor). Two percent nital and 4 percent picral etch.
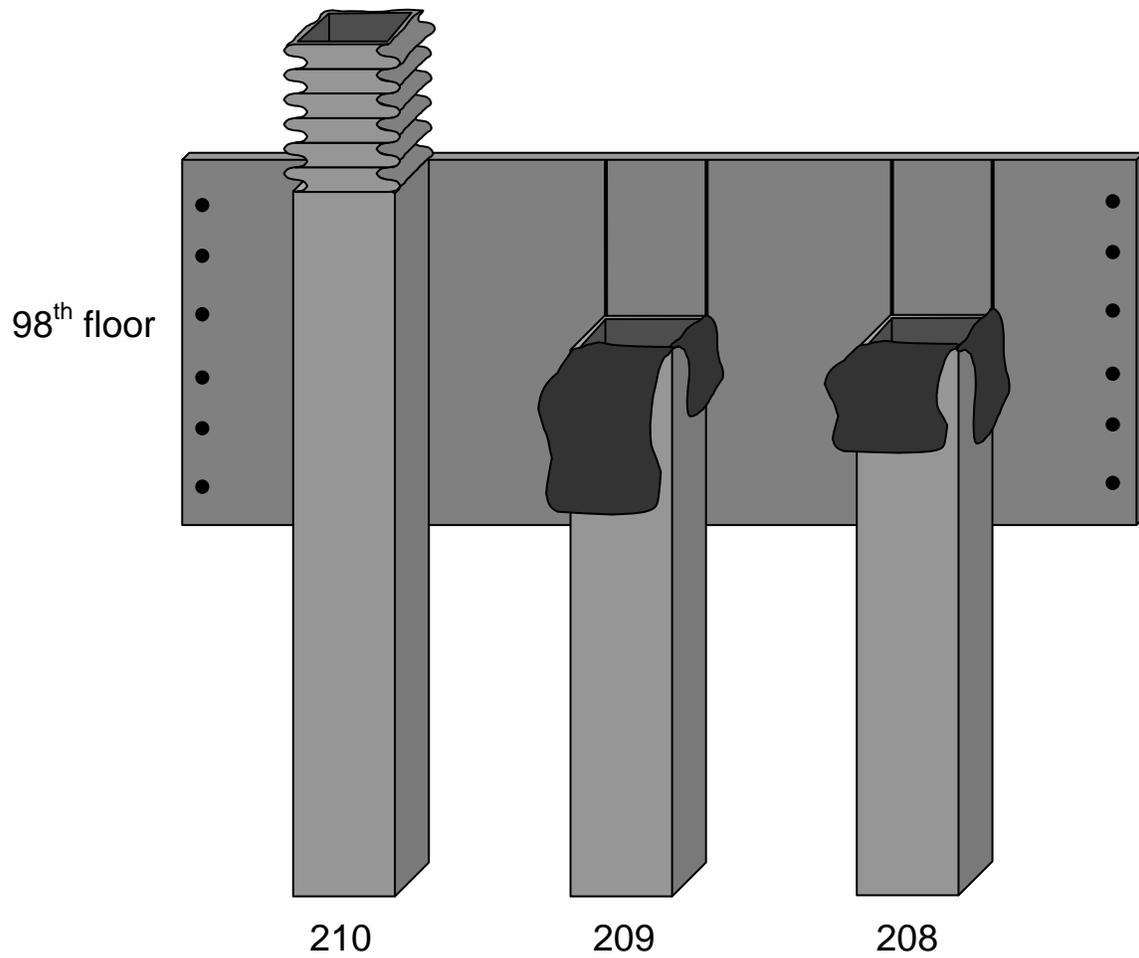
Figure 6–14. Panel K-1 from the east face of WTC 1 (A209: 97-100). a) Schematic showing the damage to the panel when viewed from outside the building looking inward.

b)

c)

Column 210 in the 98th floor level

d)

Column 210 in the 97th floor level

Source: NIST.

Figure 6–14. Panel K-1 (A209: 97-100). b) and c) crushed section above the 98th floor and d) relatively undeformed below the 98th floor spandrel. Removal areas of metallographic samples are shown in c) and d) by colored circles (cont.).

Source: Original photograph copyright Jeroen Morrien 2001.

Figure 6–15. Pre-collapse photographs of panel K-1 on the east face of WTC 1 (A209: 97-100) showing a) aluminum façade intact minutes after impact. Column 210 was indicated.

Source: Original photograph copyright Mark Stetler 2001.

Figure 6–15. Pre-collapse photographs of panel K-1 (A209: 97-100) showing b) external flaming of the panel at time 9:55:01 a.m., 34 min before collapse.
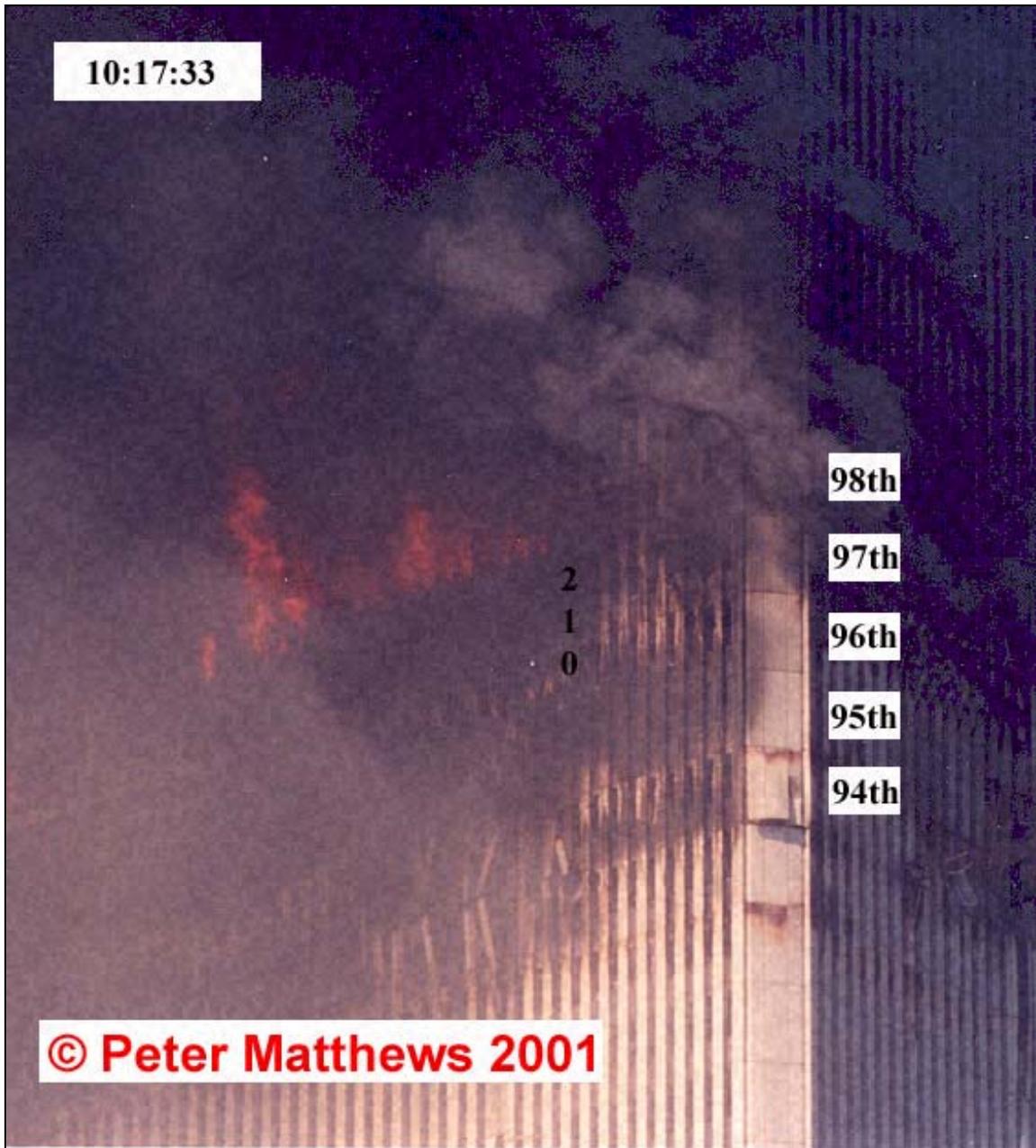
Source: Original photograph copyright Peter Matthews 2001.

Figure 6–15. Pre-collapse photographs of panel K-1 (A209: 97-100) showing c) fire has begun to recede from this area. Photograph taken approximately 12 min prior to collapse.
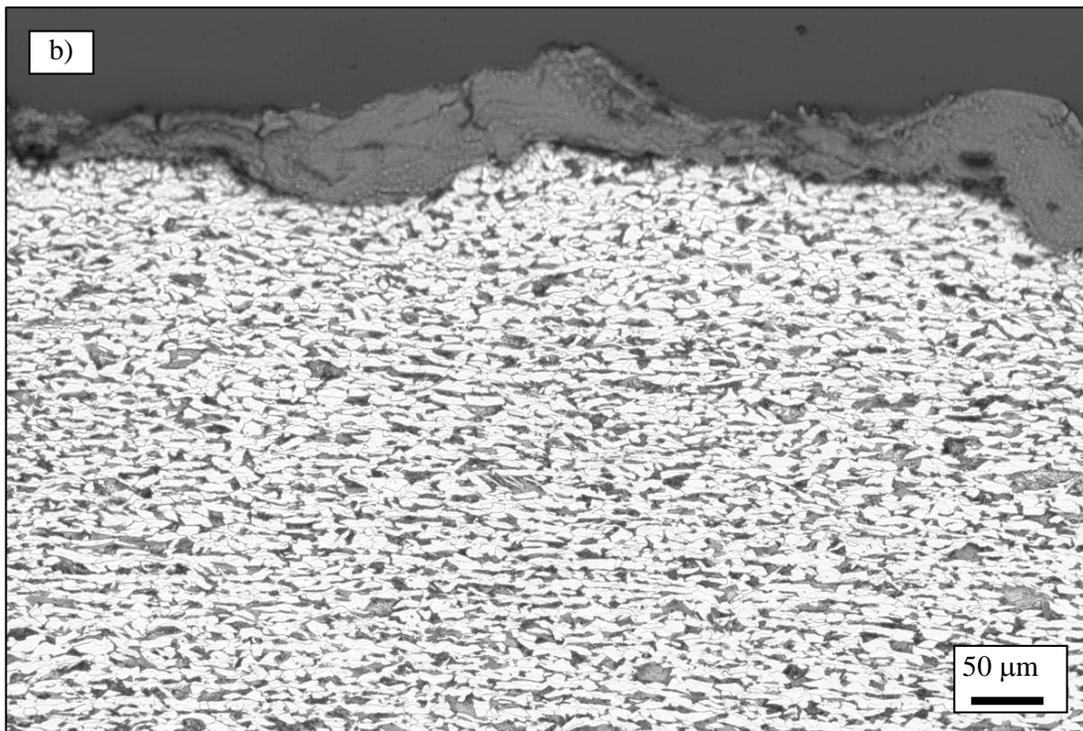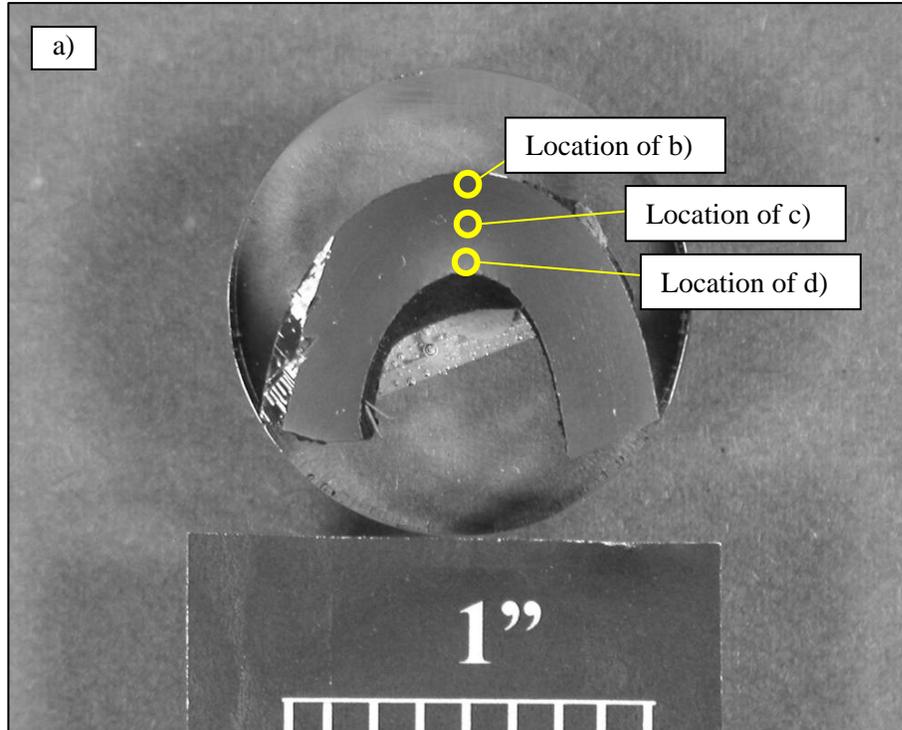
Source: NIST.

Figure 6–16. Images from a flange of column 210 of panel K-1 (A209: 97-100) from the crumpled area above the 98th floor spandrel. a) Location of micrographs taken on the bent sample, b) light optical micrograph of the outer surface of the sample showing elongated grains. Two percent nital and 4 percent picral etch.
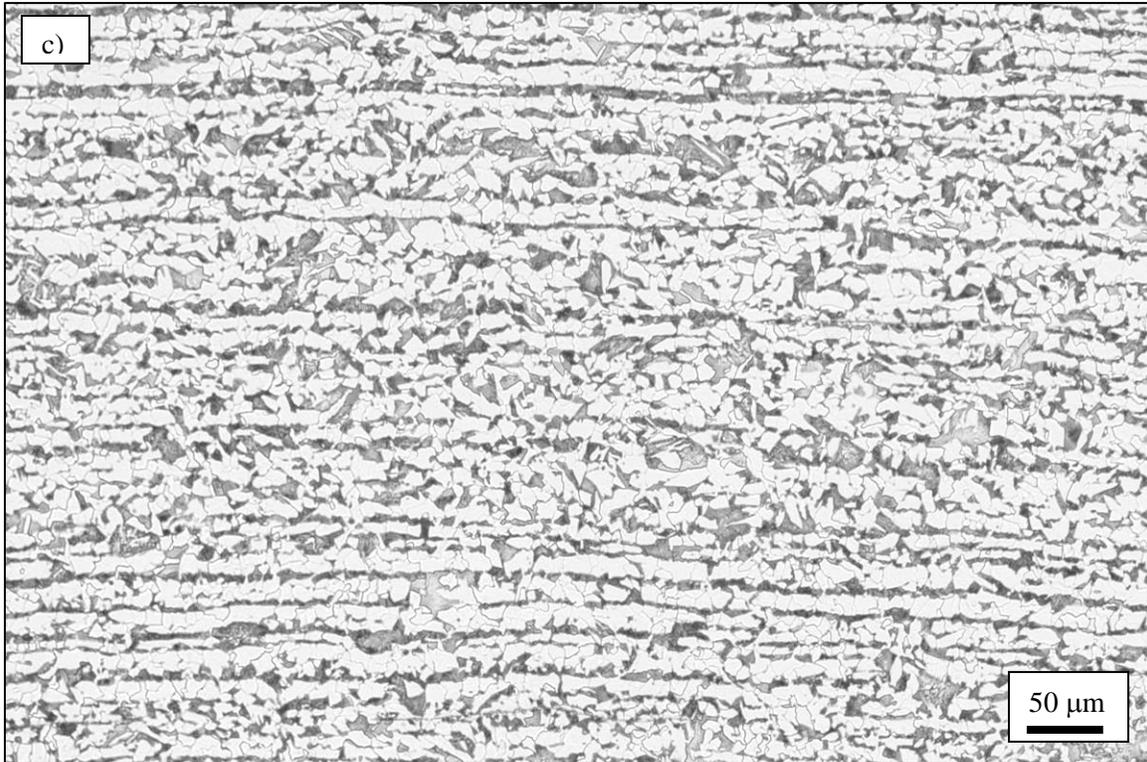
Source: NIST.

Figure 6–16. Light optical micrographs showing the microstructure from flange of column 210 of panel K-1 (A209: 97-100) from the crumpled area above the 98th floor spandrel. c) centerline of plate showing relatively undeformed grains of blocky ferrite and pearlite colonies. Two percent nital and 4 percent picral etch.
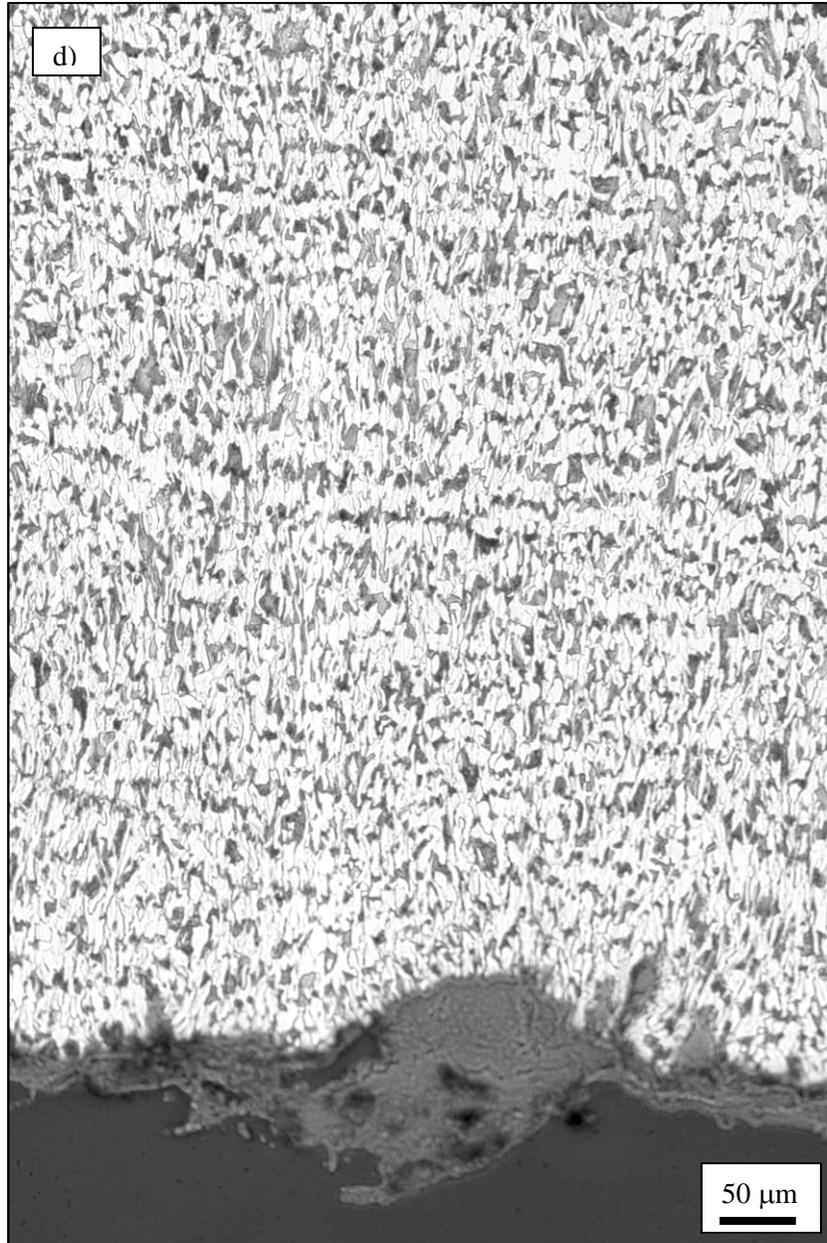
Source: NIST.

Figure 6–16. Light optical micrographs showing the microstructure from flange of column 210 of panel K-1 (A209: 97-100) from the crumpled area above the 98th floor spandrel. d) inner surface of plate showing compressed constituents of ferrite and pearlite. Two percent nital and 4 percent picral etch.
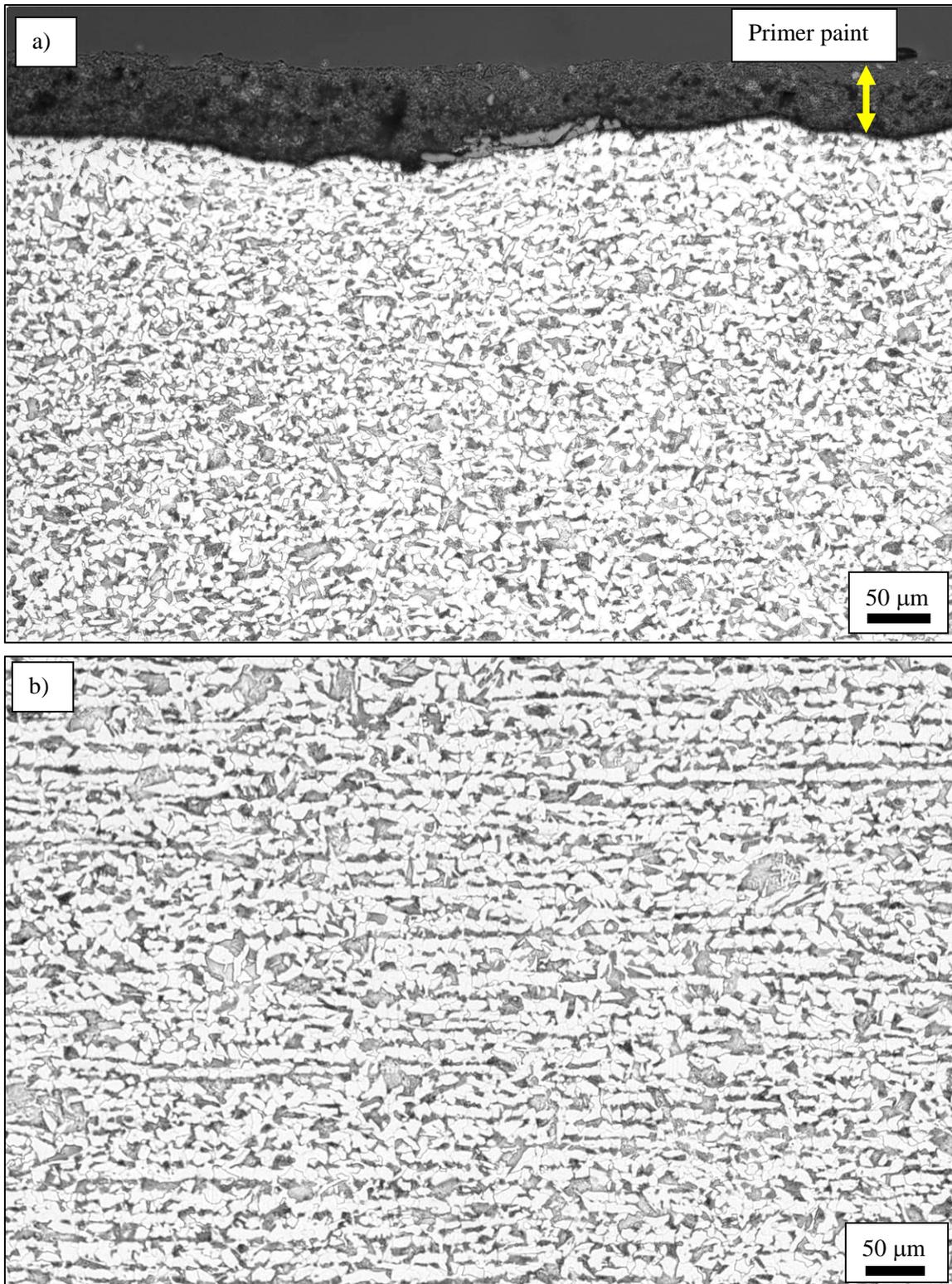
Source: NIST.

Figure 6–17. Light optical micrographs showing microstructure from flange of column 210 of panel K-1 (A209: 97-100) from the flange below the 98th floor spandrel. a) outer surface of sample and b) center line of plate. Two percent nital and 4 percent picral etch.
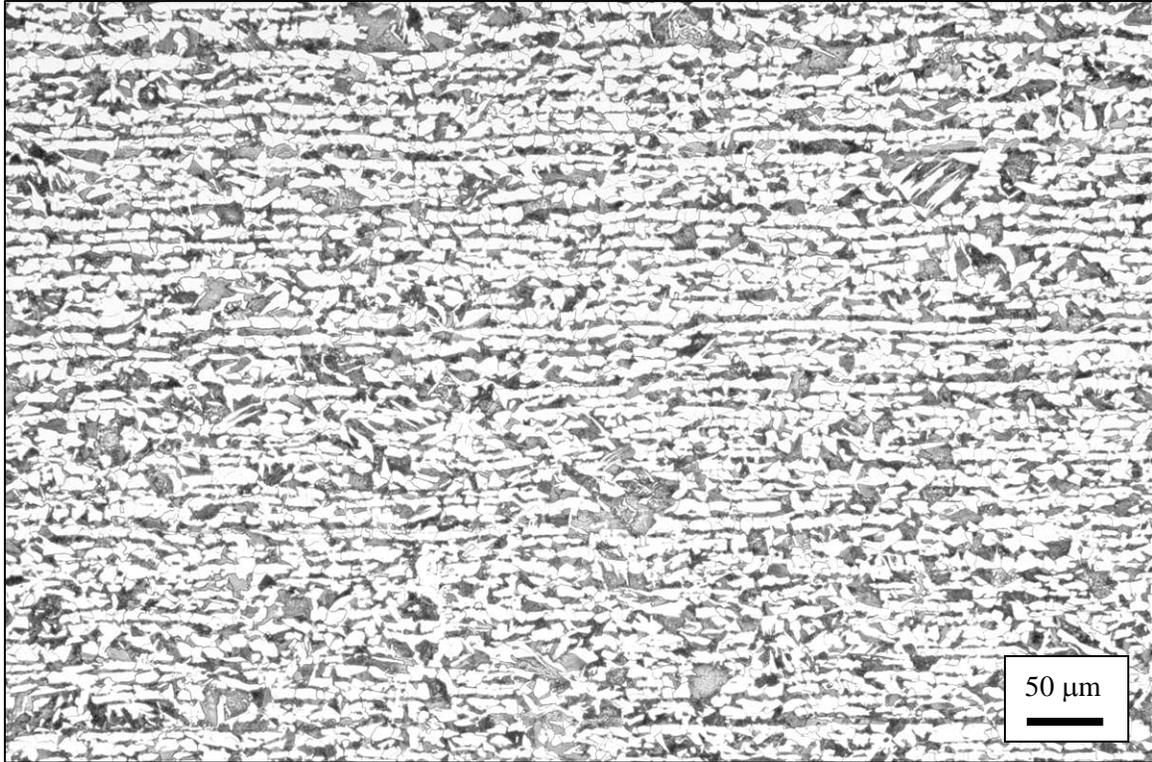
Source: NIST.

Figure 6–18. Light optical micrograph showing a characteristic microstructure taken at the centerline of a 60 ksi outer web plate. Sample is from panel C-40 (A136: 98-101), column 136 in the 99th floor region of WTC 1. Two percent nital and 4 percent picral etch.
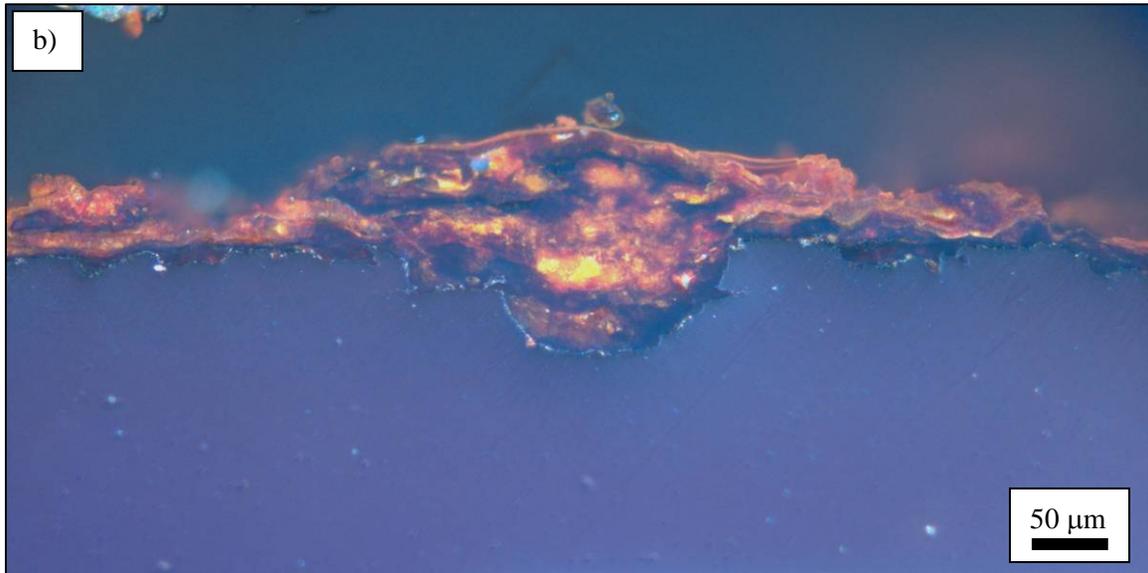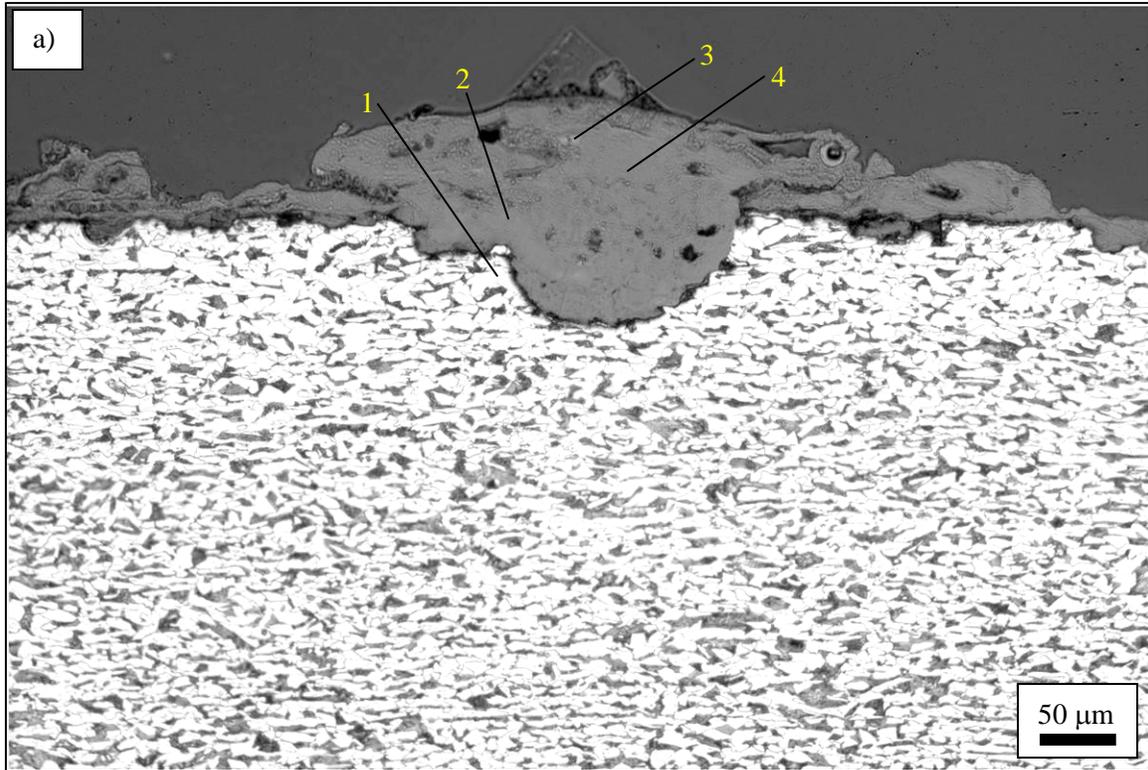
Source: NIST.

**Figure 6–19. Light optical micrographs showing microstructure from flange of column 210 of panel K-1 (A209: 97-100) from the crumpled area above the 98th floor spandrel. a) Characteristic scale formation, 2 percent nital and 4 percent picral etch. b) same area, as polished, using polarized light.**
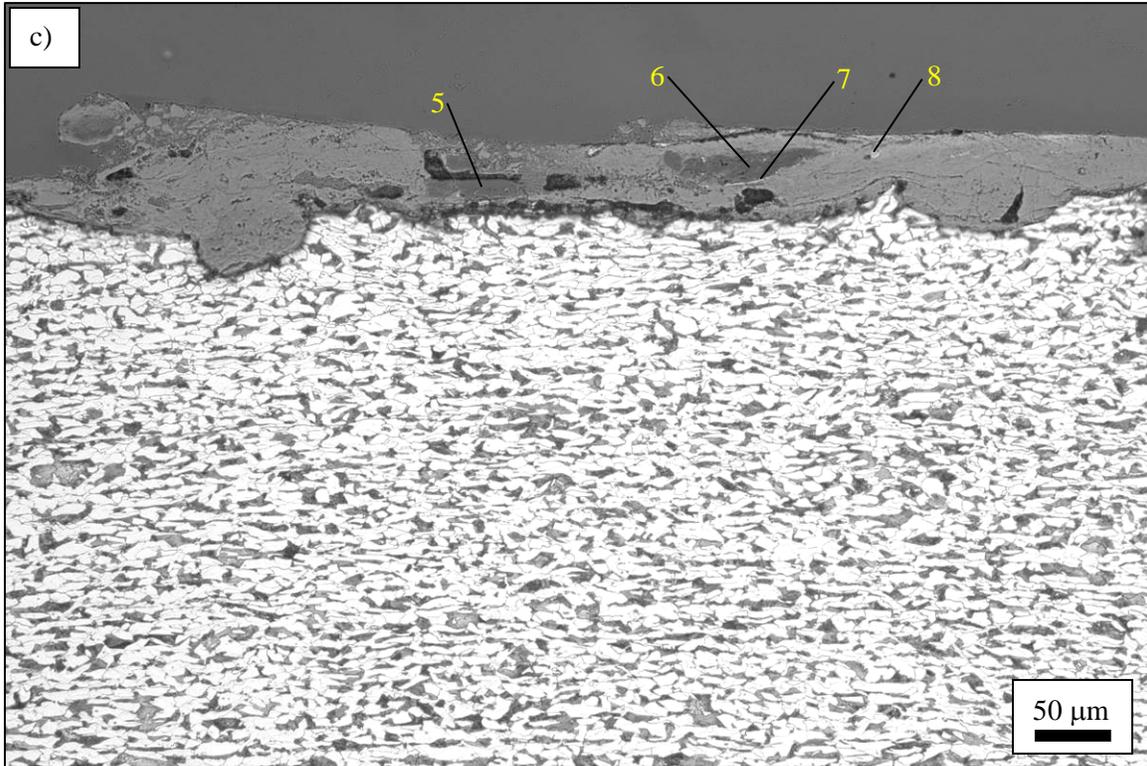
Source: NIST.

Figure 6–19. Light optical micrographs showing microstructure from flange of column 210 of panel K-1 (A209: 97-100) from the crumpled area above the 98th floor spandrel. c) Characteristic scale formation. Two percent nital and 4 percent picral etch.

Source: NIST.

Figure 6–20. a) Overall image of panel K-16 and b) images showing the deterioration of the column due to erosion/corrosion mechanisms. Red arrow indicates direction of photograph seen in Fig. 6–23.
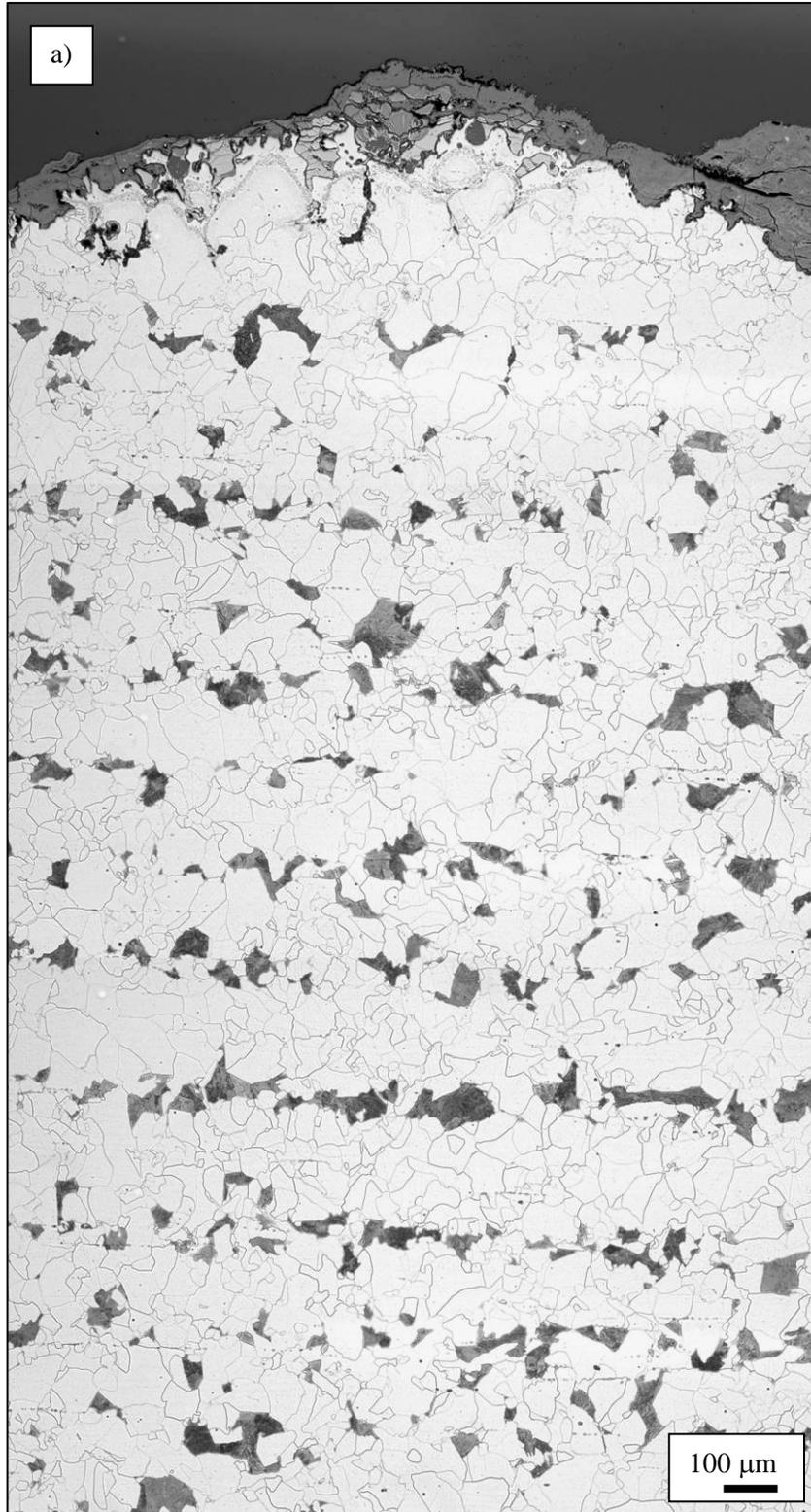
Source: NIST.

Figure 6–21. a) Light optical micrograph showing banded structure of the 50 ksi column labeled K-16 near where the extreme corrosion process occurred. As-built location was not known. Two percent nital and 4 percent picral etch.
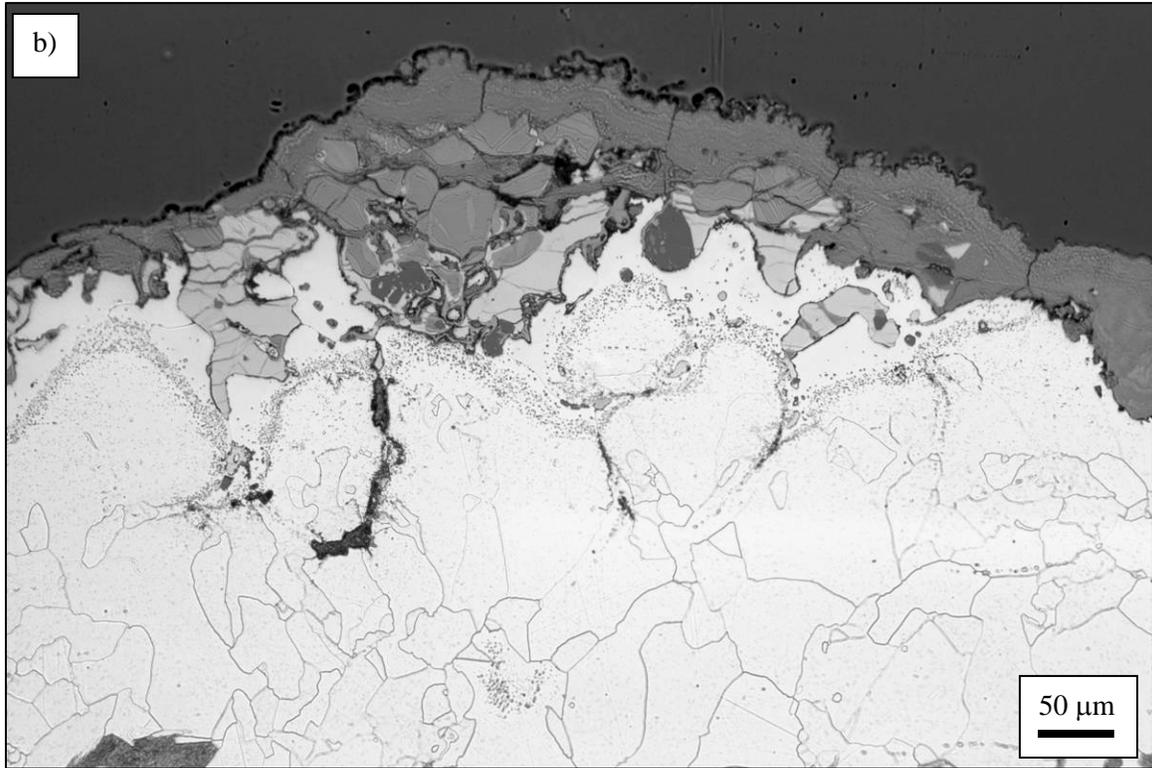
Source: NIST.

Figure 6–21. b) Light optical micrograph showing the microstructure near the metal-scale interface of the 50 ksi column labeled K-16 near where the corrosion process occurred. As-built location was not known. Two percent nital and 4 percent picral etch (cont.).
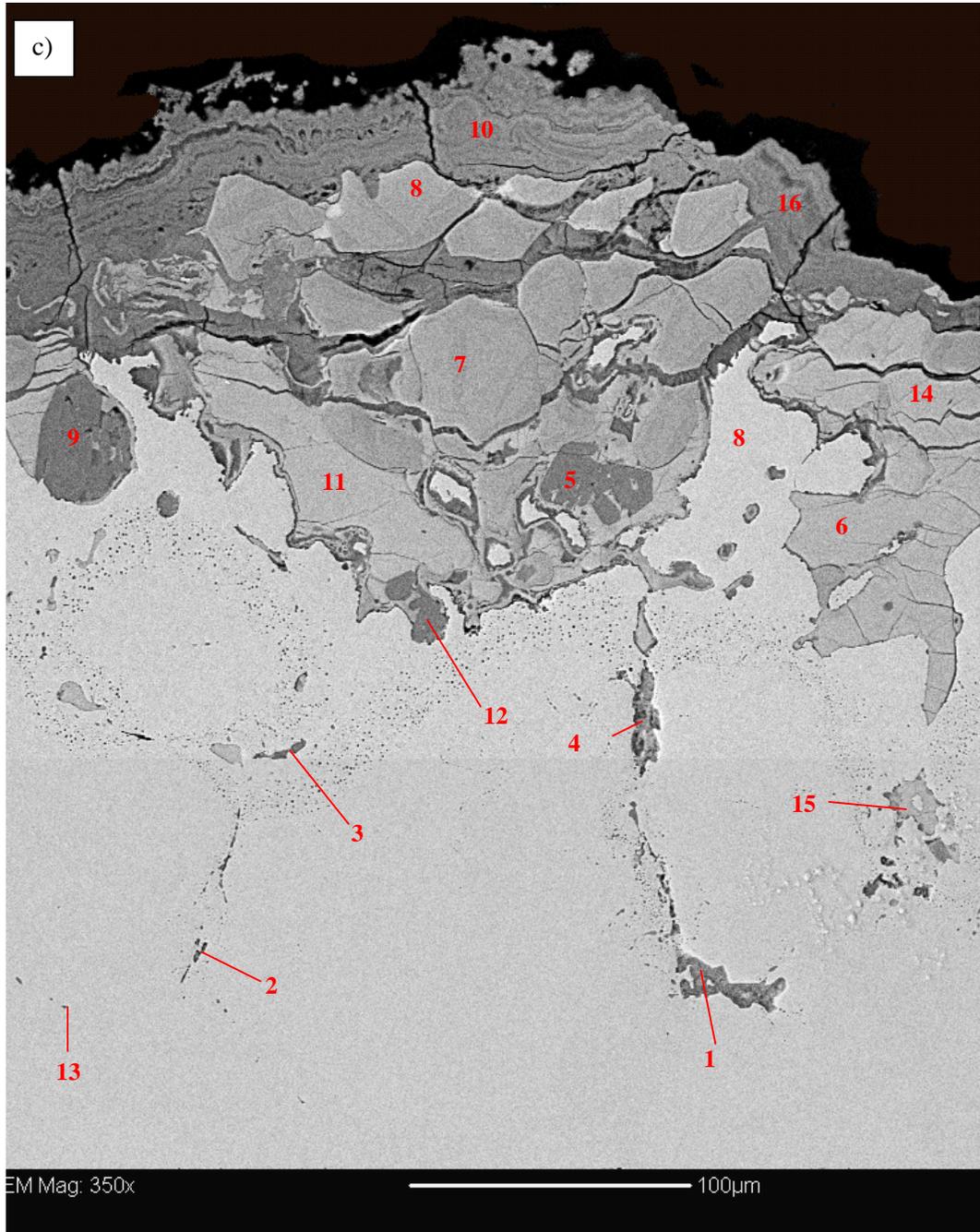
Source: NIST.

Figure 6–21. c) Secondary electron micrograph showing corrosion scale formation on panel K-16. As-built location was not known. Sample in the as-polished condition (cont.).
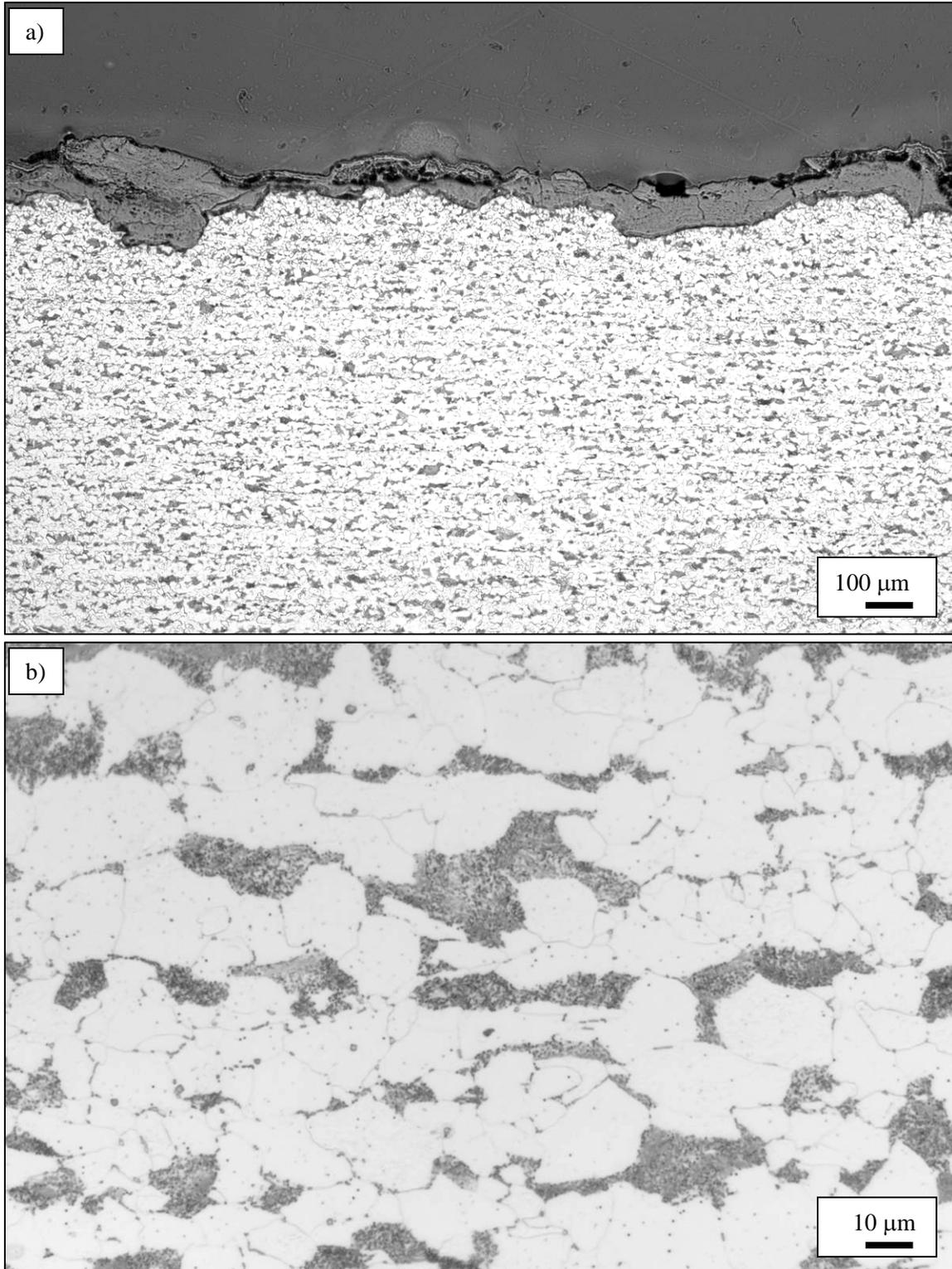
Source: NIST.

Figure 6–22. Light optical micrographs showing structure of the 50 ksi column labeled K-16 near the base of the column where the corrosion process did not occur. As-built location was not known. a) low magnification and b) pearlite has begun to spheroidize. Two percent nital and 4 percent picral etch.
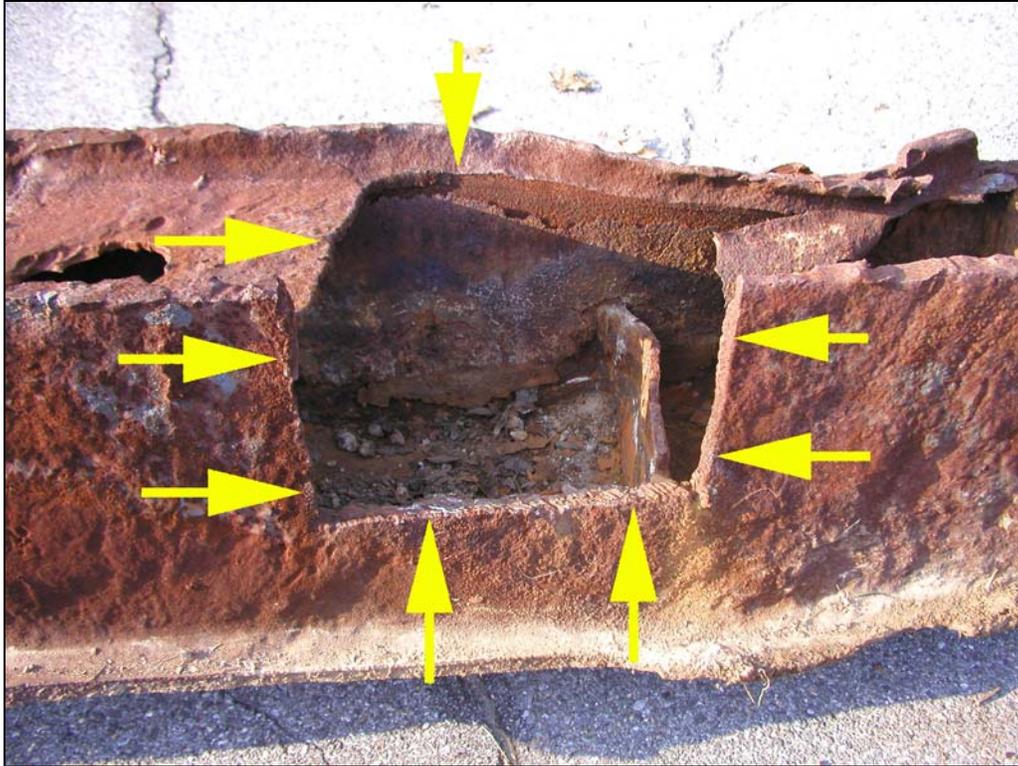
Source: NIST.

Figure 6–23. Photograph showing the location, size, shape, and orientation of sample removed from panel K-16 prior to its arrival on the NIST campus. Sample was analyzed in FEMA/BPAT study. Yellow areas indicate flame cut edges.
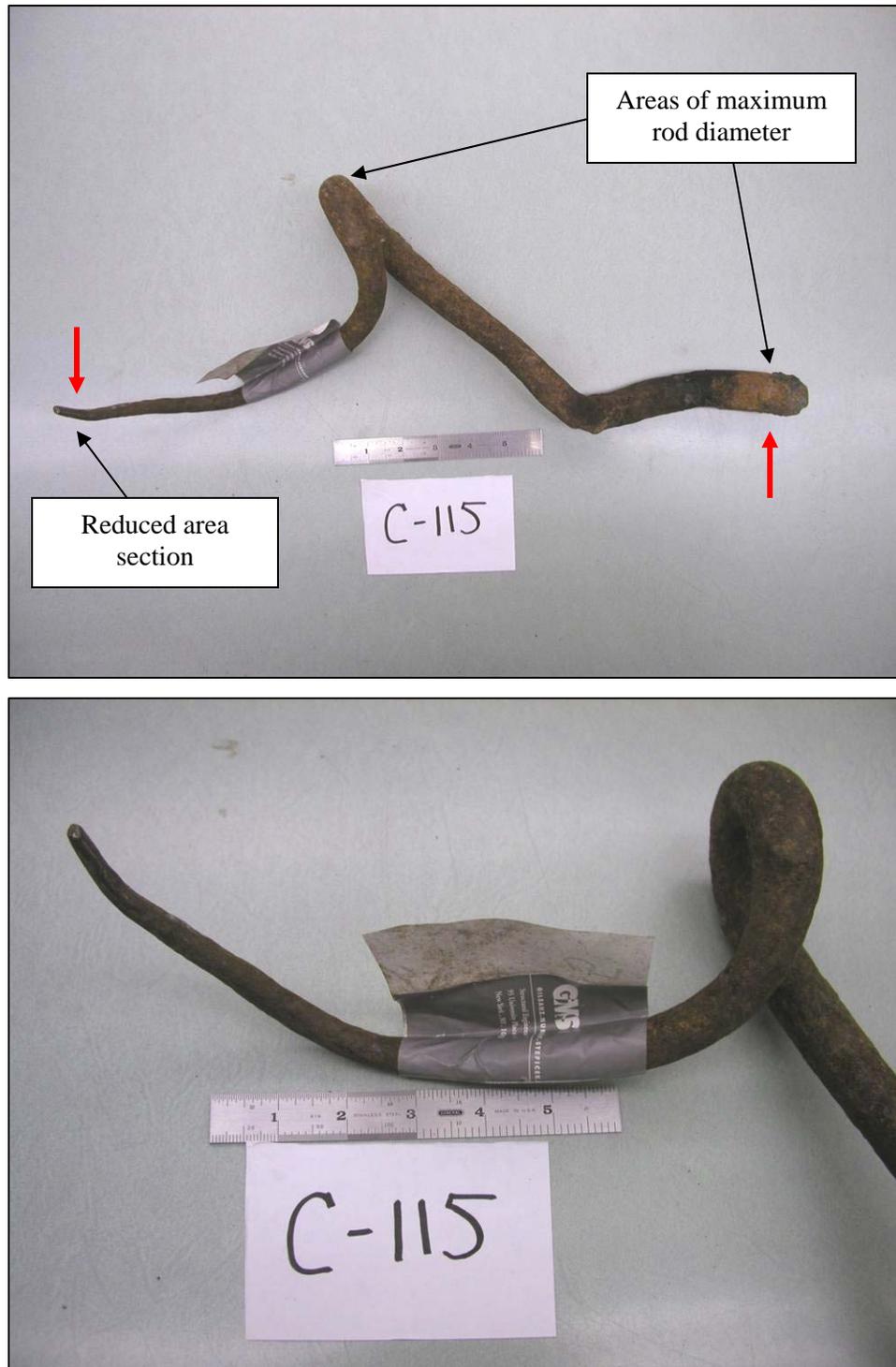
Source: NIST.

Figure 6–24. Sample C-115, an unidentified floor truss rod that has thinned down. Red arrows indicate areas of sample removal for analysis.
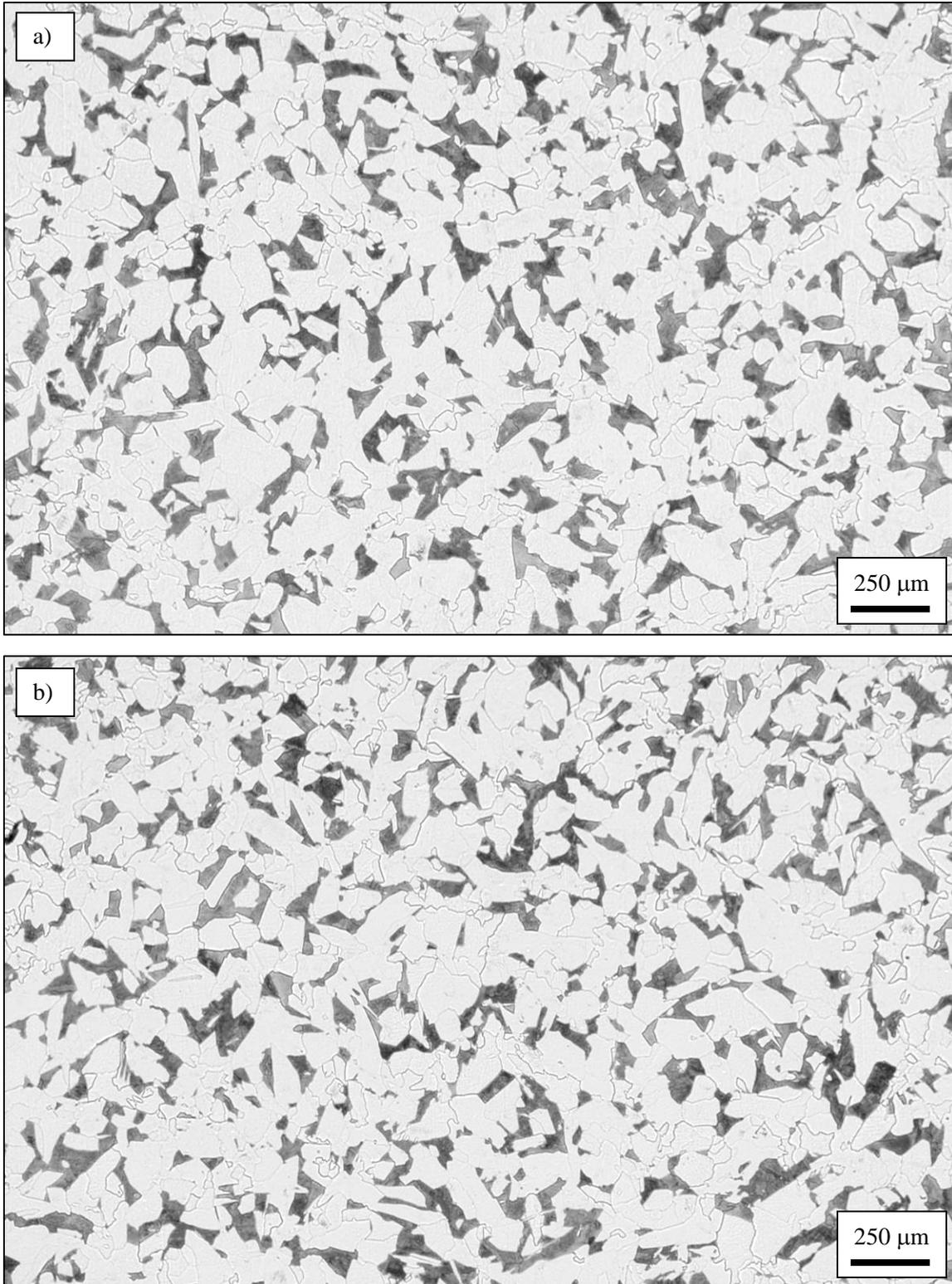
Source: NIST.
Figure 6–25. Light optical micrographs showing ferrite-pearlite structure of truss rod sample C-115. a) 1 in. section, b) reduced section. Two percent nital and 4 percent picral etch.
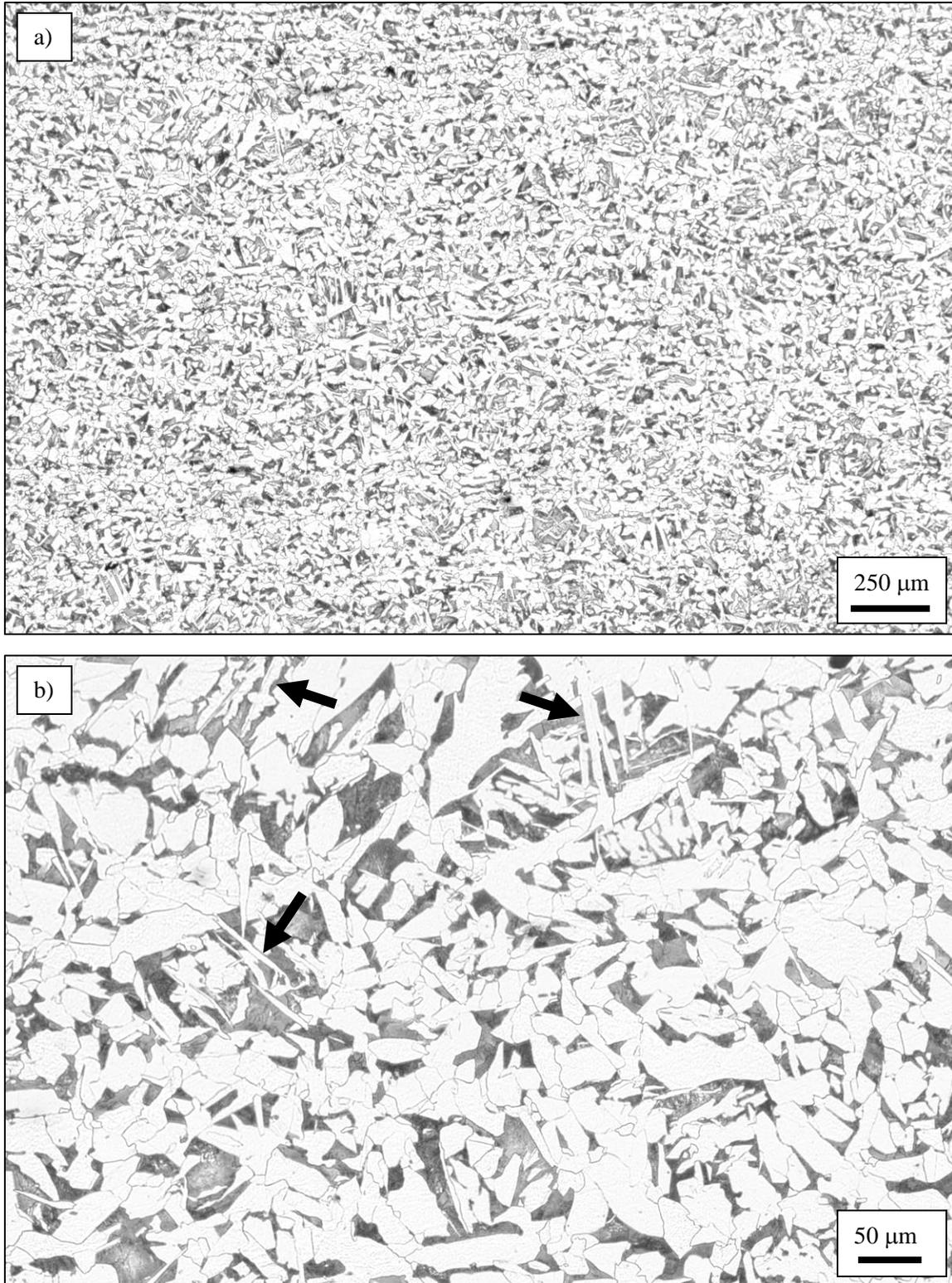
Source: NIST.

Figure 6–26. Light optical micrographs showing the structure of a typical A 242 truss rod (sample T1-LR-1). a) Overall structure at 50x, b) Widmanstatten ferrite indicated with arrows. Two percent nital and 4 percent picral etch.
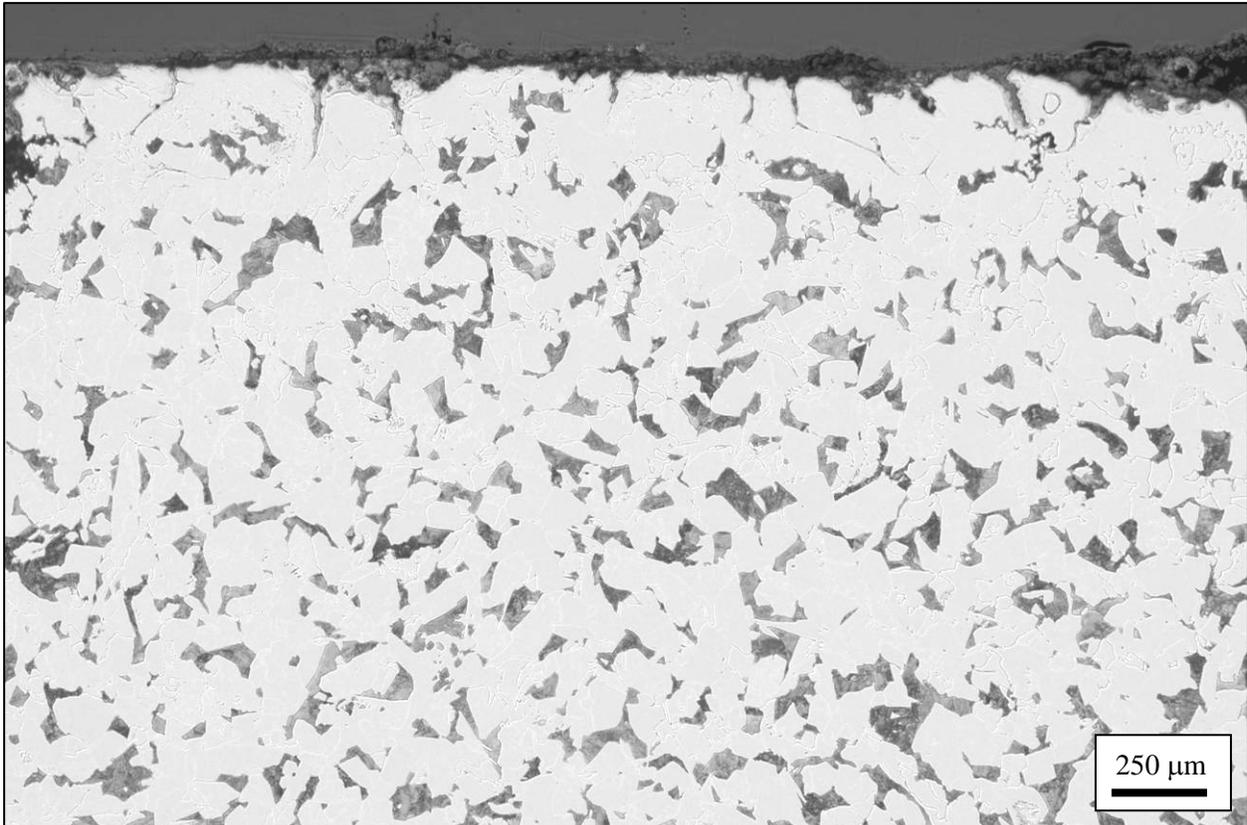
Source: NIST.

Figure 6–27. Light optical micrograph showing the structure of corrosion scale formed on sample C-115. A decarburization zone was not observed. Two percent nital and 4 percent picral etch.
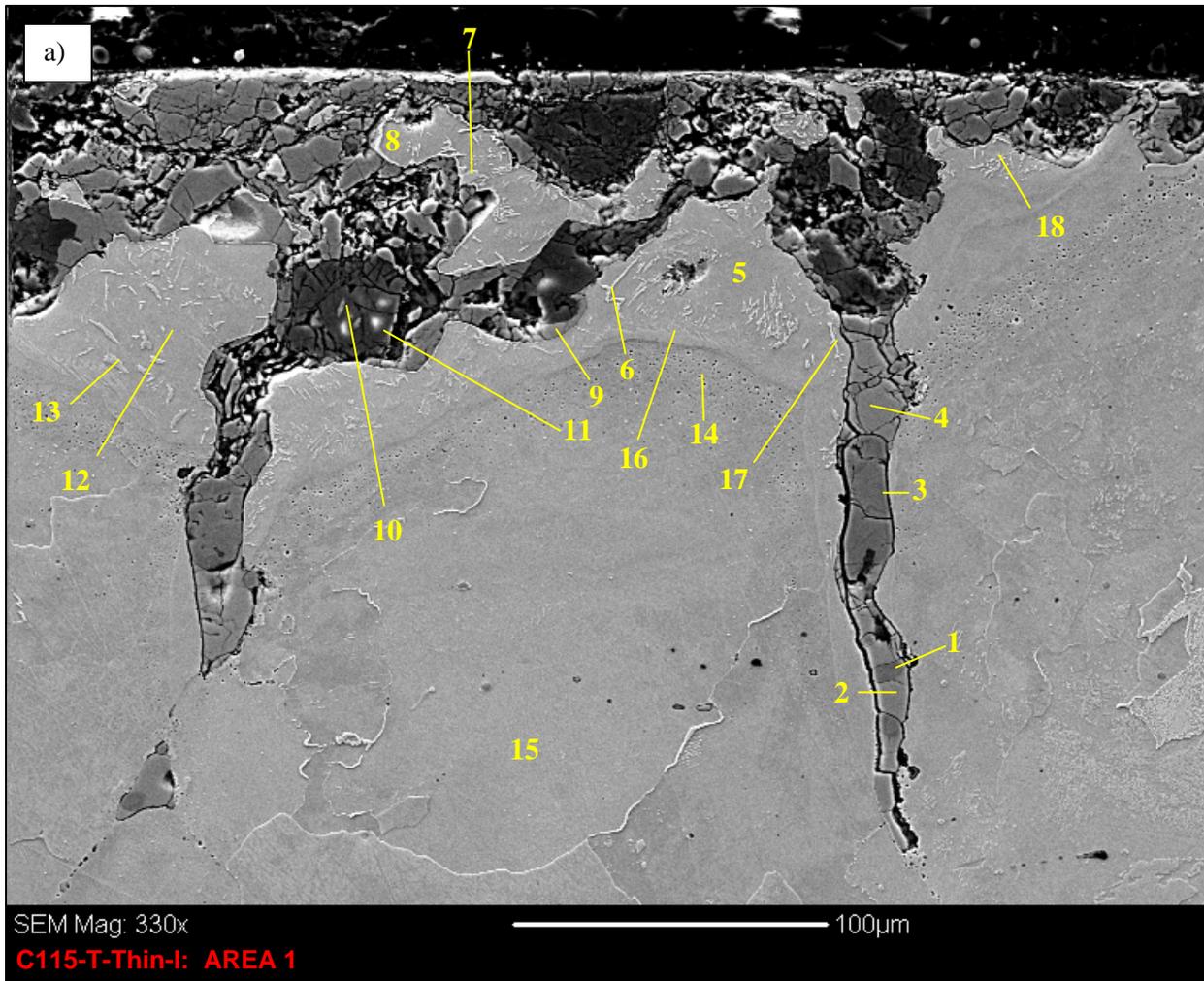
Source: NIST.

Figure 6–28. Secondary electron image showing the corrosion scale found on sample C-115. a) The location of EDS analysis (results shown in Table 6–3) were indicated. Two percent nital and 4 percent picral etch.
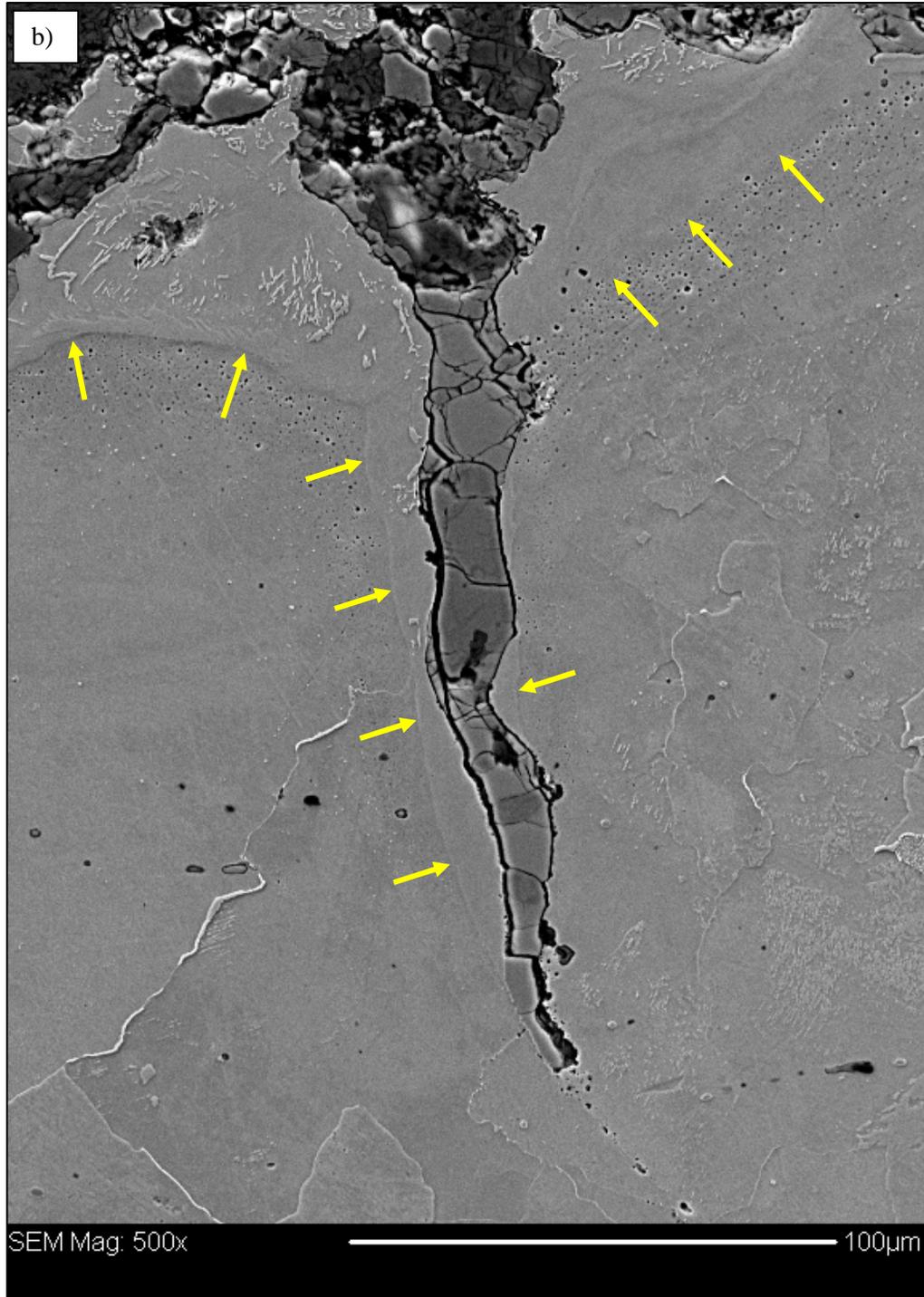
Source: NIST.

Figure 6–28. Secondary electron image showing the corrosion scale found on sample C-115. b) yellow arrows indicating the Fe-Ni layer between the penetrating corrosion product and internal oxidation zone. Two percent nital and 4 percent picral etch (cont.).
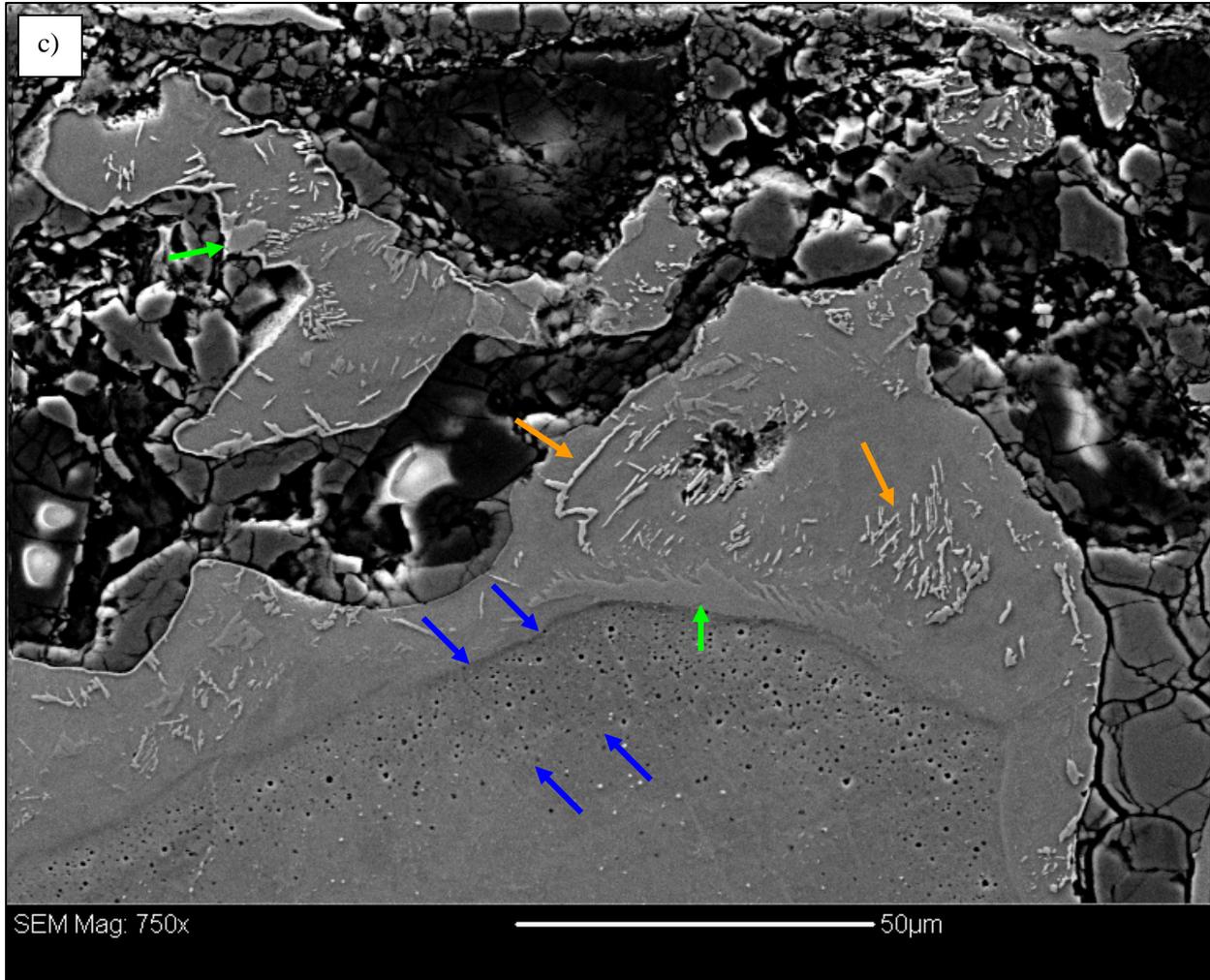
Source: NIST.

Figure 6–28. Secondary electron image showing the corrosion scale found on sample C-115. c) Blue arrows indicate the internal oxidation zone, green arrows indicate the "feathery" morphology and orange arrows indicated the "needle-like" morphology of corrosion phases observed. Two percent nital and 4 percent picral etch.

Table 6–1. Results of visual examination for fire exposure on recovered perimeter panels.

Most severe exposure prior to collapse	Condition of paint	Number of observations analyzed	Result of microscopy technique for mud cracking			
			Positive	Negative	Inconclusive	No conclusion
Any type of exposure to fire	Sufficient for analysis	68	4.5	91	4.5	0
	Insufficient for analysis	4	0	0	0	100
External flaming	Sufficient for analysis	37	5	92	3	0
	Insufficient for analysis	0				
Fire inside	Sufficient for analysis	29	3.5	93	3.5	0
	Insufficient for analysis	4	0	0	0	100
Spot fire	Sufficient for analysis	2	0	50	50	0
	Insufficient for analysis	0				
No fire evident	Sufficient for analysis	85	0	98	2	0
	Insufficient for analysis	3	0	0	0	100

Note: Unless otherwise noted, values are in percentages of observations.

Table 6–2. Microstructure and hardness results concerning specific structural elements analyzed for possible fire-related damage.

Section in Report	Sample	As-built location	Component	Floor level	Time-Fire Exposure Data		Visual Inspection		Vickers Hardness		Rockwell Hardness	
					Most severe exposure	Minimum duration of exposure (min)	Condition of surface	Microscopy technique for mud cracking	Sample HVN	Average HVN (for given F_y)	Sample HRB	Average HRB (for given F_y)
6.3.2	M-2	WTC 1, north face	Spandrel	99th	external flaming	18	Sufficient paint for analysis	negative	180 +/- 4	+/- 21 (36 ksi mate	83.8 +/- 0.7	84.7 +/- 5.8 (36 ksi material)
	N-7	WTC 1, north face	Spandrel	99th	external flaming	16	Sufficient paint for analysis	negative	172 +/- 5	+/- 16 (42 ksi mate	86.3 +/- 0.2	86.9 +/- 3.5 (42 ksi material)
	N-8	WTC 1, north face	Spandrel	99th	external flaming	18	Sufficient paint for analysis	negative	172 +/- 3	+/- 16 (42 ksi mate	82.7 +/- 0.8	86.9 +/- 3.5 (42 ksi material)
	S-10	WTC 1, east face	Spandrel	93rd	fire inside	32, discontinuous	No paint available for analysis	no conclusion	196 +/- 4	+/- 21 (50 ksi mate	93.9 +/- 0.3	93.5 +/- 1.4 (50 ksi material)
6.3.3	C-40	WTC 1, north face	Seat, C135	99th	fire inside	18	Sufficient paint for analysis	negative	143 +/- 4	183 +/- 15	83.0 +/- 1.0	86.6 +/- 2.1
	M-2	WTC 1, north face	Seat, C131	99th	external flaming	18	Sufficient paint for analysis	negative	163 +/- 13	183 +/- 15	78.9 +/- 1.4	86.6 +/- 2.1
	N-8	WTC 1, north face	Seat, C143	99th	external flaming	18	Sufficient paint for analysis	Positive on seat and standoff	148 +/- 3	183 +/- 15	86.3 +/- 0.8	86.6 +/- 2.1
	N-12	WTC 1, east face	Seat, C206	94th	external flaming	25, discontinuous	Sufficient paint for analysis	inconclusive	135 +/- 9	183 +/- 15	74.3 +/- 1.1	86.6 +/- 2.1
6.3.4.1	K-1	WTC 1, east face	Flange, C210	97th	external flaming	12	Sufficient paint for analysis	negative	216 +/- 3	220 +/- 15 (60 ksi outer web,	94.8 +/- 0.3	94.7 +/- 1.8 (60 ksi outer web, t = 0.25")
	K-1	WTC 1, east face	Flange, C210	98th	external flaming	31, discontinuous	Sufficient paint for analysis	positive	242 +/-6	220 +/- 15 (60 ksi outer web, t = 0.25")	NA	NA
6.3.4.2	K-2	WTC 1 , east face	Spandrel	93rd	fire inside	9, discontinuos	Sufficient paint for analysis	Positive below 93rd floor slab	179 +/- 6	+/- 16 (42 ksi mate	87.1 +/- 0.1	86.9 +/- 3.5 (42 ksi material)
6.3.4.3	K-16	Unknown 50 ksi column	Outer web	Upper portion of column	NA	NA	No paint available for analysis	no conclusion	132 +/- 13	205 +/- 11 (50 ksi flange, t = 0.5625")	NA	NA
	K-16	Unknown 50 ksi column	Outer web	Lower portion of column	NA	NA	No paint available for analysis	no conclusion	168 +/- 5	205 +/- 11 (50 ksi flange, t = 0.5625")	85.3 +/- 0.0	91.7 +/- 1.7 (50 ksi flange, t = 0.5625")
6.3.4.4	C-115	Unknown	Truss rod	Thinned end	NA	NA	No paint available for analysis	no conclusion	141 +/- 7	172 +/- 17 (similar diameter)	NA	NA
	C-115	Unkown	Truss rod	Unaffected end	NA	NA	No paint available for analysis	no conclusion	167 +/- 10	172 +/- 17 (similar diameter)	72.2 +/- 0.2	94.2 +/- 1.6 (similar diameter)

Table 6–3. EDS analysis from samples analyzed in Sec. 3.2.

Sample	Point	Color of scale using optical microscopy or description of morphology	EDS Analysis (Results in order of decreasing peak height)
K-1	1	matrix	Fe, Mn
	2	gray	Fe, Mn
	3	light gray	Fe, Mn
	4	gray	Fe, Mn
	5	dark gray	Fe, Ca, Mn
	6	dark gray	Fe, Ca, Mn
	7	light gray	Fe, Mn
	8	light gray	Fe, Mn
K-16	1	dark gray	Fe, Cl, S, Mn, Si
	2	dark gray	Fe, Cl, S, Si, Mn
	3	dark gray	Fe, Cl, S, Mn
	4	dark gray	Fe, Cl, S, Si, Mn
	5	dark gray	Fe, Si, Ca, Mn, S
	6	gold	S, Fe
	7	gray	Fe, Mn
	8	matrix	Fe
	9	dark gray	Fe, Si, Ca, Mn
	10	gray	Fe
	11	gold	S, Fe
	12	dark gray	Fe, Si, Ca, Mn
	13	dark gray	Fe, S, Cl, Mn, Si
	14	gold	Fe, S
	15	gold	Fe, S, Mn
	16	gray	Fe, Mn
C-115	1	gray	Fe
	2	gold	Fe, S
	3	gray	Fe
	4	gold	Fe, S
	5	matrix around needles	Fe, Ni
	6	needle phase	Fe, Ni
	7	"feathery" phase	Fe, Ni, Cu
	8	matrix around needles	Fe, Ni
	9	gold	Fe, S
	10	dark gray	Fe, Si, Ca, Mn
	11	gold	Fe, S
	12	matrix around needles	Fe, Ni
	13	"feathery" phase	Fe, Ni
	14	internal precipitate	Fe
	15	matrix away from corroded area	Fe
	16	"feathery" phase	Fe, Ni
	17	needle phase	Fe, Ni
	18	needle phase	Fe, Ni

This page intentionally left blank.

Chapter 7
FINDINGS AND CONCLUSIONS

Damage assessment and failure analysis of the recovered World Trade Center (WTC) steel resulted in the following findings and conclusions:

7.1 STRUCTURAL DAMAGE AS A RESULT OF AIRPLANE IMPACT – PERIMETER PANELS

Analysis of enhanced photographs taken of the impact hole in WTC 1 allowed for the identification of about 95 percent of the modes of failure for the exterior wall columns damaged in the collision. Gross deformation behavior observed from the photographs, coupled with analysis of the recovered steel, included:

- Whole exterior panels pushed inside the envelope of the building as a result of column connection bolt failures in the area of fuselage impact;

- Individual perimeter columns torn in a tensile mode surrounding the area of fuselage impact;

- Individual perimeter columns sliced through with little disturbance of surrounding material in areas where engines, heavier sections of the wings, and wing sections containing fuel impacted; and

- Minor damage to individual perimeter columns where lighter airplane components (e.g., wing tips) impacted and sieved through the panel openings.

Of the five panels recovered from the impact hole of WTC 1, four were directly hit by the airplane. Correlation between pre-collapse photographs and the recovered panels from the impact zone indicates that two of the four recovered impact-damaged panels (M-2 and M-30) were in a condition similar to that just prior to building collapse. Some damage can be attributed to the events during and after collapse, but the shape and appearance of the recovered pieces generally match the damage photographs. There was a lack of detailed pre-collapse visual evidence of the impact damage sustained by panels M-27 and S 9, and it was not possible to make such a comparison. The lower portion of panel N-7 did incur some damage; however, it could not be positively correlated with pre-collapse images.

The number and particularly the resolution of the photographs taken of the damage to WTC 2 were much less than those available for the analysis of WTC 1, allowing identification of only 70 percent of the exterior column failure modes. Gross deformation behavior was similar to that observed for WTC 1. In addition, failures of exterior columns due to impact by aircraft components and debris that had passed through the building and exited on the opposite side were characterized.

Of particular interest was the fracture behavior of the plates composing the recovered columns that were directly impacted by the airplane. Fractures of the outer webs of panels M-30 and S-9 exhibited ductile

behavior, including necking and thinning away from the fracture, indicating that the steel behaved ductilely under very high strain rates.

Conversely, fractures occurring parallel and directly next to welded joints exhibited few or no ductile characteristics. The geometry of the joint with respect to the direction of impact, stress concentrations due to the geometry, diminished properties of the heat-affected zone in the base metal, and the orientation of the crack propagation with respect to the rolling direction of the plate are expected to have contributed to the lack of ductility. There was no evidence to indicate that the type of joining method, materials, or welding procedures were improper. The welds appeared to perform as intended.

In general, severing of the perimeter columns hit by the heavier sections of the aircraft occurred at the internal stiffener plates or diaphragm plates (associated with the spandrel connection to column). There was a tendency for the columns hit by the plane to fracture along heat-affected zones adjacent to welds. This behavior was not observed for columns outside the impact zone.

7.2   STRUCTURAL DAMAGE AS A RESULT OF AIRPLANE IMPACT – CORE COLUMNS

Failure of the limited number (three) of recovered core columns in the impact zone was a result of both splice connection failures and fracture of the columns themselves. One recovered core column (WTC 2, column line 801, floors 77 through 80) may have sustained damage as a direct result of the airplane impact in terms of a flange bent in a direction consistent with the travel of the airplane. However, the welded splice connection to the column above survived intact.

7.3   DAMAGE TO SPRAYED FIRE-RESISTIVE MATERIAL AS A RESULT OF AIRPLANE IMPACT

Damage to sprayed fire-resistive material on the perimeter columns was examined in pre-collapse photographs. As expected, sprayed fire-resistive material was removed from pieces struck by the incoming aircraft or debris exiting the far side of the buildings. In addition, the impact caused sprayed fire-resistive material and aluminum facade panels to spall off many perimeter columns, which were not directly struck nor severed, but apparently suffered strong accelerations and forces otherwise transmitted through the structure.

A band of white features was apparent on the sprayed fire-resistive material (SFRM) wherever two aluminum panels met on the exterior columns of the buildings, becoming visible when the panels were dislodged. This appears to be a coating applied to protect the SFRM from moisture infiltration at the aluminum panel joints. This coating appears to have prevented the loss of SFRM in a number of locations where the SFRM was knocked off both above and below this location.

7.4   FIRE EXPOSURE AND TEMPERATURES REACHED BY THE STEEL

The pre-collapse photographic analysis showed that 16 recovered exterior panels were exposed to fire prior to collapse of WTC 1. None of the nine recovered panels from within the fire floors of WTC 2 were observed to have been directly exposed.

A method was developed using microscopic observations of paint cracking to determine whether steel members had experienced temperatures in excess of 250 °C. More than 170 areas were examined on 21 exterior panels. Note that these 21 panels represent only about 3 percent of the panels from fire-involved floors, and that results on these panels cannot be considered indicative of exposure of other panels. Only three locations had a positive result indicating that the steel and paint may have reached temperatures in excess of 250 °C (note that exposure could have occurred pre- or post-collapse). These areas were:

- WTC 1, east face, floor 98, column 210, inner web;

- WTC 1, east face, floor 92, column 236, spandrel; and

- WTC 1, north face, floor 98, column 143, floor truss connector.

Annealing studies on recovered steels (NIST NCSTAR 1-3E) established the set of time and temperature conditions necessary to alter the steel microstructure. The microstructures of steels known to have been exposed to fire, based on the pre-collapse photographic evidence, were characterized. These microstructures show no evidence of exposure to temperatures above 600 °C for any significant time.

Perimeter columns exposed to pre-collapse fire (determined from pre-collapse photographs) had a great tendency for local buckling of the inner web; a similar correlation did not exist for fracture in the base metal near welds.

In the two buildings, there were 329 core columns (each three stories tall) traversing floors involved in fires. National Institute of Standards and Technology (NIST) has portions of four of these columns, and on average about half of each column was recovered. While these pieces allow some comparison of metal and paint condition with the predications of the fire model, the recovered steel represents less than one percent of all the core columns intersecting floors with fire. Thus, the forensic analysis indicating moderate temperature excursions in the recovered core columns does not, and cannot, give a picture of temperatures seen by the vast majority of the core columns.

7.5   TIME-DEPENDENT DEFORMATION OF PERIMETER WALLS DUE TO FIRE AND LOAD REDISTRIBUTION

Images of WTC 1 showed gross deformations of an exterior wall prior to final collapse. Images of the south face of the tower taken approximately 5 min prior to collapse showed inward bowing of the exterior columns, reaching an observable maximum of 55 in. near column 316 on the 96th floor. The inward deflection appears to extend over the entire south face of the building at this time and is visible vertically between the 94th and 100th floors. Photographs taken approximately 30 min prior to this time do not show any inward bowing of the south face of WTC 1.

Images of WTC 2 revealed some details of how the building deformed during the time between aircraft impact and collapse and revealed how the portion of the building above the impact zone moved relative to the bottom of the building during initial stages of collapse. Approximately 18 min after the impact of the aircraft, the east face of WTC 2 exhibited inward bowing of up to 10 in. in the region of the 79th to 83rd floors. This inward bowing increased to 20 in. at a time 5 min before collapse of the tower.

Hanging floor slabs at the 82nd and 83rd floors were visible in window openings on the east and north faces, respectively, and the positions of these slabs changed over time, suggesting a slow collapse mechanism of certain parts of the flooring in this area of the tower.

At the moment of collapse of WTC 2, the top portion of the building moved to the west as it tilted to the southeast. During this tilting, a complex kink developed at the southeast corner of the top portion in the region of the 106th floor. In addition, the top portion twisted slightly clockwise (as viewed from the top) as the collapse progressed.

7.6 STRUCTURAL DAMAGE AND FAILURES AS A RESULT OF COLLAPSE

The failure mode of spandrel connections on perimeter panels differed above and below the impact zone. Spandrel connections on exterior panels at or above the impact zone were more likely to experience bolt hole tear out as a failure mode. For those exterior panels below the impact zone, there was a higher propensity for portions of the spandrels to be torn from the panels. There did not appear to be any difference in failure mode for the spandrel connections whether the exterior panels were exposed to fire or not.

With the exception of the mechanical floors, the major failure mechanism concerning perimeter panel column splices was fracture of the bolts. At mechanical floors, where column splices were welded in addition to being bolted, the majority of the splices did not fail, rather the web and flange plates composing the columns fractured near the splice.

The damage to truss seats on perimeter panels differed above and below the impact zone. The majority of perimeter panel floor truss connectors (perimeter seats) below the impact floors were either missing or bent downward. Above this level, the failure modes were more randomly distributed. This trend was observed for both towers.

Failure of the perimeter panel floor truss seats typically occurred in the heat-affected zones near welds, and the fracture location was associated with the weld geometry (i.e., in the component with the lowest cross-sectional area). These areas with the lowest cross-sectional area were typically the standoff plates. However, there was no evidence to indicate that the type of joining method, materials, or welding procedures were improper.

Of the 31 core floor truss connectors (core truss seats) recovered, 90 percent were still intact though extensive damage may have occurred. Only two were observed to have been completely torn from the channel. (This distribution may have resulted from the selection process at the salvage yards).

In the floor trusses, failure of a large majority of the electric resistance welds at the web-to-chord connections was observed. Failure of the connection between the floor truss and the perimeter panel floor truss connectors was typically a result of gusset plate (attached to top truss chord) weld and bolt failure.

7.7 STRUCTURAL STEEL IN IMPACT ZONE

Though representative examples of all strength/gauge combinations of steel plate used to fabricate the exterior panels from the impact regions of the towers have not been recovered, numerous gauges for all

14 specified grades of steel used for the perimeter panels have been recovered. Of the 28 different strength/gauge combinations for plates composing the perimeter columns in the impact region of both towers, NIST has recovered representative samples for 14. Of the 14 unrecovered strength/gauge combinations, 10 combinations had gauges very close to those in the NIST inventory (within 0.0625 in.), while three were 0.125 in. away, and one combination had a difference of 0.1875 in. Similarly, 7 of the 13 strength/gauge combinations used for the spandrel plates in the impact region were recovered. All six of these missing strength/gauge combinations of spandrel plate were within 0.0625 in. of those in the NIST inventory.

This page intentionally left blank.

Chapter 8
REFERENCES

Boeing 2004, http://www.boeing.com.

Bramfitt, B.L. and Benscoter, A.O. 2002. Metallographer's Guide: Practices and Procedures for Irons and Steels, ASM International, Materials Park, OH.

Feld, L. S. 1971. Superstructure for the 1,350-ft World Trade Center. Civil Engineering-ASCE. 41:66–70.

Kou, S. 1987. Welding Metallurgy, John Wiley and Sons, New York, NY.

Ludwigson, D.C., Speich, G.R., Gilbert, S., and Defilippi, J.D. 1982. Iron and Steelmaker, 9 (4), 38-43.

McAllister, T., ed. 2002. World Trade Center Building Performance Study: Data Collection, Preliminary Observations, and Recommendations. FEMA 403. Federal Emergency Management Agency. Washington, DC, May.

Porter, L.F. 1976. "Lamellar tearing in plate steels", United States Steel Corporation, ADUSS 16-6919-02, Aug 1976.

Russ, J.C. 1995. The Image Processing Handbook, Second Edition, CRC Press, Ann Arbor, Michigan.

Samuels, L.E. 1980. Optical Microscopy of Carbon Steels, ASM, Metals Park, OH.

Sommella, J. 1979. "Significance and control of lamellar tearing of steel plate in the shipbuilding industry", SSC-290, Ship Structure Committee, 1979.

Tide, R.H.R. 1998. "Integrity of structural steel after exposure to fire", Engineering Journal, 35 (1), 26-38.

VanderVoort, G. 2003. "Metallographic Examination of Structural Steel From the World Trade Center," poster presented at Microscopy and Microanalysis 2003, San Antonio, TX, August 3-7, 2003.

This page intentionally left blank.